BRL R 1988

BRL

AD

REPORT NO. 1988

(Supersedes IMR No. 159)

A PARAMETRIC STUDY OF GAS FLOW AND FLAME SPREADING IN PACKED BEDS OF BALL PROPELLANT. PART I. THE 108.4 MM CHAMBER WITH 7.62 MM I.D.

Norman J. Gerri

May 1977

USA ARMAMENT RESEARCH AND DEVELOPMENT COMMAND
USA BALLISTIC RESEARCH LABORATORY
ABERDEEN PROVING GROUND, MARYLAND

Destroy this report when it is no longer needed.
Do not return it to the originator.

Secondary distribution of this report by originating or sponsoring activity is prohibited.

Additional copies of this report may be obtained from the National Technical Information Service, U.S. Department of Commerce, Springfield, Virginia 22151.

The findings in this report are not to be construed as an official Department of the Army position, unless so designated by other authorized documents.

The use of trade names or manufacturers' names in this report does not constitute indorsement of any commercial product.

REPORT DOCUMENTATION PAGE

READ INSTRUCTIONS BEFORE COMPLETING FORM

1. REPORT NUMBER: BRL Report No. 1988
2. GOVT ACCESSION NO.:
3. RECIPIENT'S CATALOG NUMBER:

4. TITLE (and Subtitle): A PARAMETRIC STUDY OF GAS FLOW AND FLAME SPREADING IN PACKED BEDS OF BALL PROPELLANT. PART I. THE 108.4 MM CHAMBER WITH 7.62 MM I.D.

5. TYPE OF REPORT & PERIOD COVERED:

6. PERFORMING ORG. REPORT NUMBER:

7. AUTHOR(s): Norman J. Gerri

8. CONTRACT OR GRANT NUMBER(s):

9. PERFORMING ORGANIZATION NAME AND ADDRESS:
USA Ballistic Research Laboratory
Aberdeen Proving Ground, Maryland 21005

10. PROGRAM ELEMENT, PROJECT, TASK AREA & WORK UNIT NUMBERS:
RDT&E 1T161102A33H

11. CONTROLLING OFFICE NAME AND ADDRESS:
USA Materiel Development & Readiness Command
5001 Eisenhower Avenue
Alexandria, VA 22333

12. REPORT DATE: MAY 1977

13. NUMBER OF PAGES: 128

14. MONITORING AGENCY NAME & ADDRESS (if different from Controlling Office):

15. SECURITY CLASS. (of this report): Unclassified

15a. DECLASSIFICATION/DOWNGRADING SCHEDULE:

16. DISTRIBUTION STATEMENT (of this Report):
Approved for public release; distribution unlimited.

17. DISTRIBUTION STATEMENT (of the abstract entered in Block 20, if different from Report):

18. SUPPLEMENTARY NOTES:
This Report supercedes BRL IMR No. 159.

19. KEY WORDS (Continue on reverse side if necessary and identify by block number):
Gas Flow
Flame Spreading
Convective Burning Mechanism
Porous Propellant Beds
Model Validation

20. ABSTRACT (Continue on reverse side if necessary and identify by block number) (meg)

A parametric study of gas flow and flame spreading in porous beds of ball propellant was carried out in three vented chambers, 58.5 mm, 108.4 mm, and 201.6 mm, with 7.62 mm I.D. In Part I of this study, the bed length was maintained at 108.4 mm while the principle variables were the primer vent geometry and the shot start pressure is simulated by a shear disc. The results indicate that (1) the initial primer pulse and the primer vent geometry set the stage for all subsequent events, (2) intergranular pressure transmission contributes to the (Cont'd)

20. Abstract (Cont'd)

rupture of the shear disc, (3) propellant grain deformation and frictional forces at the chamber walls greatly effect the progress of the combustion wave through the bed. The major conclusions are that predictive modeling efforts cannot (1) assume homogeneous ignition across the face of the bed, (2) ignore the void space created by the initial primer blast and (3) ignore bed compaction by the initial primer blast and subsequent progress of the combustion wave through the bed. Other factors which must be considered are intergranular stresses, propellant deformation, and frictional forces at the chamber walls.

TABLE OF CONTENTS

LIST OF ILLUSTRATIONS

LIST OF ILLUSTRATIONS (Cont'd)

I. INTRODUCTION

The current demand for high performance weapons of the larger calibers has centered attention on the development of propelling charges capable of generating high chamber pressures in a rapid, controlled manner. Although it has already been demonstrated that porous beds of granulated propellants can be tailored to provide the ultra high burning rates necessary to satisfy these demands, the combination of high chamber pressures and high burning rates immediately raises the spectre of erratic pressure regimes which affect the muzzle velocity, the velocity variability and, in extreme cases, may cause failure of the tube.

Unstable or erratic burning of the propelling charge may be (1) an inherent characteristic of the charge caused by exceeding or failing to meet some critical value of a design parameter, or (2) due to the failure of some component in the ignition train giving rise to an undesirable ignition mode, an ever increasing possibility where performance demands a reduced ignition time. A reduced ignition time, in turn, prohibits usual variations in the ignition train component performance.

This study is confined primarily to the importance of the propellant bed length as a design parameter, with side excursions into primer vent geometry, shot start pressure, and primer strength.

II. BACKGROUND

The complexities of modern weapons coupled with the spiralling cost of development and testing practically demands that charge design become less dependent on "state-of-the-art" techniques and follow a more rigorous approach. Toward this end much emphasis has been placed on the development of mathematical models describing the combustion process from ignition to shot start. Some models are designed to be independent of the overall interior ballistic model, but will ultimately provide an additional input to that model.

Such a model has been demonstrated by the work of Kuo, Vichnevetsky, and Summerfield,[1] who obtained rough agreement between a mathematical model of gas flow and flame spreading in short beds (38.5 mm) of porous propellant, with experimental results obtained by Squire.[2]

---

[1] K.K. Kuo, R. Vichnevetsky, and M. Summerfield, "Generation of an Accelerated Flame Front in a Porous Propellant," AIAA Paper 71-210. Presented at the AIAA 9th Aerospace Sciences Meeting, New York, January 1971.

[2] W. H. Squire, Private communication with K. K. Kuo, 1970-1971.

The theoretical considerations led to the conclusion that: (1) the velocity of the combustion wave accelerates rapidly and continuously in porous beds, and (2) in beds only slightly longer than already reported the flame front could easily attain detonation velocities. These predictions imply the existence of a critical bed length dependent on the burning rate, bed porosity, and propellant geometry. Such predictions are of concern since higher chamber pressures are often obtained by axially increasing the size of the propelling charge.

It was the purpose of this program to: (1) test the general predictive capabilities of the KVS model[1] when applied to longer propellant beds than already reported; (2) test the specific predictions with respect to the transitions of the flame front velocity from deflagration to detonation; (3) provide a sorely needed data base for future comparison between theory and practice; and (4) identify critical parameters related to ignition and gas flow which may have been ignored or underestimated.

Toward this end, a parametric study based on the work of Squire et al.[2,3] had as its principle variant the length of the propellant bed. For comparative purposes, Kitchens[4,5] employed the method of characteristics to extend the KVS model over the experimental range of bed lengths.

The experimental studies were carried out in three chambers - 58.8 mm, 108.4 mm and 201.6 mm in length. All chambers had a 7.62 mm internal diameter. Due to the large number of variables and the specific characteristics of each chamber, this report will deal largely with the experimental results obtained in 108.4 mm chamber shown in Figure 1 with brief reference to the data obtained in the other chambers for comparative purposes. Results obtained from the other chambers will be published under separate titles.

III. EXPERIMENTAL

Pressure measurements were made with four piezo-electric pressure transducers, Kistler model C-4, axially mounted in a spiral configuration with a 90° offset. Shot start conditions are simulated by a shear disc at the forward end of the chamber. A light sensitive diode, mounted in

---

[3] *W.H. Squire and M. P. Devine, "The Interface Between Primer and Propellant," Part I and Part II, Presented 4 June 1969, AOA Paper, published by Frankford Arsenal, 1969.*

[4] *C. W. Kitchens, Jr., "Flame Spreading in Small Arms Ball Propellant," Ballistic Research Laboratories Report 1604, August 1972, AD #750567.*

[5] *C. W. Kitchens, Jr., and N. J. Gerri, "Numerical and Experimental Investigation of Flame Spreading and Gas Flow in Gun Propellants," Proceedings of the 9th JANNAF Combustion Conference, Monterey, California, Vol. 1, September 1971. CPIA Publication No. 231, December 1972, pp. 115-125.*

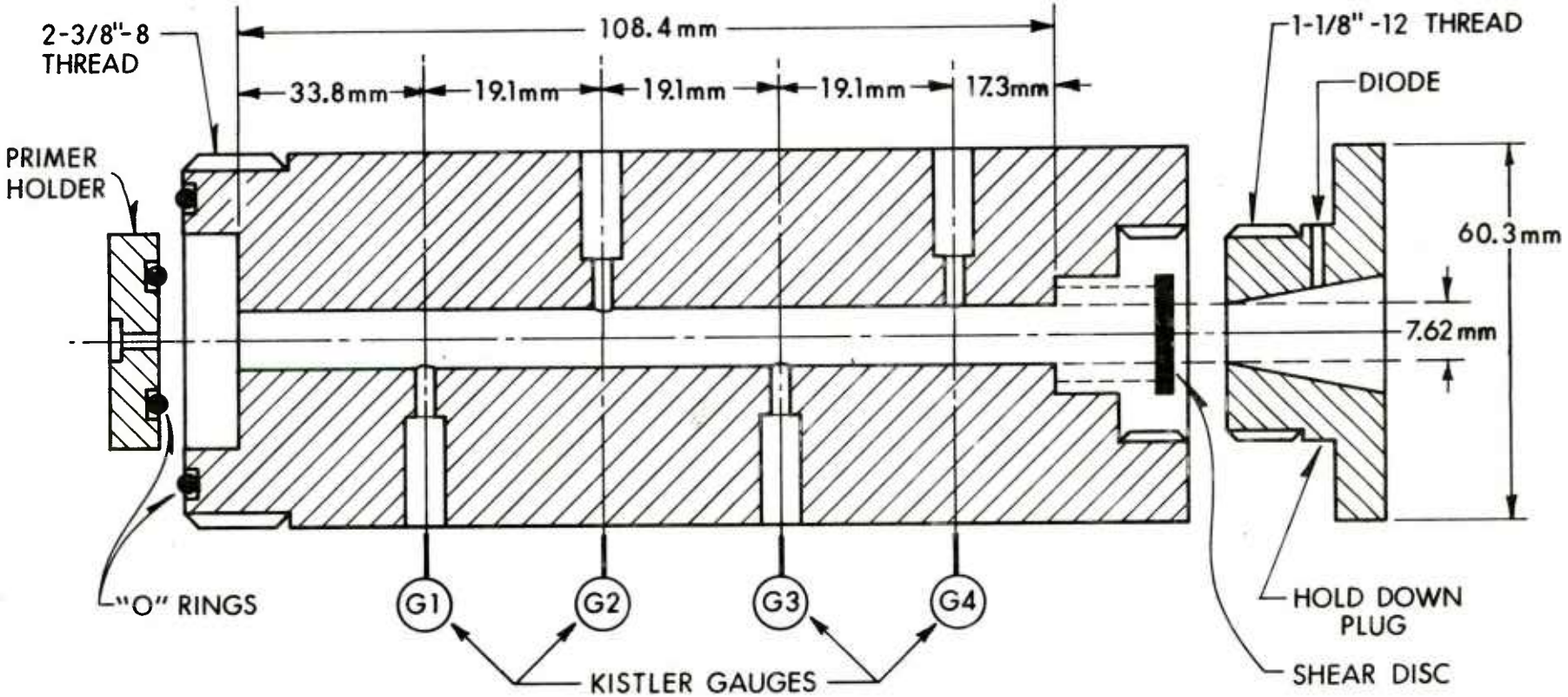

Figure 1. The 7.62 mm I.D. Vented Chamber (108.4 mm Bed Length).

the hold down plug, signals the rupture of the shear disc. The chamber is fired by the solenoid arrangement shown in Figure 2 fitted with a "make" circuit to signal when the firing pin strikes the primer.

All data channels including the firing pin and diode are recorded on 1 inch analog tape at 120 ips. Characteristic frequency response is 80 kHz ($\sim$ 3 μs rise time). The analog data is digitized at a 400 kHz sampling rate and replotted in MKS units. Time marks included on the records are measured from a common fiducial placed simultaneously across all channels prior to the initiation of the firing sequence. Variations in the position of the record along the time axis is a function of the mechanical devices in the firing lines such as safety interlocks and solenoids.

Due to the number of parameters it is convenient to arbitrarily define, for comparative purposes, a standard set of run conditions for all chambers. Following Kuo et al.[1] and Squire,[2] a standard run consists of a 7.62 mm diameter chamber, 100 percent volumetrically loaded with WC-846 (Winchester Cartridge - Olin Matheson Designation), a surface coated, deterred ball propellant. The chamber is fired in the vertical position by a FA-41 (Frankford Arsenal) primer located at the base of the propellant bed and mounted in the primer vent hole configuration shown in Figure 3(F), which is the normal vent configuration. Other configurations shown in Figure 3 will be described later. Venting is provided by a #304 stainless steel shear disc 0.79 mm thick and 19.0 mm in diameter. During the loading process, care is taken to eliminate voids and packing so that the average loading density (1.03 g/cc[3]) closely approximates the bulk density.

The pressure-time (P-t) records presented in the main body of the report are representative samples of the parametric studies carried out in the 108.4 mm chamber. A complete tabulation of all runs and the experimental results plotted in three formats [pressure-time (P-t), pressure-distance (P-x), and differential pressure-time (ΔP-t)], is given in Appendix A. Appendix B gives the propellant, primer, gage, diode and shear disc specifications.

IV. RESULTS

The typical set of pressure records shown in Figure 4 were obtained under standard conditions in the 108.4 mm chamber. The baseline pressure at each gage position has been displaced vertically and scaled according to the gage locations shown in Figure 1. This format will be used in the main body of the report when space permits.

The first set of arrows (↑) indicate the passage of the primer pulse, while the second set (↓) the initial pressure rise arbitrarily defined as the first distinct, continuous pressure rise after the primer pulse. The first major peak at each gage position will be designated as the primary (1°) peak and the second major peak as the secondary

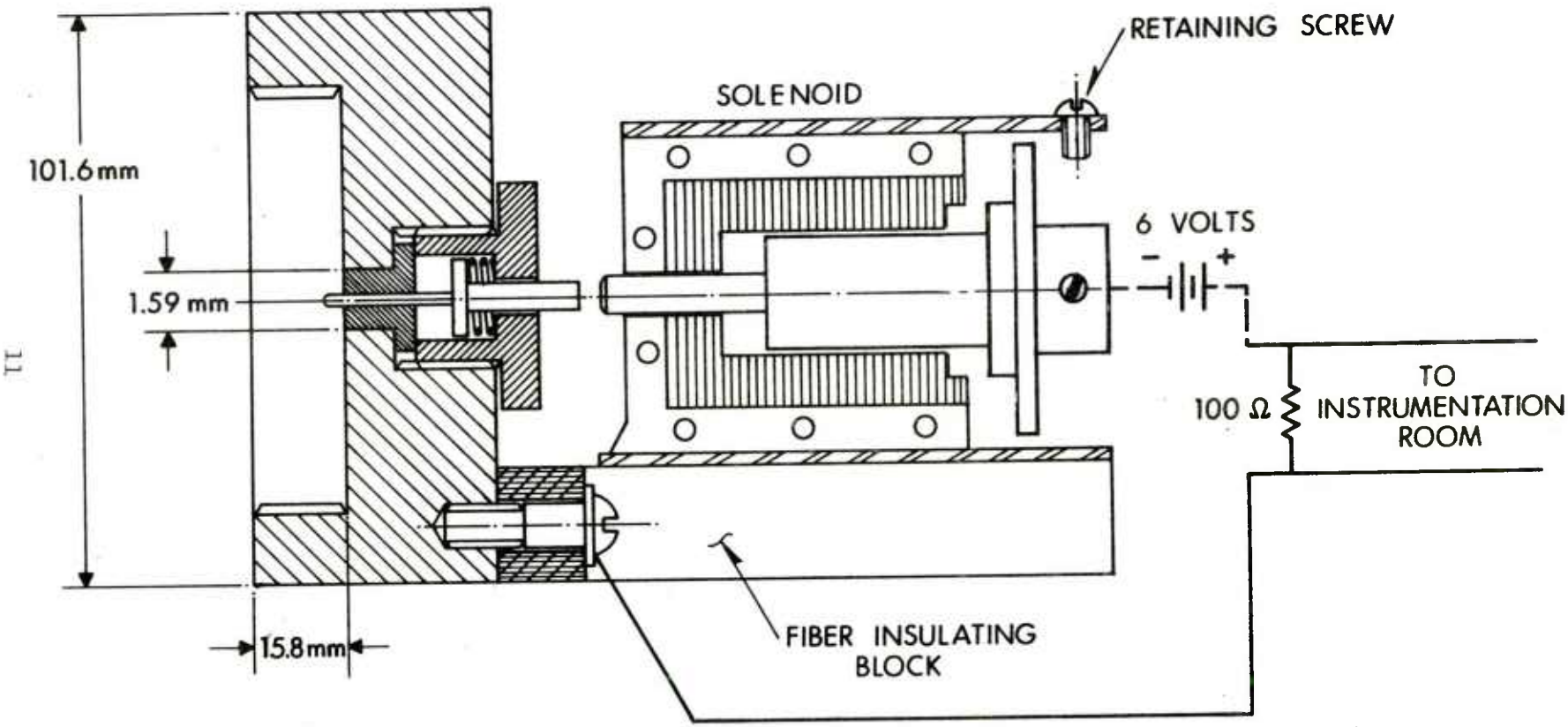

Figure 2. Schematic Diagram of Base Plate and Firing Device.

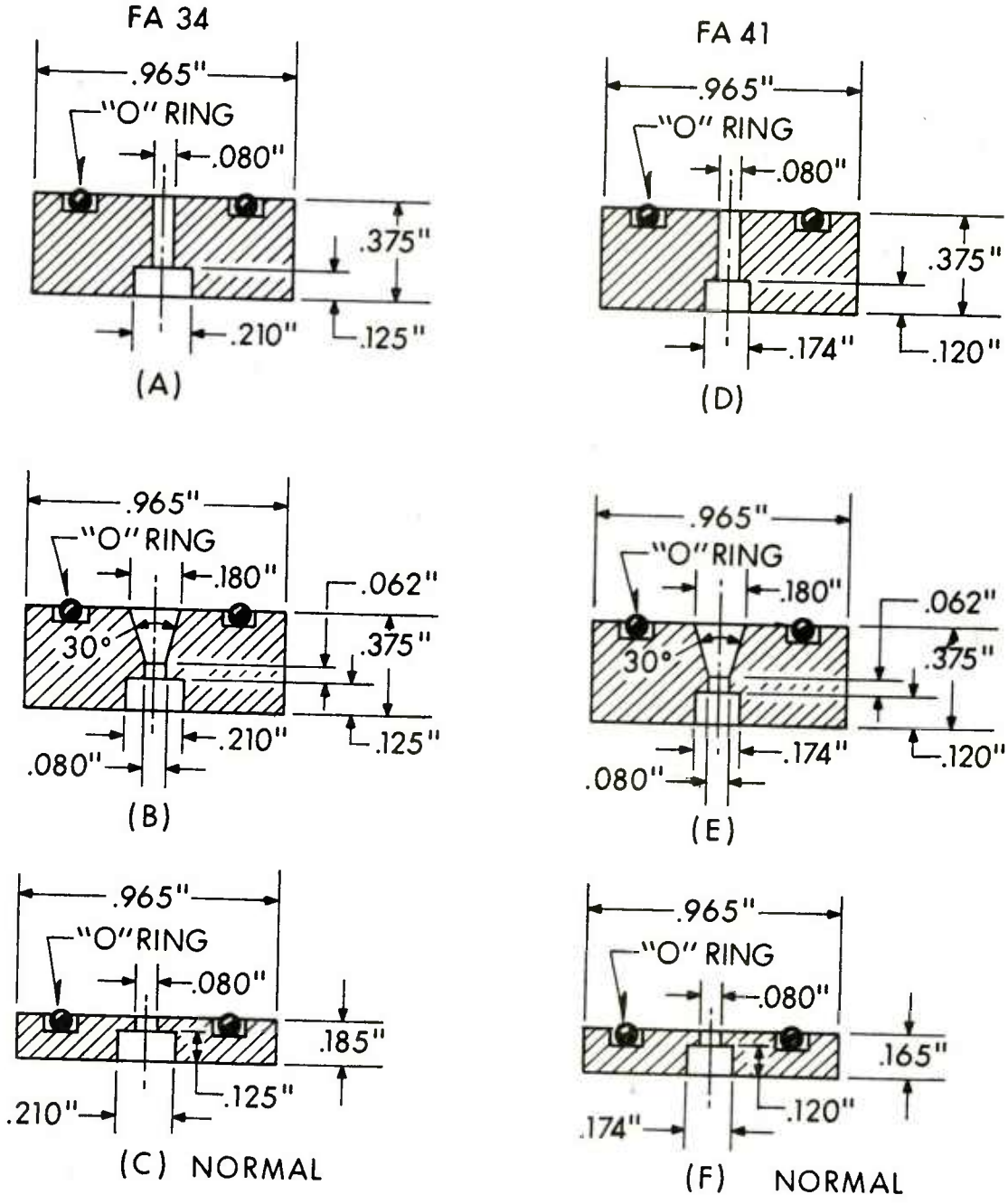

Figure 3. Primer Vent Configurations.

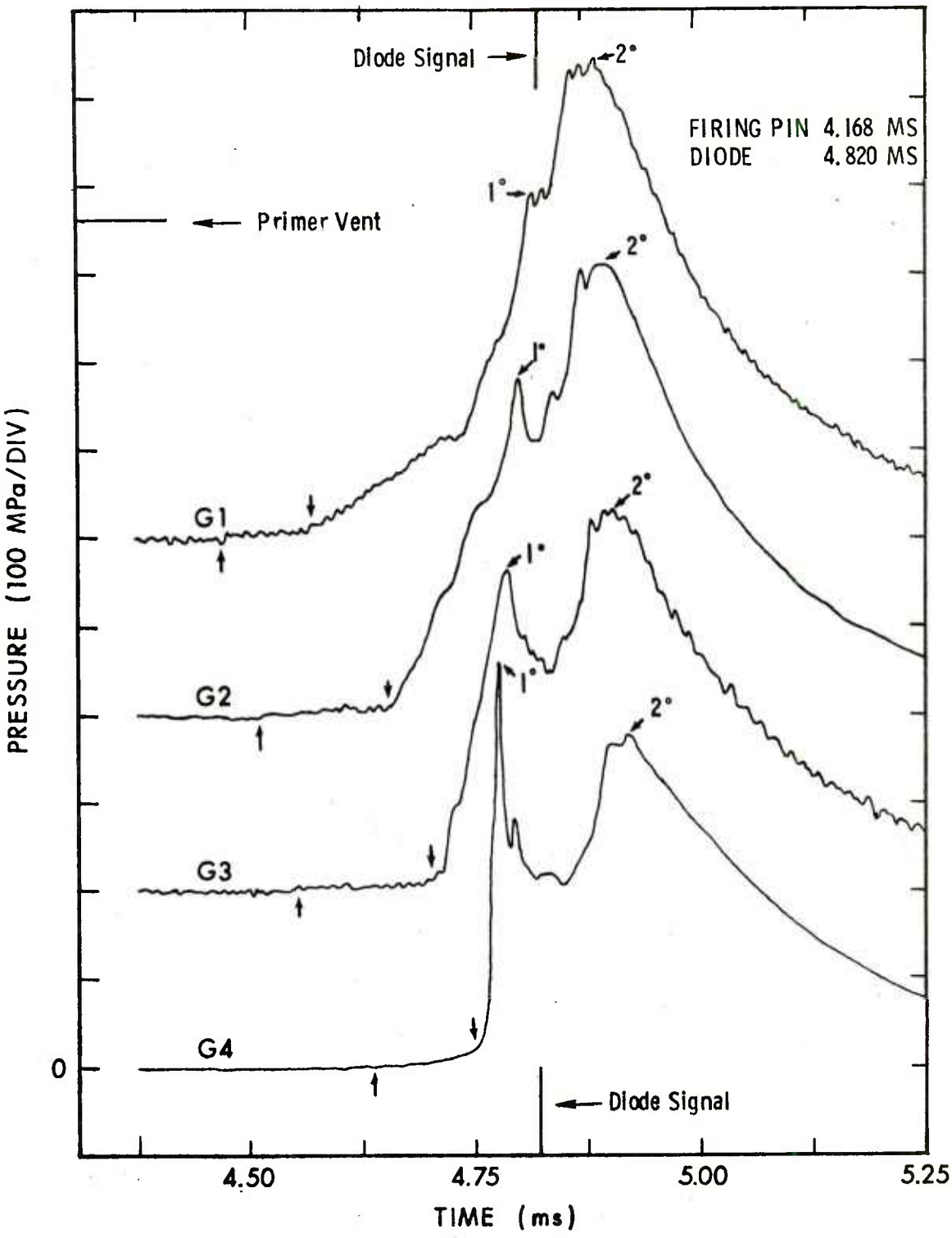

Figure 4. P-t Records Obtained Under Standard Conditions in the 108.4 mm Chamber. Standard Run 127-48.

(2°) peak. This nomenclature will be used whenever the peaks are well defined and unambiguous.

Occasionally (2 of 7 runs), a run performed under standard conditions yielded pressure-time curves at variance with the data shown in Figure 4. The results of such a run are shown in Figure 5.

Experimental studies of the propellant primer-interface were carried out by substituting a conical primer vent, Figure 6, lengthening the primer vent, Figure 7, and increasing the primer charge, Figure 8.

The effects of varying the shot start pressure were studied by halving the thickness of a standard shear disc, Figure 9, while the records shown in Figure 10 were obtained with a plate glass shear disc.

To complete the study, a different propellant, WC-844, was substituted for the WC-846, Figure 11.

All the firings listed above were carried out under standard conditions except for the specific changes noted.

V. DISCUSSION

As the P-t records shown in Figure 4 will be used as a standard of comparison for the experimental parametric study, the degree of reproducibility is of some importance. Figures 12 and 13 are composites of seven standard runs carried out over a one year time span with two lots of WC-846. In order to present this data on a common time scale the firing pin time is set at t_o. This choice of a reference point automatically includes all fluctuations in primer performance and propellant ignition. The reproducibility of the significant features could be improved by choosing a well defined reference point directly on the P-t records, i.e., the primary peak at gage 4. This procedure would place the major variations in the pressure records where they obviously belong, in the initiation sequence.

A. The Standard Configuration

The experimental results, Figure 4, suggest that the initial primer blast creates a void space at the primer end of the chamber and axially varying compaction of the bed. This void space combined with the low initial pressure provided by the primer and the reduced burning rate due to the deterrent coating results in the slow initial pressure rise at gage 1, Figure 4. As the flame front advances into the bed the pressure generated by the burning propellant drives gas into the bed ahead of the front as well as toward the low pressure reservoir created by the primer blast at the rear of the chamber.

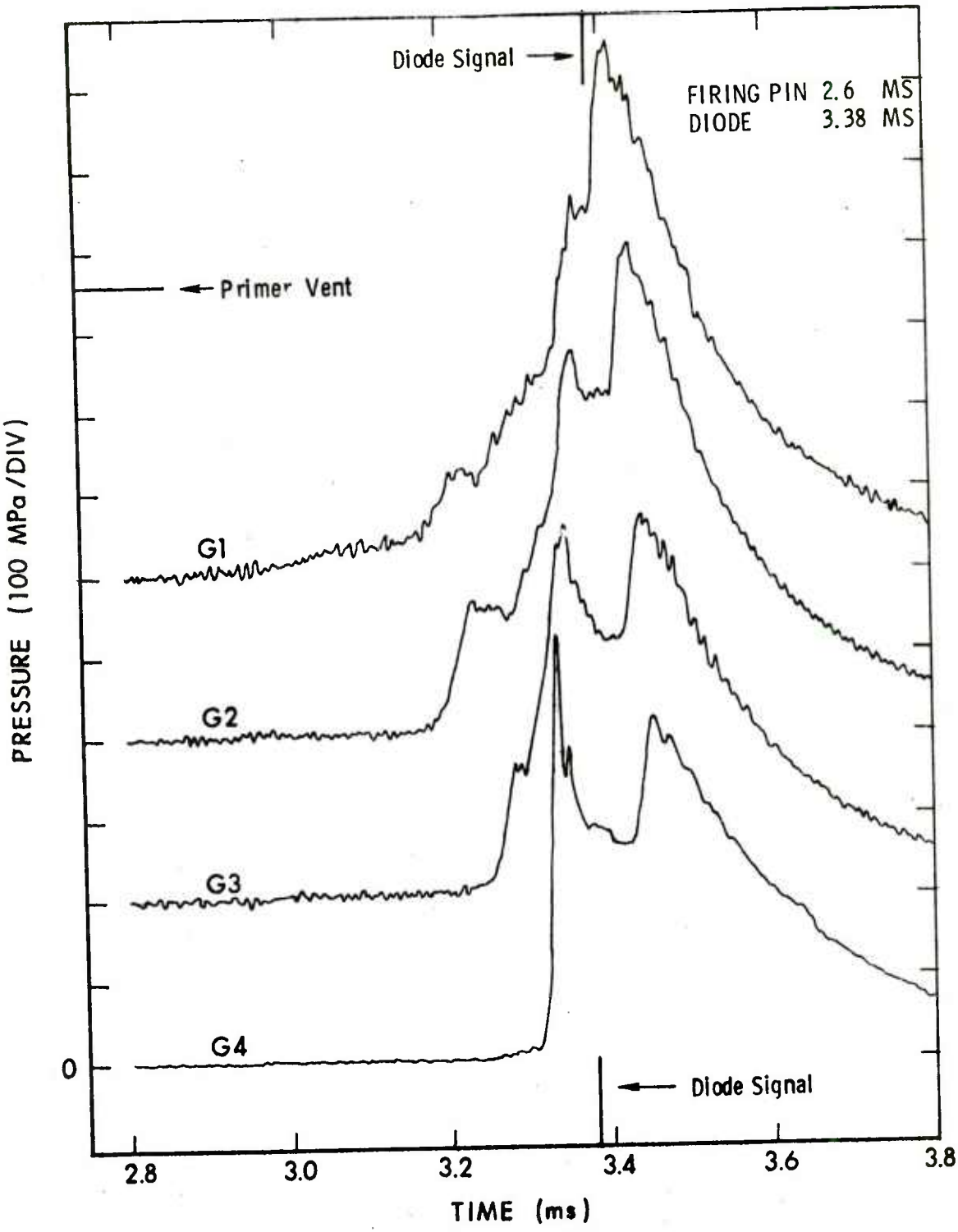

Figure 5. "Abnormal" P-t Records Obtained Under Standard Conditions. Standard Run 127-44.

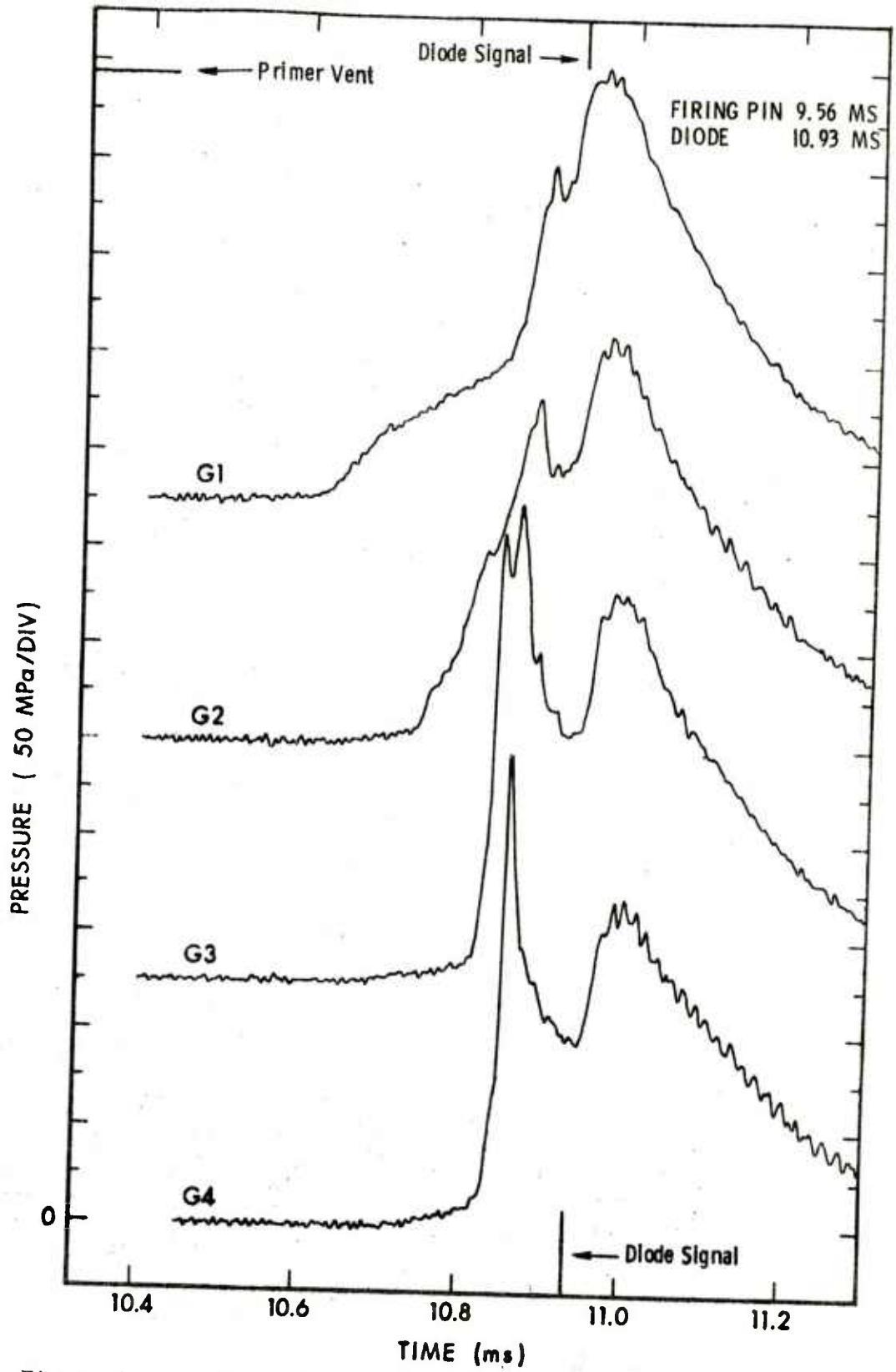

Figure 6. P-t Records Obtained With Conical Primer Vent, Configuration E, Figure 3. Run 138-43.

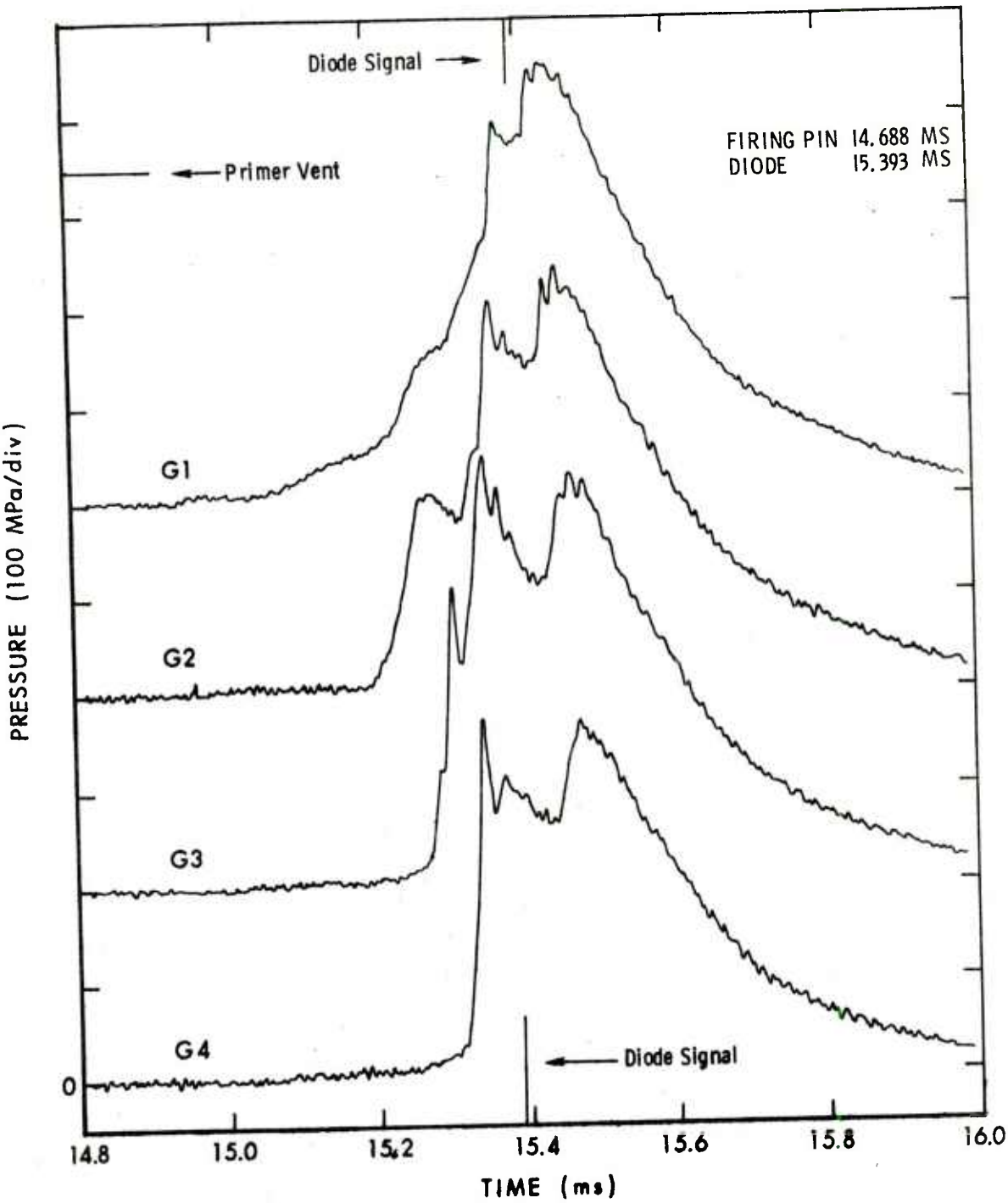

Figure 7. P-t Record Obtained by Lengthening the Primer Vent, Configuration D, Figure 3. Run 138-39.

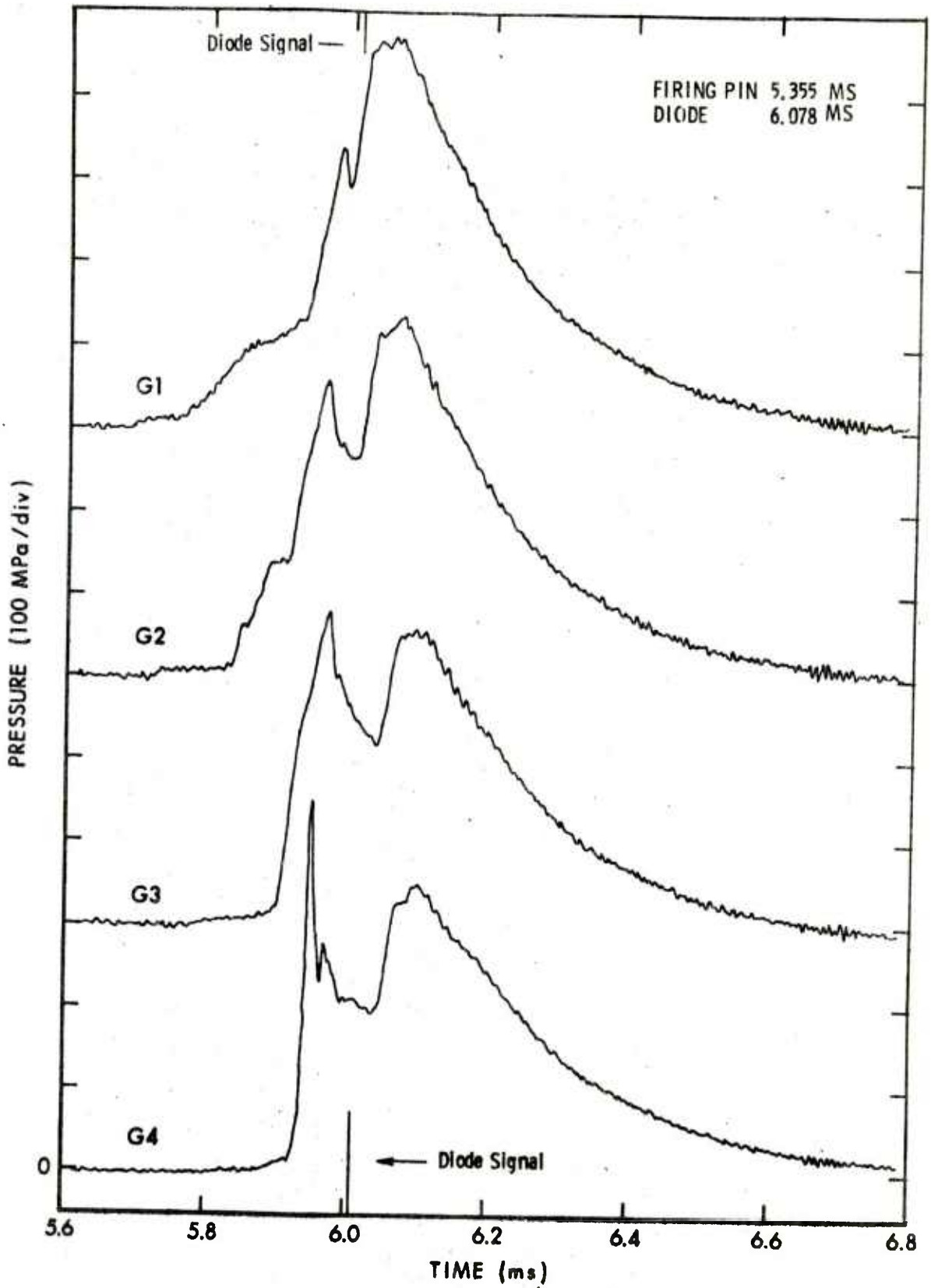

Figure 8. P-t Records Obtained With FA-34 Primer. Run 127-36.

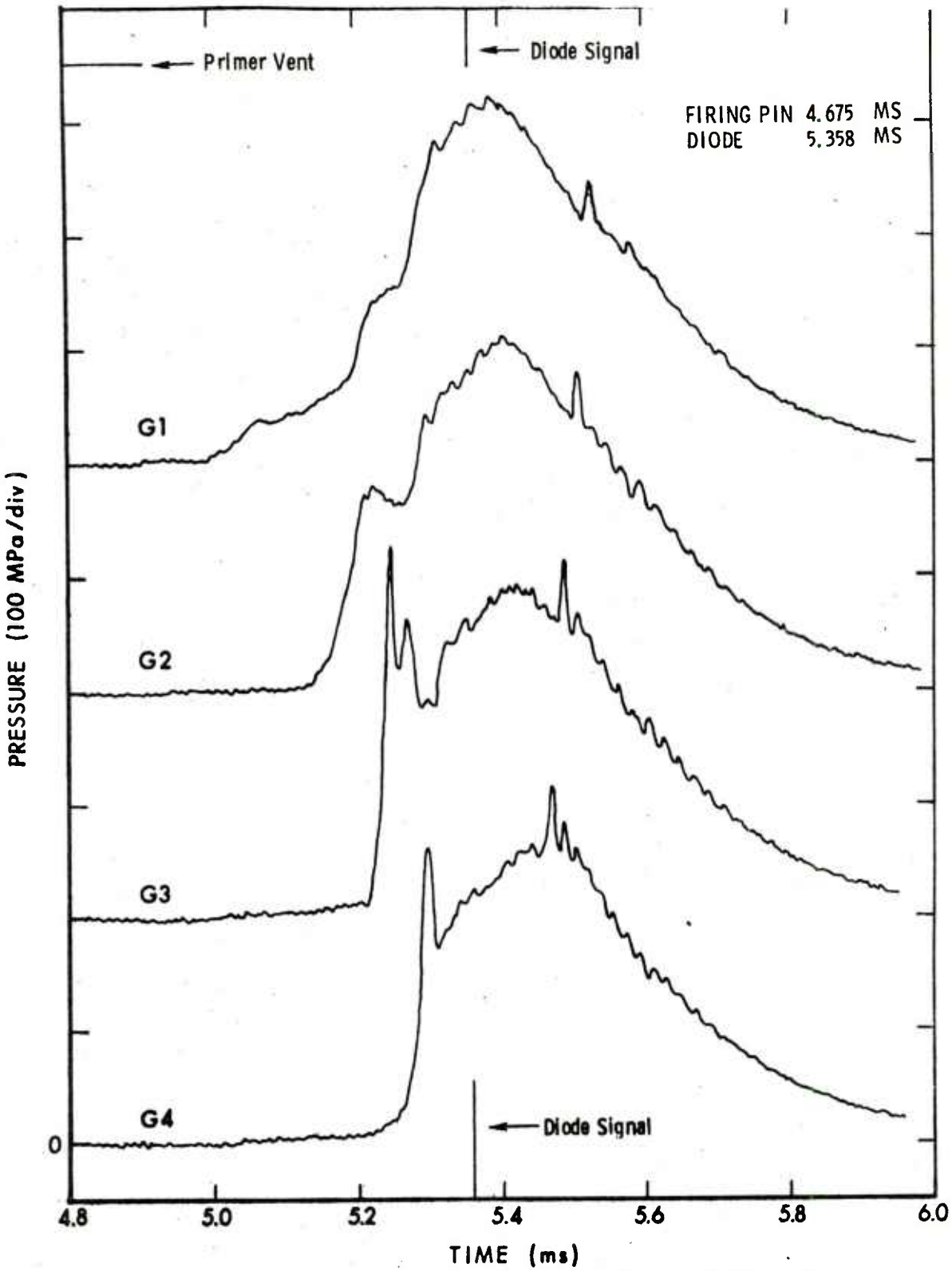

Figure 9. P-t Records Obtained With a Thin (.38 mm) Shear Disc. Run 139-17.

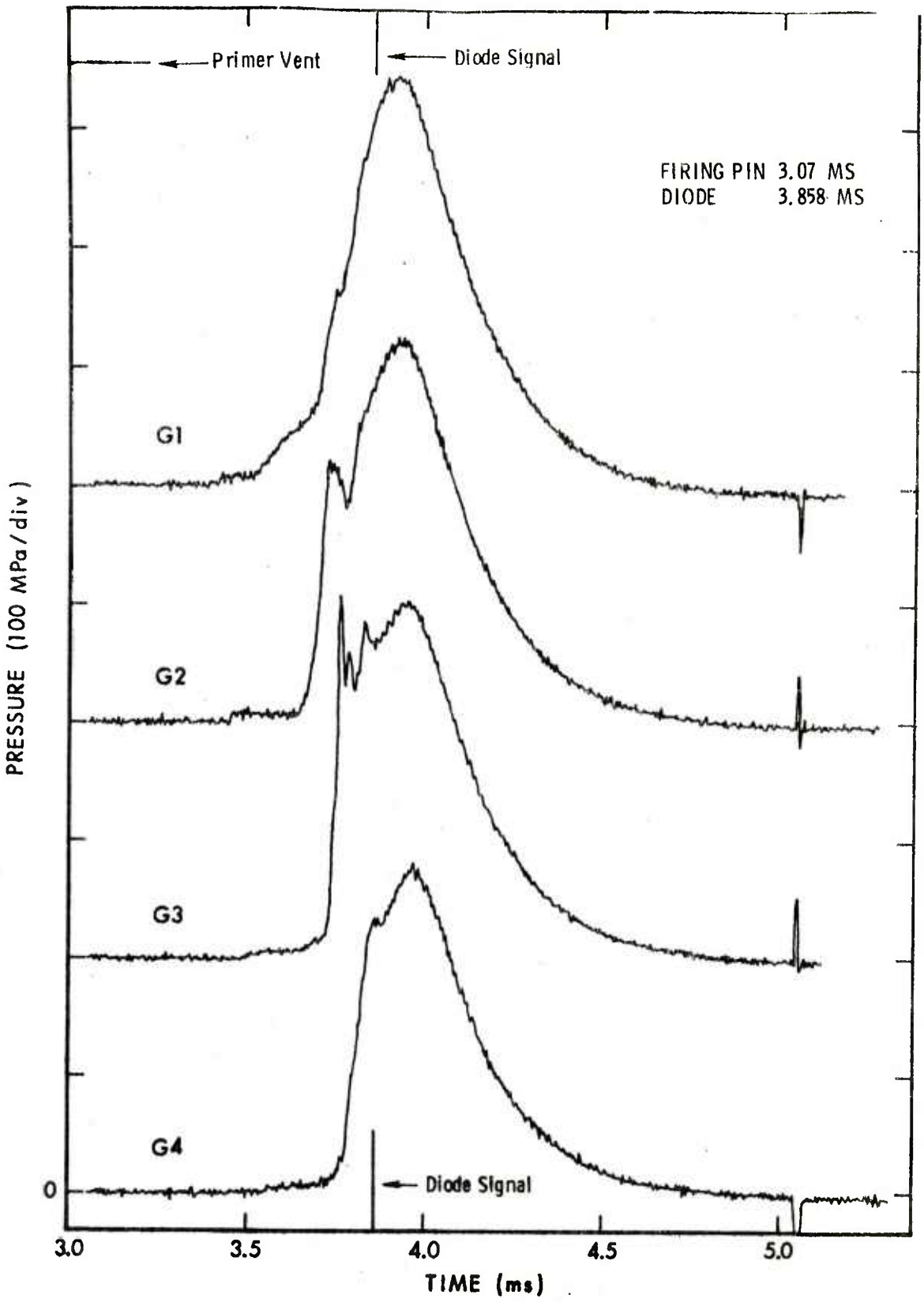

Figure 10. P-t Records Obtained With Glass Shear Disc (1.5 mm). Run 138-60.

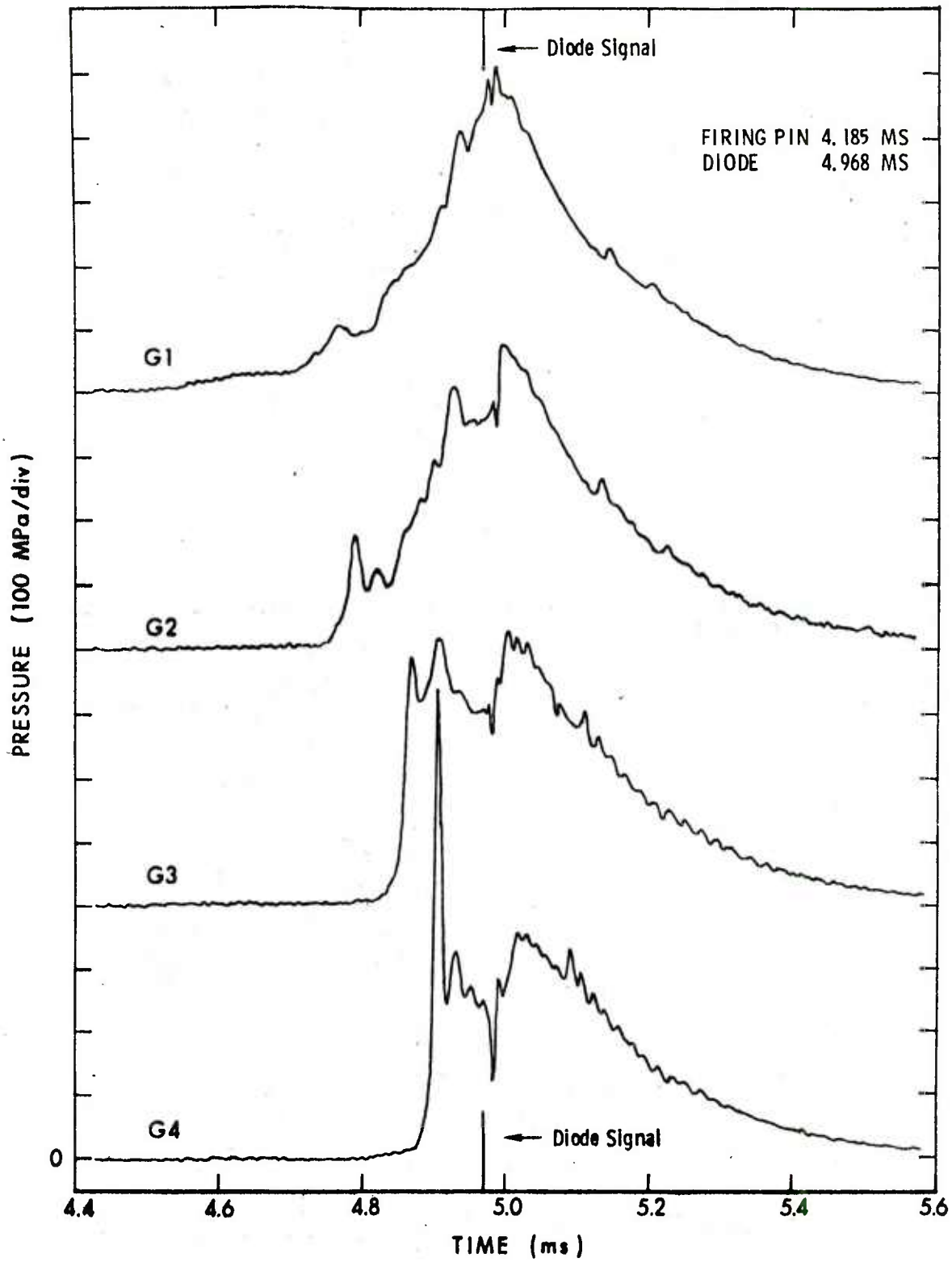

Figure 11. P-t Records Obtained With WC-844 Propellant. Run 139-19.

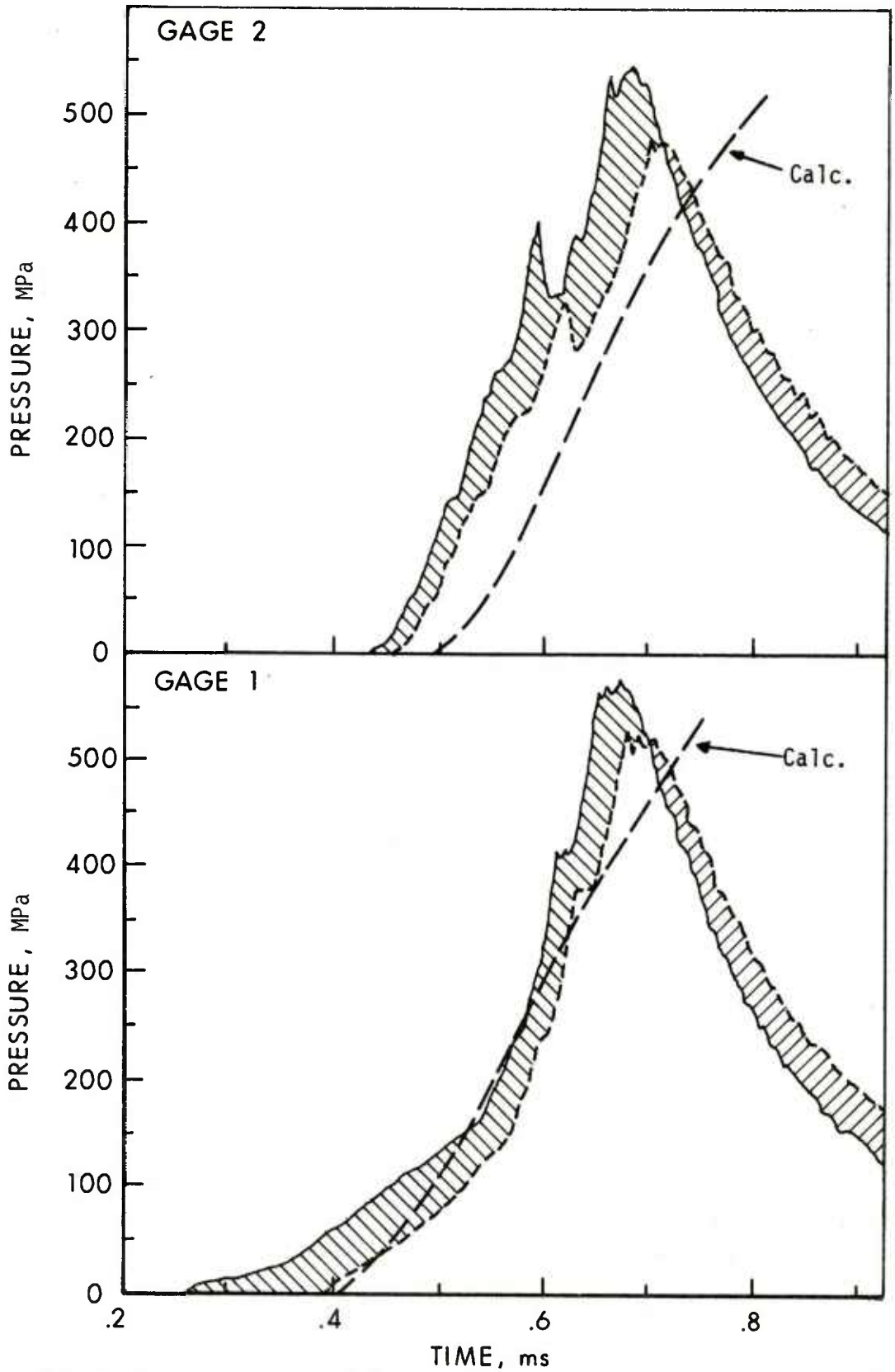

Figure 12. Composite of 7 Standard Runs Compared to Theoretical Calculations (Kitchens, BRL) (Gage Positions 1 and 2).

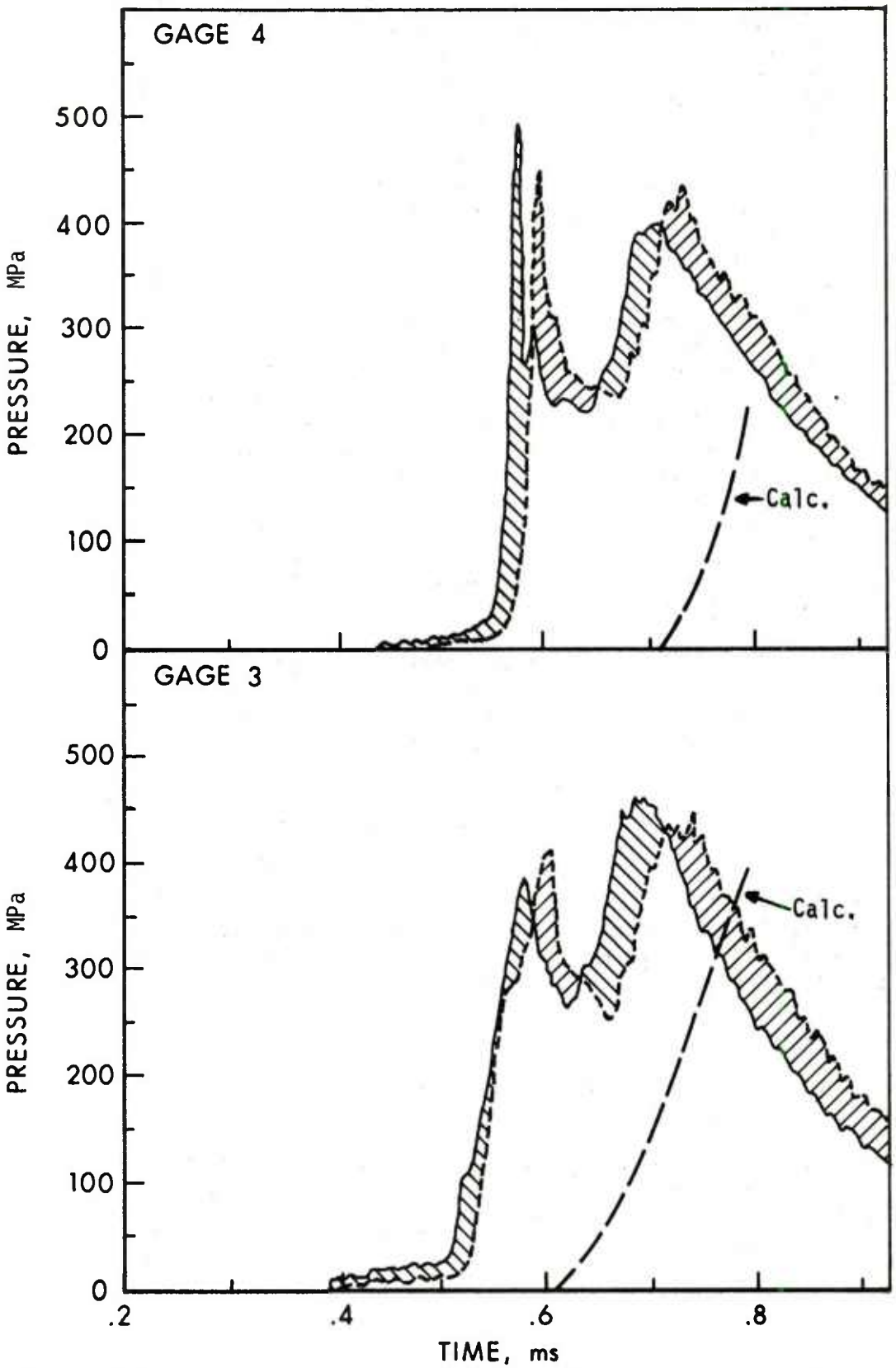

Figure 13. Composite of 7 Standard Runs Compared to Theoretical Calculations (Kitchens, BRL) (Gage Positions 3 and 4).

As the pressure increases, the bed is further compacted, reducing the degree of penetration of the bed by hot gases ahead of the front. At the rear of the chamber the pressure has risen to a point where there is but a small differential. Under these conditions, the forward edge of the combustion (compression) wave develops the increasingly sharp gradient shown at the successive gage positions. When the pressure is sufficient to rupture the shear disc the resulting expansion (rarefraction) wave propagates back through the chamber, relieving the pressure of the primary peaks. The naturally decreasing amplitude of the expansion wave, which is further attenuated by the burning propellant, causes the primary peaks to be successively less well defined as the wave approaches the rear of the chamber. By the time the expansion wave reaches the primer end of the chamber, the two phase choked flow condition established at the shear disc vent allows the pressure in the chamber to build up again, particularly at the base. As the choked condition relieves itself, the secondary (2°) compression wave propagates through the bed and completes the venting of the chamber. Since the expansion wave has had little effect in relieving the pressure at the primer end of the chamber, the propellant has continued to burn during the entire sequence of events, accounting for the high chamber pressure at gage 1 and the origin of the secondary compression wave. It should be noted that at the time of rupture of the shear disc, the highest pressure is at, or in the vicinity of, the shear disc and would tend to hold the bed in place until the pressure is relieved by the expansion wave, allowing the pressure at the breech to become dominant.

The chronological order of appearance of specific events and relevant pressures have been summarized for run no. 127-48, Figure 4 in Table I and plotted in Figure 14. The even spaced dashed lines are smooth extensions of the data points to the extremities of the chamber.

To gain a clearer picture of the pressure regimes over the length of the 108.4 mm chamber, the data shown in Figure 4 have been replotted in a P-x format. The time span in Figure 15a covers the passage of the primary combination wave, Figure 15b, the returning expansion wave, and Figure 16a, the secondary compression wave. The ΔP-t plot shown in Figure 16b again employs the same data to show wave propagation in the chamber over the entire combustion process.

B. Venting

The sequence of events immediately prior and subsequent to the rupture of the shear disc is not well defined.

The 25 μs interval from initial pressure rise to peak pressure at gage 4 practically prohibits passage of the combustion wave to the shear disc and the return of the expansion wave. Apparently, rupture occurs before the pressure wave reaches the shear disc, probably while in the vicinity of gage 4. Should this be the case, pressure relief

Table I. Summary of Characteristic Times for Run No. 127-48

t(ms)/P(MPa)	G-1	G-2	G-3	G-4
Primer Pulse	4.48/	4.52/	4.558/	4.635/
Initial Pressure Rise	4.565/	4.653/	4.708/	4.755/
1° P_{max}	4.815/390	4.803/377	4.790/367	4.783/452
Expansion Wave (P_{min})	4.823/385	4.82/310	4.835/248	4.853/208
2° P_{max}	4.885/548	4.888/509	4.903/432	4.923/378

Firing Pin - 4.168 ms

Diode - 4.820 ms

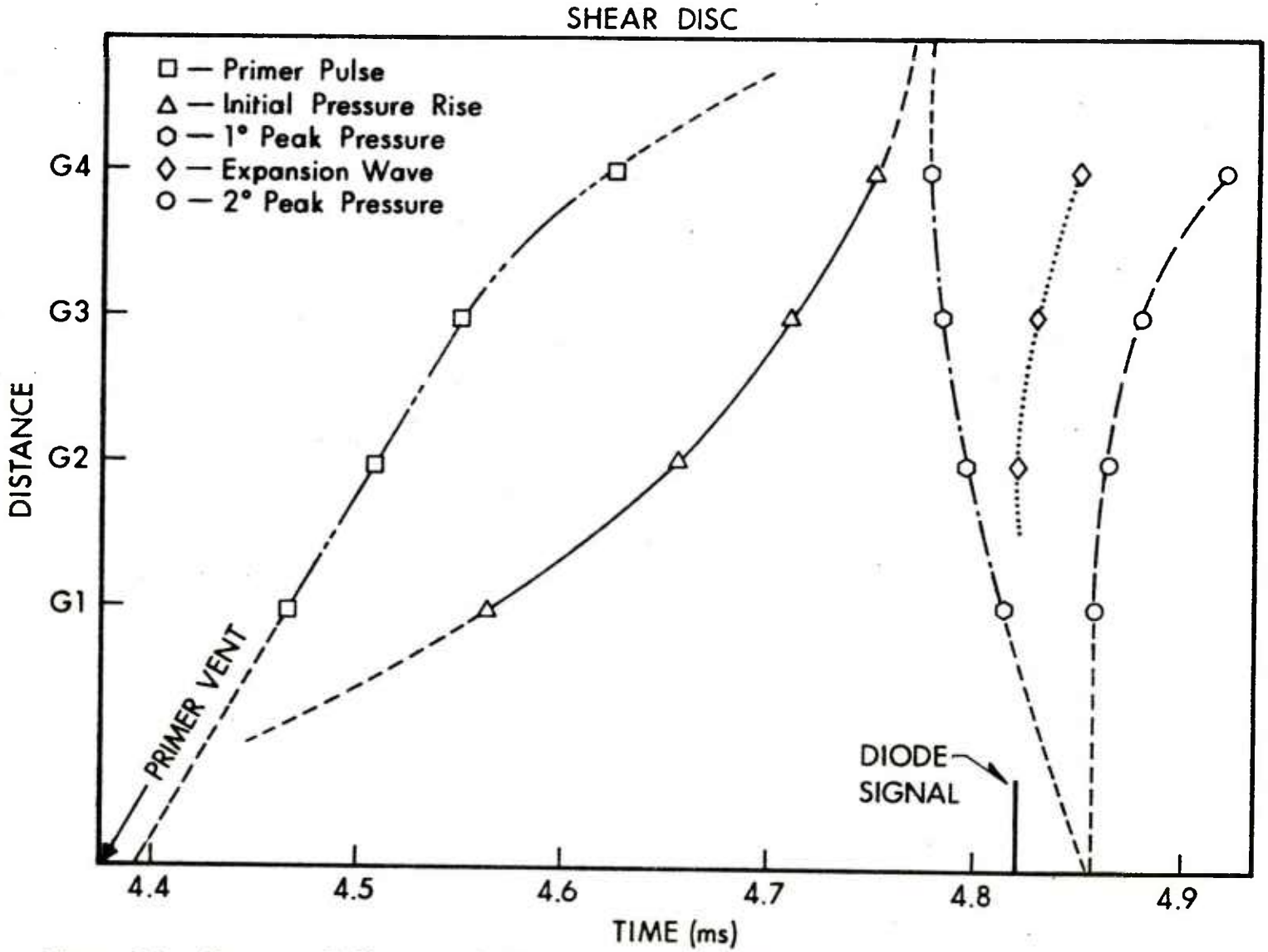

Figure 14. Summary of Characteristic Times for Standard Run 127-48. (See Figure 4).

would be almost immediate due to movement of the bed, whereas the rest of the unburnt propellant would have to clear the chamber before the diode could be triggered. This interpretation is at least partially reinforced by the long time delay from initial pressure rise at gage 4 to the diode signal.

If, as suggested by Figure 14, the compression wave accelerates rapidly between gage 4 and the shear disc, and does in fact directly load and rupture the disc, the diode signal would appear prior to the peak pressure at gage 4 created by the returning expansion wave. It has been estimated that under the loading conditions which exist at gage 4, the fracture time of the shear disc is 10 to 20 μsec.

C. Velocity of the Combustion Wave

There are at least three criteria to consider when estimating the velocity of the combustion wave: the initial pressure rise, the rate of pressure rise, and the flame front. Of these, the initial pressure rise is a poor choice as it is a function of the sensitivity of the measuring device and is often complicated by the primer pulse and low pressure transients. The KVS model locates the flame front at the point of inflection on the axial pressure gradient and uses this criteria to predict a rapidly accelerating flame front as the wave propagates through the bed. It is clear from Figure 15 that there are insufficient data points to use the KVS criteria. Implied, however, in the KVS model, is a close association between the maximum rate of pressure rise, and the inflection point on the computed gradient curves. Accepting the maximum rate of pressure rise as a criteria and referring to the ΔP-t plot, Figure 16b, it is evident that by either criteria, significant initial pressure rise, or maximum rate of pressure rise, there is little evidence of more than a nominal acceleration of the combustion wave through the bed. The average velocity between gage 2 and gage 4 is $\sim$ 0.46 mm/μsec. The lack of an appreciable acceleration is attributed to the continuous bed compaction ahead of the flame front.

D. 30° Conical Primer Vent

The use of a 30° conical primer vent was a rough attempt to distribute the primer output evenly over the face of the propellant bed. The results, Figure 6, were among the most interesting and informative of the entire study.

The time interval from the firing pin to the initial pressure rise at gage 1 was more than twice that of a standard run, Table A-1. A distinct primer pulse proceeding the initial pressure rise is not distinguishable and a long, slow, initial pressure rise is observed at each gage position. The rate of pressure rise, the magnitude of the pressure rise and the double peak at gage 3 also differ from a standard run.

The experimental results suggest that the initial primer blast is almost completely absorbed in the uniform axial compaction of the bed for a few chamber diameters and that ignition occurs only at the face of the bed. The flame front must now burn its way through the compacted region, at best a slow process due to the reduced surface area, the deterrent coating, and the adjacent void space. Once through the compacted zone, the combustion wave is confronted by a bed whose porosity is little changed from the initial loading density. The combination of a relatively high pressure behind the flame front, and the uncompacted bed allows rapid gas penetration of the bed. The pressure relief afforded is reflected in the decreased rate of pressure rise at gage 1.

The first peak of the doublet at gage 3 is attributed to a sudden movement of the bed in the vicinity of the flame front; probably due to bed compaction by the rapidly advancing pressure wave. The low peak pressure at gage 4 and the slower pressure rise than that encountered in the standard run are consistent with the creation of a void space in the vicinity of gage 3. This temporary pause in the development of the combustion wave results in the long time from the initial pressure rise at gage 4 to the diode signal.

The acceleration of the combustion wave obtained with the conical primer vent, shown in Run Nos. 138-41 and 138-43, Appendix A, is the closest approach to the theoretical considerations obtained in this study.

E. The Elongated Primer Vent

In contrast to the 30° conical primer vent the elongated vent provides a more coherent, but reduced primer output, resulting in deeper penetration of bed, compaction within the bed, and localized ignition, also within the bed.

The results, Figure 7, are in many respects similar to the "abnormal" standard run, Figure 5, particularly with respect to the low initial pressure rise at gage 1 followed by the plateau or weak peak propagation through the chamber. The origin of the plateau can be accounted for if the assumptions are made that: (1) the initial primer blast forms a compact "plug" of propellant fixed in place by frictional forces at the wall, and (2) ignition occurs within, or downstream of the plug. Now the flame front must propagate toward the primer end of the chamber as well as downstream. If the pressure in the chamber overcomes the forces holding the plug before the burn through occurs, the plug and part of the burning bed will be thrown to the rear of the chamber creating the almost simultaneous plateaus at gages 1 and 2. If on the other hand burn-through occurs first, the gases will flow toward the rear of the chamber causing the more orderly propagation of the resulting expansion wave as observed in the "abnormal" standard run, Figure 5.

F. The 0.38 mm Stainless Steel (SS) Shear Disc

To estimate the degree of pressure transmission through the propellant bed, the shot start pressure was lowered by reducing the thickness of the shear disc. Substituting a 0.38 mm disc for the standard 0.79 mm disc yielded the complex results reproduced in Figure 9.

Note in particular (1) the reversed order of appearance of the primary peaks as compared to the standard run, (2) the rapid fall in the rate of pressure rise after the initial surge, (3) the weak expansion wave, (4) the lower maximum pressure in the chamber, and (5) the long delay from the initial pressure rise at gage 4 to the diode signal. Another factor is that the recovered shear disc had an uneven appearance around the perimeter of the vent hole, in marked contrast to the smooth, cleanly punched out hole found in the standard run.

These observations suggest that rupture occurs early in the run as a direct result of the primer blast. Should this occur, it is likely that the major portion of the bed, burning at the primer end, will move out of the chamber much in the manner of a traveling charge. The small, sharp primary spikes which indicate the passage of the flame front at the rear of the moving bed, are consistent with the hypotheses of early shear disc rupture. The secondary compression wave is due to the venting of the remainder of the bed as the dominant pressure shifts to the primer end of the chamber. The uneven edges of the shear disc may be caused by distortion of the disc prior to rupture, indicative of some resistance to the primer blast.

Apparently, there is an interaction between the primer output and the shear disc coupled by the porous bed which is rapidly attenuated, provided the disc can withstand the initial stress. If the force of the primer and subsequent pressure wave were transmitted continuously, the pressure in the standard run could not reach the 500 MPa level, shown in Figure 4.

The relatively noisy gage outputs and multiple pressure spikes in these runs have been attributed to (1) pressure wave reflection from the ragged edges of the shear disc, (2) uneven resistance to movement of the bed by these edges, and (3) vibration of the disc.

G. The Glass Shear Disc

The use of a plate glass shear disc, Figure 10, was intended to lower the shot start pressure without introducing complications due to distortion prior to rupture and to use the diode signal to estimate the proximity of the flame front to the shear disc at rupture.

As with the thin (0.38 mm) steel disc, the primary peaks are in reverse order, the expansion wave is weak, the pressure rise at gage 1 is slow, and maximum pressures developed in the chamber are low when

compared to a standard run. Exclusive to the glass disc is the relatively weak pressure rise at gage 4 and the very short delay from the primary peak at gage 4 to the diode signal. Another factor to consider is the short delay between the initial pressure rise at gages 3 and 4.

Although there is too little information available to evaluate the results, it is interesting to speculate that most of the events can be accounted for if the assumptions are made that (1) the primer blast breaks the shear disc but ejects only a small portion of the bed, creating a larger void space and accounting for the slow pressure rise at gage 1, (2) as the combustion wave propagates through the bed, the pressure buildup overcomes the weak frictional forces at the wall and causes the bed to move out of the chamber starting in the vicinity of gage 2, (3) as the bed moves, the combustion wave propagates rapidly through the bed, forming a thick burning zone, as suggested by Kuo, (4) by the time the moving, burning bed passes gage 4, affording a small pressure relief, the flame front downstream of gage 4 has triggered the diode, and (5) the pressure buildup at the primer end of the chamber forces the rest of the bed, originally left behind, out of the chamber causing the secondary peak. At the time of pressure relief at gage 4, the pressure at gage 4 is the lowest in the chamber, Table II.

Table II. Chamber Pressure at Venting

t = 3.2525	GL	G2	G3	G4
P(MPa)	316	289	267	233

Of interest are the "clean" gage outputs and uncomplicated structuring of the pressure records, offering some support to the idea that distortion, vibration, and uneven rupture contributed to the records obtained with the 0.38 mm shear disc.

H. The FA-34 Primer

The FA-34 primer contains about 50 percent more charge than the FA-41 primer; yet surprisingly, the results in Figure 8 were almost identical to those under standard conditions. At gage 1, the difference from a standard run are: (1) shorter times from primer delivery (firing pin plus action time) to the appearance of the primer pulse, (2) shorter time from primer pulse to initial pressure rise, (3) slightly steeper initial pressure rise, and (4) a broader plateau at the end of the initial pressure rise. At subsequent gage positions the records are almost identical to Figure 4.

The differences, apparently confined to the initial stages, are consistent with the expected creation of a larger void space and increased bed compaction.

A conclusion to be drawn from these results is that above a certain primer output, additional output becomes decreasingly effective beyond the first few diameters of bed length.

I. Abnormal Standard Run

The primer vent studies tend to support the obvious implication that the slow development of the combustion wave is caused by a poor ignition within the bed. The orderly sequential progression of the plateau, which appears before the 1° peak at gage positions 1, 2, and 3, indicates an event which occurs between the primer vent and gage 1, probably due to burn through of densely compacted region of the bed caused by the primer blast. It should be noted that despite the successful attempts to artificially reproduce the slow initial pressure rise, the long delay from the initial pressure rise, and the plateau prior to the primary peaks, the abnormally high peak pressure at gage 1 was not duplicated. This failure is attributed to the inability of the substituted primer vents to cause the same bed response as the standard primer.

J. The 58.8 mm and 201.6 mm Chambers

Figures 17 and 18 are typical results obtained under standard conditions in the 58.8 mm (Figure 19a) and 201.6 mm (Figure 19b) chambers, respectively.* The wave velocity in the 58.8 mm chamber between the last two gage positions is $\sim$ 0.26 mm/μsec, the decreasing peak pressure starting at gage 1 coupled with the weak expansion wave and the short delay between the peak pressure at gage 3 and the diode signal are all indications of shear disc rupture prior to the arrival of the combustion wave at the shear disc location.

On the other hand the data from the 201.6 mm chamber yields a wave velocity of 0.9 mm/μsec and extremely high pressure rise at gage 4, estimated at > than 900 MPa (130 kpsi). The implication is that excessive bed compaction occurs in the vicinity of the last gage position.

The results obtained under standard conditions for all three chambers is summarized in Figure 20. For this plot t_o is the firing pin time.

The most striking feature of the plot is the tendency of the combustion wave velocity, measured by the initial pressure rise, to approach a constant value in the neighborhood of 1.0 mm/μsec at long bed lengths, a situation not predicted by current models.

---

* *As each of these chambers will be the subject of separate reports currently in preparation, these results are presented for comparative purposes with only general comments.*

VI. EXPERIMENT DIFFICULTIES

A. Shear Disc as a Venting Device

There have been few attempts to compare absolute pressure magnitude from run to run due to the unknown fracture mechanics of the shear disc. At the loading rates encountered in these experiments, it is possible for the burst rating, measured under static conditions, to be exceeded by a factor of two or three under dynamic conditions. In any case, small variations in the rupture time of the shear disc of a few microseconds can easily lead to large pressure fluctuations.

There is the added problem that thin metallic shear discs are easily distorted and drum-like vibrations can cause an elastic compression-rarefraction wave in the chamber.

A rigid shear disc, or better yet, a heavy slug would have been a more suitable choice.

B. The Firing Mechanism

Early in the program it was found that the action time of the primer, defined as the delay between the time of impact by the firing pin to light emission at the vent hole, was dependent on the voltage supplied to the solenoid. The problem was overcome by increasing the voltage until the results were consistent. Still there is some doubt that the solenoid will always provide a consistent stroke. A spring loaded firing pin or ball drop technique would have been better.

C. Compaction Studies

Interpretation of the experimental results suffers from the lack of an inert material, not only of the same size and shape and density of the propellant, but also with similar mechanical, cohesive and adhesive properties. Such a material is not only crucial to the studies of bed compaction and ignition modes at the propellant primer interface, but also to pressure transmission, mobility, elastic, and inelastic deformation studies.

A few crude experiments with starchy substances (macaroni, tapioca) as a mechanical property analog, yielded, under standard conditions in a 58.8 mm chamber, approximately 12.0 mm of void space, adjacent to the primer, followed by 5 mm of loose material, 20.0 mm of a dense fixed plug, and 13.5 mm loose grain. The 20.0 mm plug was so firmly fixed in place it had to be drilled out.

In the 108.4 mm chamber, the void space and depth of loose material was $\sim$ 20.0 mm and 5.0 mm, respectively.

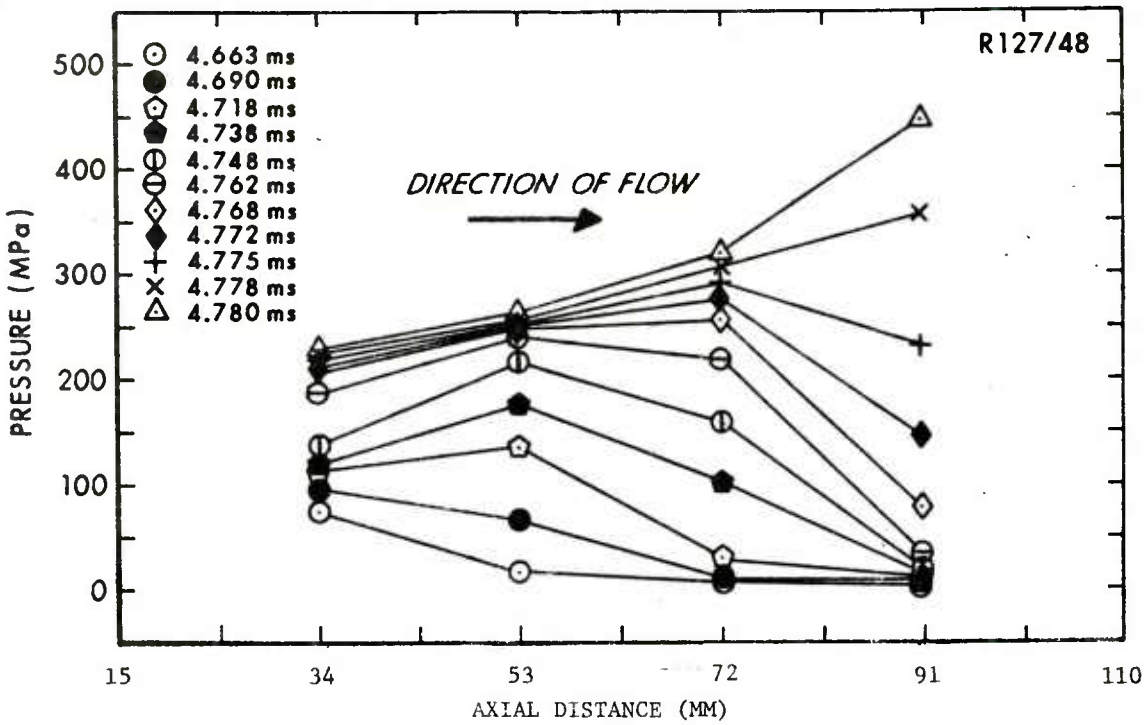

Figure 15a. Primary (1°) Compression Wave Pressure vs Axial Distance Curves at Selected Times for Run 127-48. (See Figure 4)

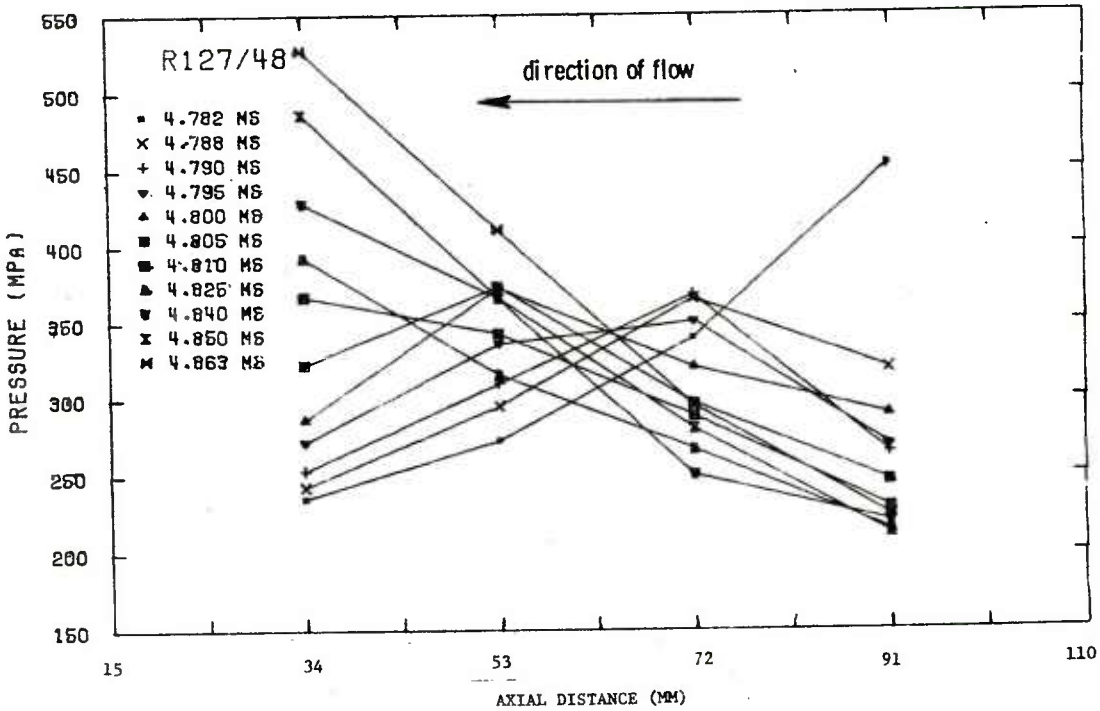

Figure 15b. Expansion Wave Pressure vs Axial Distance Curves at Selected Times for Run 127-48. (See Figure 4)

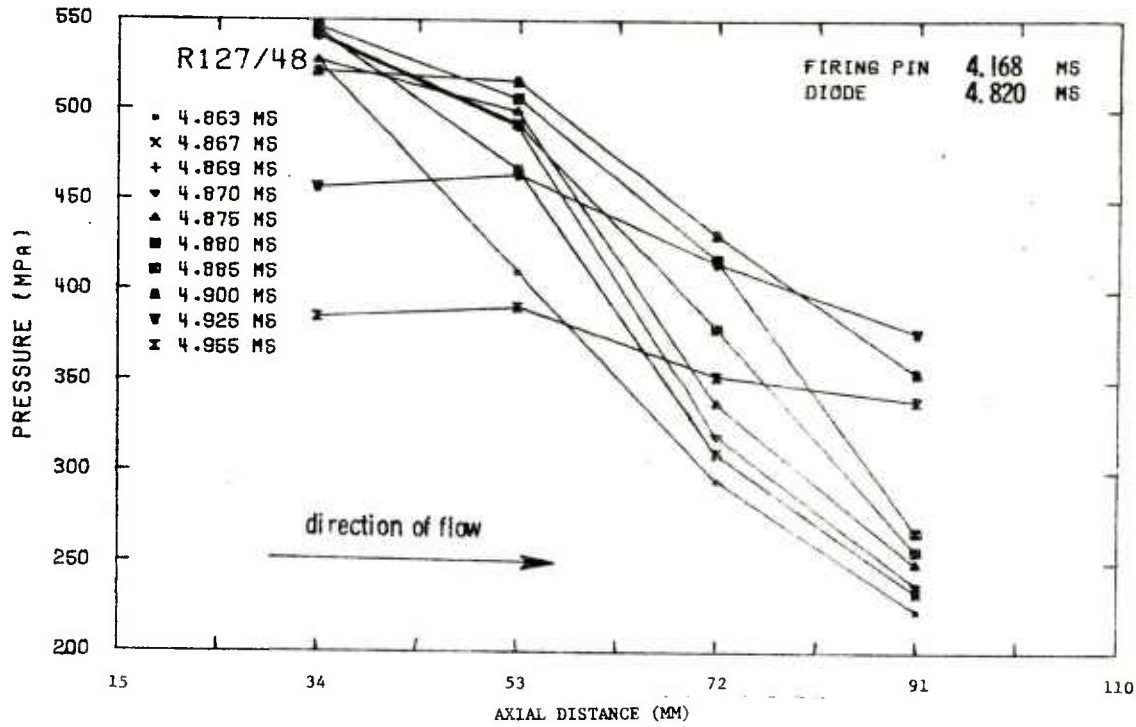

Figure 16a. Secondary (2°) Compression Wave Pressure vs Axial Distance Curves at Selected Times for Run 127-48. (See Figure 4)

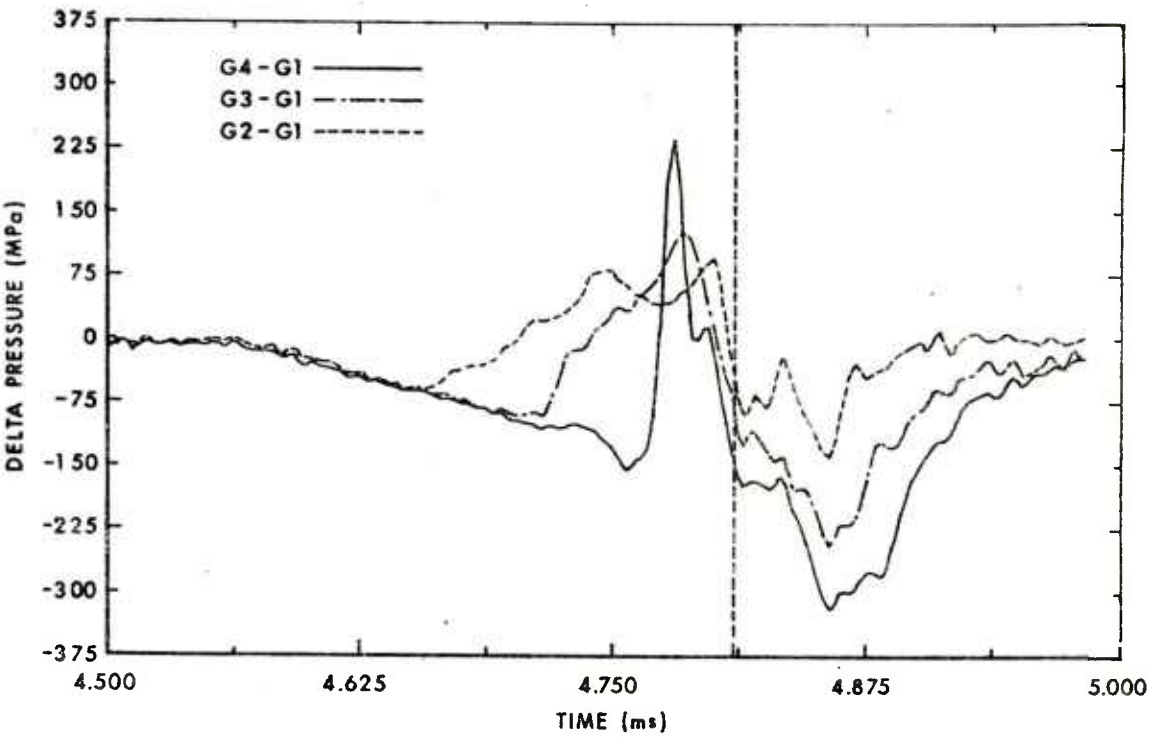

Figure 16b. Differential P-t Curves for Run 127-48. (See Figure 4)

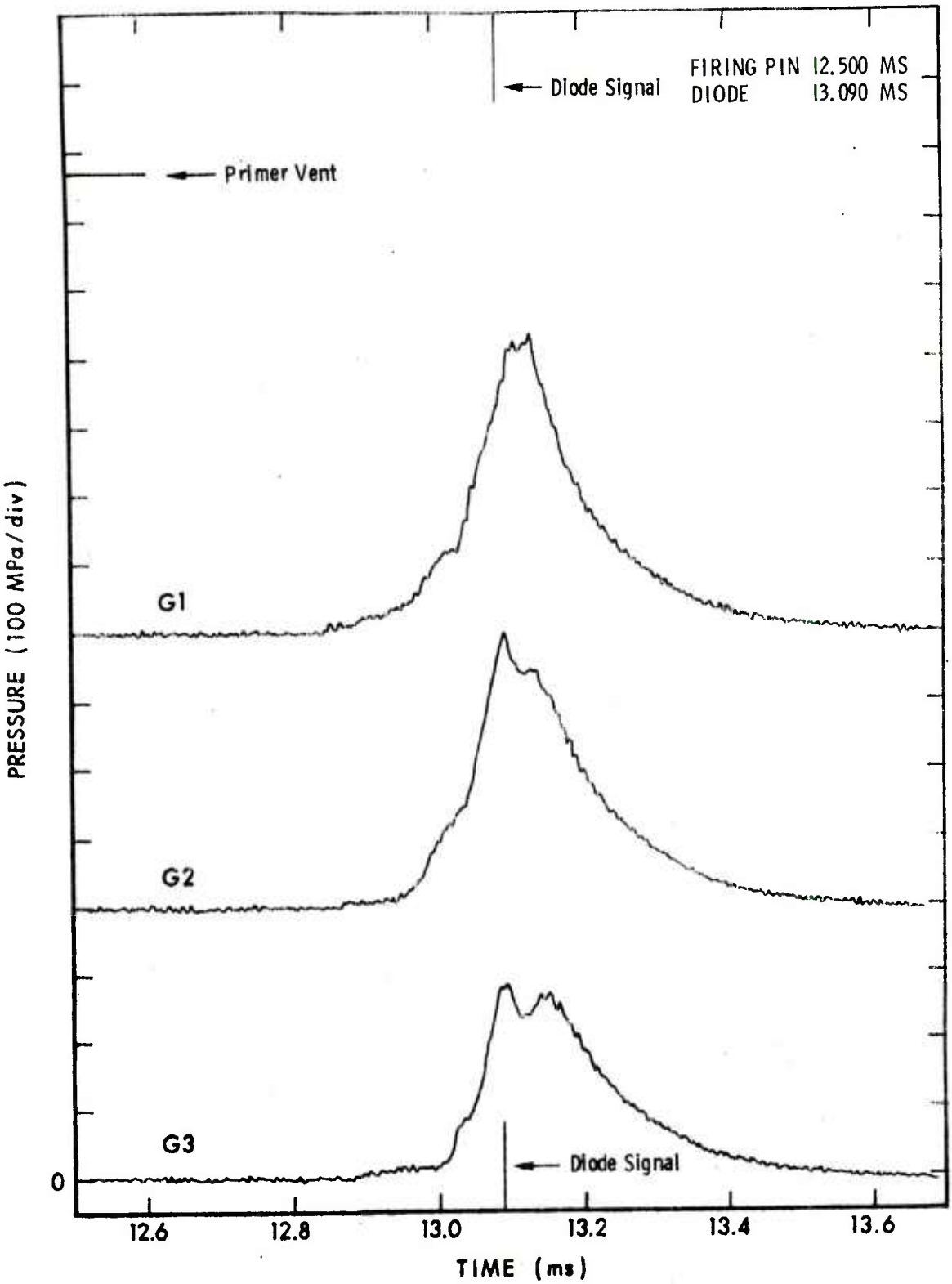

Figure 17. P-t Records Obtained Under Standard Conditions in the 58.5 mm Chamber.

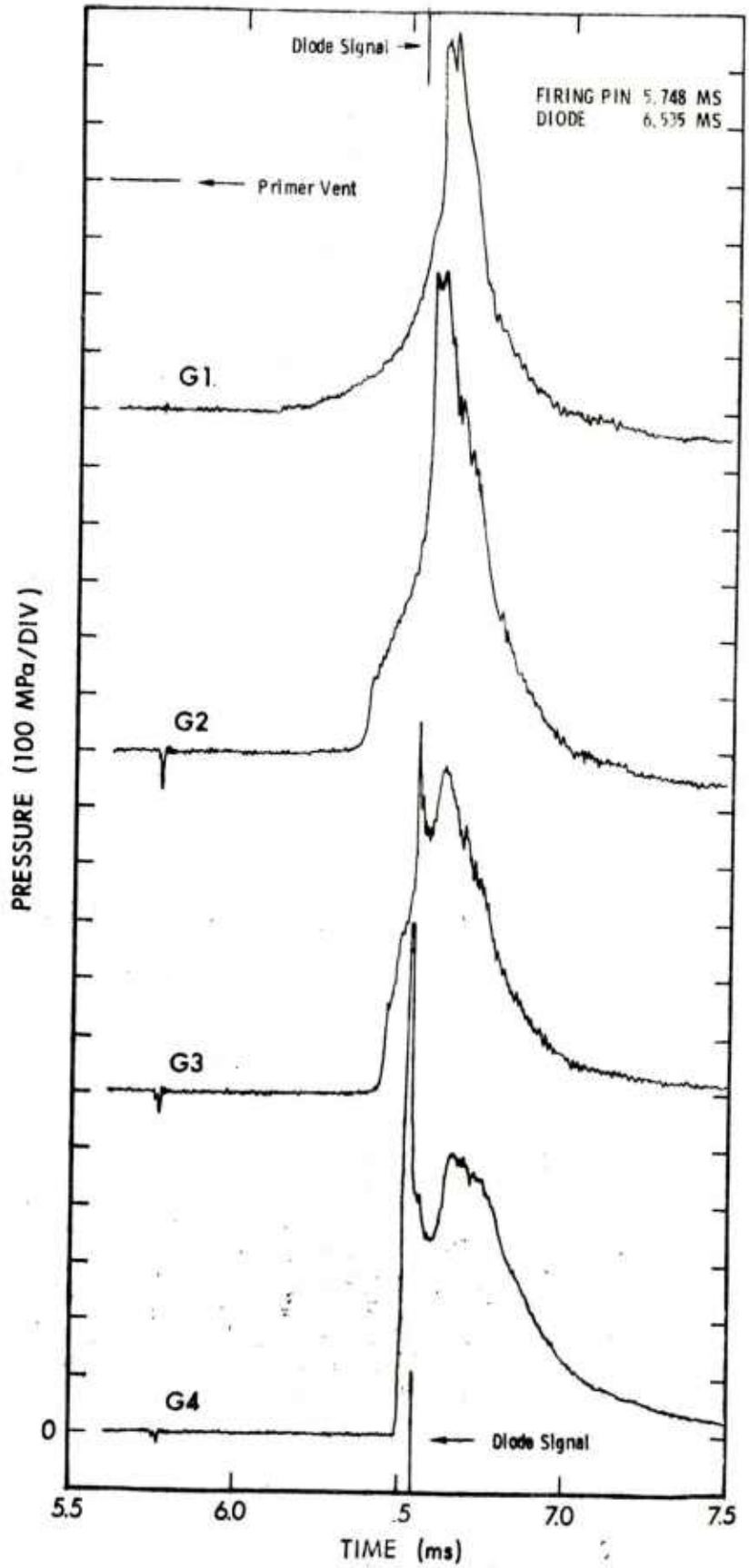

Figure 18. P-t Records Obtained Under Standard Conditions in the 201.6 mm Chamber.

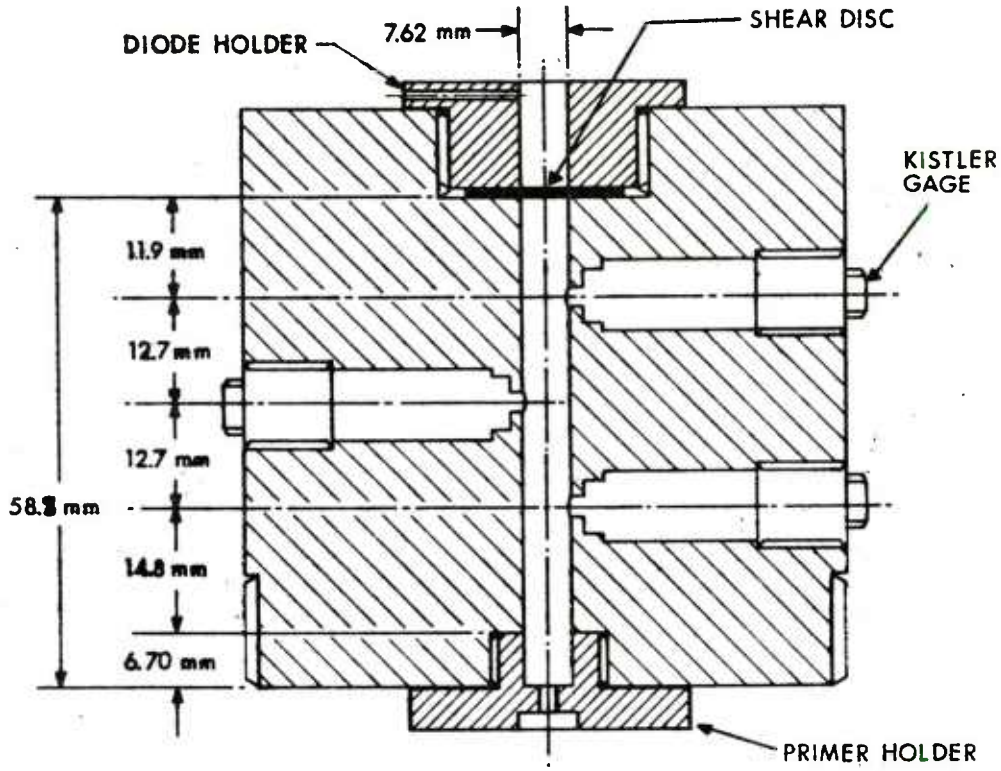

Figure 19a. 7.62 mm Vented Chamber (58.8 mm Bed Length).

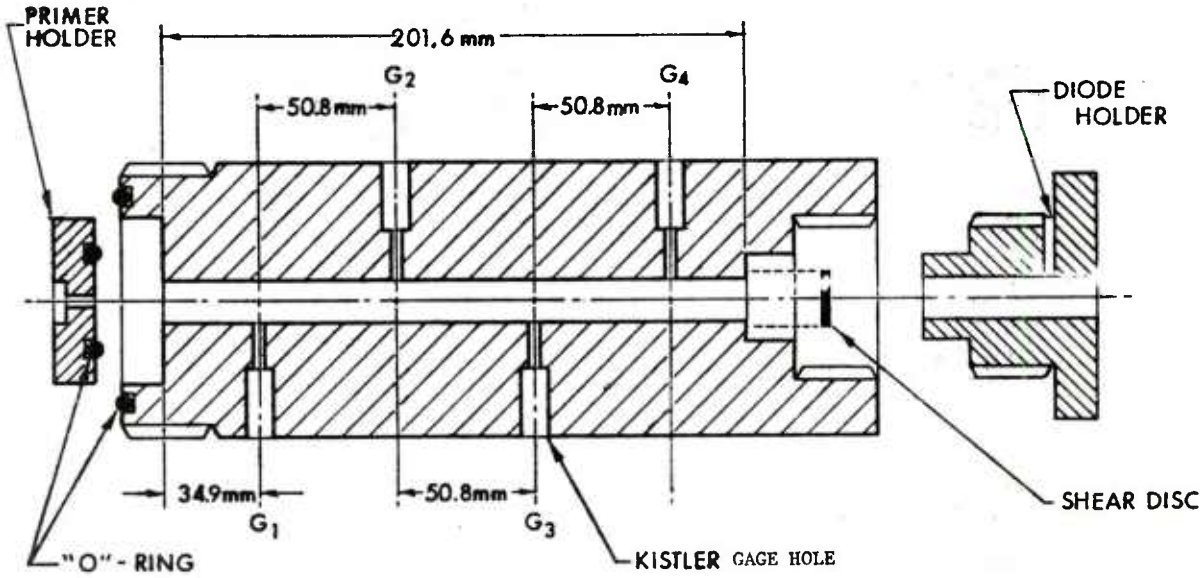

Figure 19b. 7.62 mm Vented Chamber (20.16 mm Bed Length).

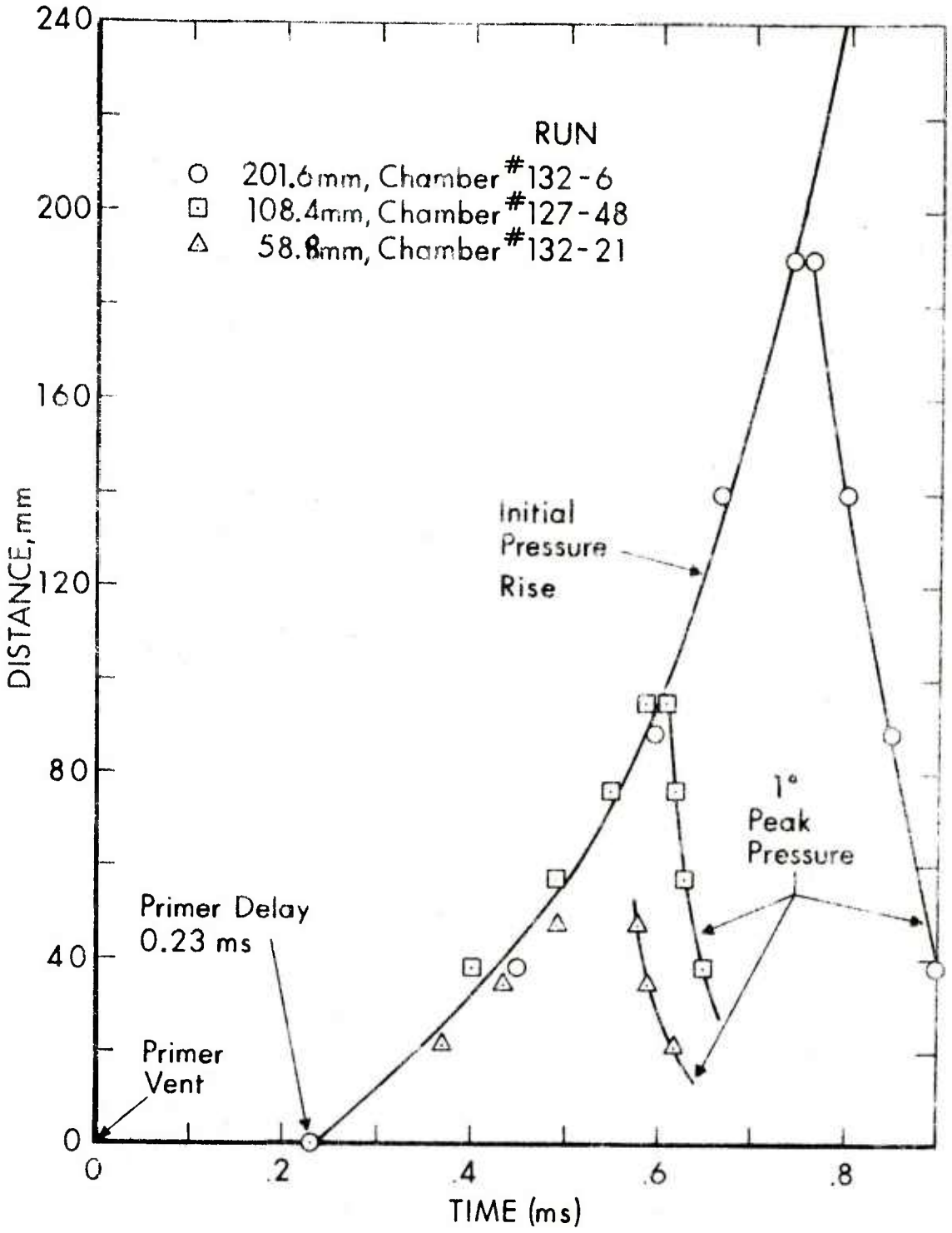

Figure 20. Summary of Initial Pressure Rise and Primary (1°) Peak Pressure Rise vs Time for Runs Carried Out Under Standard Conditions in the 58.8 mm, 108.4 mm, 201.6 mm Chambers.

VII. THEORETICAL CONSIDERATIONS

While an in-depth discussion of mathematical models used to predict the pressure regimes in porous beds is beyond the scope of this report, some brief observations on the KVS model are in order.

This model assumes a void space adjacent to the primer vent and a fixed bed ahead of the combustion wave (i.e., no compaction allowed by the primer or subsequent pressure buildup). These conditions permit the hot product gases ahead of the ignition front to penetrate the bed, thermally preconditioning the bed to a depth and magnitude depending on the pressure and the loading density. At the same time the product gases behind the flame front are permitted access to the void space giving rise to the "continental divide" and a continuously accelerated flame front with increasing pressure.

In the experiment, the initial primer blast causes about a 20 percent decrease in the average porosity followed by the continuous compaction by the advancing combustion wave. On the one hand, compaction tends to decrease penetration of the bed, reduce the available surface area, and encourage heat transfer by conduction - all factors which inhibit the progress of the wave. On the other hand, bed compaction provides steeper pressure gradients, increased pressure rise times, and higher pressures, factors which, through the dynamic burning rates, assist the propagation of the flame front. The comparison between experiment and model prediction implies that the second set of factors tend to become predominant in longer beds.

Although comprehensive definitive mathematical models must await the future, it is perhaps in this area parametric studies of the type carried out by Kitchens[6] can be of immediate use.

VIII. CONCLUSIONS

The complex interrelationship between the variables in this study, both induced and naturally occurring, render definitive interpretation, at best, a difficult task. However, some conclusions are readily drawn from the experimental results.

In dealing with either operational systems or mathematical models, two factors are of the utmost importance for base ignited charges with higher L/D ratios than normally considered: (1) the propellant-primer interface, a complex function of the primer charge, manner of delivery, and the primary ignition mode, has been shown to exert an immediate and fundamental influence over subsequent events; (2) the degree of bed

---

[6] C.W. Kitchens, Jr., "Parametric Sensitivity Study of a Numerical Model for Flame Spreading", BRL Memorandum Report No. 2546, October 1975. (AD #A018135)

compaction provided by the initial primer blast and subsequent progress of the combustion wave through the bed. Although compaction is a partial function of the primer action and chamber length, the bed itself influences the combustion mechanism through the size and shape of the particles, the degree of elastic and inelastic deformation and the magnitude of the friction forces with the walls of the chamber - important factors when estimating contribution to shot start pressure by intergranular forces.

With regard to the other objectives of this study there is little doubt that the bed length is a critical parameter. Under standard conditions, the combustion wave rapidly establishes a velocity level dependent on the chamber length and shows little tendency toward rapid acceleration, which is in some disagreement with the theoretical prediction. Of more importance, in a practical sense, is the development of high pressures at the extremities of the chamber. The sharp pressure rise in the vicinity of the shear disc, although disturbing in appearance, amounts to a fast transient if venting occurs soon after the rise. At the breech end of the chamber, however, pressure buildup occurs at a high rate for some time after venting occurs. Consequently, small delays in venting or partial venting which may relieve the pressure buildup at the vent will result in catastrophic pressure regimes of long duration at the breech.

Some criticism has been made that the studies carried out in the 108.4 mm chamber were unrealistic as no weapon exists today nor is there much likelihood of one being designed to accommodate long beds of ball propellant. It should be pointed out that the experiments were designed to create extreme conditions in order to identify areas of importance which might be obscured under ordinary conditions. Secondly, most of the characteristic features of wave propagation through porous beds found in these studies, have been shown to exist in detonation studies[7] and in large caliber rounds[8].

---

[7] *D. Price and R.R. Bernecker, "Sensitivity of Porous Explosives to Transition from Deflagration to Detonation", Combustion & Flame, Volume 25, page 91, 1975.*

[8] *W.G. Soper, "Ignition Waves in Gun Chambers", Combustion & Flame, Volume 20, page 157, 1973.*

REFERENCES

1. K. K. Kuo, R. Vichnevetsky, and M. Summerfield, "Generation of an Accelerated Flame Front in a Porous Propellant," AIAA Paper 71-210. Presented at the AIAA 9th Aerospace Sciences Meeting, New York, January 1971.

2. W. H. Squire, Private communication with K. K. Kuo, 1970-1971.

3. W. H. Squire and M. P. Devine, "The Interface Between Primer and Propellant," Part I and Part II, Presented 4 June 1969, AOA Paper, published by Frankford Arsenal, 1969.

4. C. W. Kitchens, Jr., "Flame Spreading in Small Arms Ball Propellant," Ballistic Research Laboratories Report 1604, August 1972, AD #750567.

5. C. W. Kitchens, Jr., and N. J. Gerri, "Numerical and Experimental Investigation of Flame Spreading and Gas Flow in Gun Propellants," Proceedings of the 9th JANNAF Combustion Conference, Monterey, California, Vol. 1, September 1971. CPIA Publication No. 231, December 1972, pp. 115-125.

6. C. W. Kitchens, Jr., "Parametric Sensitivity Study of a Numerical Model for Flame Spreading," Ballistic Research Laboratories Memorandum Report 2546, October 1975. (AD #A018135)

7. D. Price and R.R. Bernecker, "Sensitivity of Porous Explosives to Transition from Deflagration to Detonation," Combustion & Flame, Volume 25, page 91, 1975.

8. W.G. Soper, "Ignition Waves in Gun Chambers," Combustion & Flame, Volume 20, page 157, 1973.

APPENDIX A. SUMMARY OF EXPERIMENTAL PARAMETERS, PEAK PRESSURES, CHARACTERISTIC TIMES P-t, P-x, AND ΔP-t CURVES FOR ALL RUNS CARRIED OUT IN THE 108.4 MM CHAMBER

Table A-1, Appendix A, lists each run carried out in the 108.4 mm chamber by run number. The adjacent columns identify respectively, the primer, primer vent configuration, propellant and shear disc, used in each run. For all runs the chamber was 100% volumetrically loaded and fired in the upright position with the primer down.

The remaining columns give the firing pin time (t_o), diode signal time, and the highest pressure recorded at each gage position during the passage of the primary (1°) and secondary (2°) compression waves.* All times were measured from the start of the firing sequence timer.

For each run listed in Table A-1, and in the same order as the listing, the analog pressure data accumulated at each gage position was digitized, normalized and replotted in three different formats: pressure vs. time (two plots, two gages each), pressure vs. distance (at pre-selected times) and differential pressure vs. time.

---

* *See page 10.*

Table A-1. Experimental Parameters, Peak Pressures, Diode and Firing Pin Times for all Runs in the 108.4 mm Chamber.

RUN NO.	PRIMER	VENT CONFIGURATION (FIGURE 3)	PROPELLANT	SHEAR DISC* (mm)	FIRING PIN (ms)	G-1 1° Pmax/2° Pmax (MPa)	G-2 1° Pmax/2° Pmax (MPa)	G-3 1° Pmax/2° Pmax (MPa)	G-4 1° Pmax/2° Pmax (MPa)	DIODE SIGNAL (ms)
127-44	FA-41	F	WC 846[a]	0.787*	2.600	459/649	469/598	453/466	515/416	3.385
127-45	FA-41	F	WC 846[a]	0.787	2.503	333/493	351/467	360/393	429/340	3.145
127-48	FA-41	F	WC 846[a]	0.787	4.168	390/548	377/518	367/432	452/378	4.820
127-50	FA-41	F	WC 846[a]	0.787	3.733	376/507	362/475	367/400	449/350	4.355
127-51	FA-41	F	WC 846[a]	0.787	3.773	389/475	370/451	294/373	351/330	4.433
147-4	FA-41	F	WC 846[b]	0.787	13.813	370/474	324/428	364/422	411/402	ns
147-6	FA-41	F	WC 846[b]	0.787	11.090	361/512	328/459	382/454	428/413	11.765
139-18	FA-41[d]	F	WC 844[c]	0.787	5.473	353/437	380/394	422/345	601/301	6.363
139-19	FA-41[d]	F	WC 844[c]	0.787	4.185	408/508	409/473	418/430	742/359	4.968
147-7	FA-41	F	WC 844[c]	0.787	12.640	409/509	400/470	395/461	355/382	13.410
147-8	FA-41	F	WC 844[c]	0.787	11.368	415/463	370/425	327/431	346/345	12.093
138-38	FA-41	D	WC 846[a]	0.787	7.888		- /425	405/379	318/355	8.560
138-39	FA-41	D	WC 846[a]	0.787	14.688	395/455	409/444	448/426	374/371	15.393
138-44	FA-41	D	WC 846[a]	0.787	6.200	429/512	470/493	569/465	498/377	7.035
138-45	FA-41	D	WC 846[a]	0.787	6.908	388/465	420/451		322/348	7.753
138-41	FA-41	E	WC 846[a]	0.787	6.550	351/455	360/426	493/389	442/355	8.020
138-43	FA-41	E	WC 846[a]	0.787	9.560	357/457	368/428	523/409	493/341	10.930
139-14	FA-41[d]	F	WC 846[b]	0.394*	1.415	- /320	- /307	- /296	288/300	2.105
139-16	FA-41[d]	F	WC 844[c]	0.394	-	161/198	175/192	265/200	224/223	7.603
139-17	FA-41[d]	F	WC 844[c]	0.394	4.675	- /318	- /313	327/292	263/316	5.358
138-57	FA-41	F	WC 846[a]	glass**	3.745	- /388	- /336	342/321	260/290	4.483
138-60	FA-41	F	WC 846[a]	glass	3.070	- /344	- /323	309/303	233/279	3.858
127-36	FA-34	C	WC 846[a]	0.787	5.355	334/465	356/435	386/366	452/350	6.078
127-37	FA-34	C	WC 846[a]	0.787	5.653	346/472	354/444	374/366	494/357	6.308
139-22	FA-34	C	WC 846[b]	0.787	5.690	304/473	329/424	451/390	518/332	6.330
139-20	FA-34	C	WC 844[c]	0.787	4.178	- /498	- /474	421/408	534/349	4.975
139-21	FA-34	C	WC 844[c]	0.787	5.510	- /498	307/495	377/430	575/360	6.223
138-53	FA-34	A	WC 846[a]	0.787*	8.568	344/511	363/456	456/405	347/373	9.353
138-55	FA-34	A	WC 846[a]	0.787	.750	388/470	341/438	434/392	359/350	1.865
147-2	FA-34	A	WC 846[b]	0.787	6.713	438/500	338/387	426/439	474/366	7.715
147-3	FA-34	A	WC 846[b]	0.787	6.273	442/496	292/400	413/451	393/387	7.045
138-50	FA-34	B	WC 846[a]	0.787	7.768	327/453	356/420	436/378	318/351	8.468
138-52	FA-34	B	WC 846[a]	0.787	6.453	410/500	423/466	467/398	304/360	7.355
139-38	FA-34	C	WC 844[c]	0.394	1.605	343/357	216/348	380/332	250/285	2.385
139-39	FA-34	C	WC 844[c]	0.394	0.630	231/339	271/305	341/288	336/247	1.320
139-40	FA-34	C	WC 844[c]	0.394	4.103	- /369	234/342	366/317	290/272	4.803
139-41	FA-34	C	WC 844[c]	0.394	5.120	208/276	257/257	294/288	310/291	ns

* = + .025 mm
** = 7.5 mm plate glass
\- = not well defined
a = lot no. AL 46892
b = lot no. LCSP 859
c = no lot designation
d = commercial version of FA-41 primer
ns = no signal

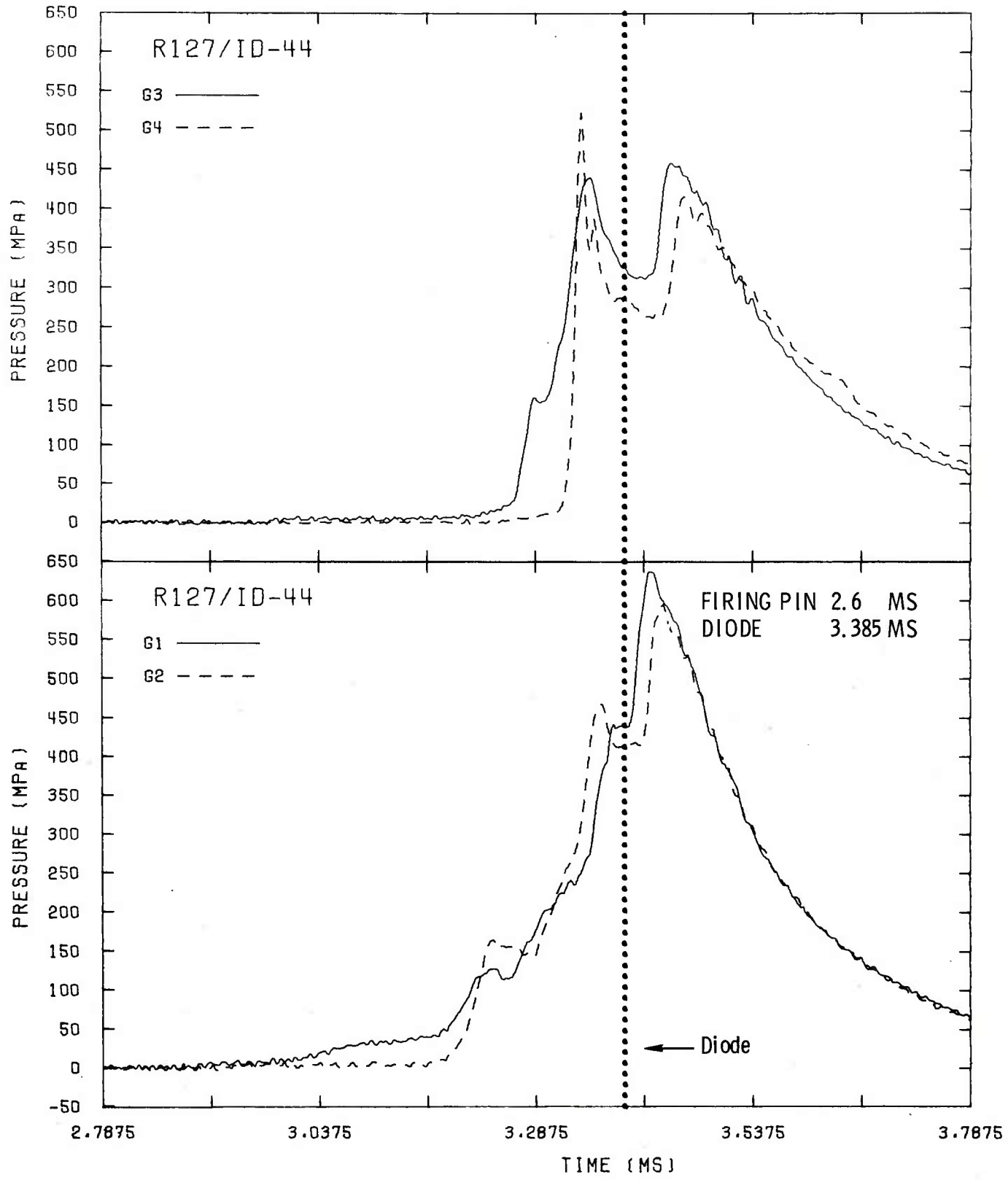
R127/ID-44
G3
G4
PRESSURE (MPA)
650
600
550
500
450
400
350
300
250
200
150
100
50
0
R127/ID-44
G1
G2
FIRING PIN 2.6 MS
DIODE 3.385 MS
Diode
-50
2.7875
3.0375
3.2875
3.5375
3.7875
TIME (MS)

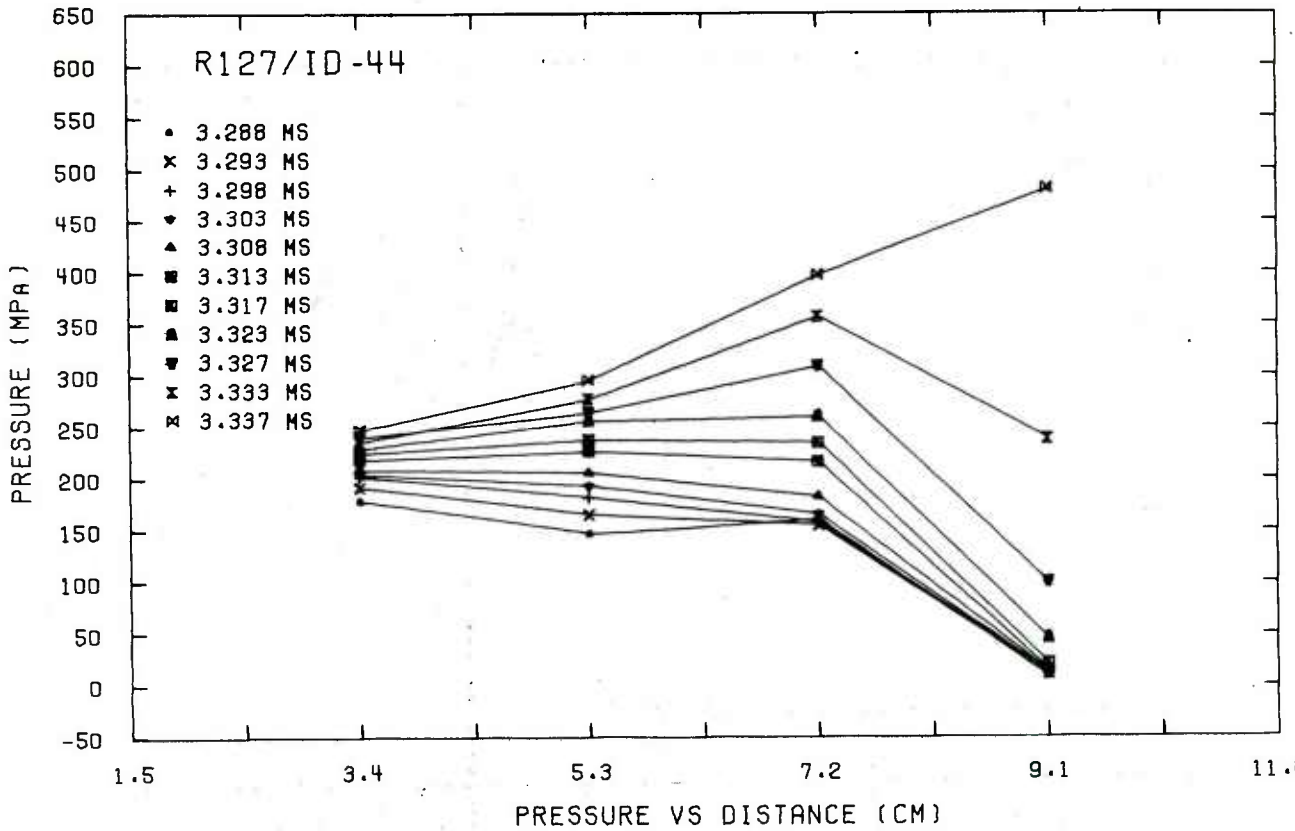
R127/ID-44
3.288 MS
3.293 MS
3.298 MS
3.303 MS
3.308 MS
3.313 MS
3.317 MS
3.323 MS
3.327 MS
3.333 MS
3.337 MS
PRESSURE (MPA)
650
600
550
500
450
400
350
300
250
200
150
100
50
0
-50
1.5
3.4
5.3
7.2
9.1
11.0
PRESSURE VS DISTANCE (CM)

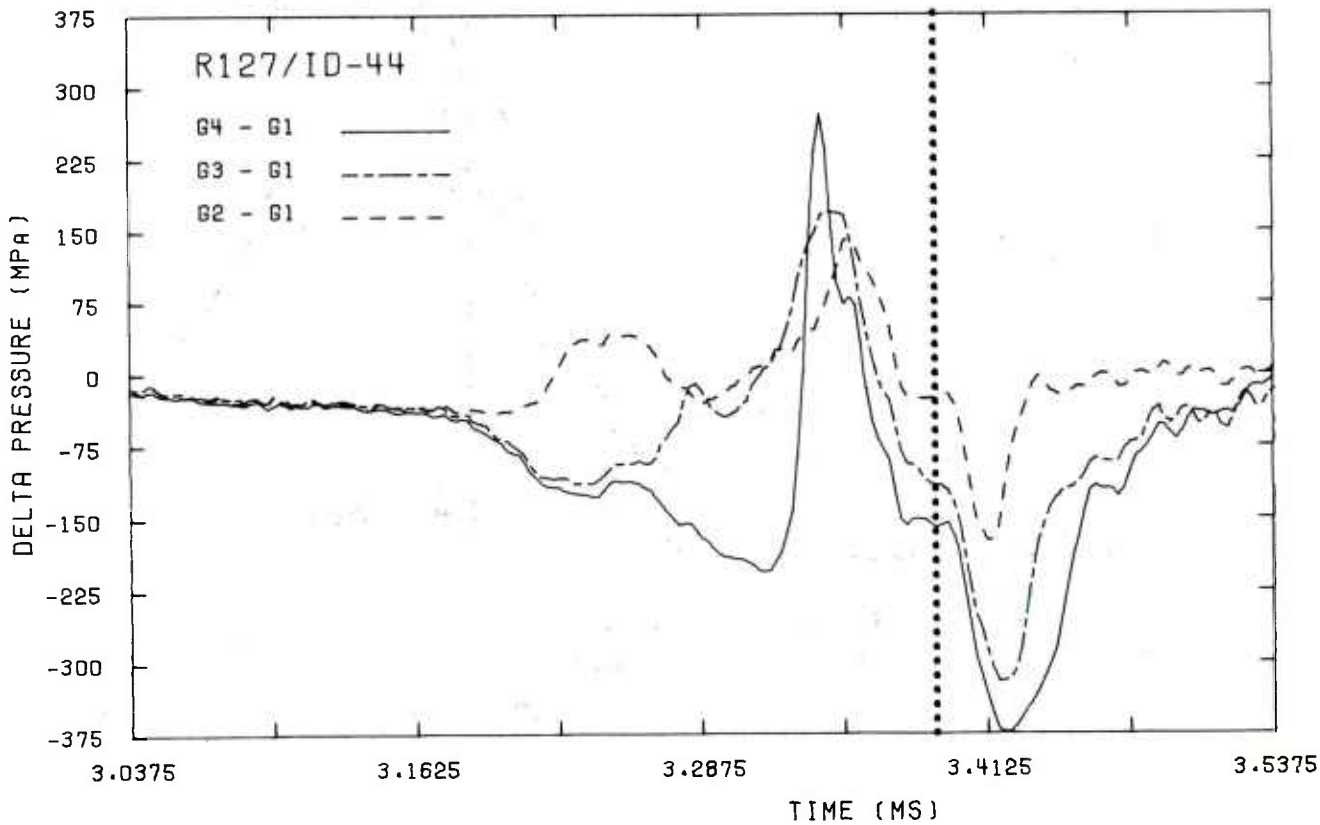
R127/ID-44
G4 - G1
G3 - G1
G2 - G1
DELTA PRESSURE (MPA)
375
300
225
150
75
0
-75
-150
-225
-300
-375
3.0375
3.1625
3.2875
3.4125
3.5375
TIME (MS)

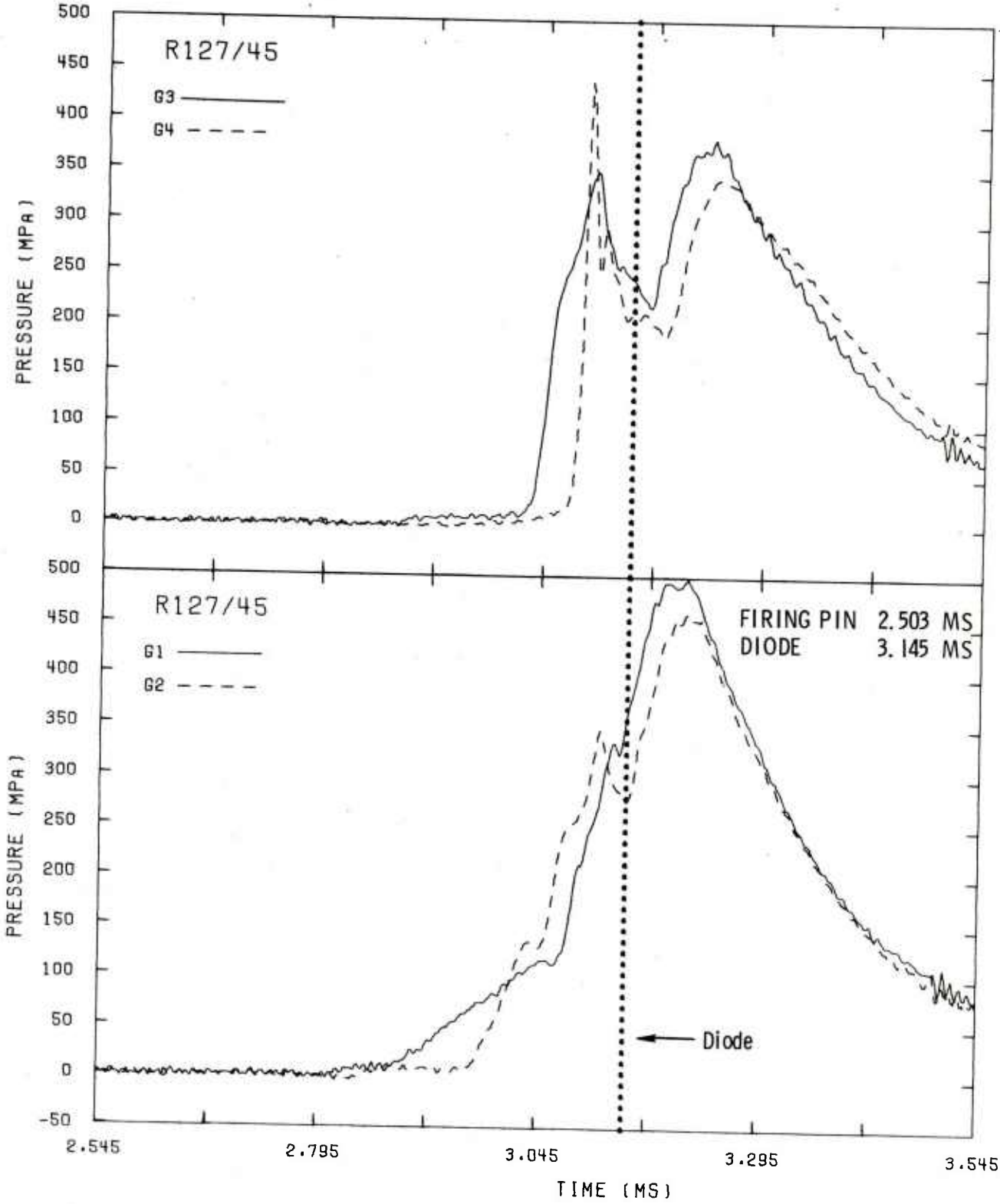
R127/45
G3
G4
PRESSURE (MPa)
500
450
400
350
300
250
200
150
100
50
0
R127/45
G1
G2
FIRING PIN 2.503 MS
DIODE 3.145 MS
Diode
-50
2.545
2.795
3.045
3.295
3.545
TIME (MS)

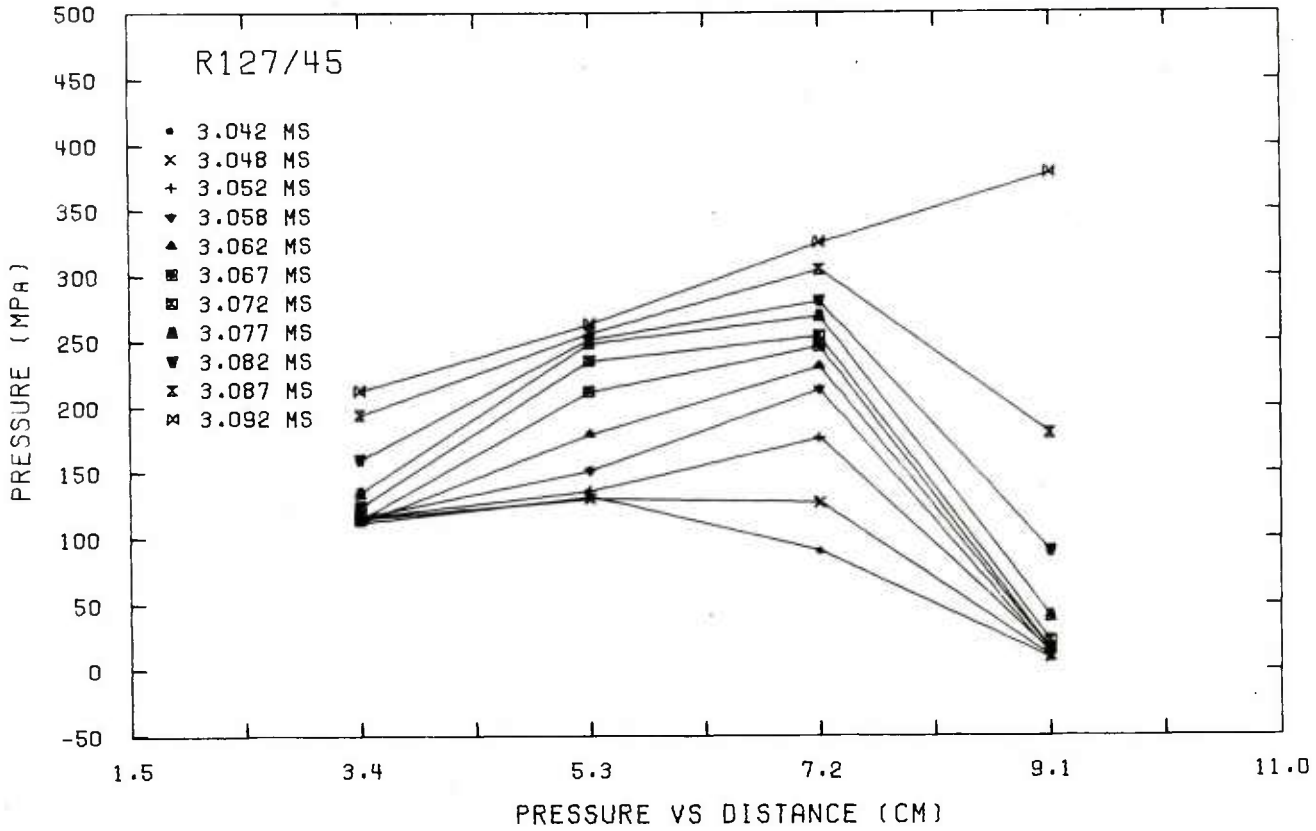
R127/45
3.042 MS
3.048 MS
3.052 MS
3.058 MS
3.062 MS
3.067 MS
3.072 MS
3.077 MS
3.082 MS
3.087 MS
3.092 MS
PRESSURE (MPa)
500
450
400
350
300
250
200
150
100
50
0
-50
1.5
3.4
5.3
7.2
9.1
11.0
PRESSURE VS DISTANCE (CM)

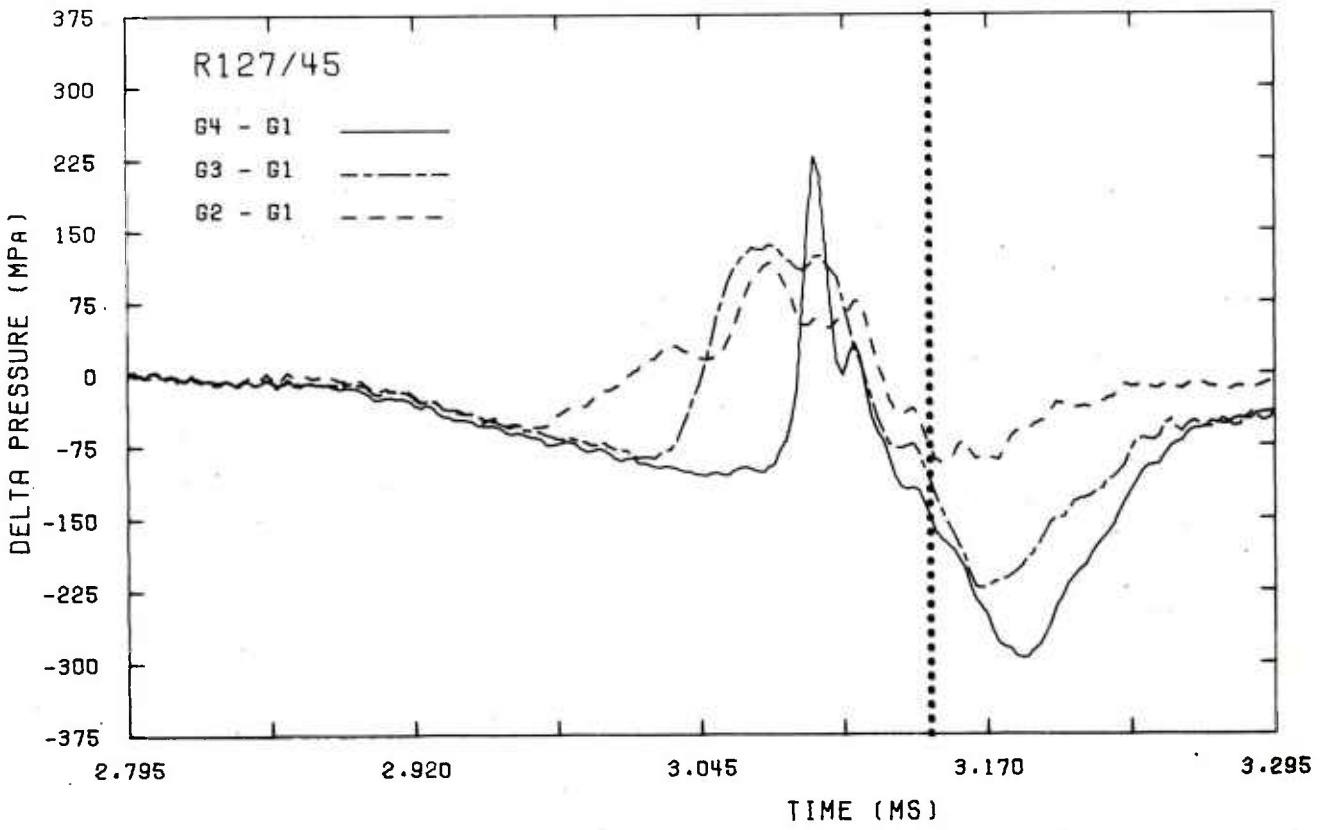
R127/45
G4 - G1
G3 - G1
G2 - G1
DELTA PRESSURE (MPa)
375
300
225
150
75
0
-75
-150
-225
-300
-375
2.795
2.920
3.045
3.170
3.295
TIME (MS)

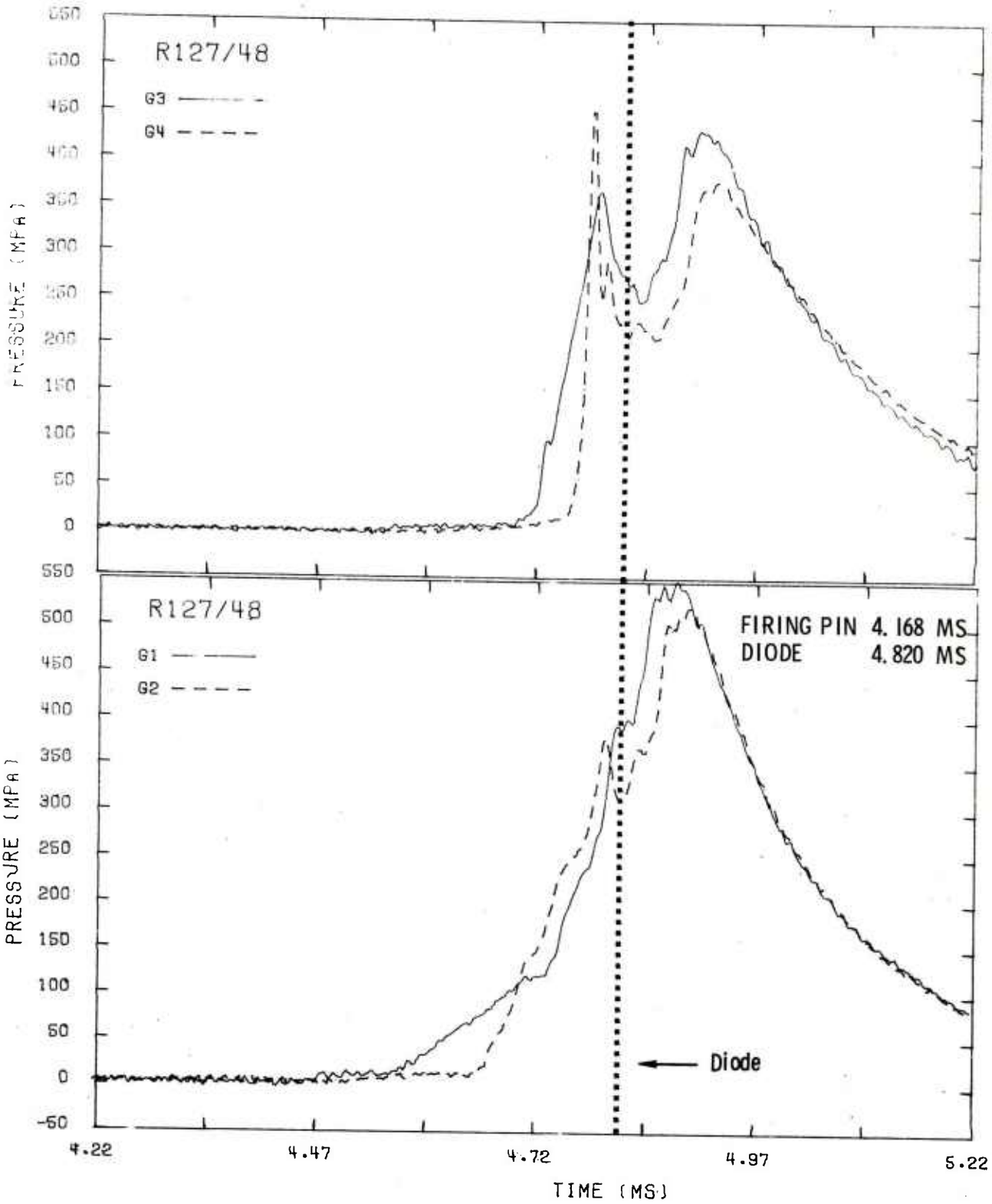
R127/48
G3
G4
R127/48
G1
G2
FIRING PIN 4.168 MS
DIODE 4.820 MS
Diode
PRESSURE (MPA)
PRESSURE (MPA)
TIME (MS)
4.22
4.47
4.72
4.97
5.22

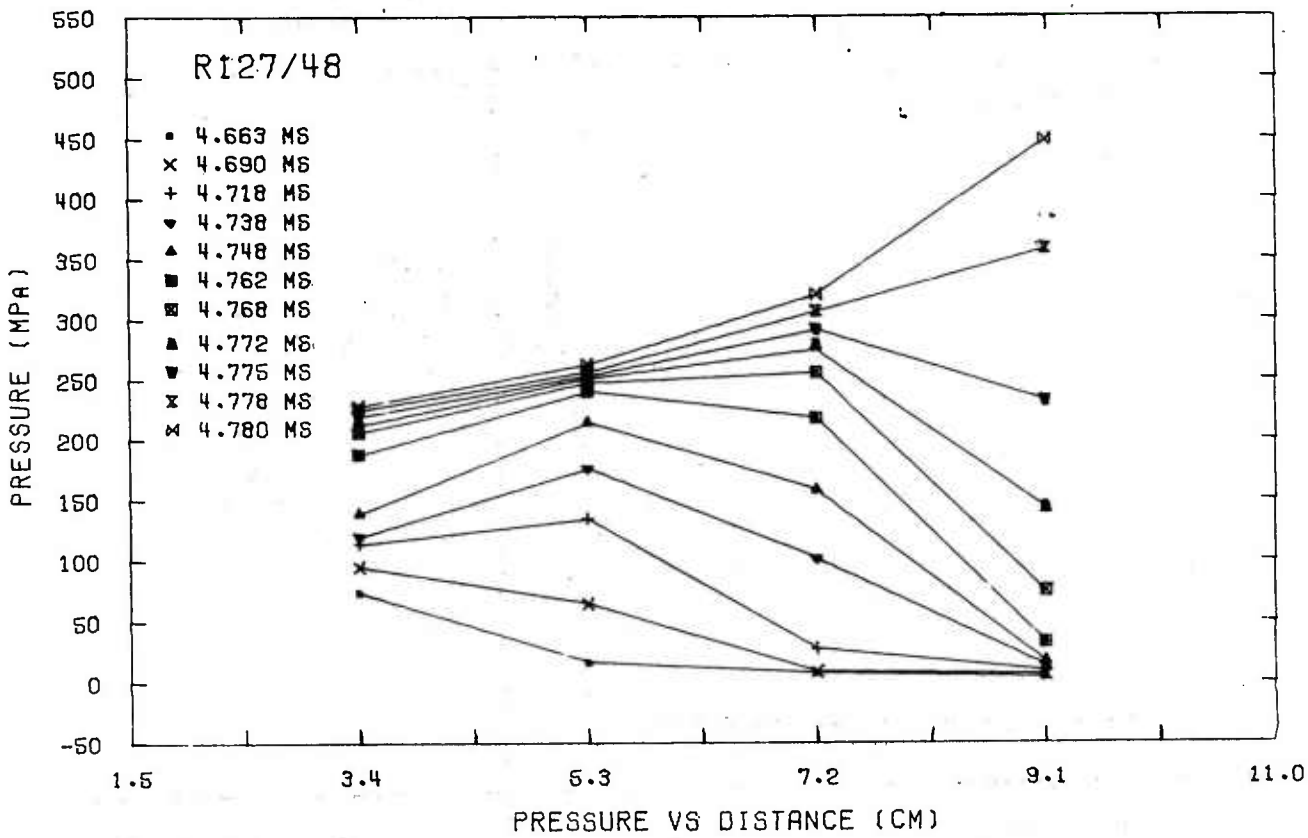
R127/48
4.663 MS
4.690 MS
4.718 MS
4.738 MS
4.748 MS
4.762 MS
4.768 MS
4.772 MS
4.775 MS
4.778 MS
4.780 MS
PRESSURE (MPA)
550
500
450
400
350
300
250
200
150
100
50
0
-50
1.5
3.4
5.3
7.2
9.1
11.0
PRESSURE VS DISTANCE (CM)

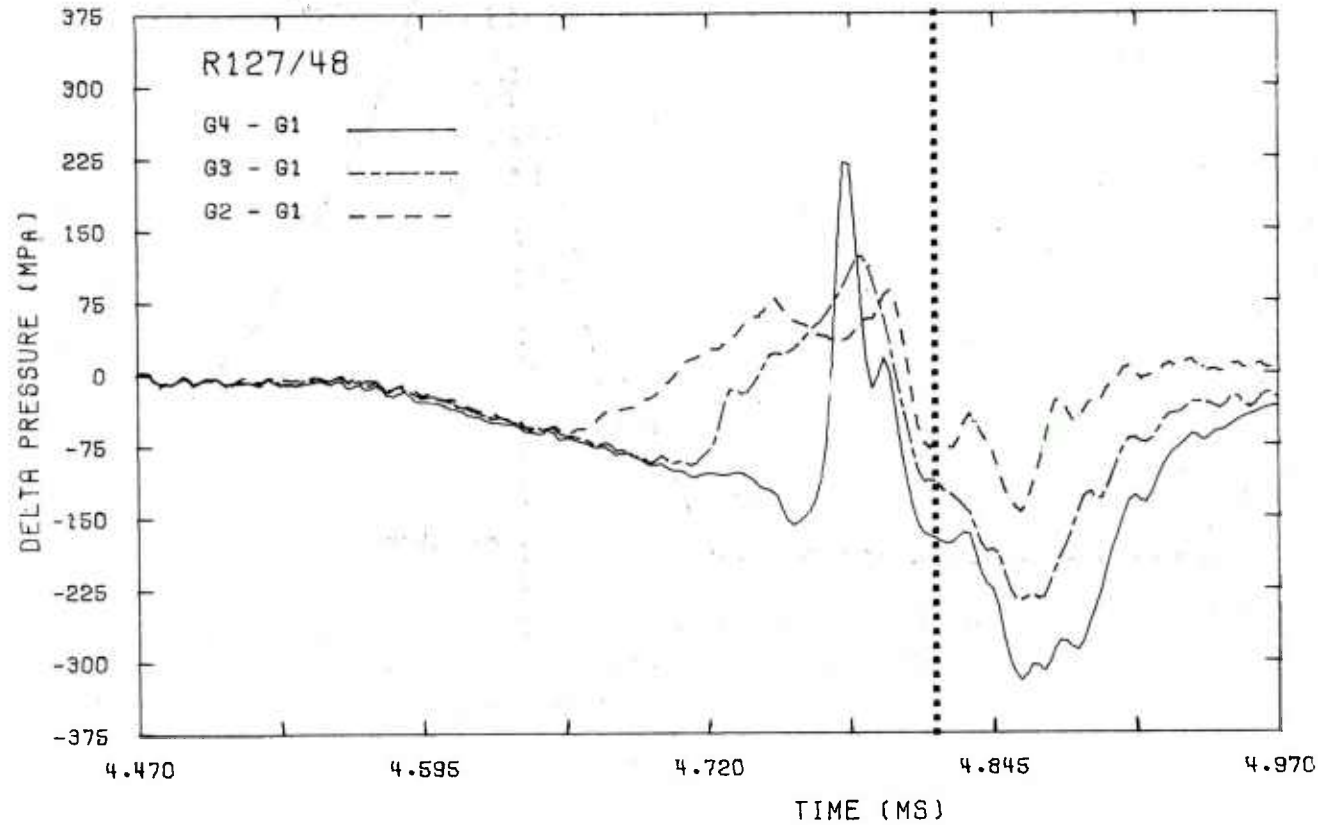
R127/48
G4 - G1
G3 - G1
G2 - G1
DELTA PRESSURE (MPA)
375
300
225
150
75
0
-75
-150
-225
-300
-375
4.470
4.595
4.720
4.845
4.970
TIME (MS)

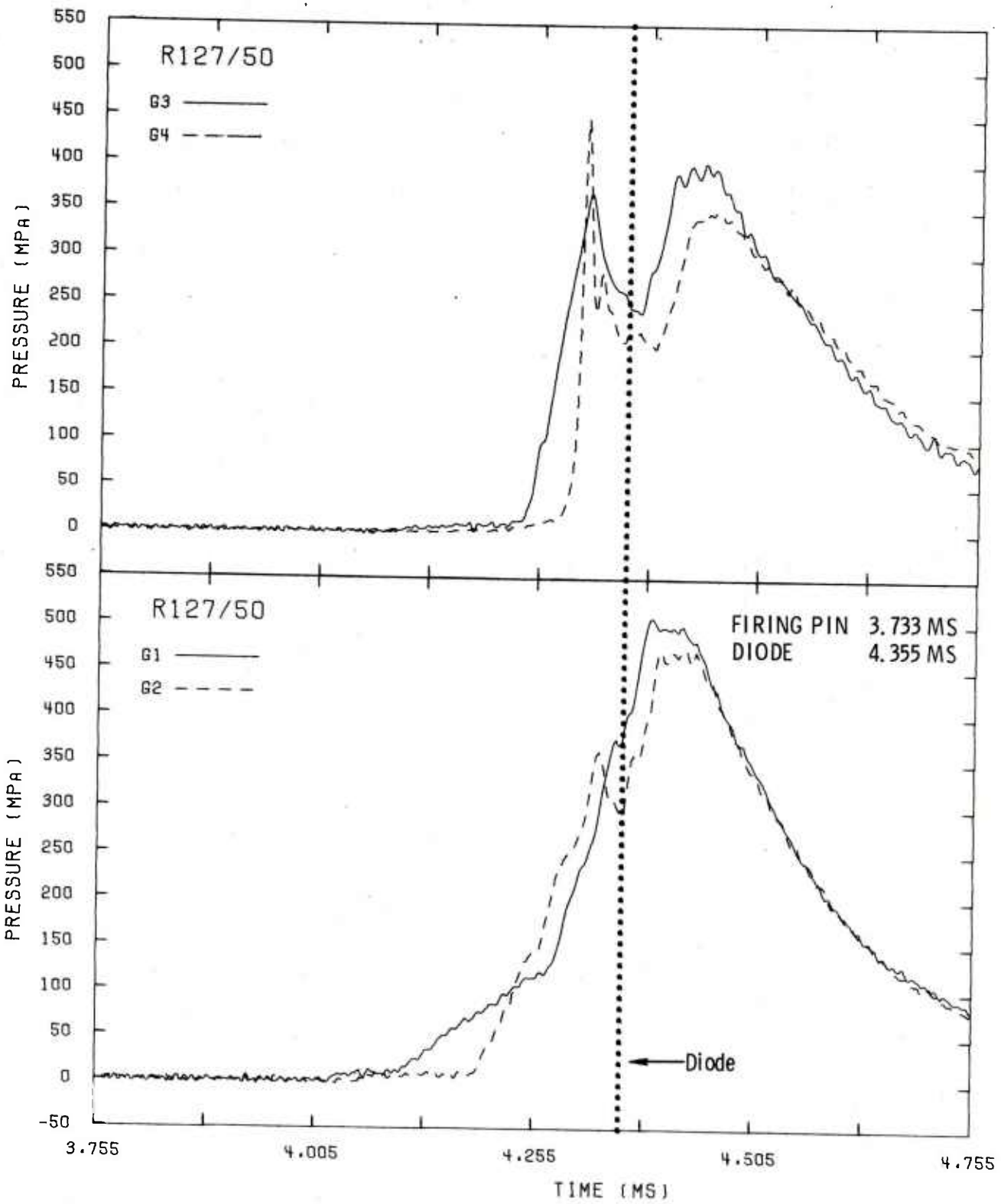
R127/50
G3
G4
PRESSURE (MPA)
550
500
450
400
350
300
250
200
150
100
50
0
R127/50
G1
G2
FIRING PIN 3.733 MS
DIODE 4.355 MS
Diode
-50
3.755
4.005
4.255
4.505
4.755
TIME (MS)

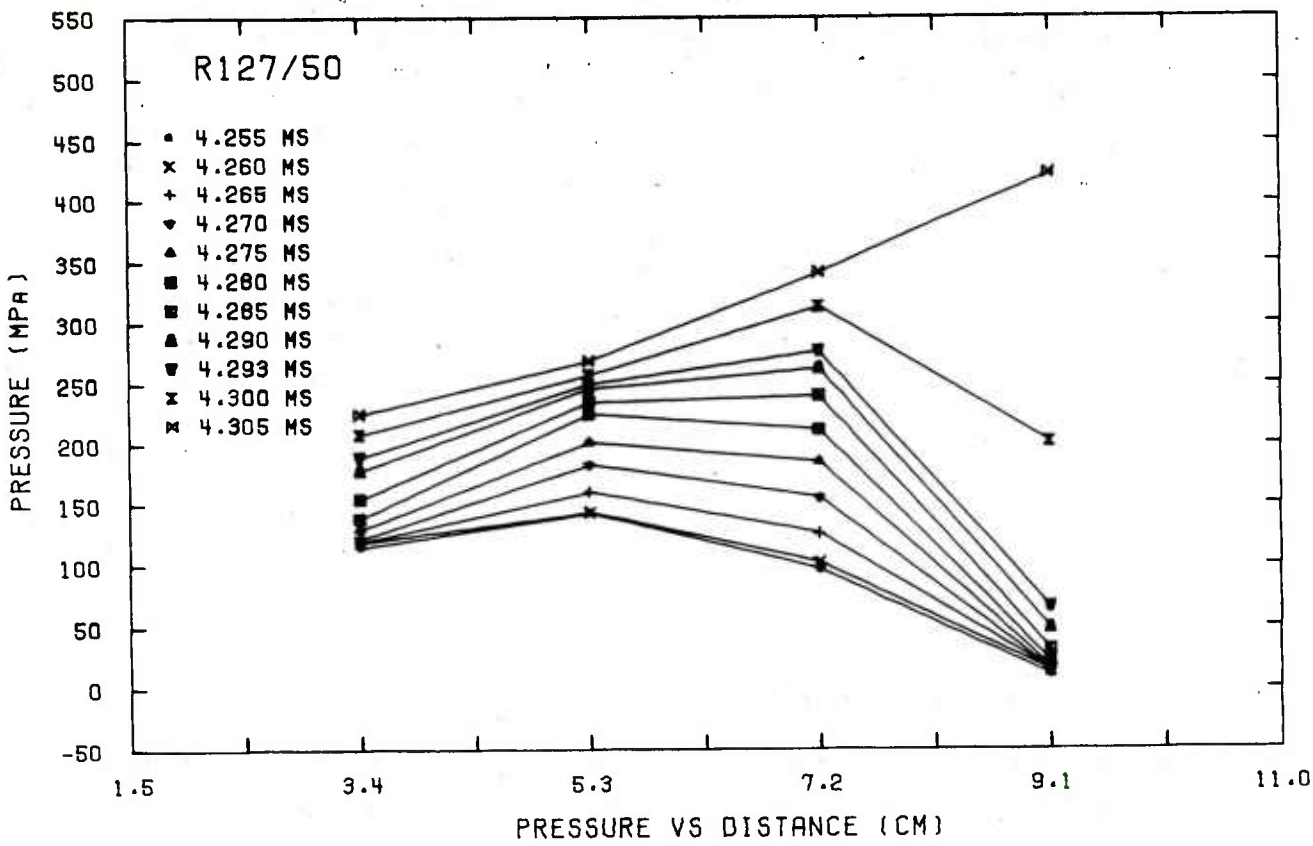
R127/50
4.255 MS
4.260 MS
4.265 MS
4.270 MS
4.275 MS
4.280 MS
4.285 MS
4.290 MS
4.293 MS
4.300 MS
4.305 MS
PRESSURE (MPa)
550
500
450
400
350
300
250
200
150
100
50
0
-50
1.5
3.4
5.3
7.2
9.1
11.0
PRESSURE VS DISTANCE (CM)

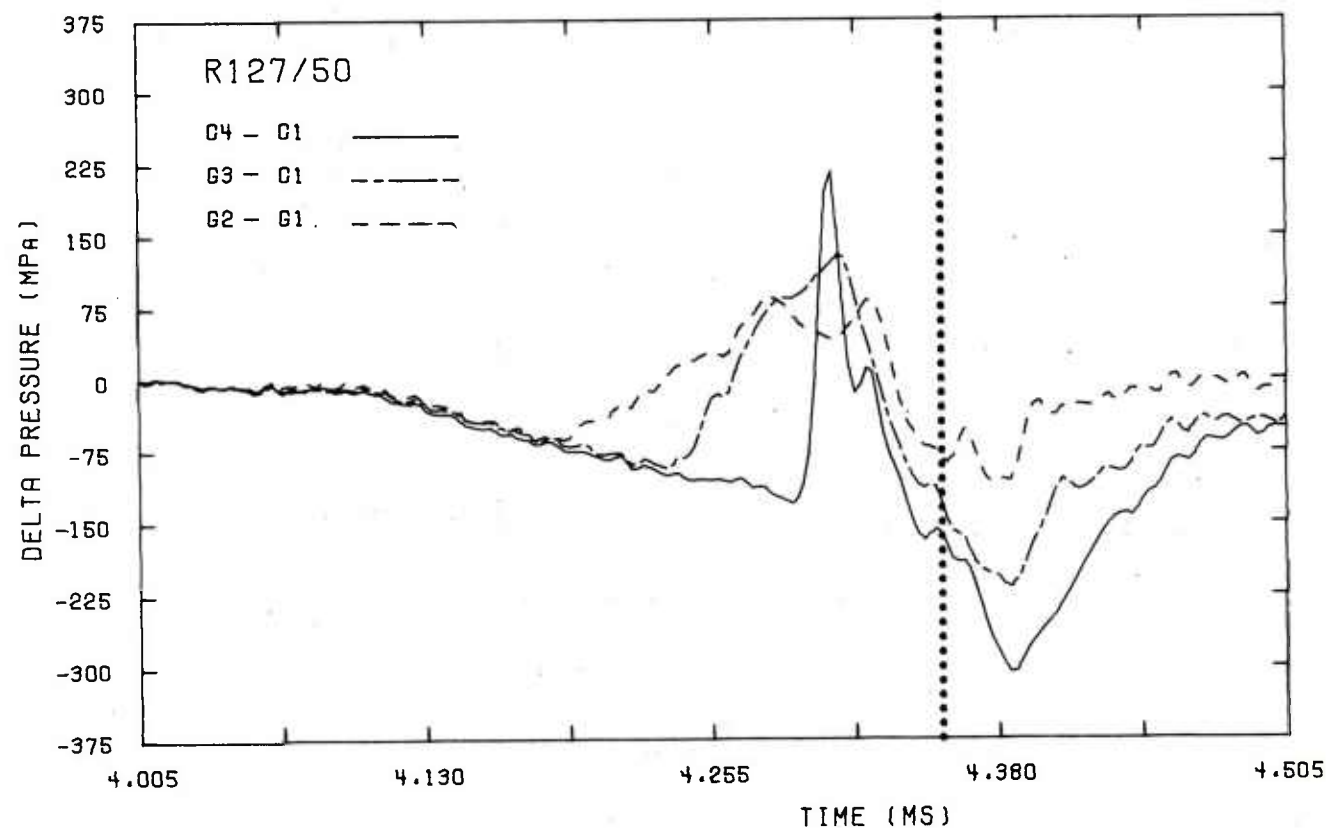
R127/50
G4 – G1
G3 – G1
G2 – G1
DELTA PRESSURE (MPa)
375
300
225
150
75
0
-75
-150
-225
-300
-375
4.005
4.130
4.255
4.380
4.505
TIME (MS)

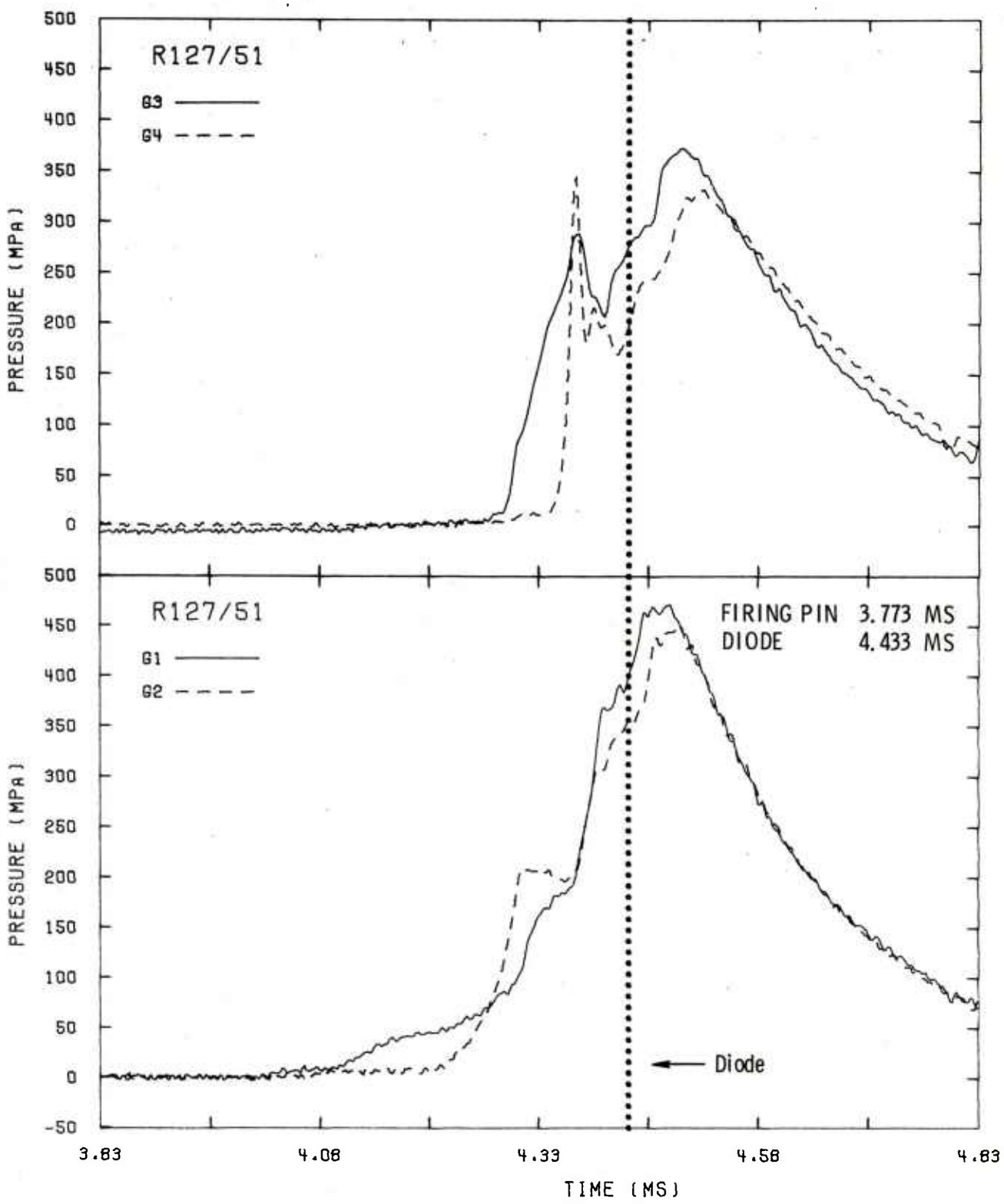
R127/51
G3
G4
PRESSURE (MPa)
500
450
400
350
300
250
200
150
100
50
0
R127/51
G1
G2
FIRING PIN 3.773 MS
DIODE 4.433 MS
Diode
-50
3.83
4.08
4.33
4.58
4.83
TIME (MS)

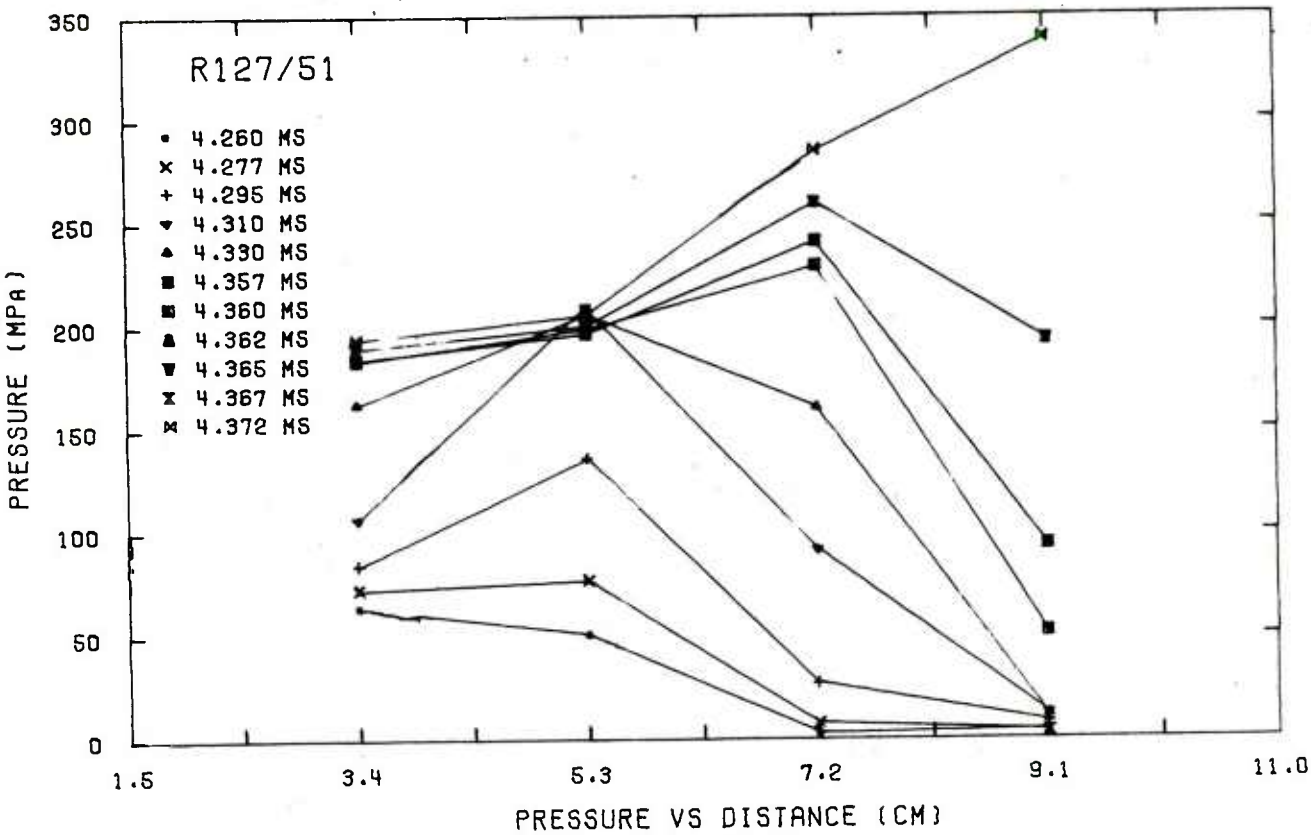
R127/51
4.260 MS
4.277 MS
4.295 MS
4.310 MS
4.330 MS
4.357 MS
4.360 MS
4.362 MS
4.365 MS
4.367 MS
4.372 MS
PRESSURE (MPa)
350
300
250
200
150
100
50
0
1.5
3.4
5.3
7.2
9.1
11.0
PRESSURE VS DISTANCE (CM)

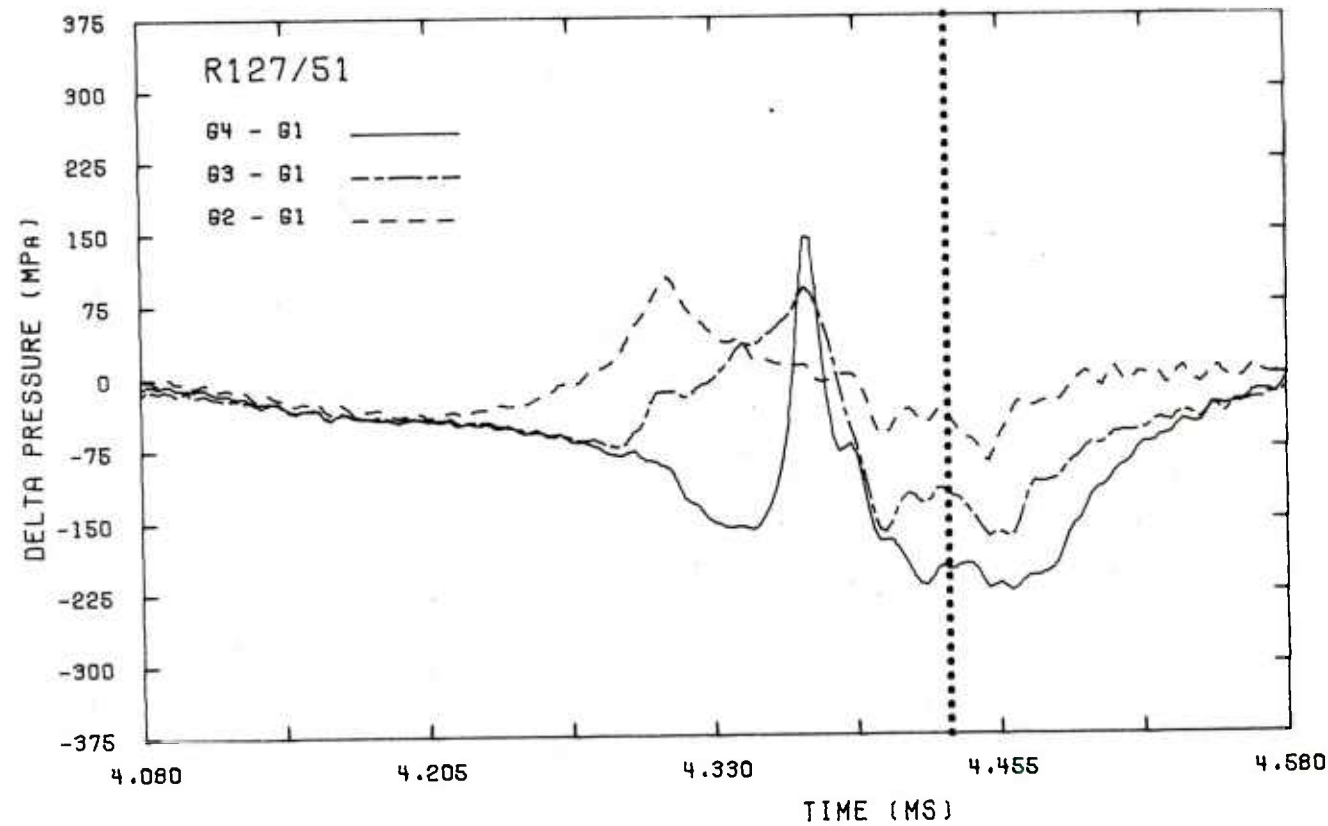
R127/51
G4 - G1
G3 - G1
G2 - G1
DELTA PRESSURE (MPa)
375
300
225
150
75
0
-75
-150
-225
-300
-375
4.080
4.205
4.330
4.455
4.580
TIME (MS)

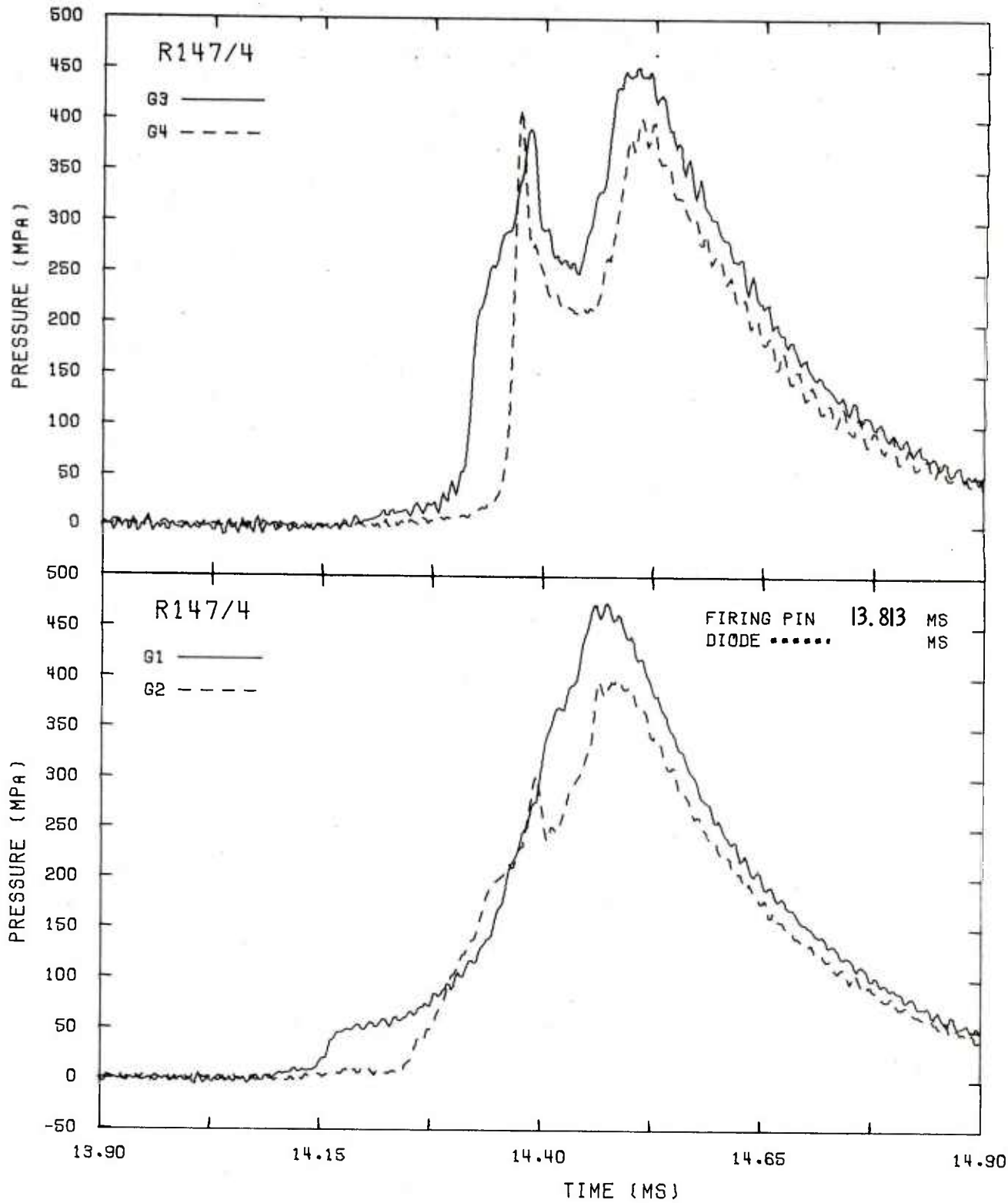
R147/4
G3
G4
PRESSURE (MPa)
500
450
400
350
300
250
200
150
100
50
0
R147/4
G1
G2
FIRING PIN
DIODE
13.813 MS
MS
-50
13.90
14.15
14.40
14.65
14.90
TIME (MS)

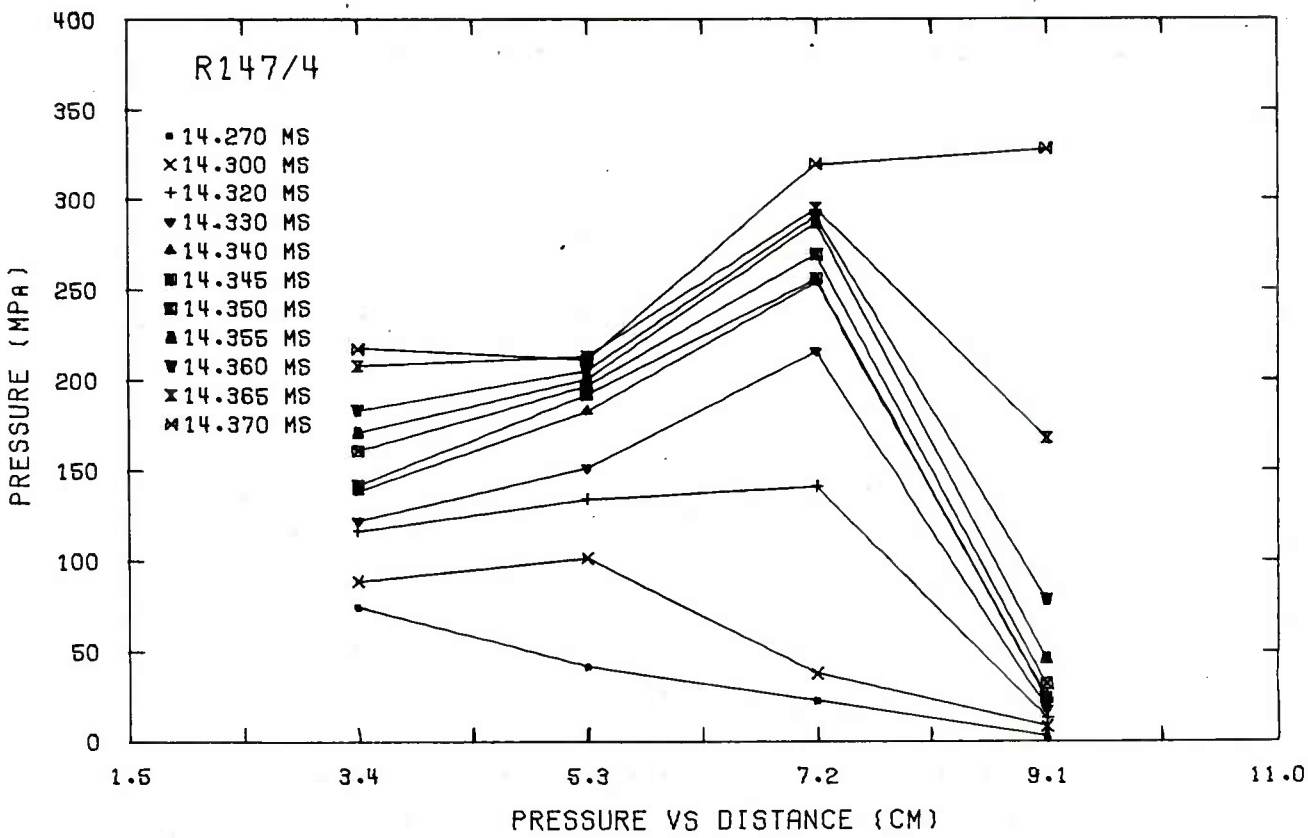
R147/4
•14.270 MS
×14.300 MS
+14.320 MS
▼14.330 MS
▲14.340 MS
■14.345 MS
■14.350 MS
▲14.355 MS
▼14.360 MS
⧗14.365 MS
⋈14.370 MS
PRESSURE (MPa)
400
350
300
250
200
150
100
50
0
1.5
3.4
5.3
7.2
9.1
11.0
PRESSURE VS DISTANCE (CM)

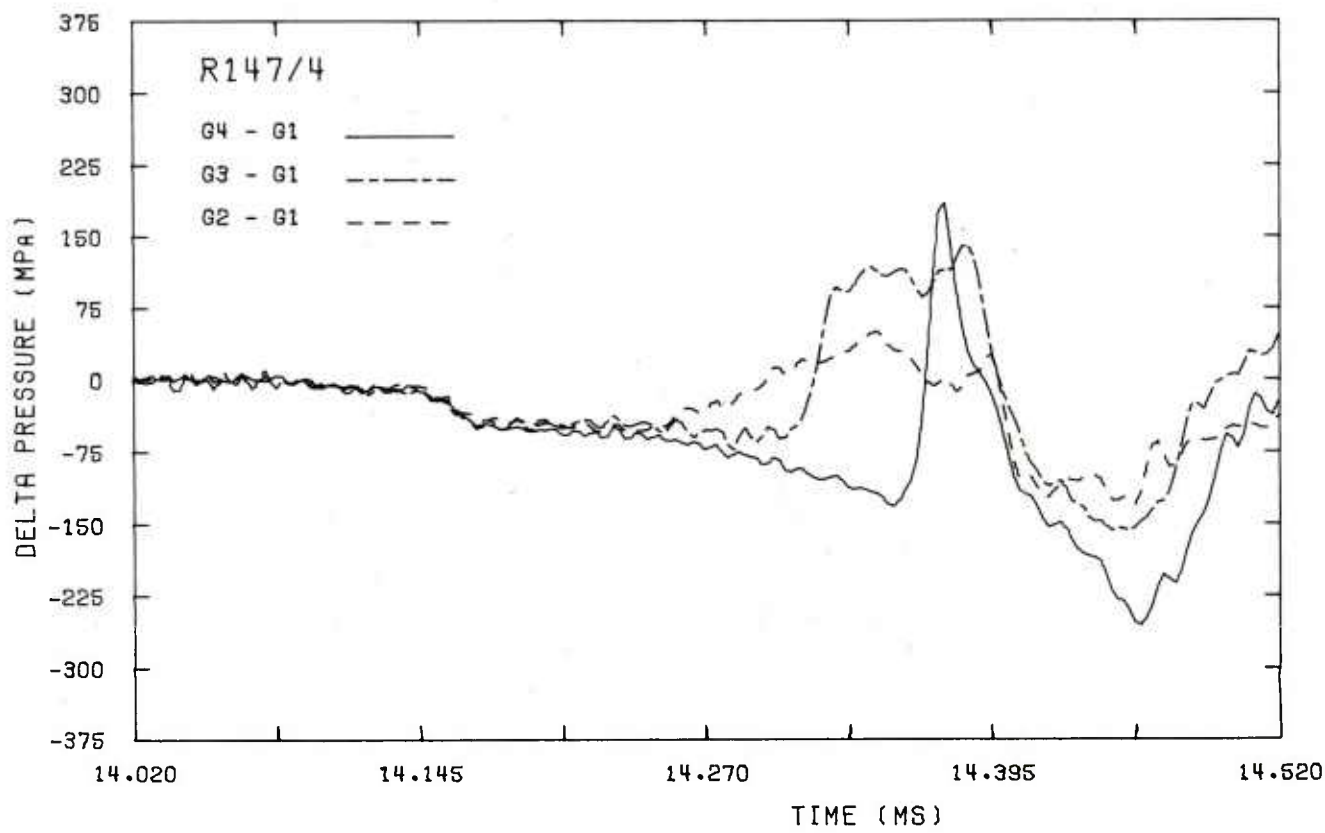
R147/4
G4 - G1
G3 - G1
G2 - G1
DELTA PRESSURE (MPa)
375
300
225
150
75
0
-75
-150
-225
-300
-375
14.020
14.145
14.270
14.395
14.520
TIME (MS)

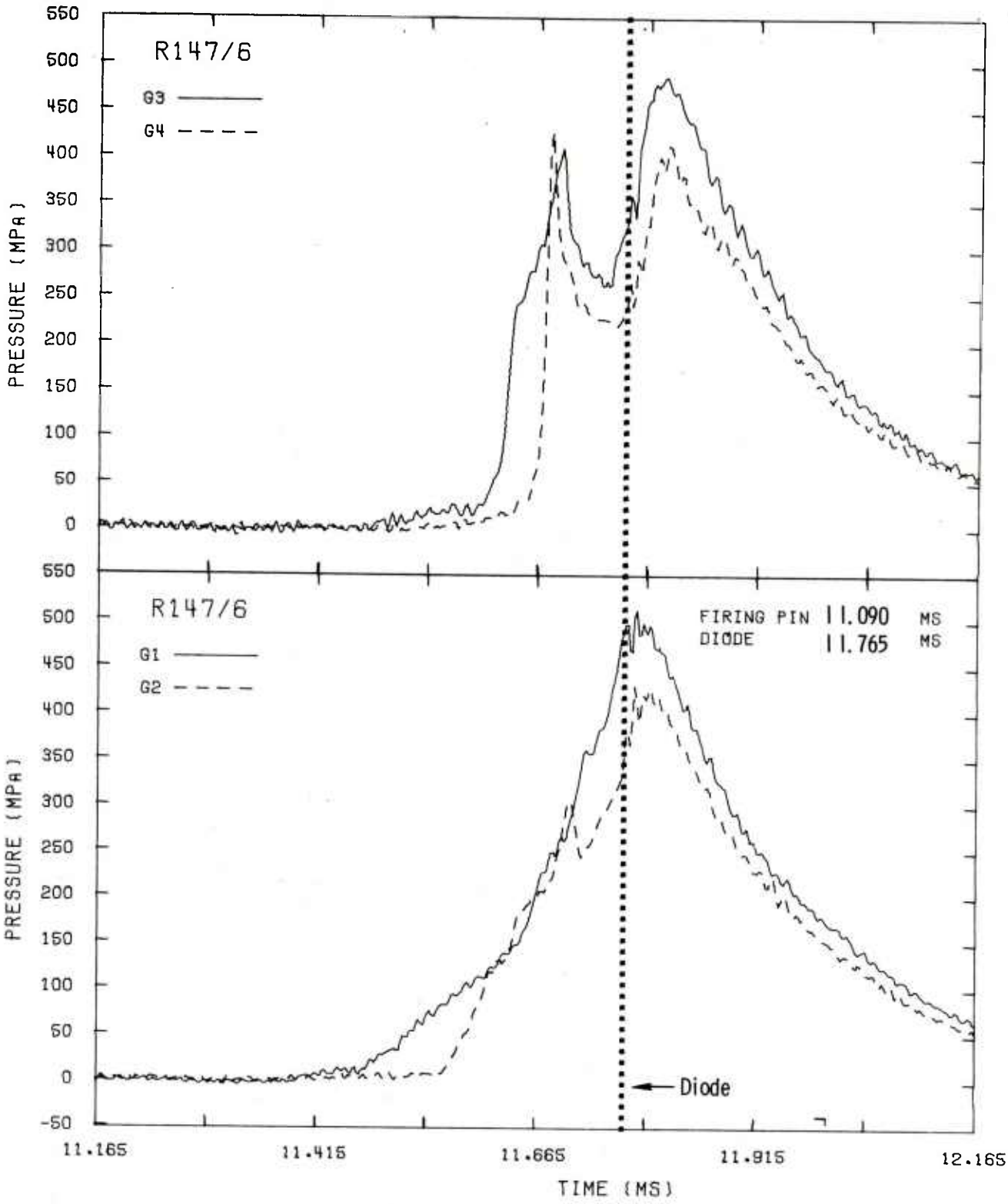
R147/6
G3
G4
PRESSURE (MPa)
R147/6
G1
G2
FIRING PIN 11.090 MS
DIODE 11.765 MS
Diode
PRESSURE (MPa)
TIME (MS)
11.165
11.415
11.665
11.915
12.165

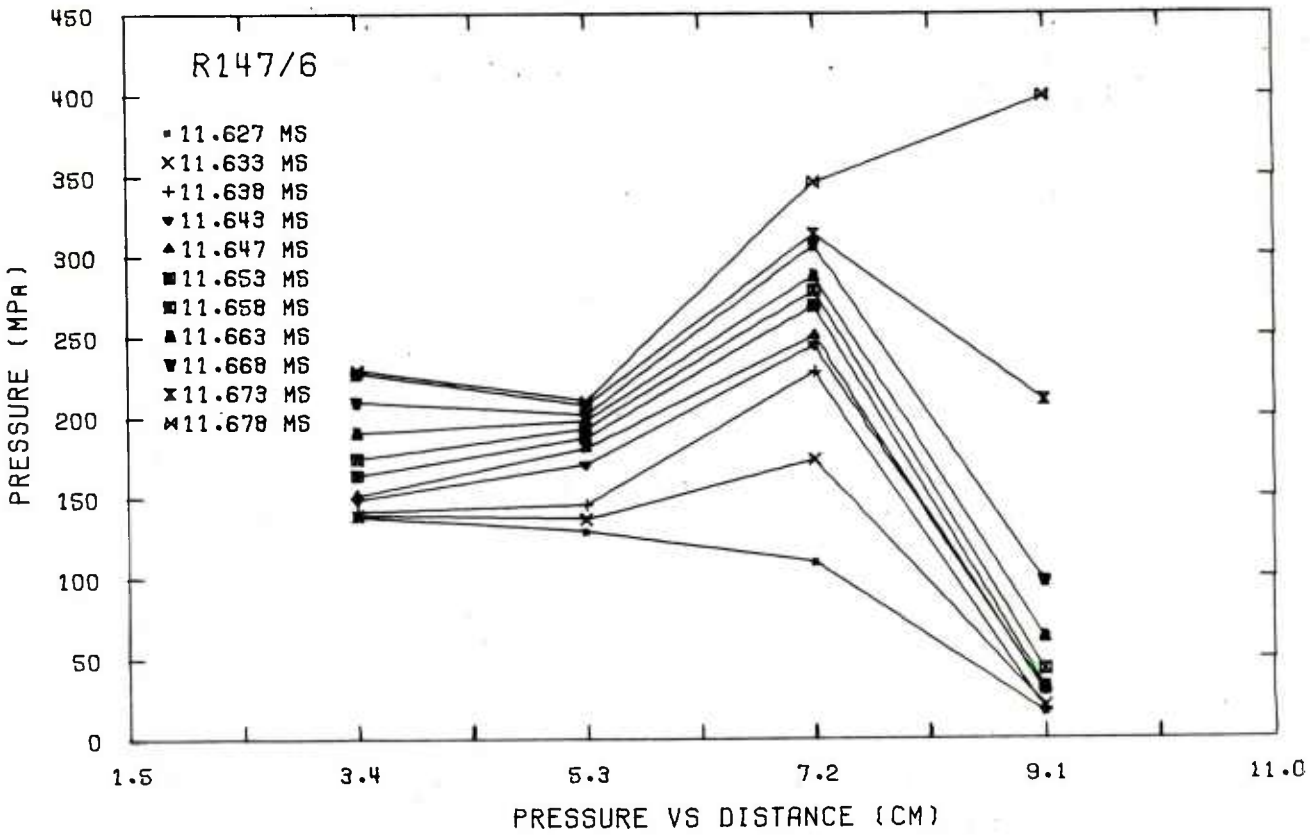
R147/6
11.627 MS
11.633 MS
11.638 MS
11.643 MS
11.647 MS
11.653 MS
11.658 MS
11.663 MS
11.668 MS
11.673 MS
11.678 MS
PRESSURE (MPA)
450
400
350
300
250
200
150
100
50
0
1.5
3.4
5.3
7.2
9.1
11.0
PRESSURE VS DISTANCE (CM)

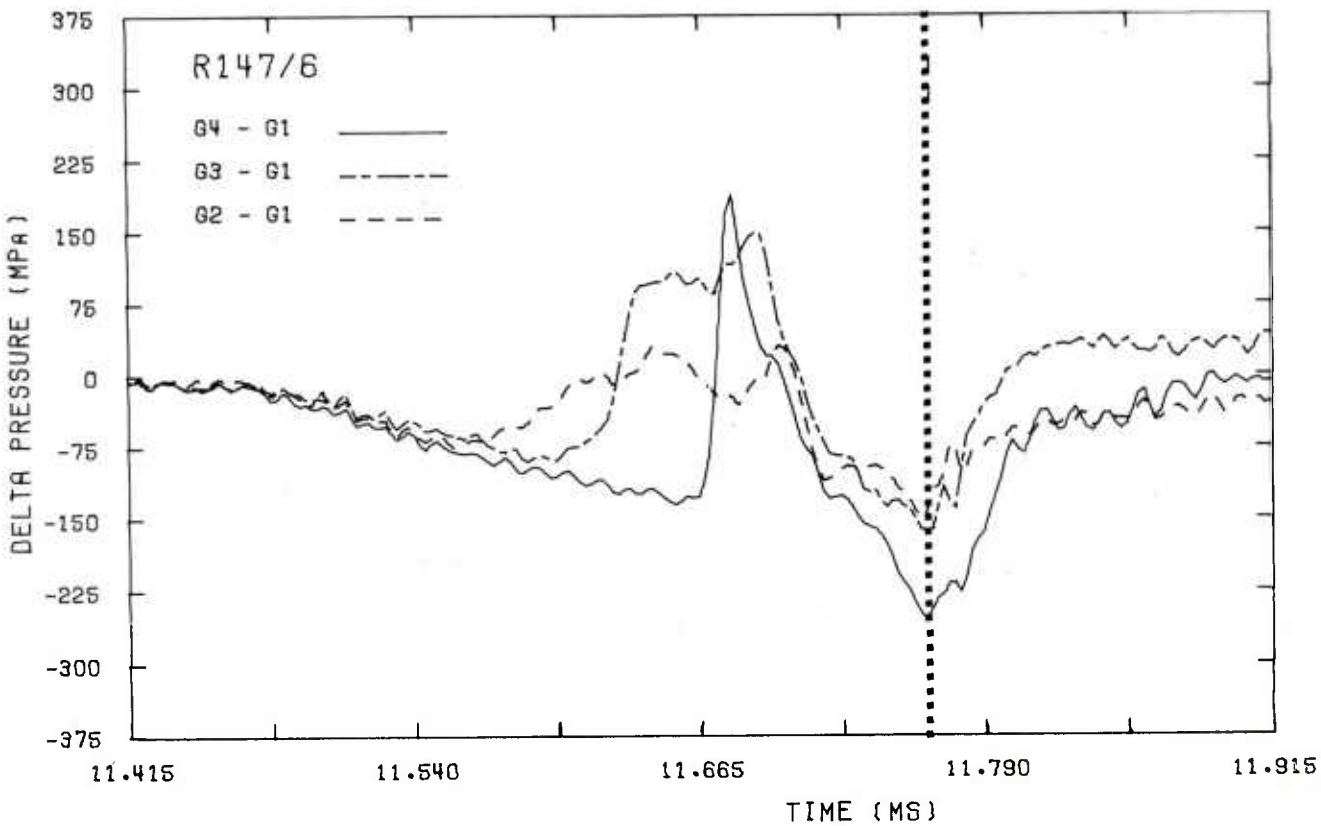
R147/6
G4 - G1
G3 - G1
G2 - G1
DELTA PRESSURE (MPA)
375
300
225
150
75
0
-75
-150
-225
-300
-375
11.415
11.540
11.665
11.790
11.915
TIME (MS)

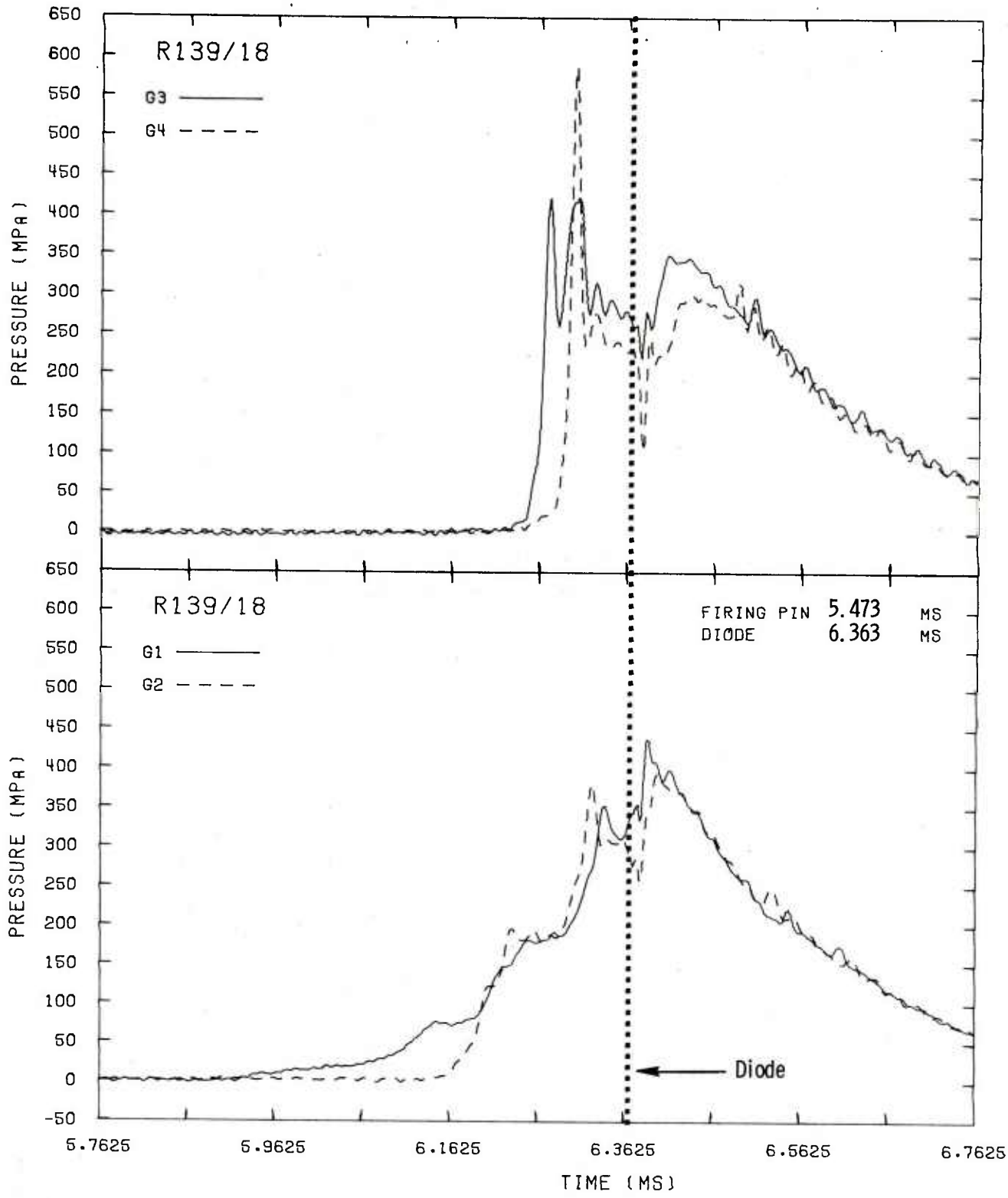
R139/18
G3
G4
PRESSURE (MPa)
650
600
550
500
450
400
350
300
250
200
150
100
50
0
R139/18
G1
G2
FIRING PIN 5.473 MS
DIODE 6.363 MS
Diode
-50
5.7625
5.9625
6.1625
6.3625
6.5625
6.7625
TIME (MS)

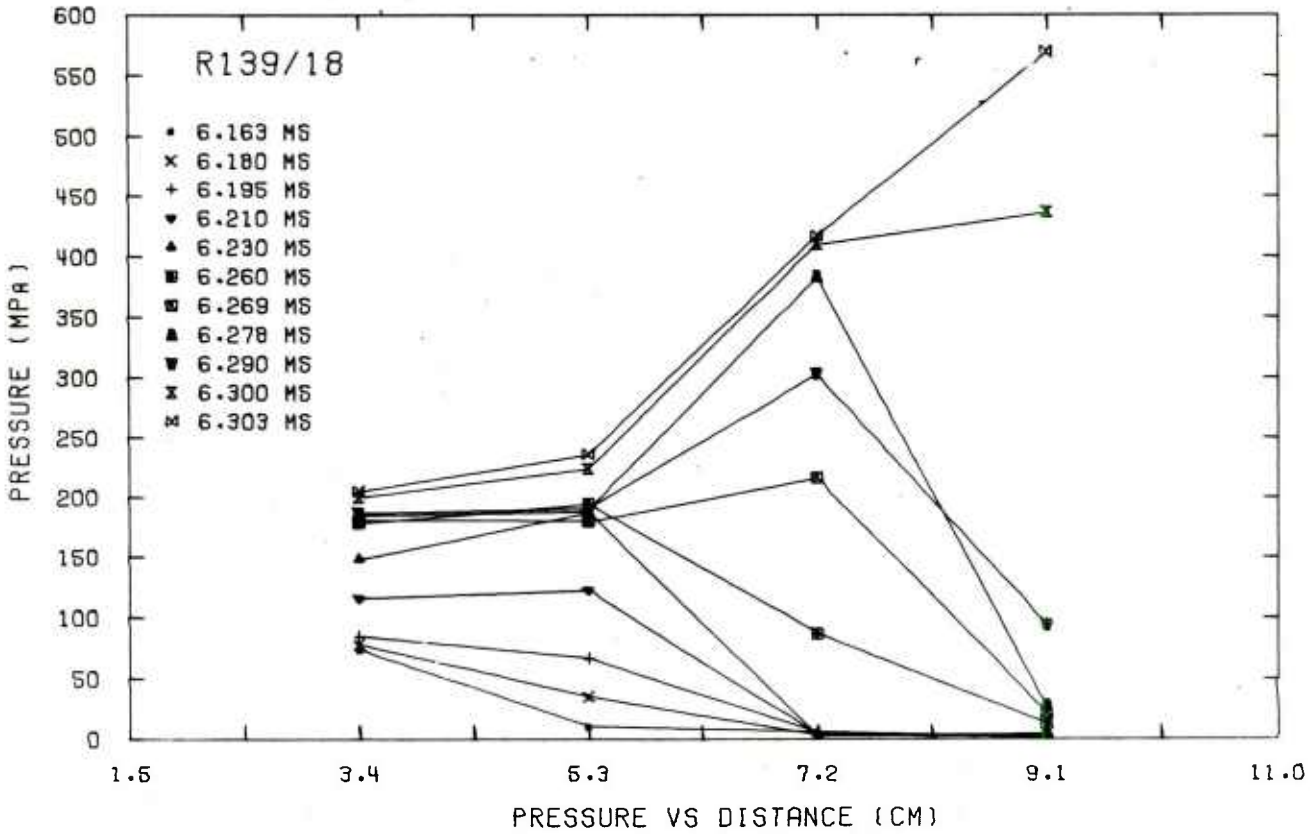
R139/18
6.163 MS
6.180 MS
6.195 MS
6.210 MS
6.230 MS
6.260 MS
6.269 MS
6.278 MS
6.290 MS
6.300 MS
6.303 MS
PRESSURE (MPa)
600
550
500
450
400
350
300
250
200
150
100
50
0
1.5
3.4
5.3
7.2
9.1
11.0
PRESSURE VS DISTANCE (CM)

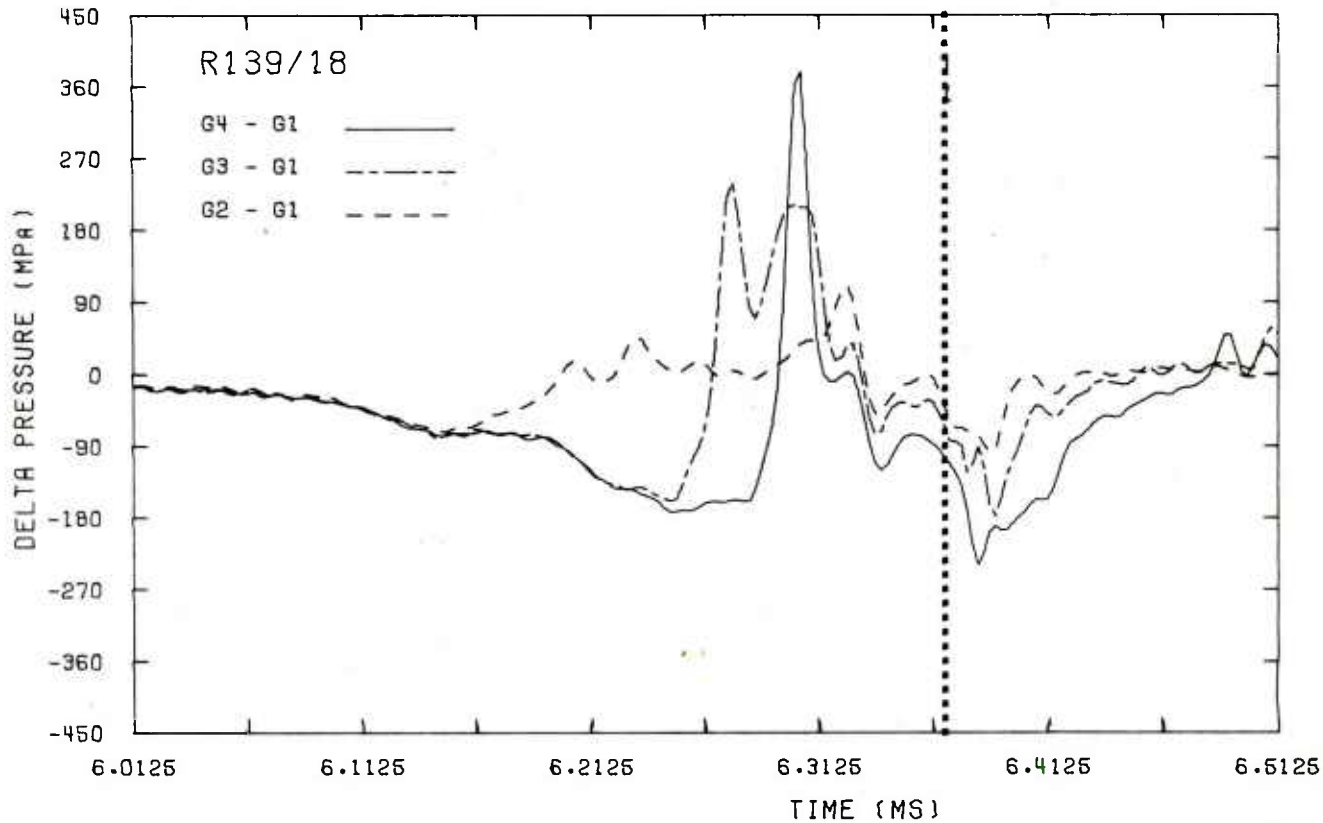
R139/18
G4 - G1
G3 - G1
G2 - G1
DELTA PRESSURE (MPa)
450
360
270
180
90
0
-90
-180
-270
-360
-450
6.0125
6.1125
6.2125
6.3125
6.4125
6.5125
TIME (MS)

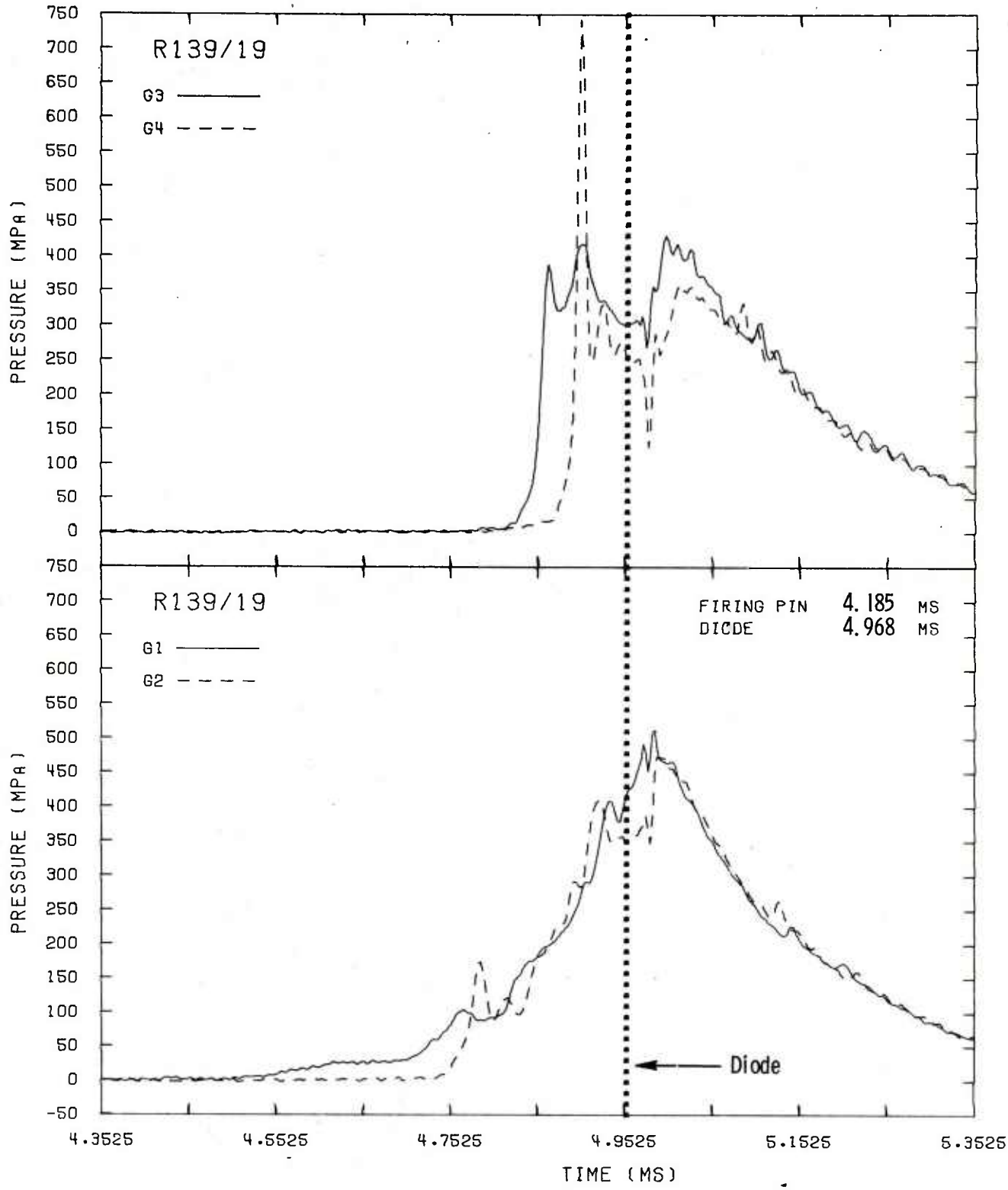
R139/19
G3
G4
PRESSURE (MPa)
R139/19
G1
G2
FIRING PIN 4.185 MS
DICDE 4.968 MS
Diode
PRESSURE (MPa)
TIME (MS)

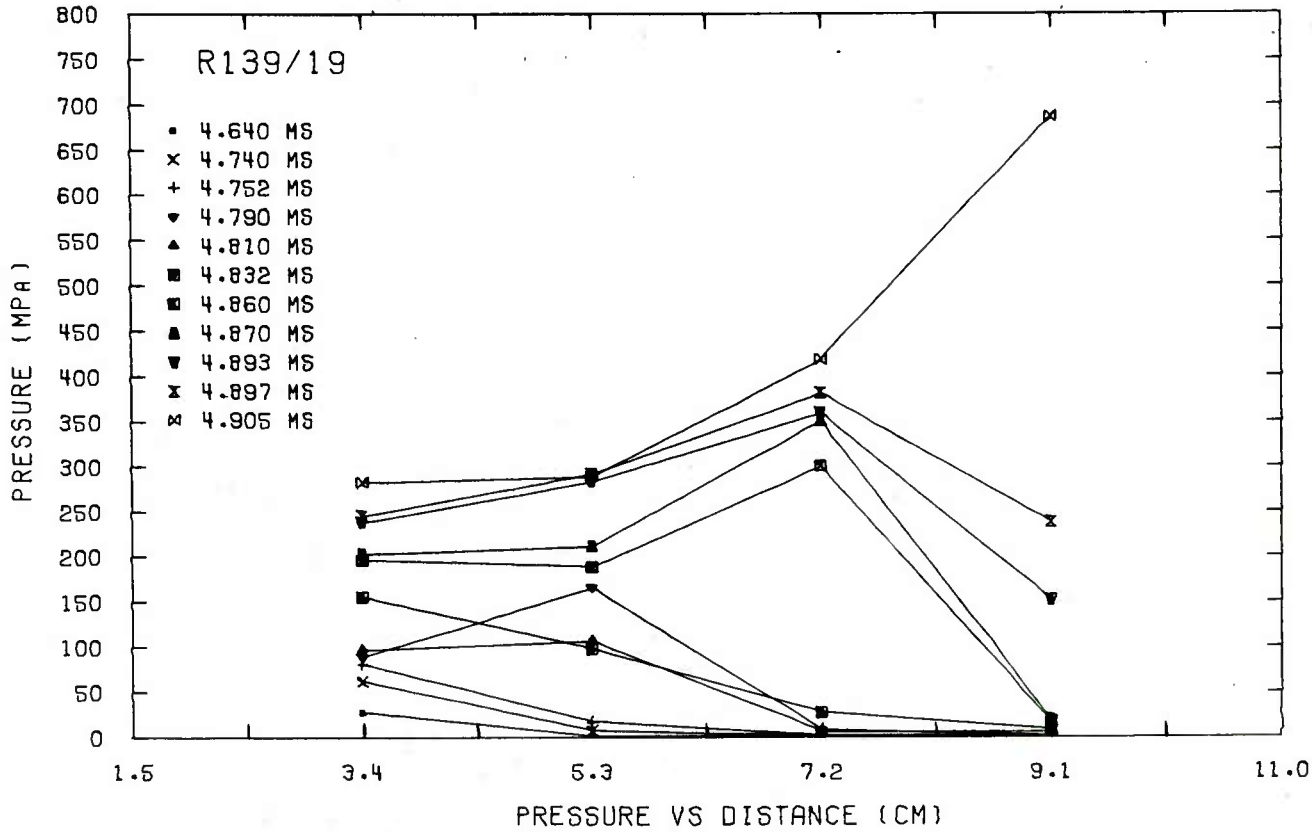
R139/19
4.640 MS
4.740 MS
4.752 MS
4.790 MS
4.810 MS
4.832 MS
4.860 MS
4.870 MS
4.893 MS
4.897 MS
4.905 MS
PRESSURE (MPa)
800
750
700
650
600
550
500
450
400
350
300
250
200
150
100
50
0
1.5
3.4
5.3
7.2
9.1
11.0
PRESSURE VS DISTANCE (CM)

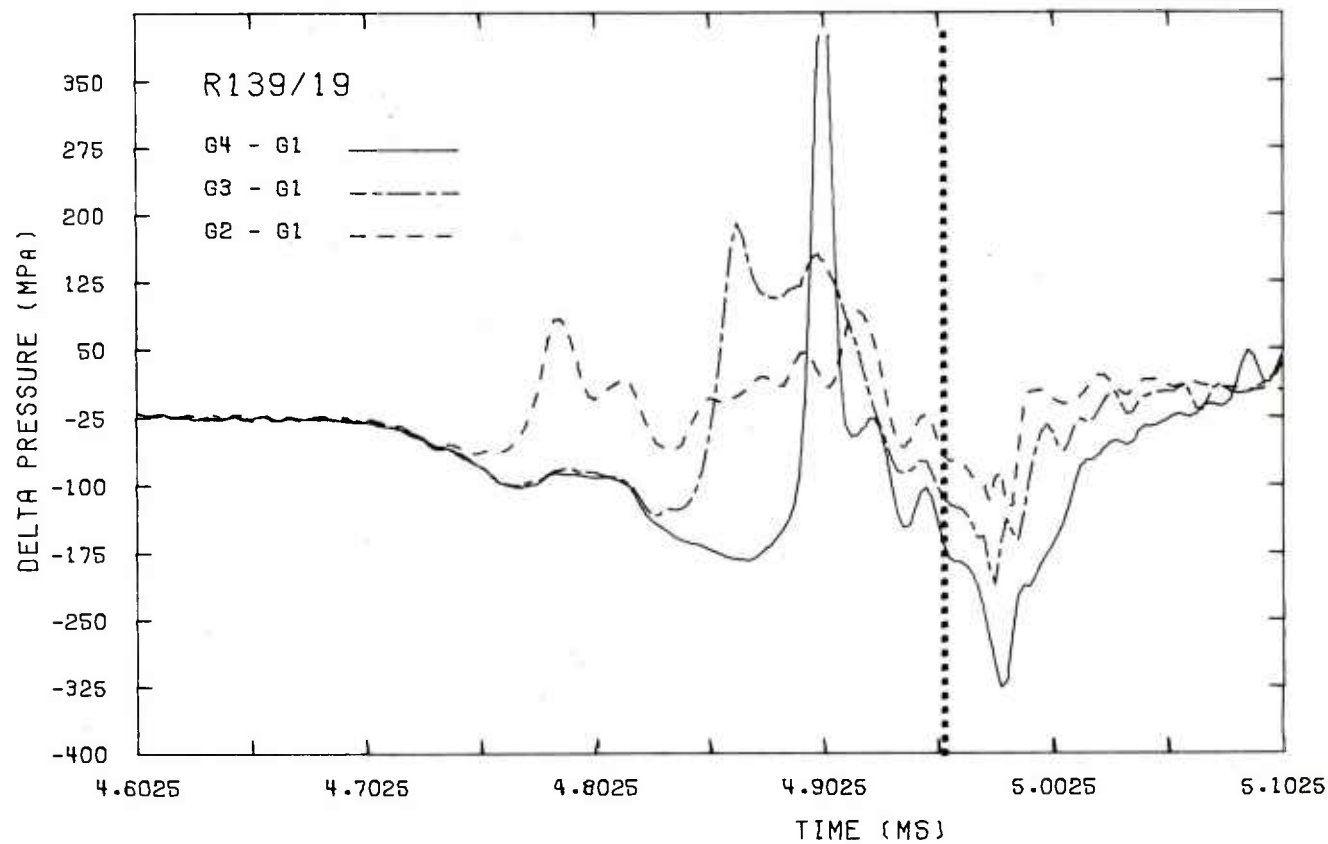
R139/19
G4 - G1
G3 - G1
G2 - G1
DELTA PRESSURE (MPa)
350
275
200
125
50
-25
-100
-175
-250
-325
-400
4.6025
4.7025
4.8025
4.9025
5.0025
5.1025
TIME (MS)

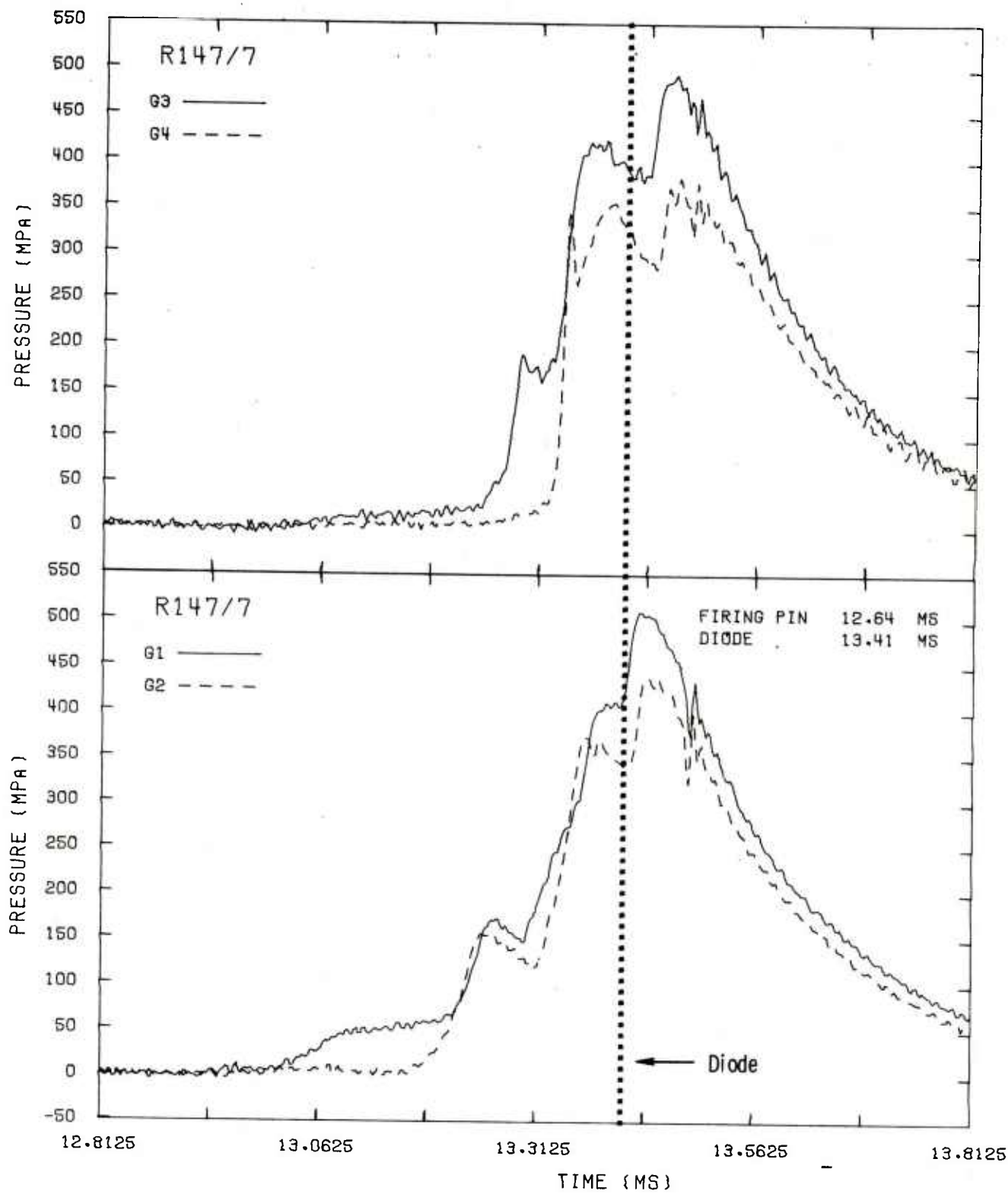
R147/7
G3
G4
PRESSURE (MPa)
R147/7
G1
G2
FIRING PIN 12.64 MS
DIODE 13.41 MS
Diode
PRESSURE (MPa)
TIME (MS)
12.8125
13.0625
13.3125
13.5625
13.8125

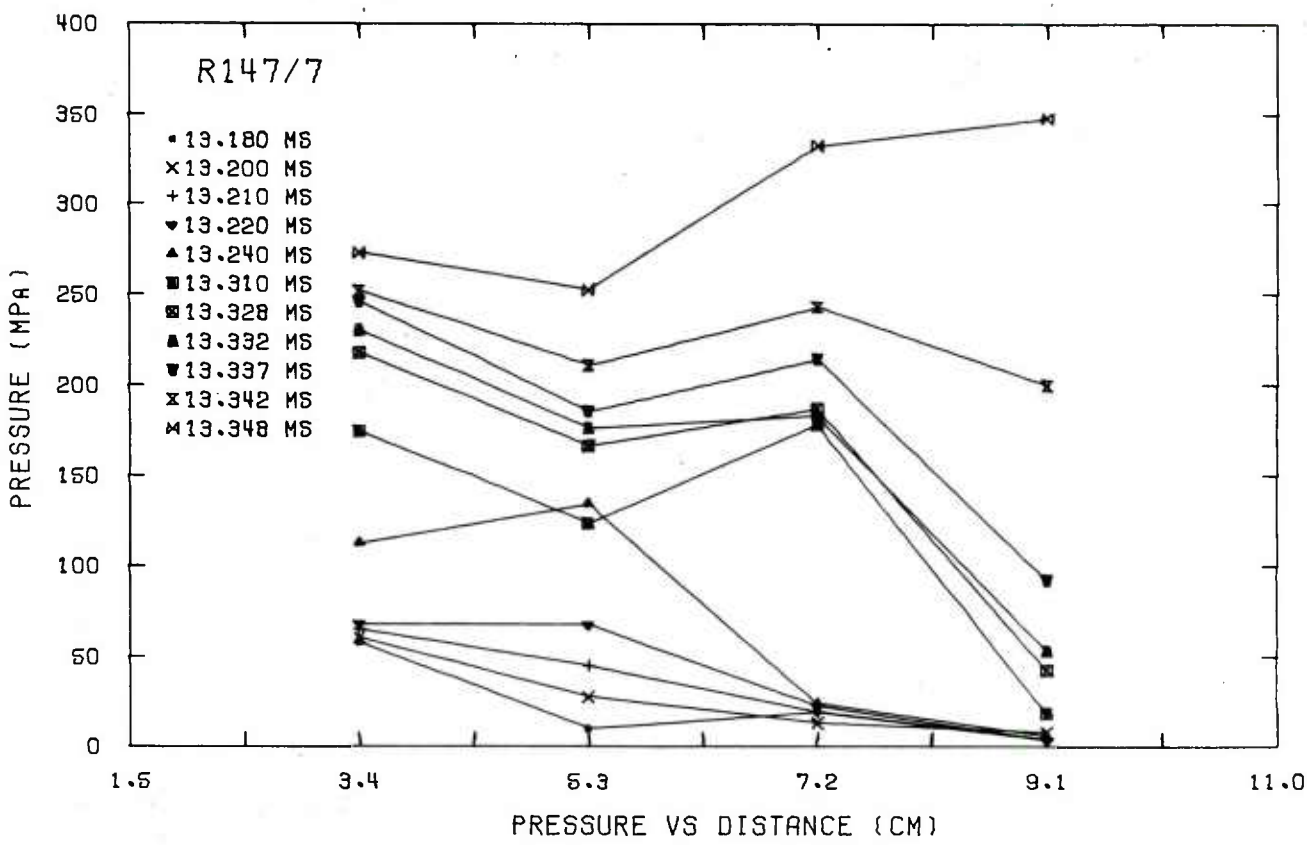
R147/7
13.180 MS
13.200 MS
13.210 MS
13.220 MS
13.240 MS
13.310 MS
13.328 MS
13.332 MS
13.337 MS
13.342 MS
13.348 MS
PRESSURE (MPa)
400
350
300
250
200
150
100
50
0
1.5
3.4
5.3
7.2
9.1
11.0
PRESSURE VS DISTANCE (CM)

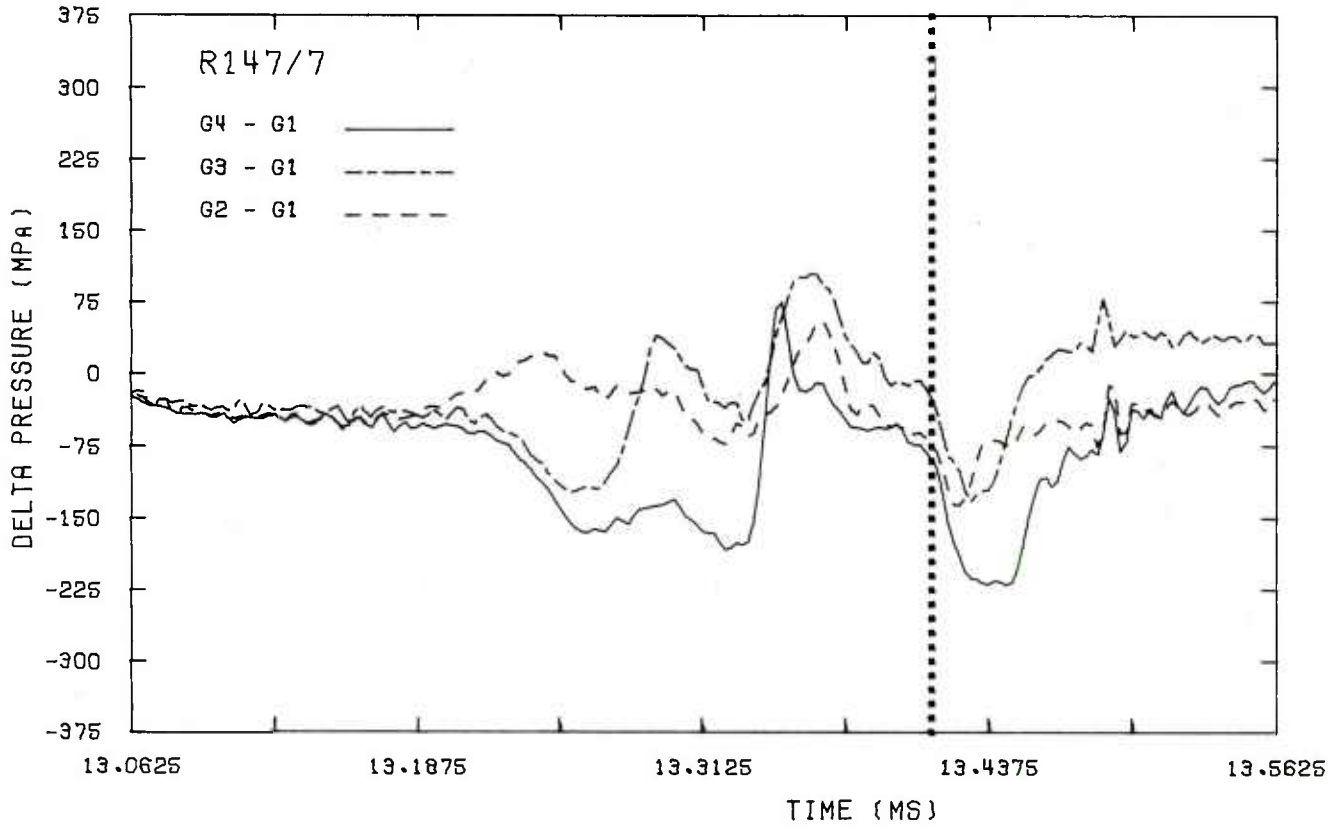
R147/7
G4 - G1
G3 - G1
G2 - G1
DELTA PRESSURE (MPa)
375
300
225
150
75
0
-75
-150
-225
-300
-375
13.0625
13.1875
13.3125
13.4375
13.5625
TIME (MS)

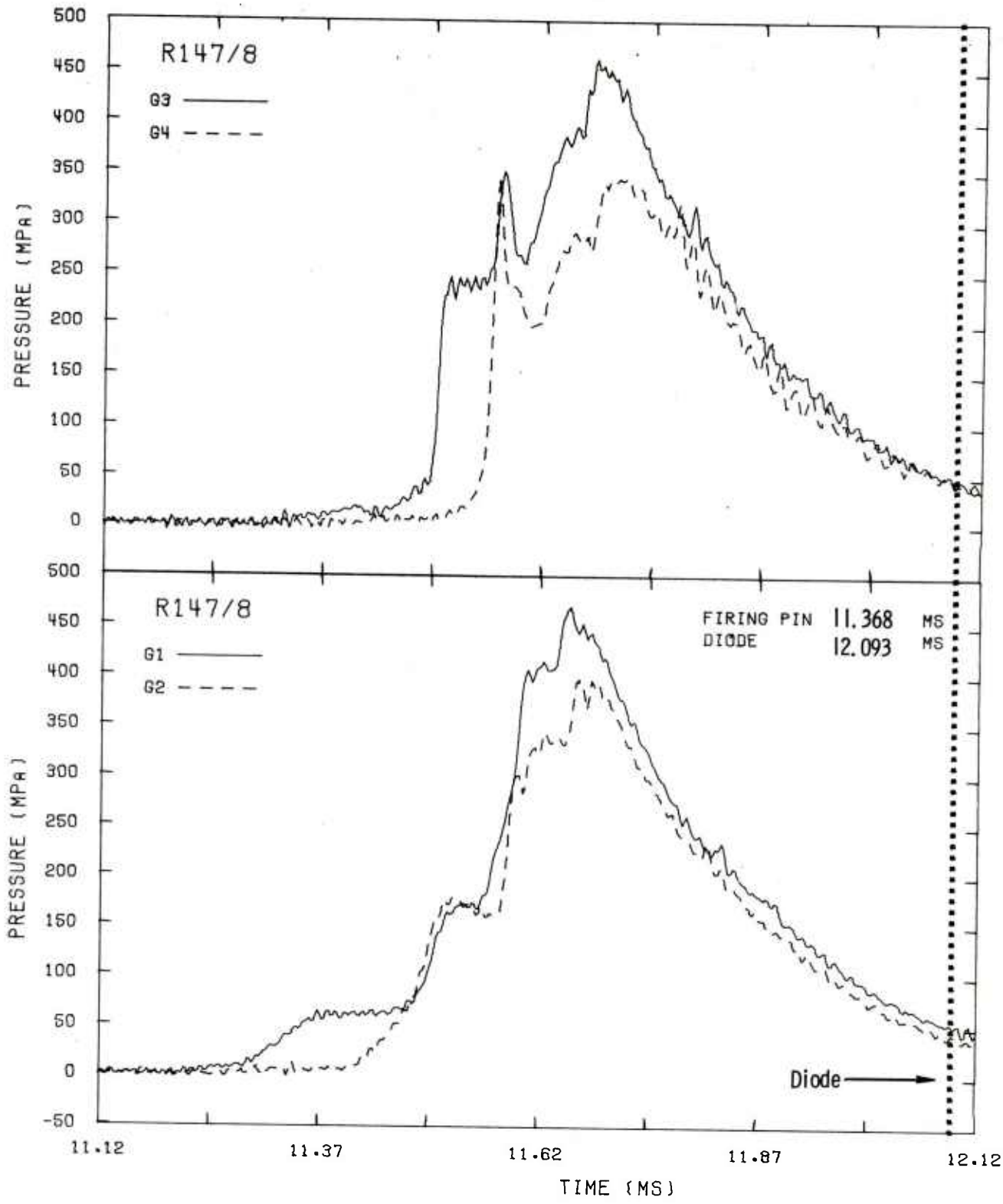
R147/8
G3
G4
PRESSURE (MPa)
500
450
400
350
300
250
200
150
100
50
0
R147/8
G1
G2
FIRING PIN 11.368 MS
DIODE 12.093 MS
Diode
-50
11.12
11.37
11.62
11.87
12.12
TIME (MS)

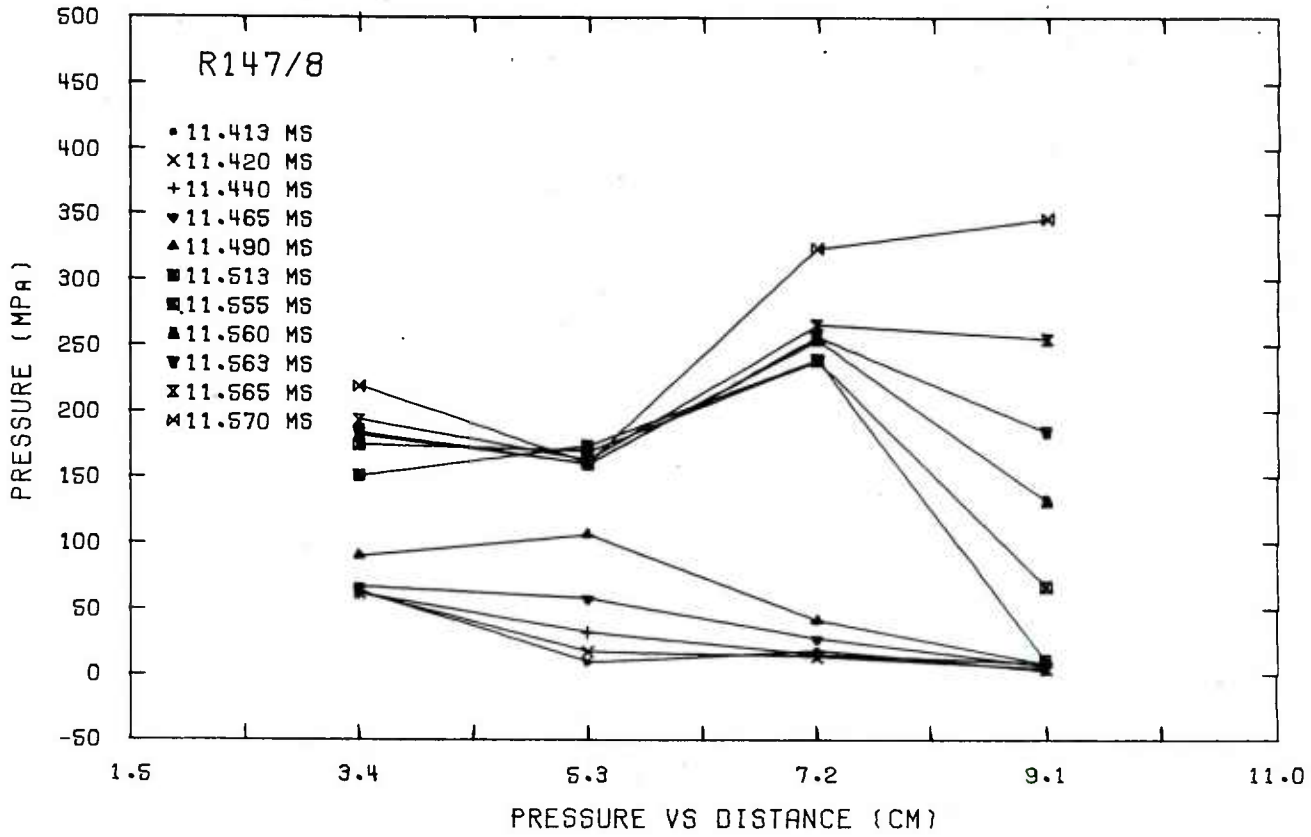
R147/8
•11.413 MS
×11.420 MS
+11.440 MS
▾11.465 MS
▴11.490 MS
■11.513 MS
■11.555 MS
▲11.560 MS
▼11.563 MS
⧗11.565 MS
⋈11.570 MS
PRESSURE (MPa)
500
450
400
350
300
250
200
150
100
50
0
-50
1.5
3.4
5.3
7.2
9.1
11.0
PRESSURE VS DISTANCE (CM)

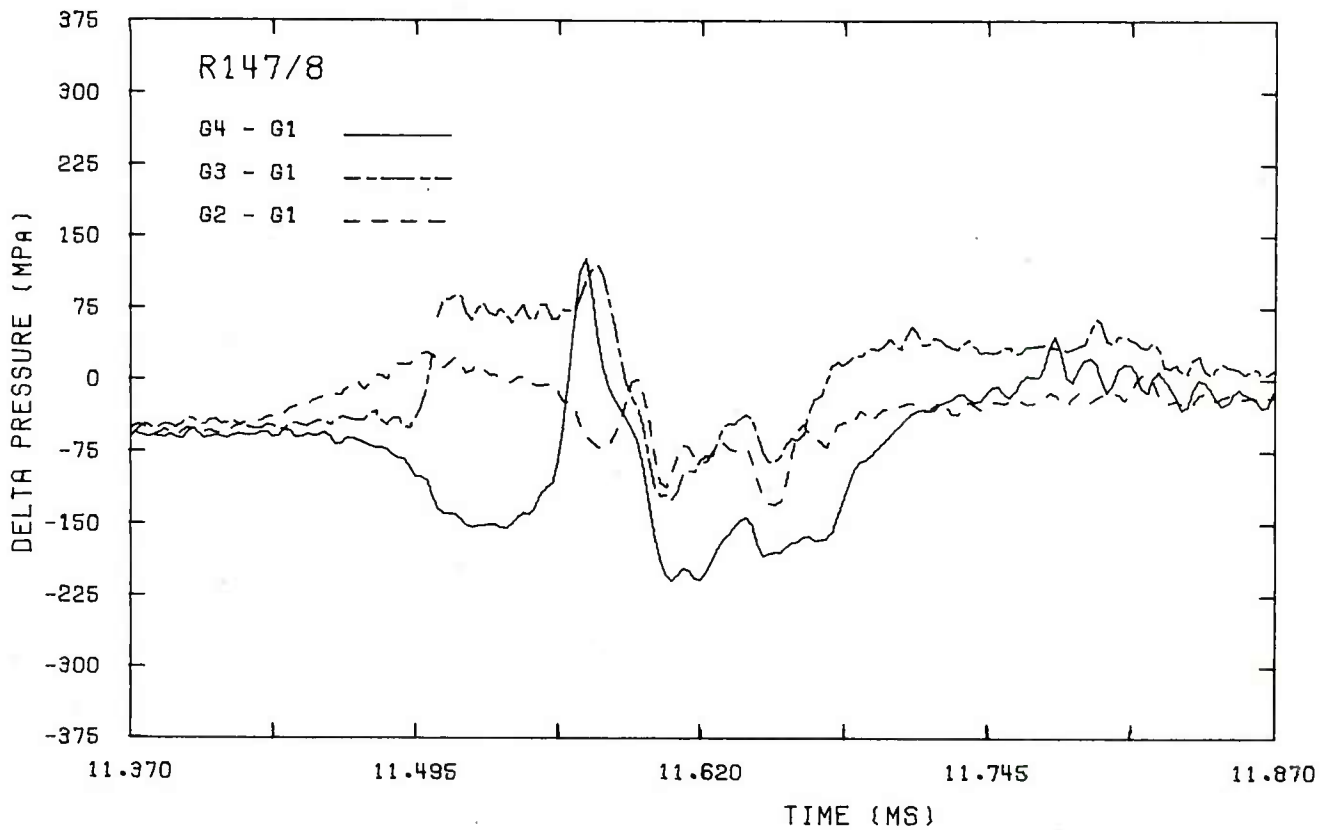
R147/8
G4 - G1
G3 - G1
G2 - G1
DELTA PRESSURE (MPa)
375
300
225
150
75
0
-75
-150
-225
-300
-375
11.370
11.495
11.620
11.745
11.870
TIME (MS)

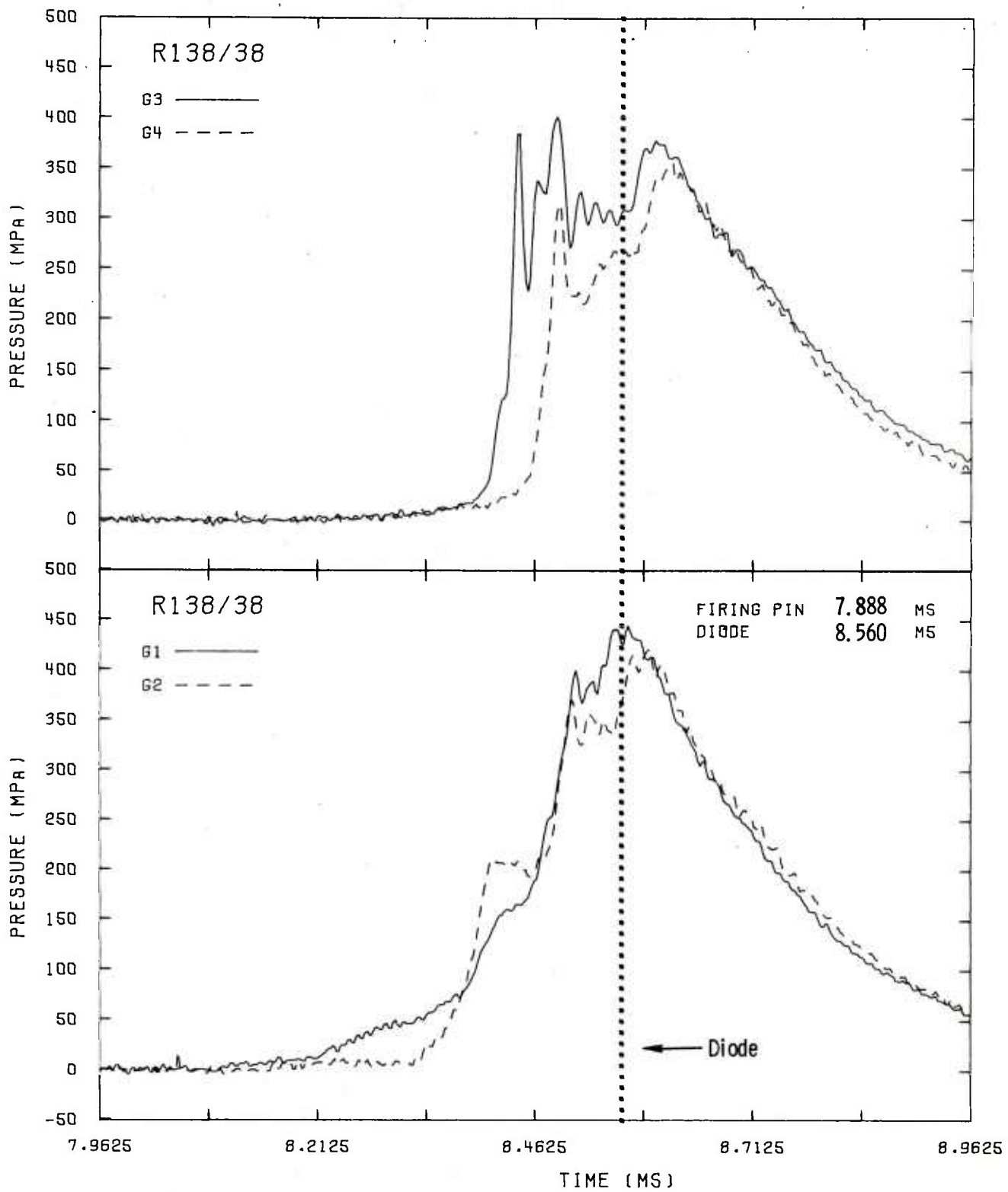
R138/38
G3
G4
PRESSURE (MPa)
500
450
400
350
300
250
200
150
100
50
0
R138/38
G1
G2
FIRING PIN 7.888 MS
DIODE 8.560 MS
Diode
-50
7.9625
8.2125
8.4625
8.7125
8.9625
TIME (MS)

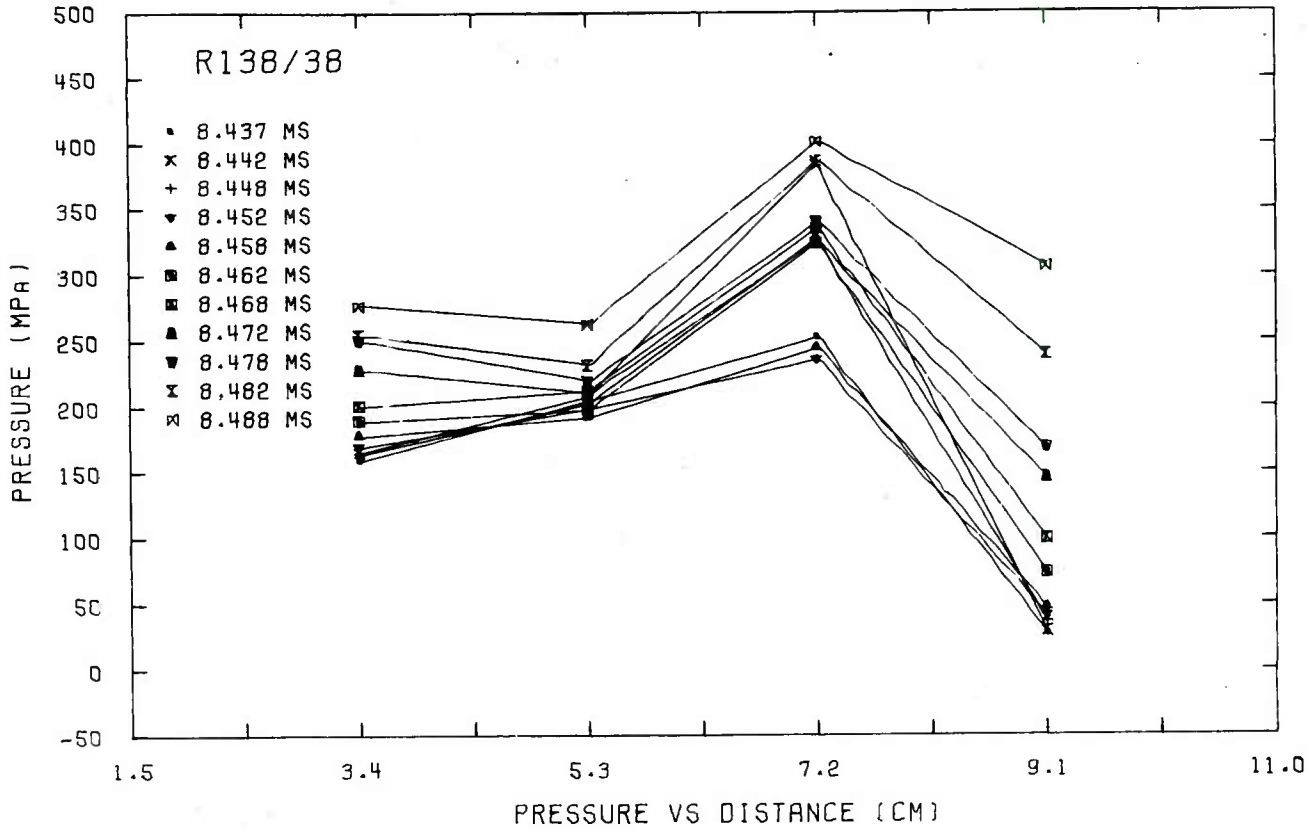
R138/38
8.437 MS
8.442 MS
8.448 MS
8.452 MS
8.458 MS
8.462 MS
8.468 MS
8.472 MS
8.478 MS
8.482 MS
8.488 MS
PRESSURE (MPa)
500
450
400
350
300
250
200
150
100
50
0
-50
1.5
3.4
5.3
7.2
9.1
11.0
PRESSURE VS DISTANCE (CM)

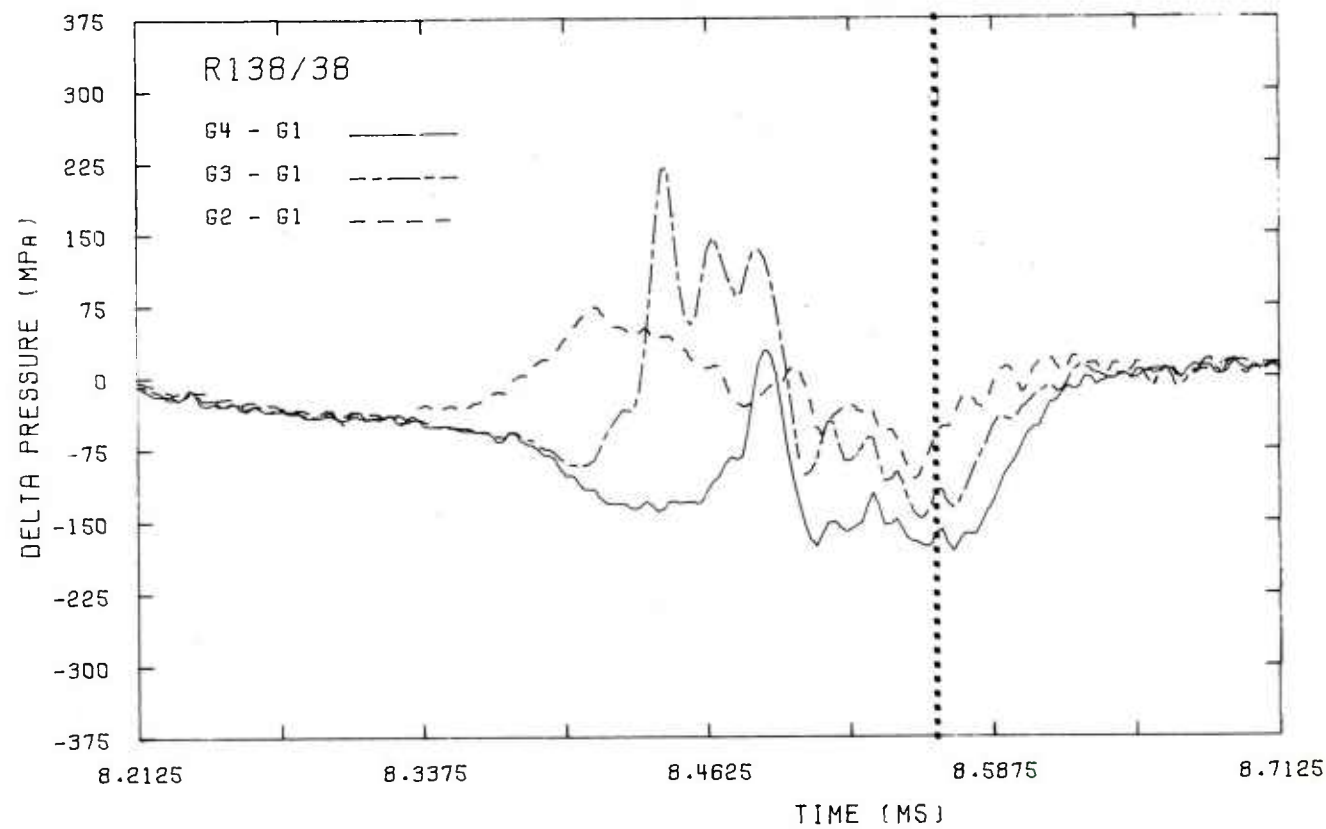
R138/38
G4 - G1
G3 - G1
G2 - G1
DELTA PRESSURE (MPa)
375
300
225
150
75
0
-75
-150
-225
-300
-375
8.2125
8.3375
8.4625
8.5875
8.7125
TIME (MS)

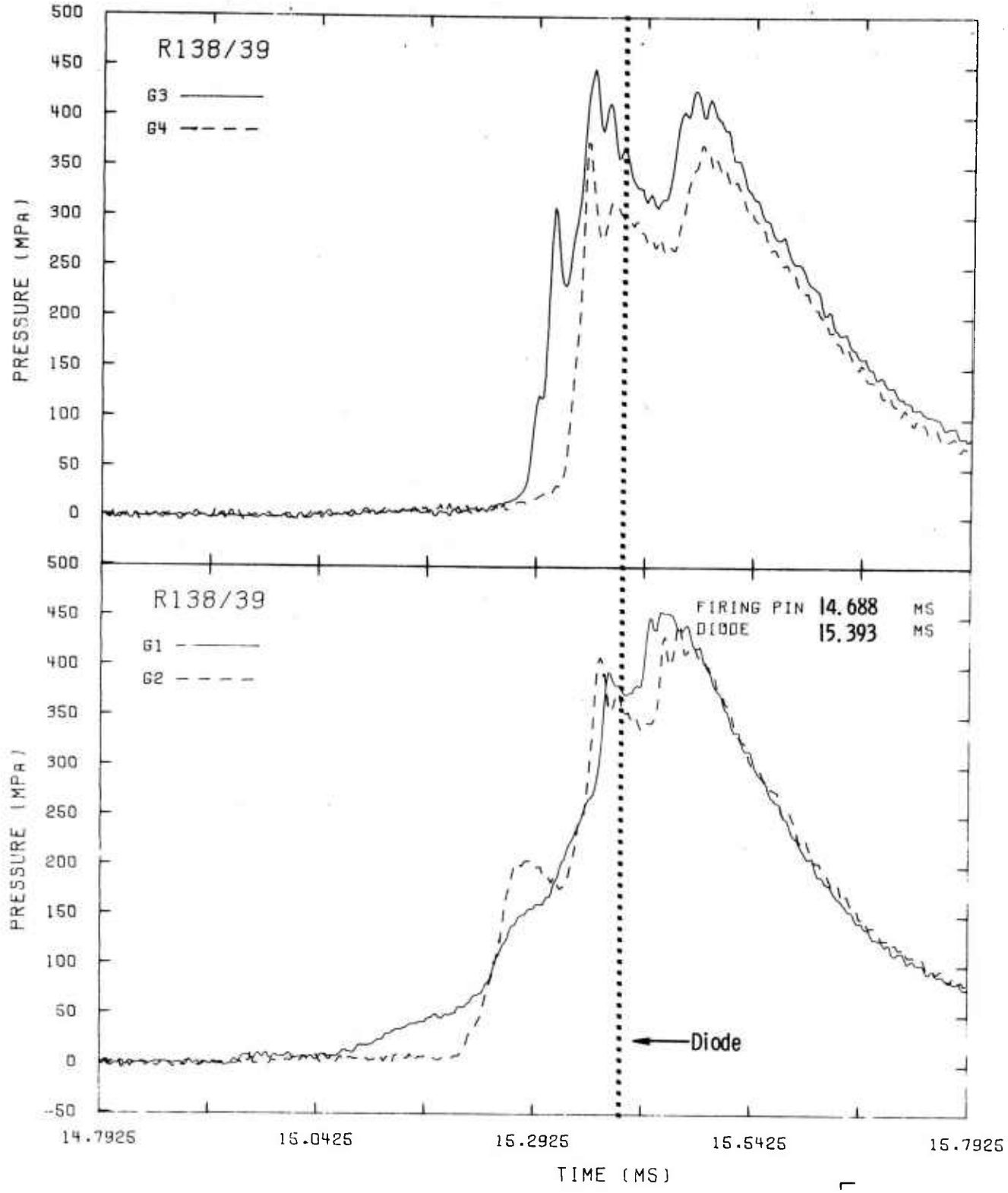
R138/39
G3
G4
PRESSURE (MPa)
R138/39
G1
G2
FIRING PIN 14.688 MS
DIODE 15.393 MS
Diode
PRESSURE (MPa)
TIME (MS)
14.7925
15.0425
15.2925
15.5425
15.7925

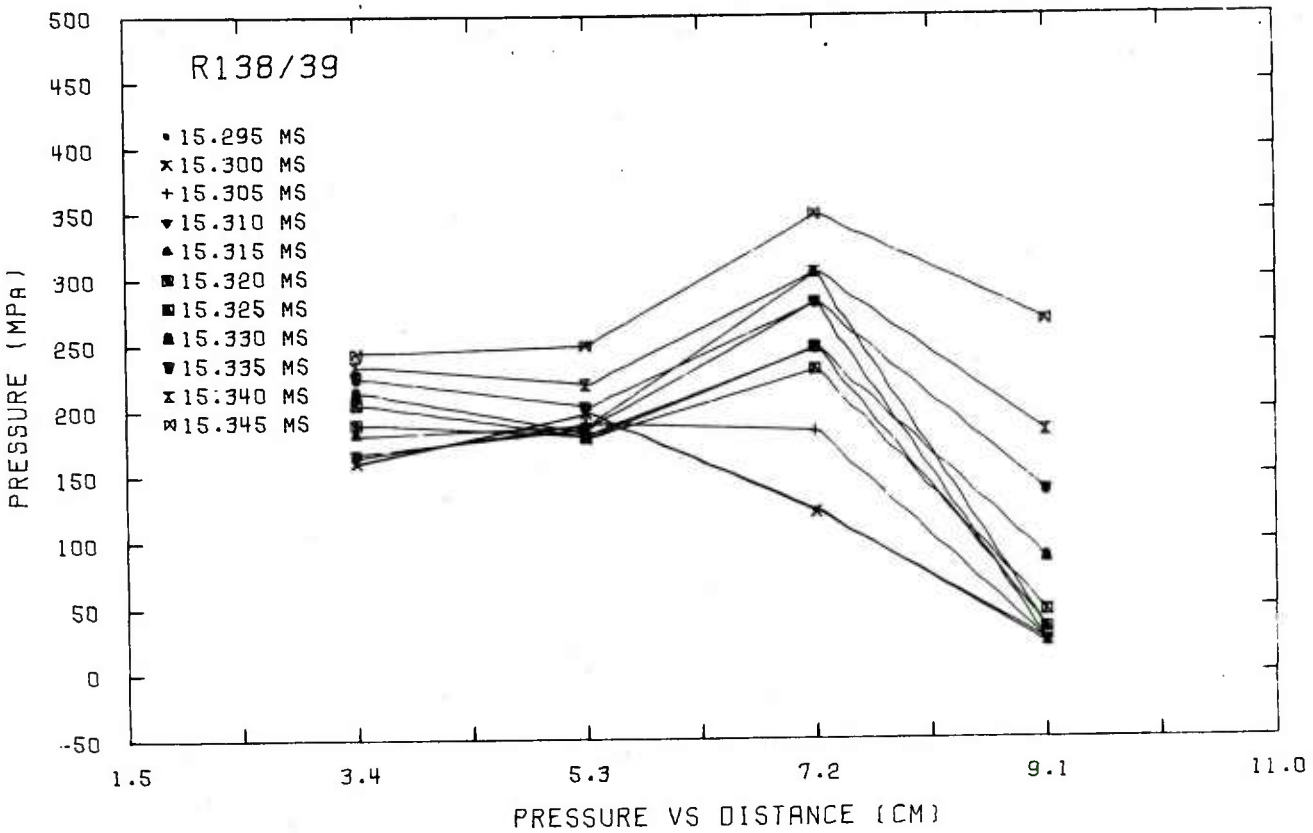
R138/39
• 15.295 MS
× 15.300 MS
+ 15.305 MS
▼ 15.310 MS
▲ 15.315 MS
■ 15.320 MS
■ 15.325 MS
▲ 15.330 MS
▼ 15.335 MS
⧗ 15.340 MS
⧗ 15.345 MS
PRESSURE (MPa)
500
450
400
350
300
250
200
150
100
50
0
-50
1.5
3.4
5.3
7.2
9.1
11.0
PRESSURE VS DISTANCE (CM)

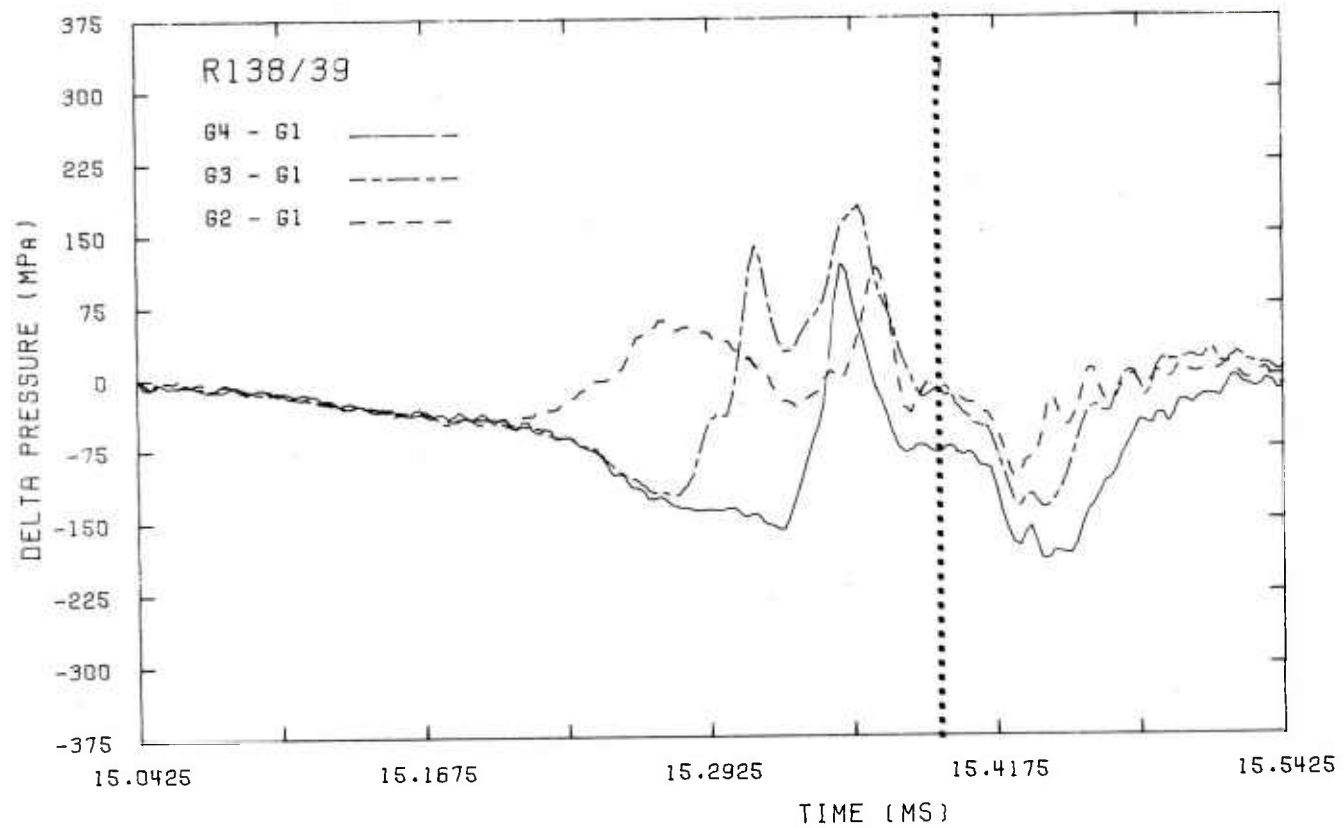
R138/39
G4 - G1
G3 - G1
G2 - G1
DELTA PRESSURE (MPa)
375
300
225
150
75
0
-75
-150
-225
-300
-375
15.0425
15.1675
15.2925
15.4175
15.5425
TIME (MS)

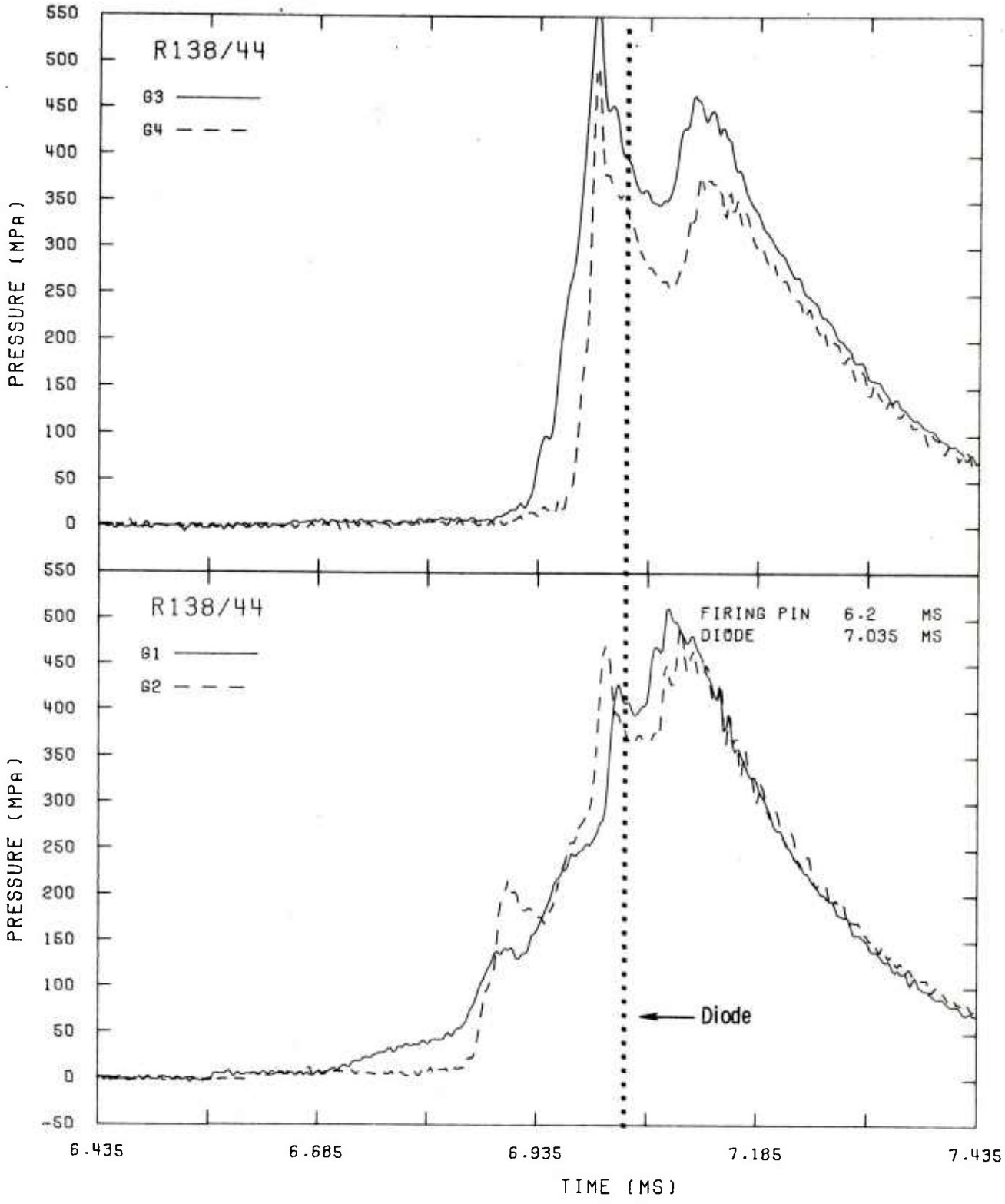
R138/44
G3
G4
PRESSURE (MPa)
550
500
450
400
350
300
250
200
150
100
50
0
R138/44
G1
G2
FIRING PIN 6.2 MS
DIODE 7.035 MS
Diode
-50
6.435
6.685
6.935
7.185
7.435
TIME (MS)

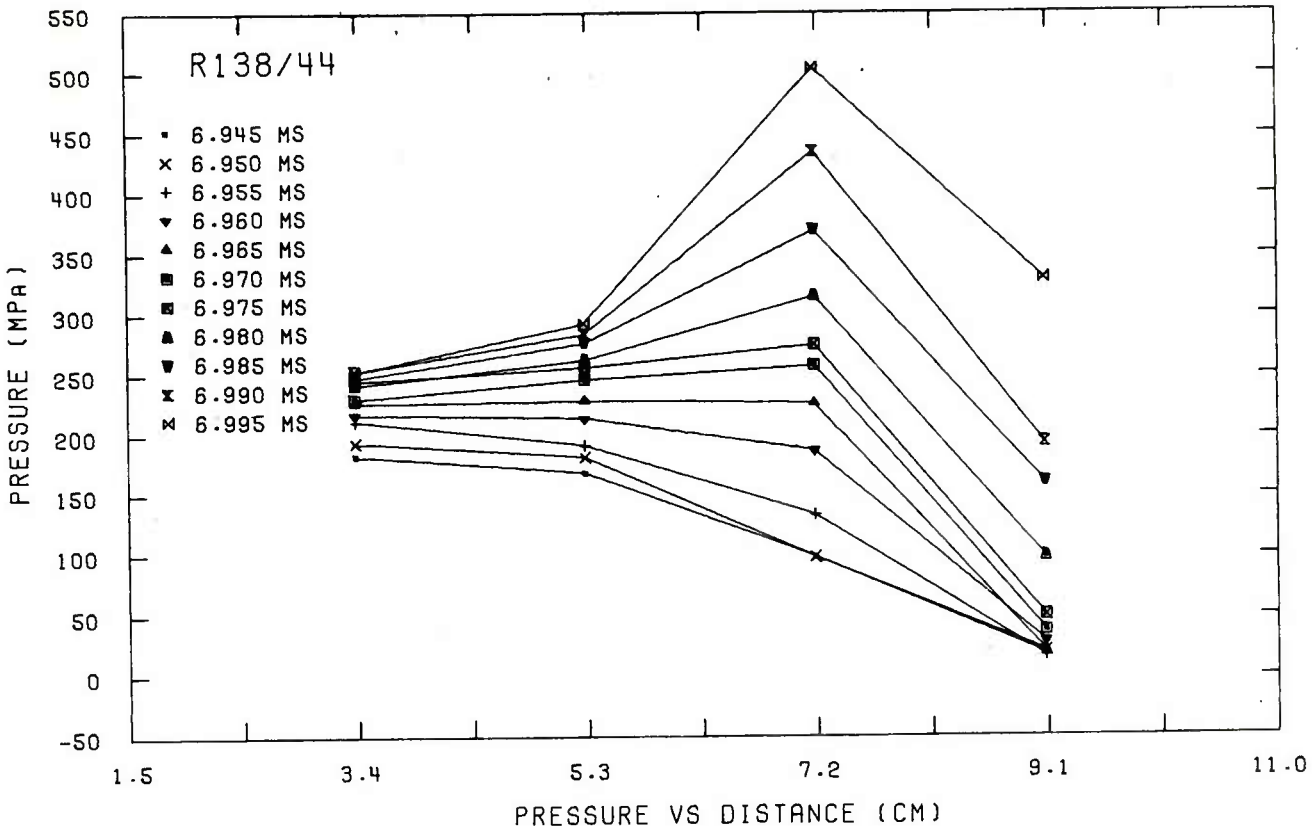
R138/44
6.945 MS
6.950 MS
6.955 MS
6.960 MS
6.965 MS
6.970 MS
6.975 MS
6.980 MS
6.985 MS
6.990 MS
6.995 MS
PRESSURE (MPa)
550
500
450
400
350
300
250
200
150
100
50
0
-50
1.5
3.4
5.3
7.2
9.1
11.0
PRESSURE VS DISTANCE (CM)

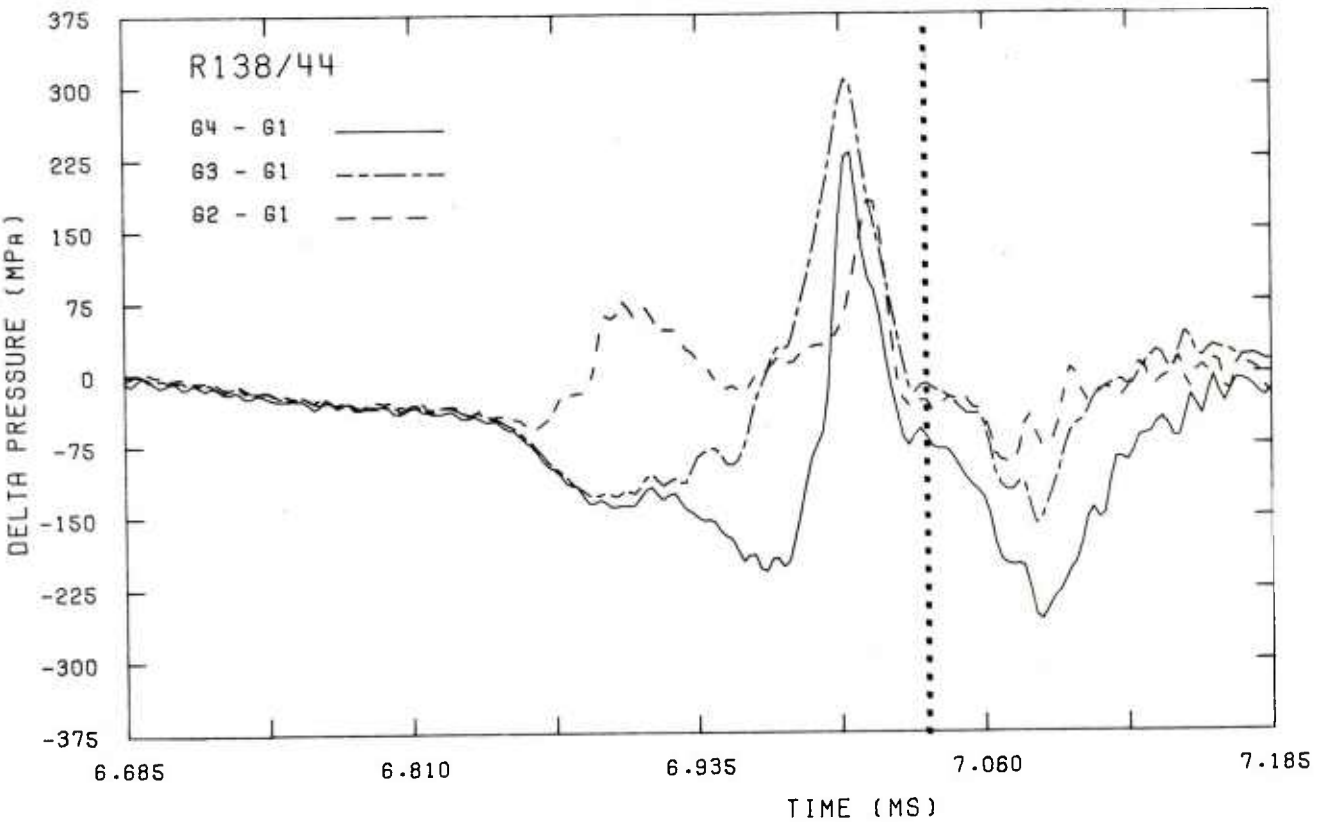
R138/44
G4 - G1
G3 - G1
G2 - G1
DELTA PRESSURE (MPa)
375
300
225
150
75
0
-75
-150
-225
-300
-375
6.685
6.810
6.935
7.060
7.185
TIME (MS)

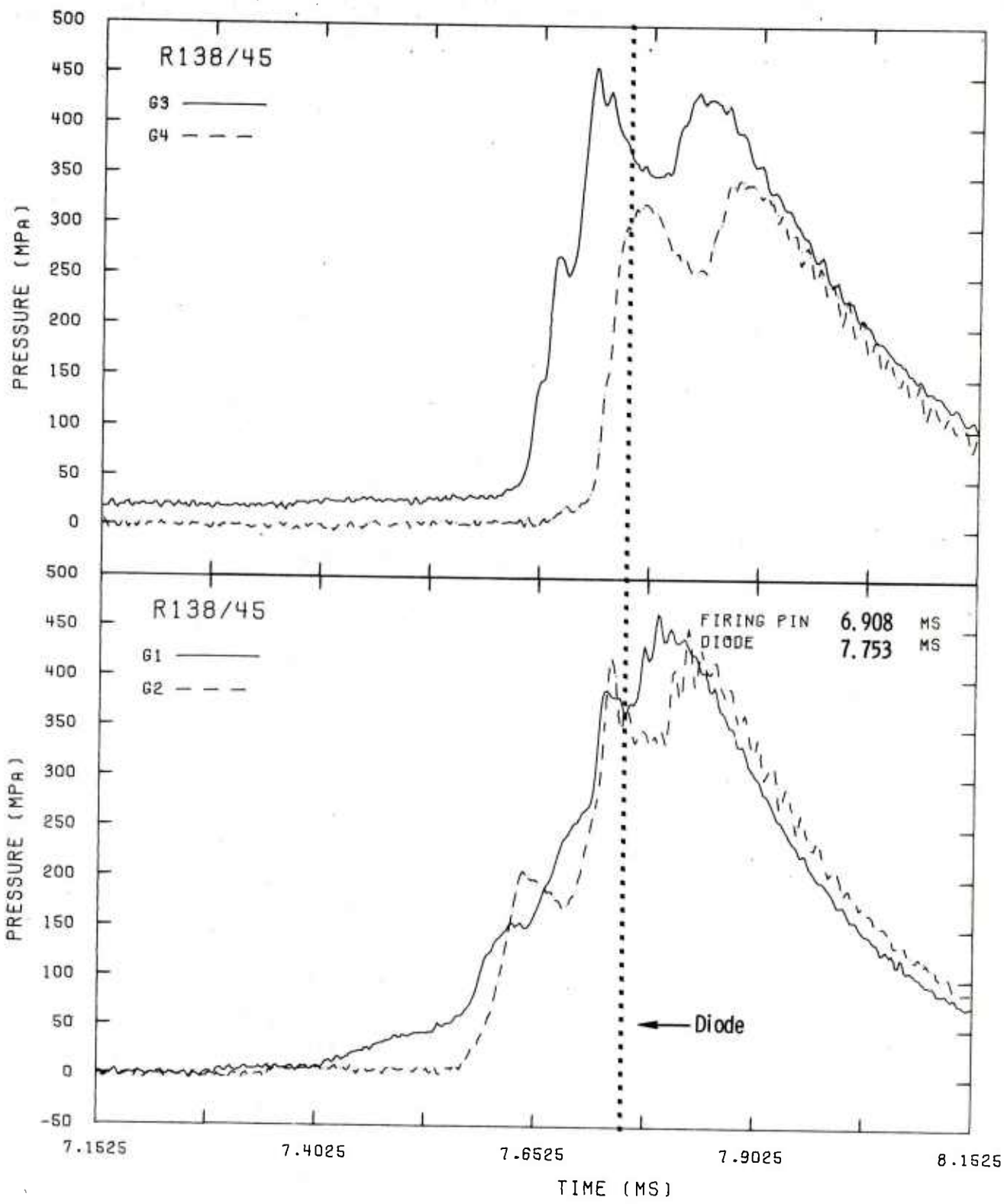
R138/45
G3
G4
PRESSURE (MPa)
500
450
400
350
300
250
200
150
100
50
0
R138/45
G1
G2
FIRING PIN 6.908 MS
DIODE 7.753 MS
Diode
-50
7.1525
7.4025
7.6525
7.9025
8.1525
TIME (MS)

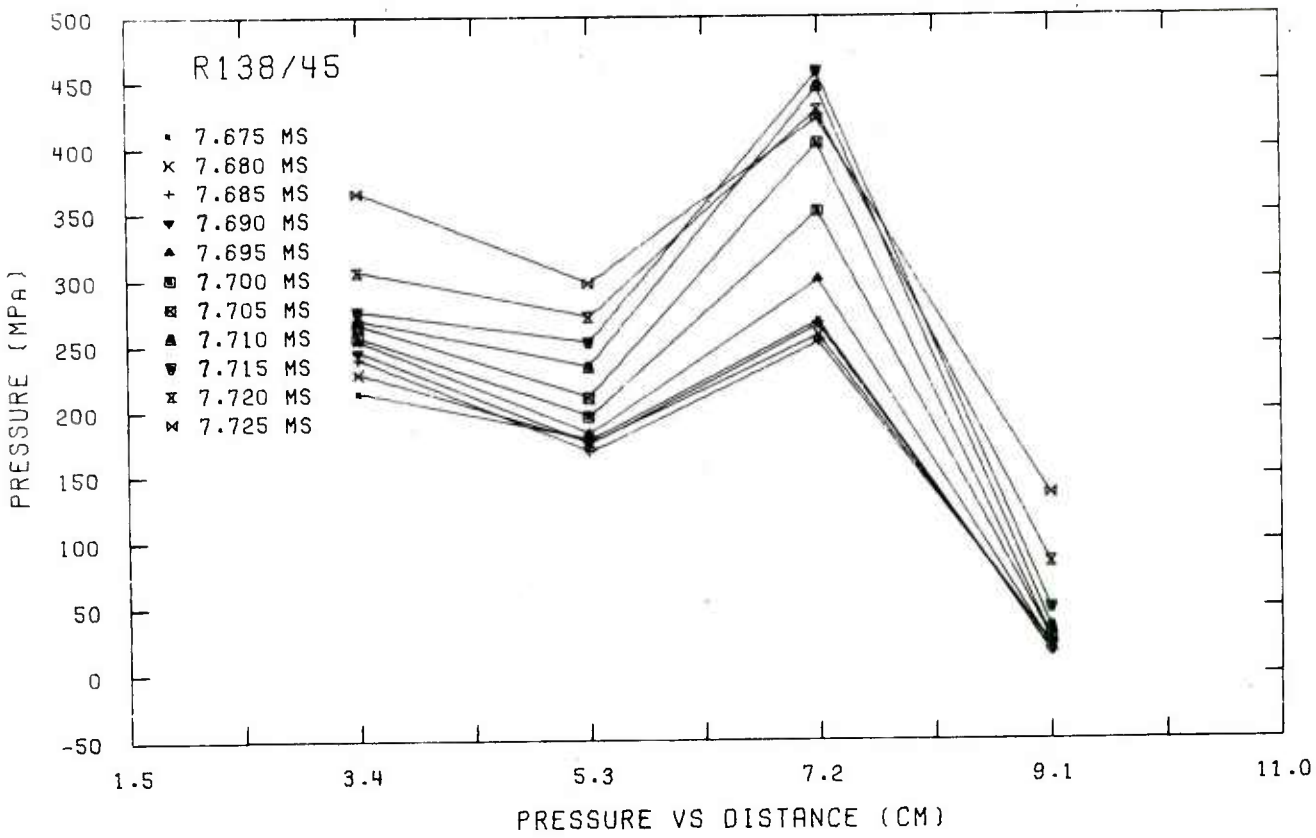
R138/45
7.675 MS
7.680 MS
7.685 MS
7.690 MS
7.695 MS
7.700 MS
7.705 MS
7.710 MS
7.715 MS
7.720 MS
7.725 MS
PRESSURE (MPa)
500
450
400
350
300
250
200
150
100
50
0
-50
1.5
3.4
5.3
7.2
9.1
11.0
PRESSURE VS DISTANCE (CM)

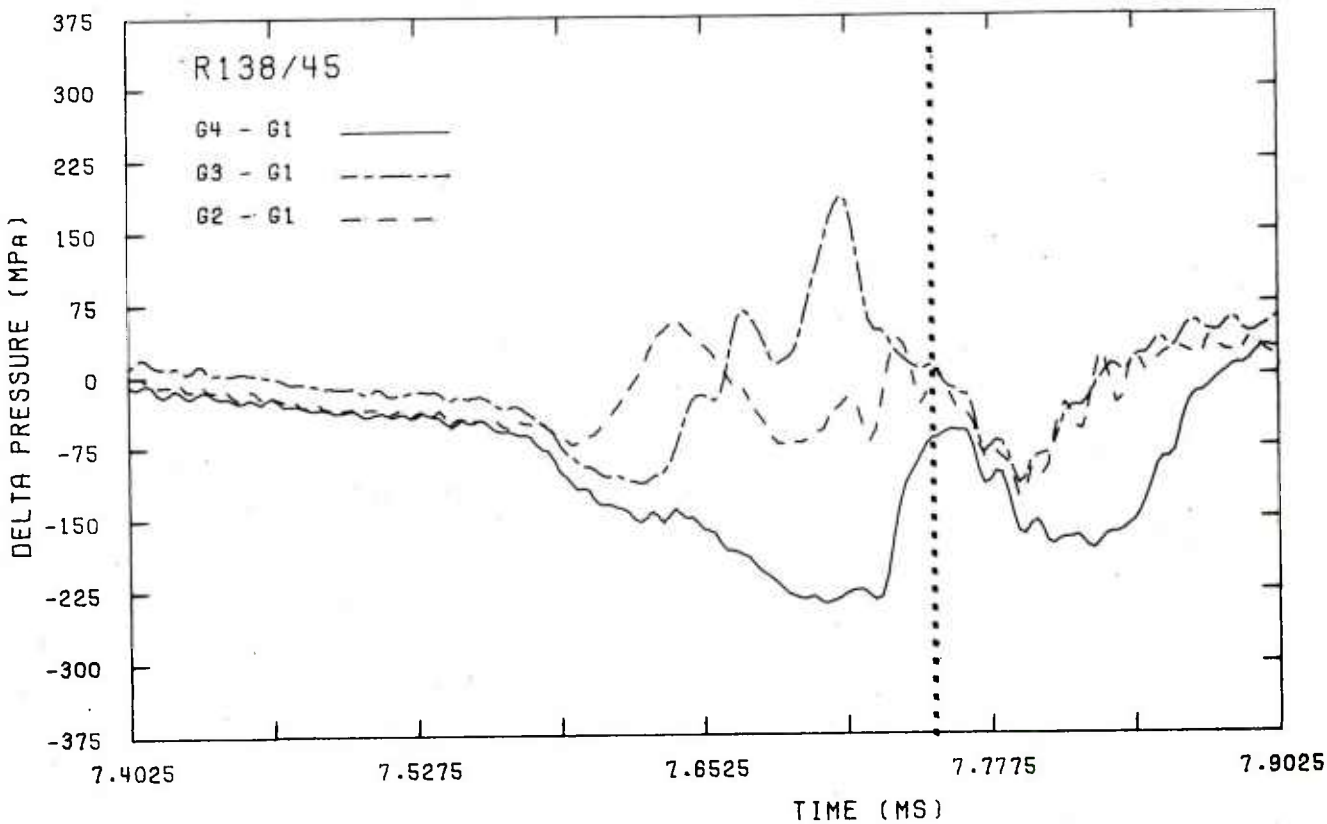
R138/45
G4 - G1
G3 - G1
G2 - G1
DELTA PRESSURE (MPa)
375
300
225
150
75
0
-75
-150
-225
-300
-375
7.4025
7.5275
7.6525
7.7775
7.9025
TIME (MS)

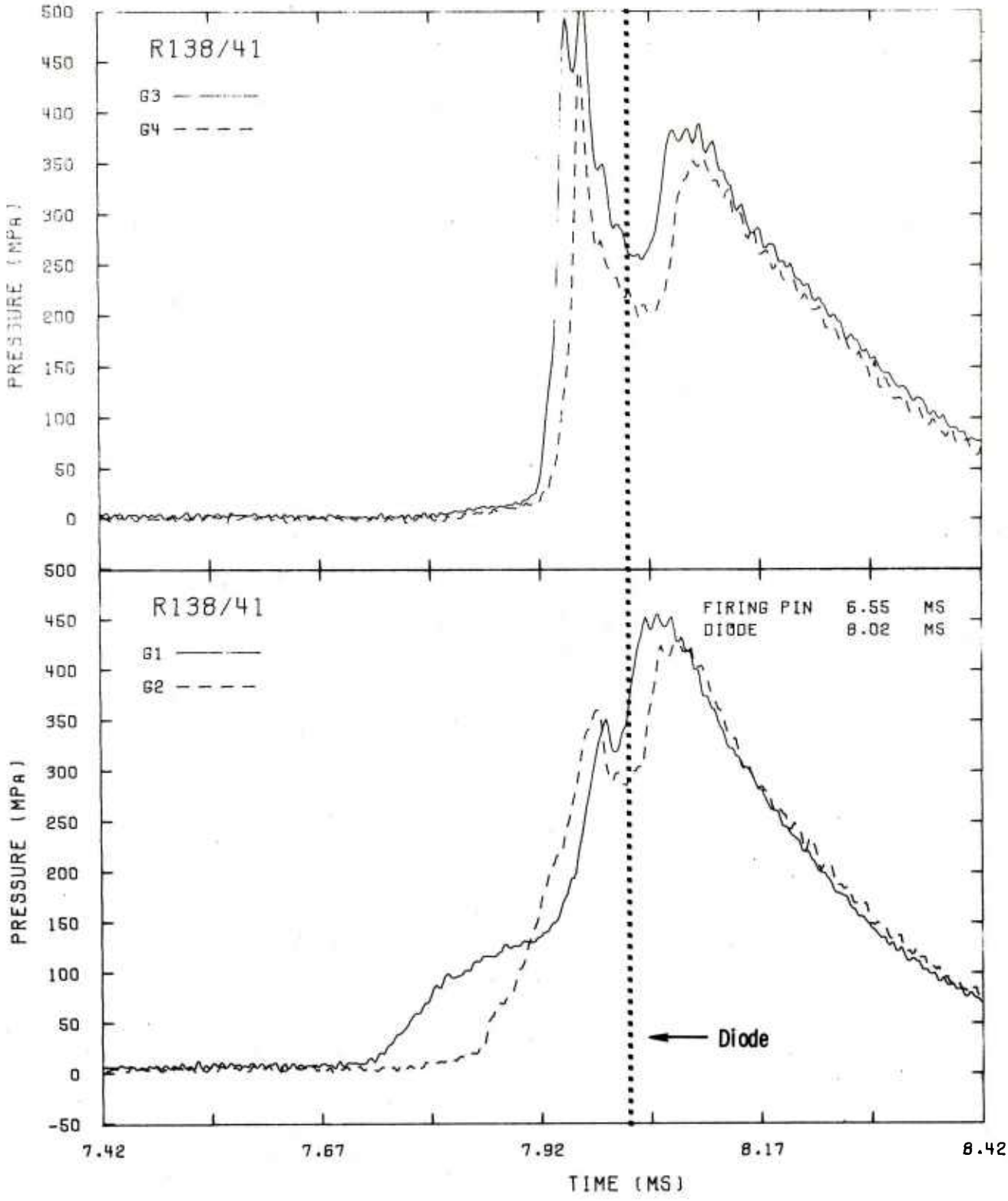
R138/41
G3
G4
PRESSURE (MPa)
500
450
400
350
300
250
200
150
100
50
0
R138/41
G1
G2
FIRING PIN 6.55 MS
DIODE 8.02 MS
Diode
PRESSURE (MPa)
500
450
400
350
300
250
200
150
100
50
0
-50
7.42
7.67
7.92
8.17
8.42
TIME (MS)

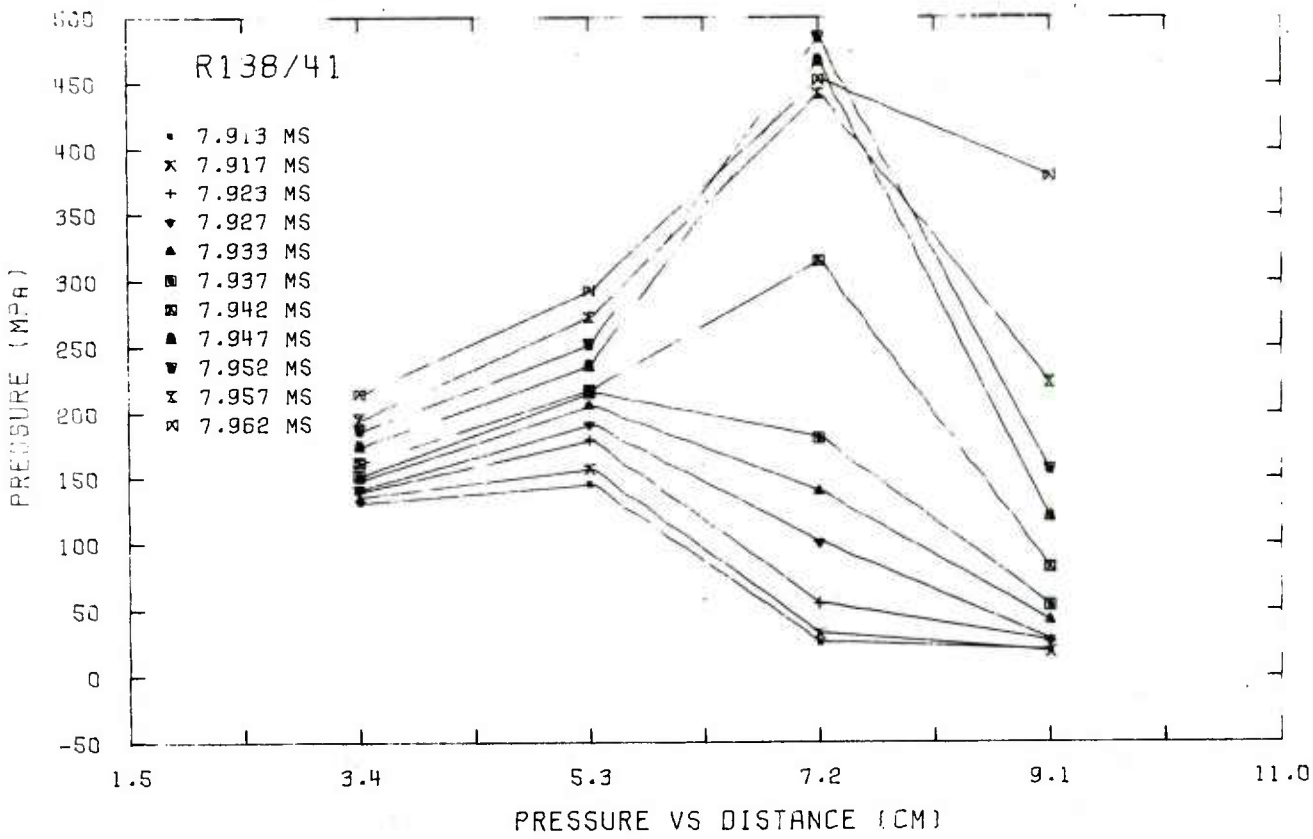
R138/41
7.913 MS
7.917 MS
7.923 MS
7.927 MS
7.933 MS
7.937 MS
7.942 MS
7.947 MS
7.952 MS
7.957 MS
7.962 MS
PRESSURE (MPa)
500
450
400
350
300
250
200
150
100
50
0
-50
1.5
3.4
5.3
7.2
9.1
11.0
PRESSURE VS DISTANCE (CM)

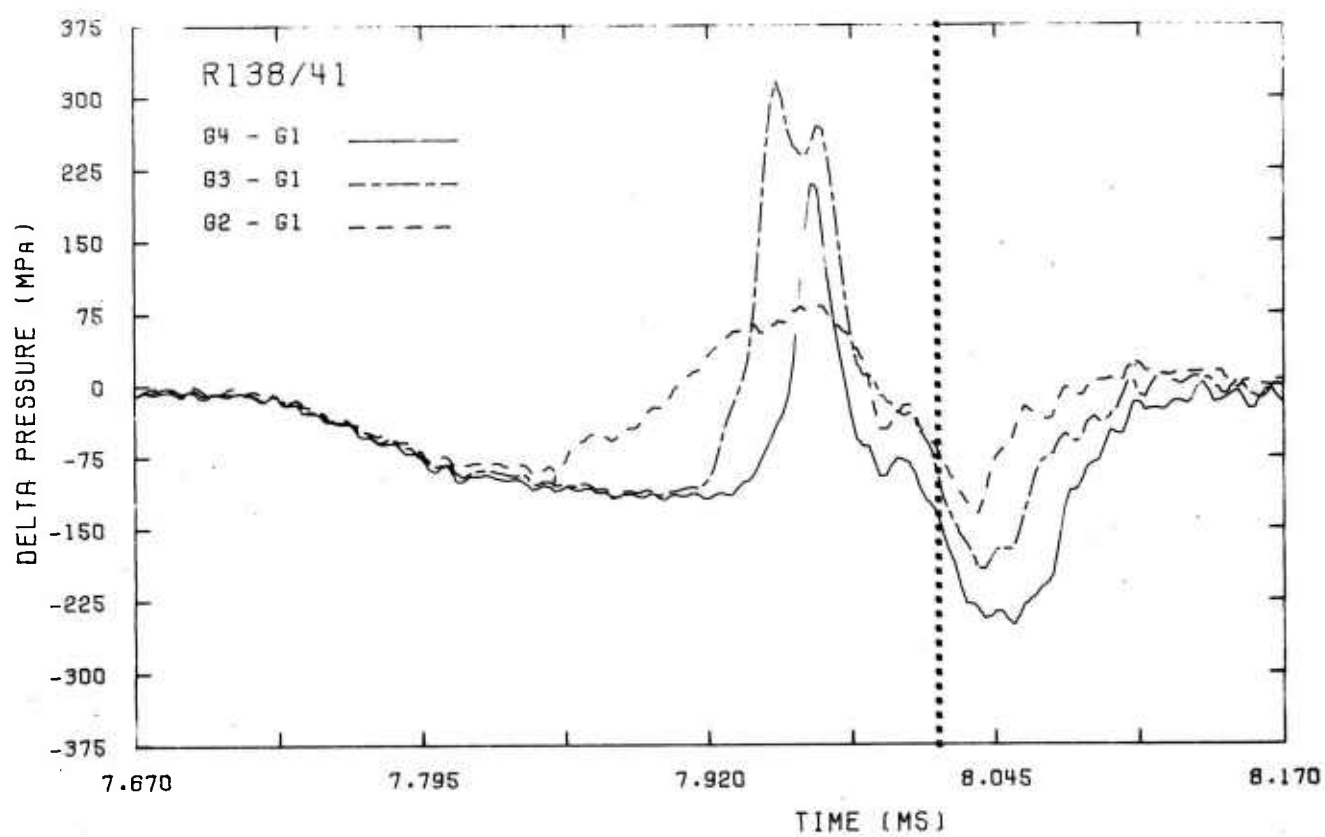
R138/41
G4 - G1
G3 - G1
G2 - G1
DELTA PRESSURE (MPa)
375
300
225
150
75
0
-75
-150
-225
-300
-375
7.670
7.795
7.920
8.045
8.170
TIME (MS)

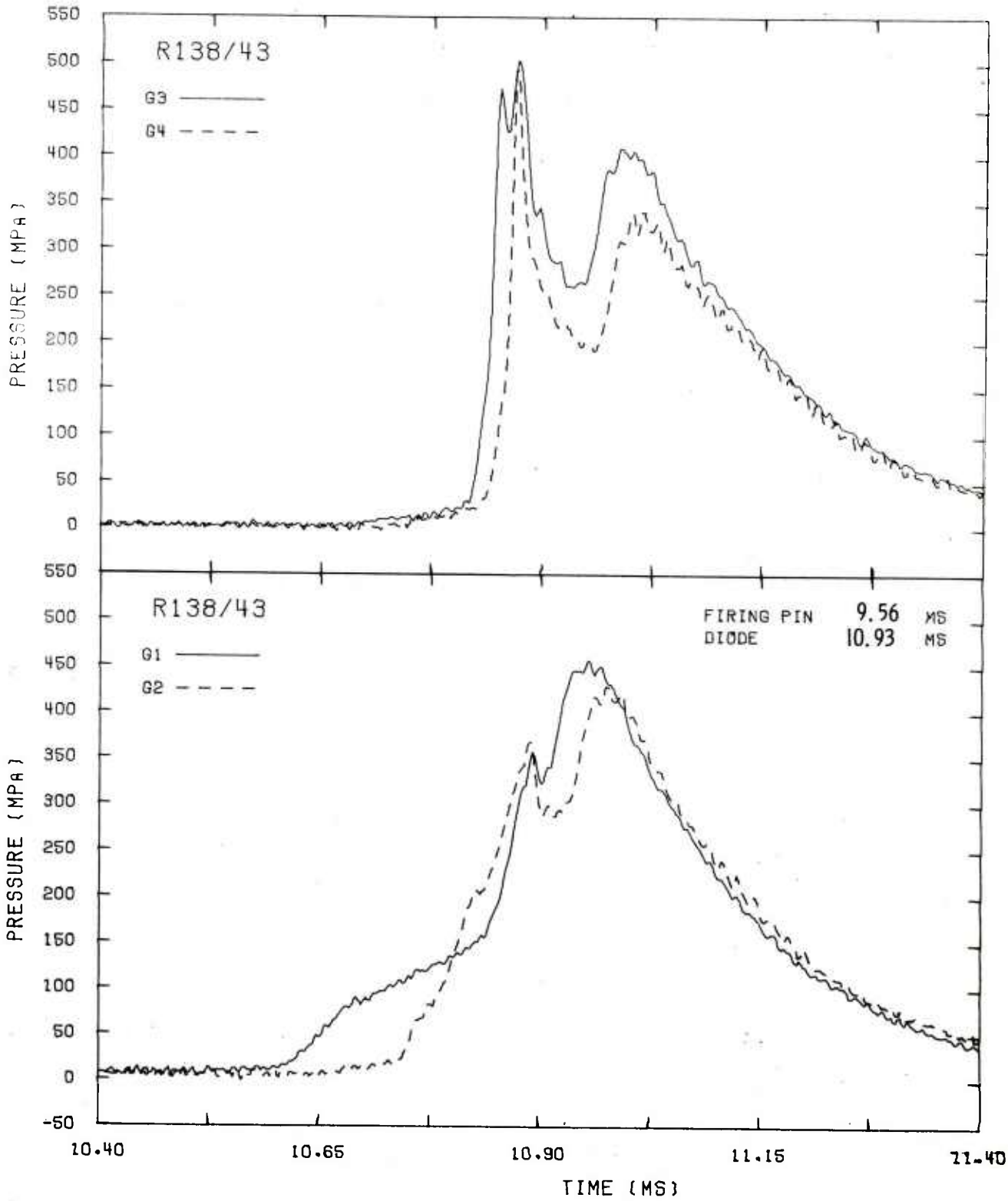
R138/43
G3
G4
PRESSURE (MPa)
550
500
450
400
350
300
250
200
150
100
50
0
R138/43
G1
G2
FIRING PIN 9.56 MS
DIODE 10.93 MS
PRESSURE (MPa)
-50
10.40
10.65
10.90
11.15
11.40
TIME (MS)

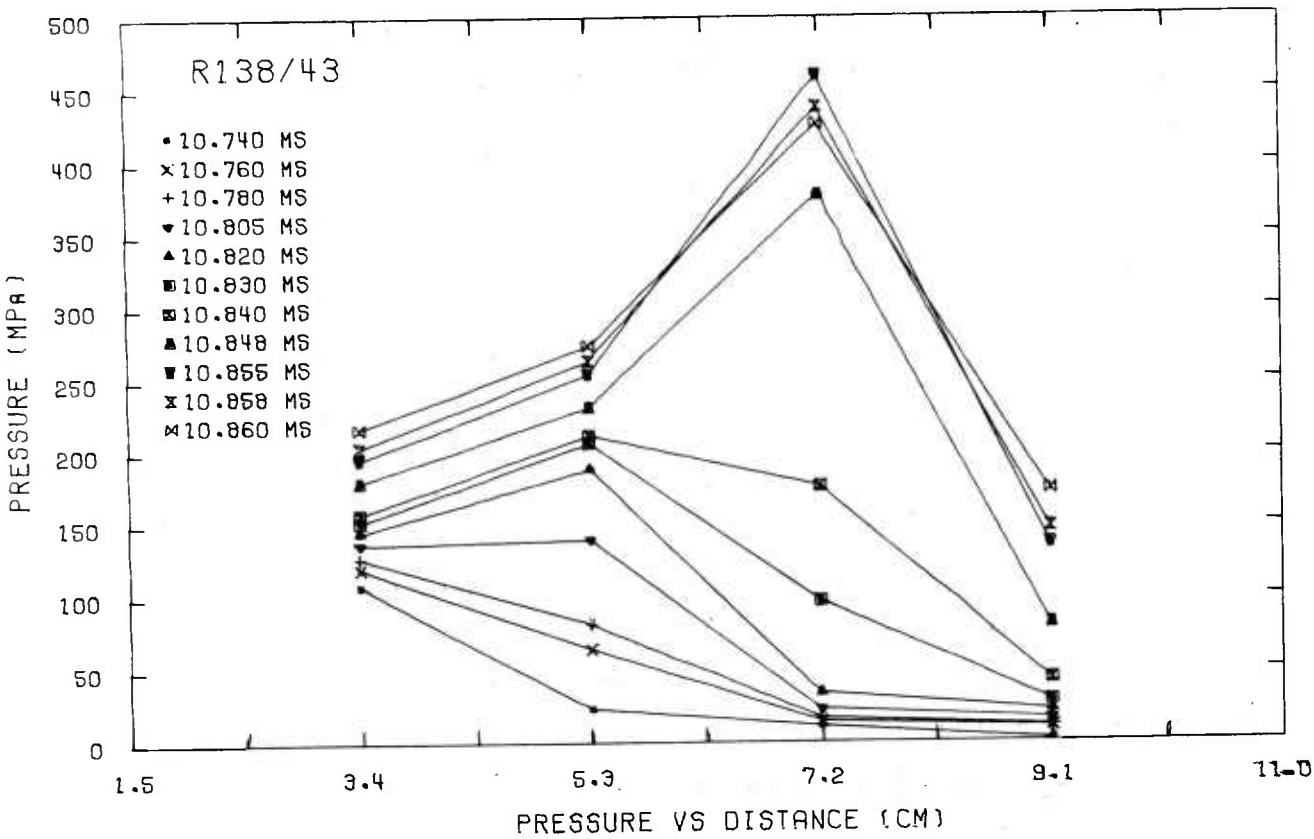
R138/43
•10.740 MS
×10.760 MS
+10.780 MS
▾10.805 MS
▲10.820 MS
■10.830 MS
⊠10.840 MS
▲10.848 MS
▼10.855 MS
⧗10.858 MS
⋈10.860 MS
PRESSURE (MPa)
500
450
400
350
300
250
200
150
100
50
0
1.5
3.4
5.3
7.2
9.1
11.0
PRESSURE VS DISTANCE (CM)

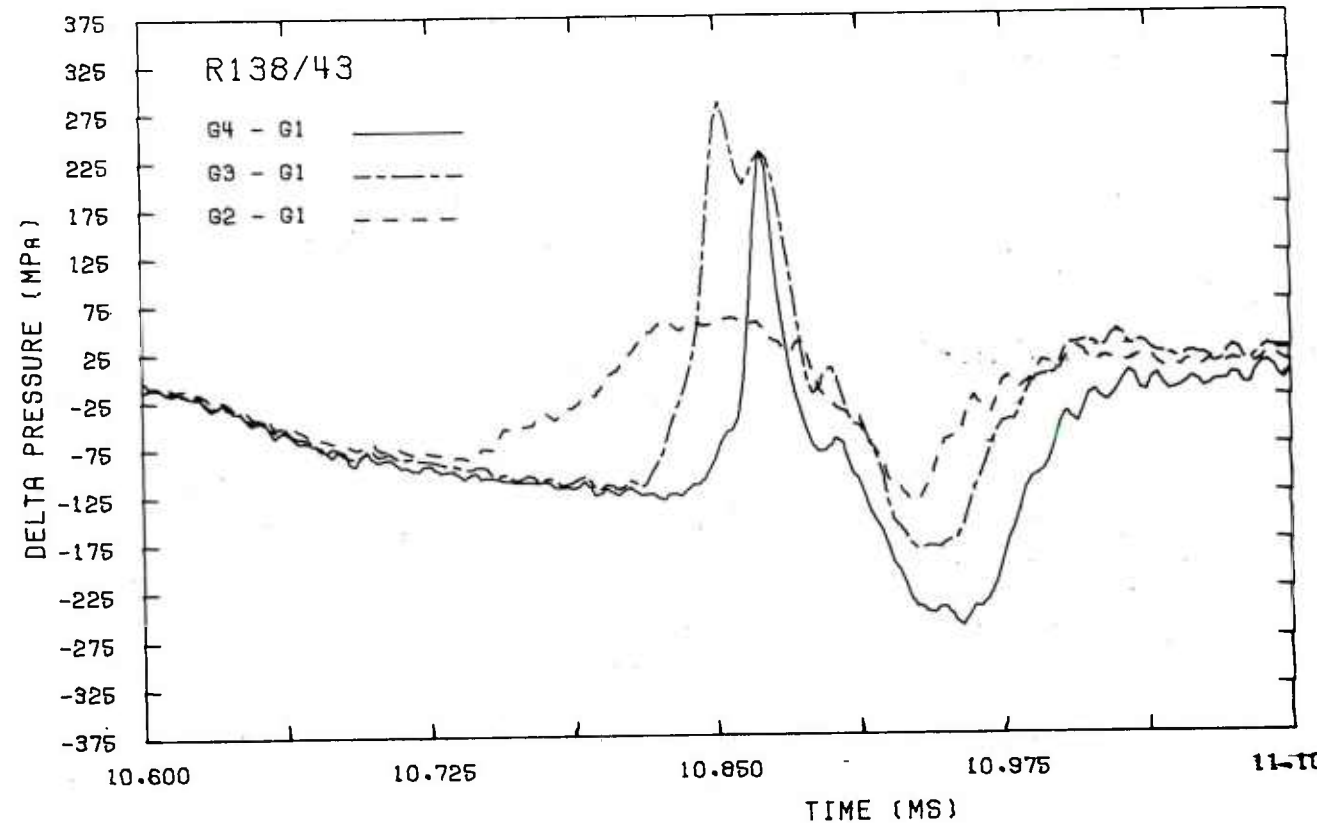
R138/43
G4 - G1
G3 - G1
G2 - G1
DELTA PRESSURE (MPa)
375
325
275
225
175
125
75
25
-25
-75
-125
-175
-225
-275
-325
-375
10.600
10.725
10.850
10.975
11.100
TIME (MS)

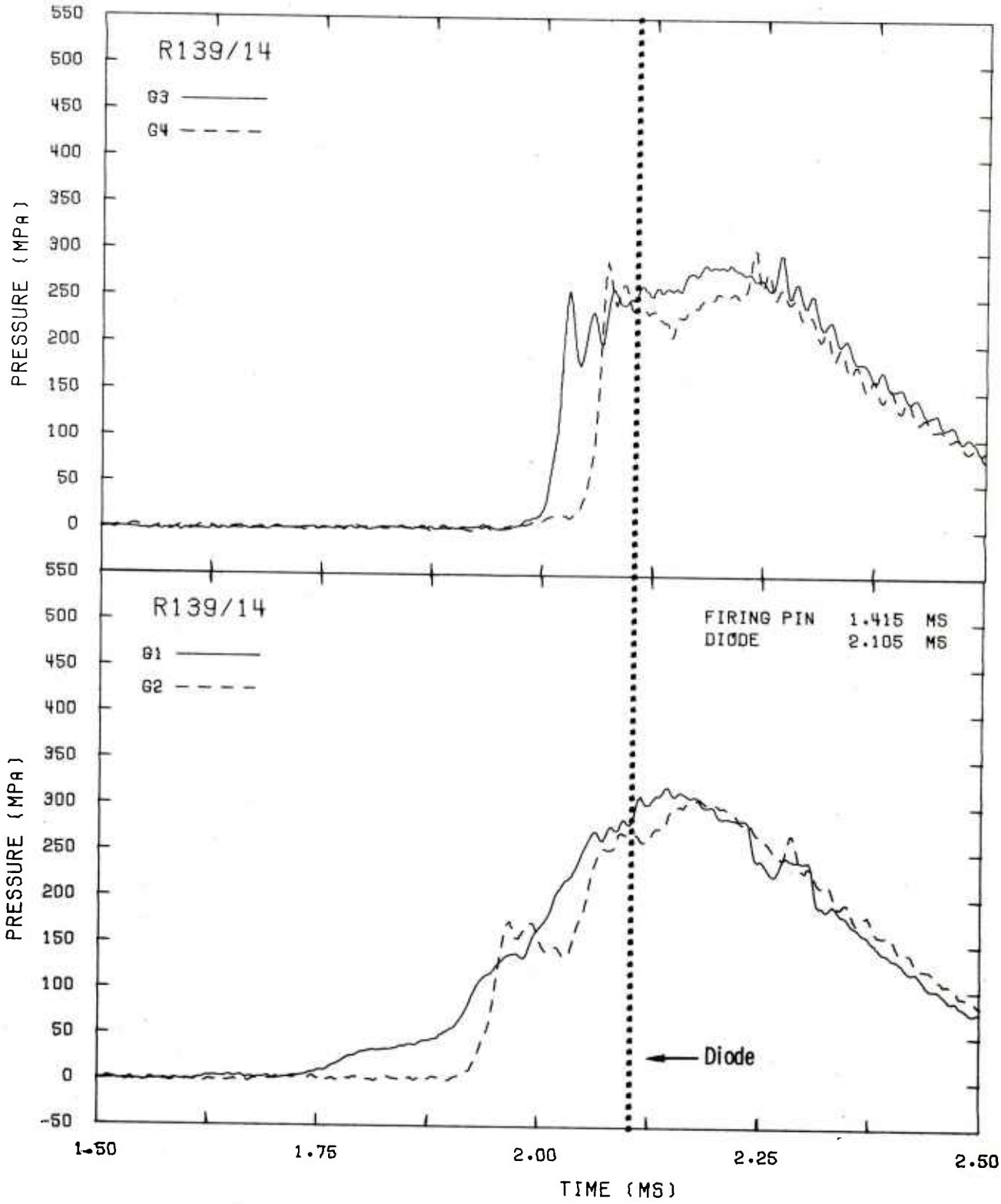
R139/14
G3
G4
PRESSURE (MPa)
550
500
450
400
350
300
250
200
150
100
50
0
R139/14
G1
G2
FIRING PIN 1.415 MS
DIODE 2.105 MS
Diode
-50
1.50
1.75
2.00
2.25
2.50
TIME (MS)

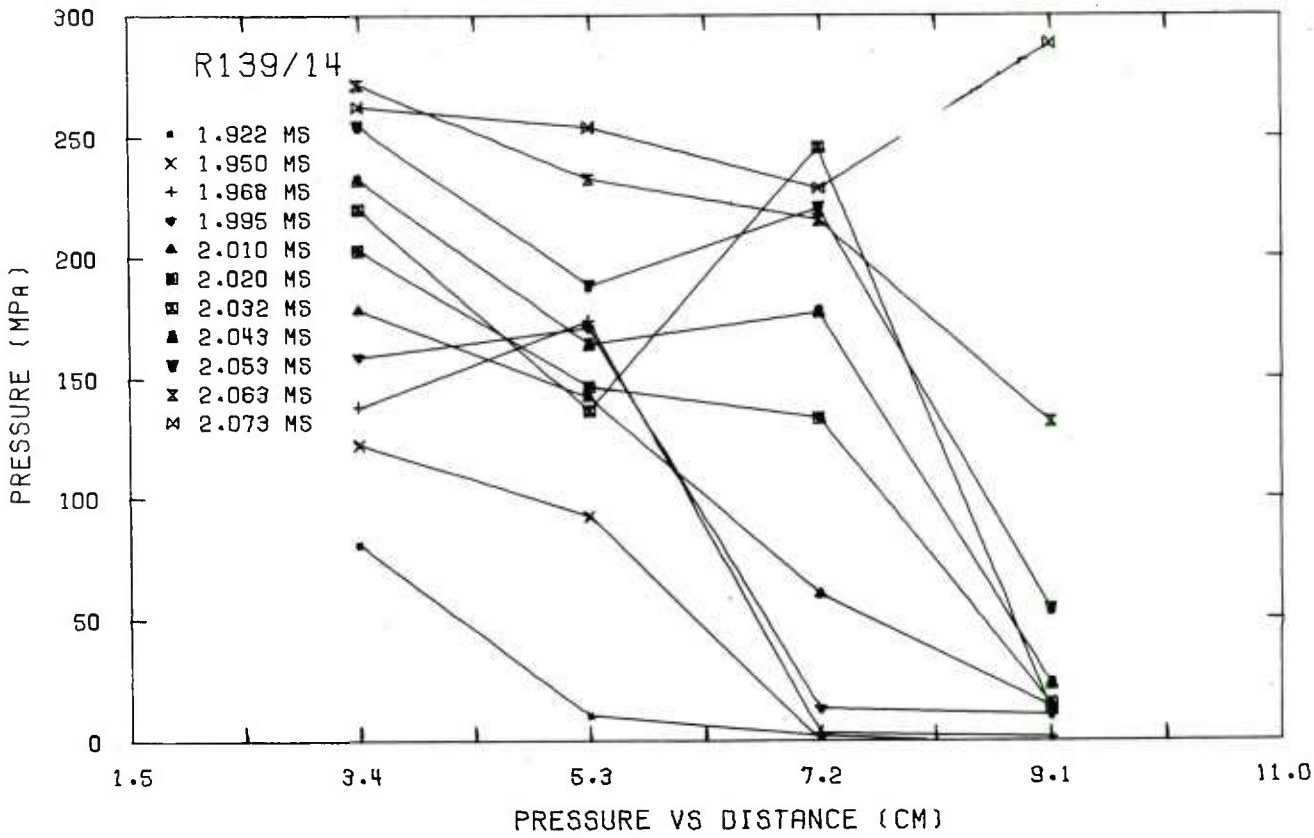
R139/14
1.922 MS
1.950 MS
1.968 MS
1.995 MS
2.010 MS
2.020 MS
2.032 MS
2.043 MS
2.053 MS
2.063 MS
2.073 MS
PRESSURE (MPa)
300
250
200
150
100
50
0
1.5
3.4
5.3
7.2
9.1
11.0
PRESSURE VS DISTANCE (CM)

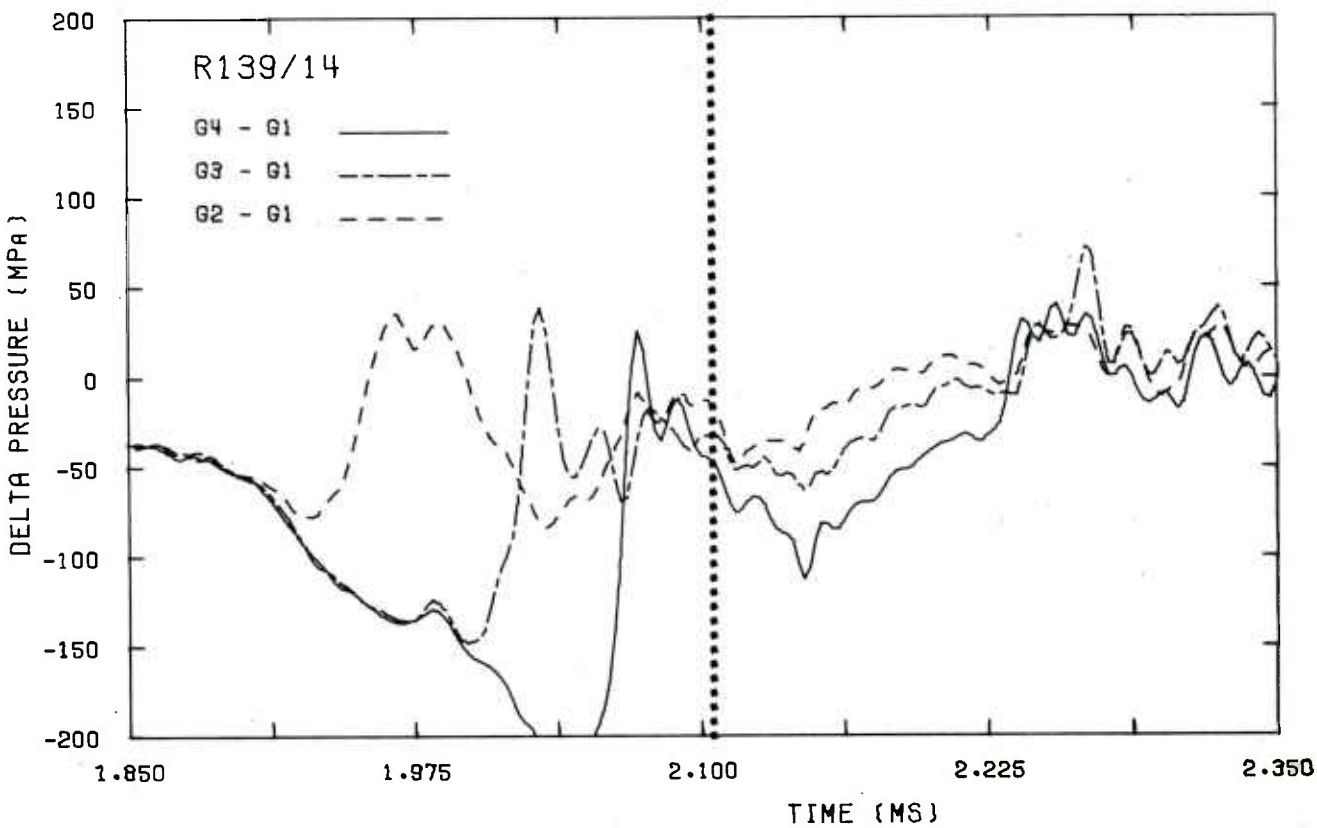
R139/14
G4 - G1
G3 - G1
G2 - G1
DELTA PRESSURE (MPa)
200
150
100
50
0
-50
-100
-150
-200
1.850
1.975
2.100
2.225
2.350
TIME (MS)

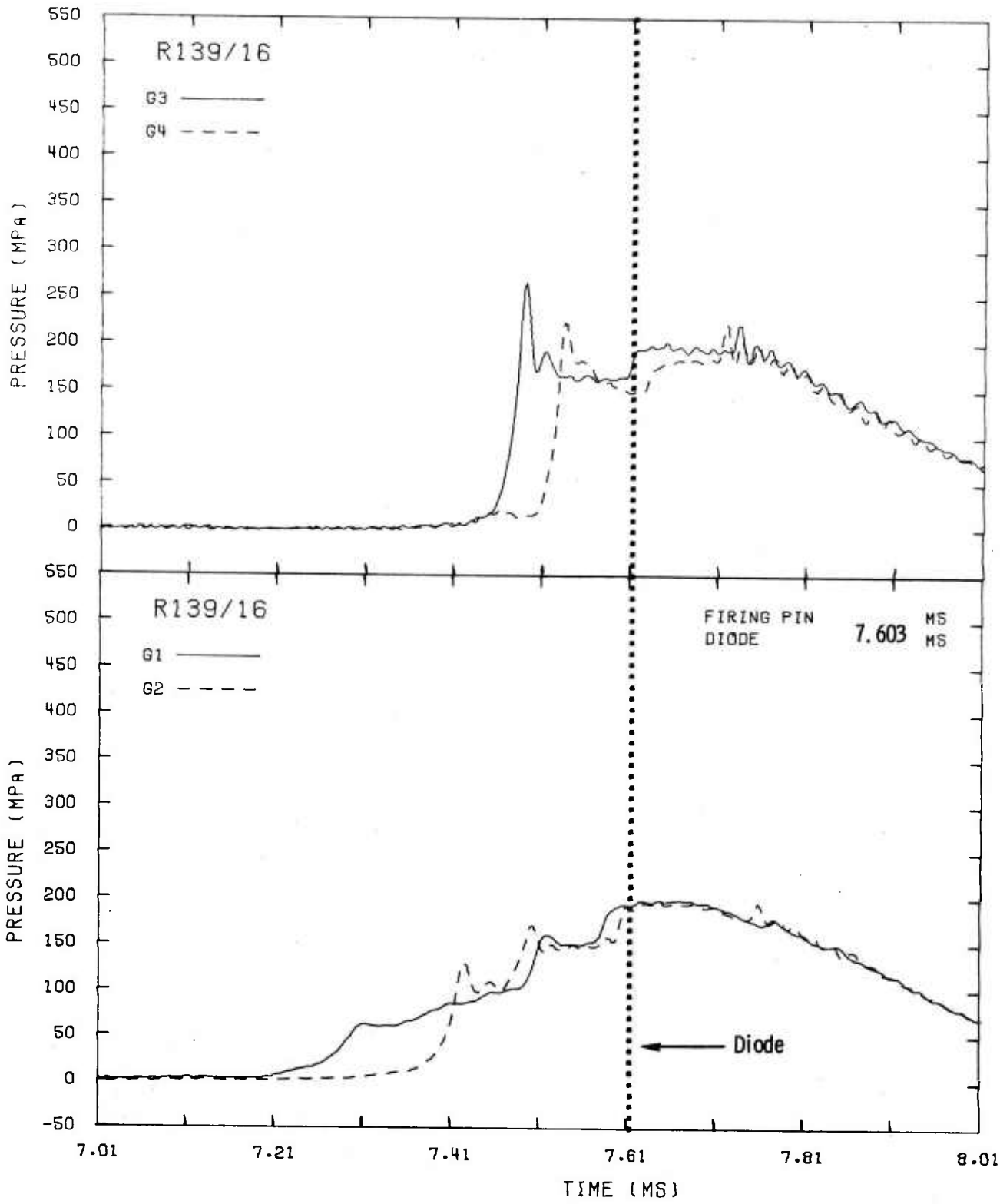
R139/16
G3
G4
PRESSURE (MPA)
R139/16
G1
G2
FIRING PIN
DIODE
7.603 MS
MS
Diode
PRESSURE (MPA)
TIME (MS)
550
500
450
400
350
300
250
200
150
100
50
0
-50
7.01
7.21
7.41
7.61
7.81
8.01

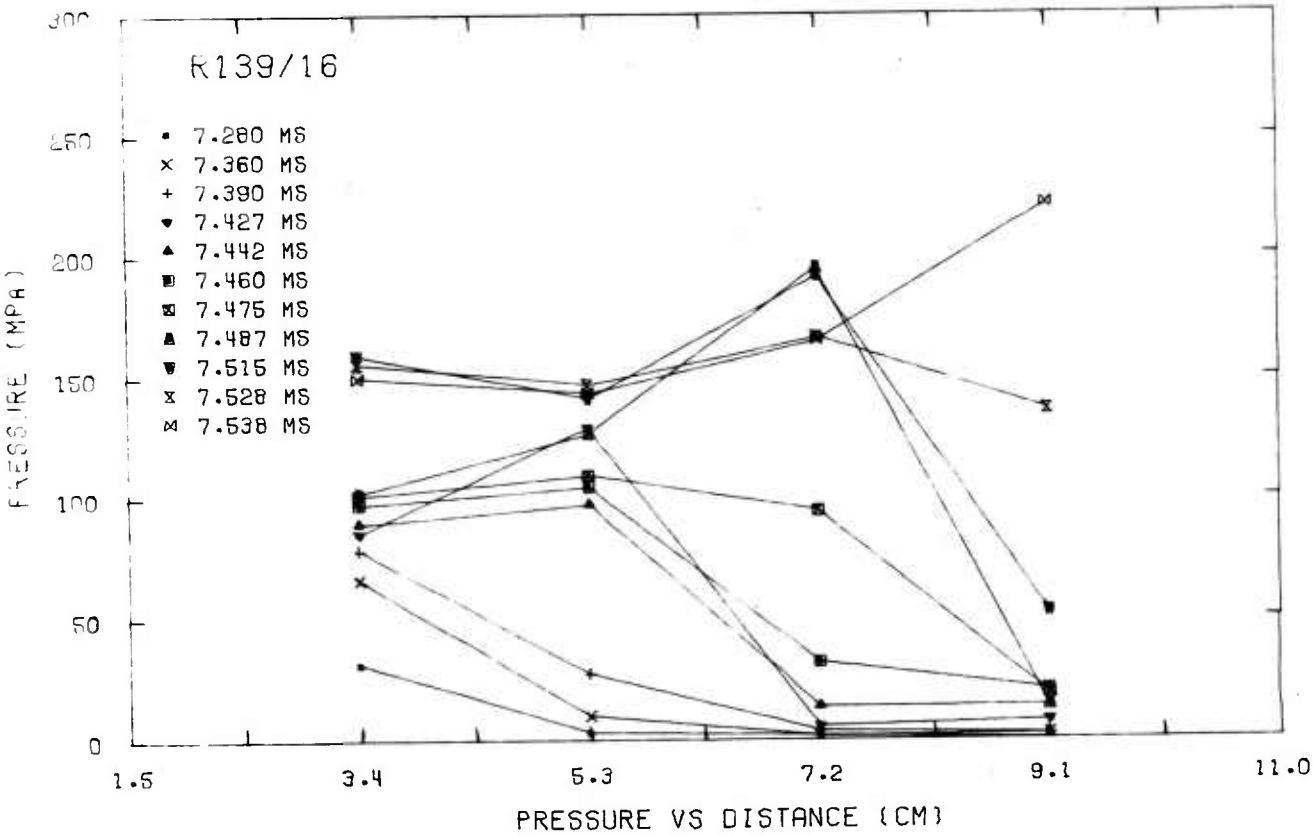
R139/16
7.280 MS
7.360 MS
7.390 MS
7.427 MS
7.442 MS
7.460 MS
7.475 MS
7.487 MS
7.515 MS
7.528 MS
7.538 MS
PRESSURE (MPA)
300
250
200
150
100
50
0
1.5
3.4
5.3
7.2
9.1
11.0
PRESSURE VS DISTANCE (CM)

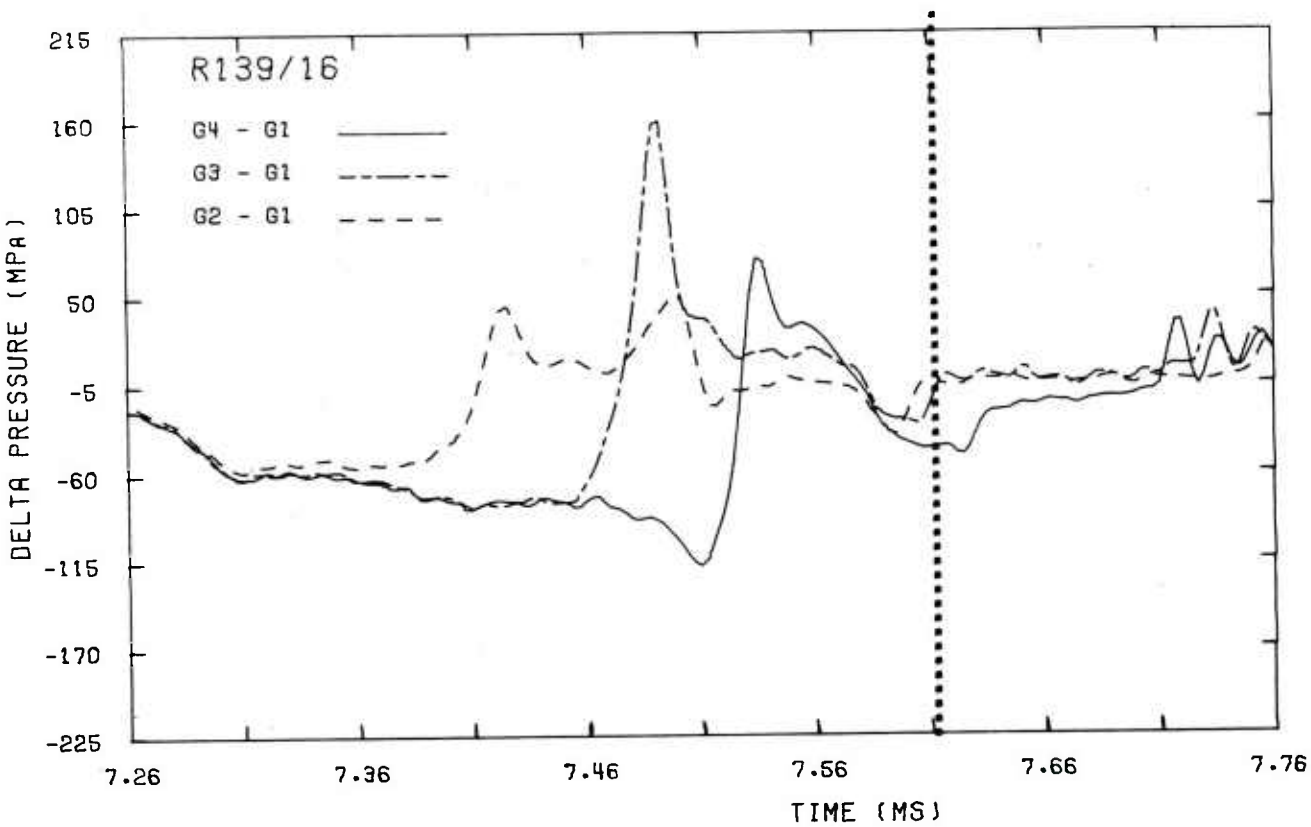
R139/16
G4 - G1
G3 - G1
G2 - G1
DELTA PRESSURE (MPA)
215
160
105
50
-5
-60
-115
-170
-225
7.26
7.36
7.46
7.56
7.66
7.76
TIME (MS)

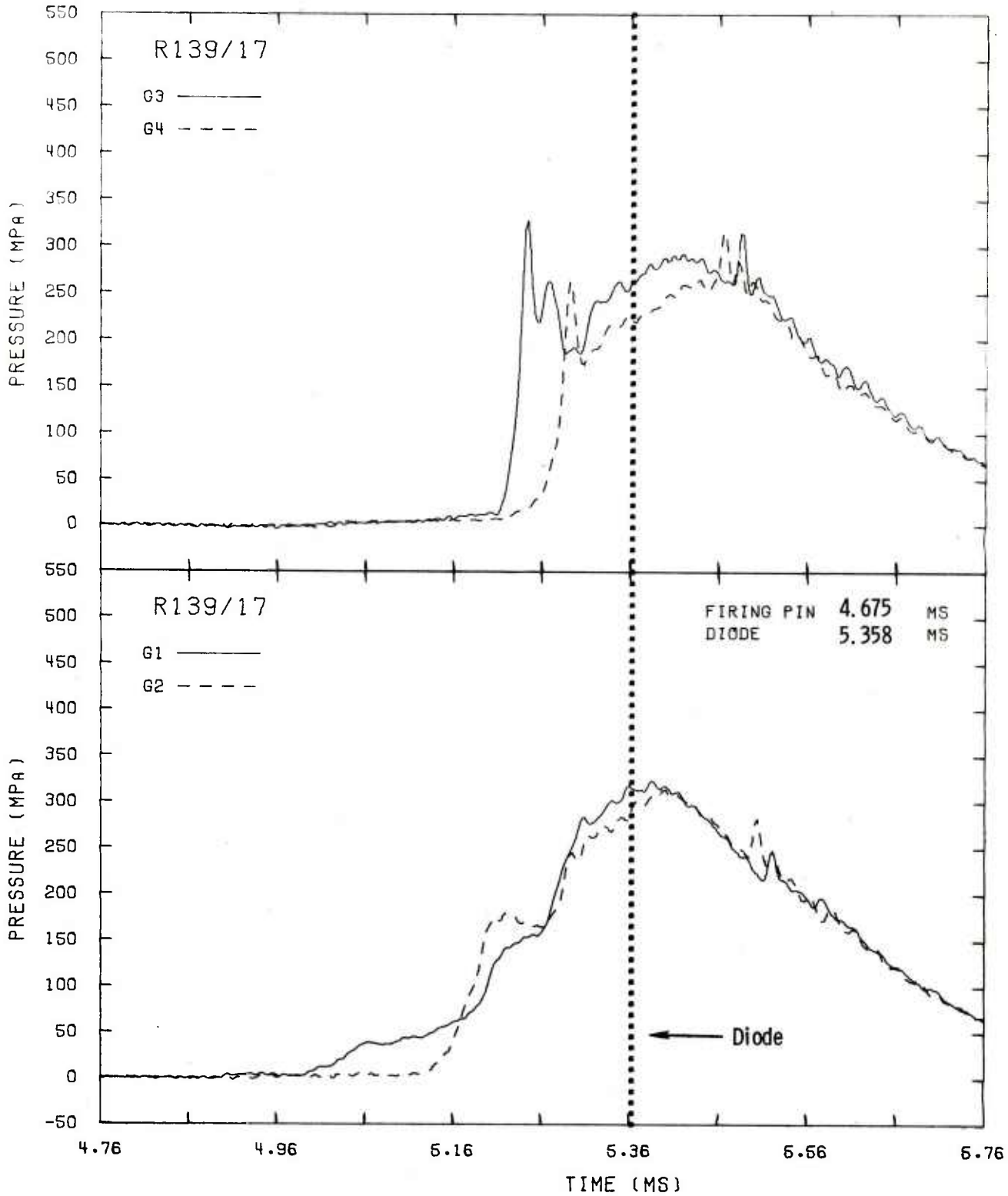
R139/17
G3
G4
PRESSURE (MPa)
R139/17
G1
G2
FIRING PIN 4.675 MS
DIODE 5.358 MS
Diode
PRESSURE (MPa)
TIME (MS)

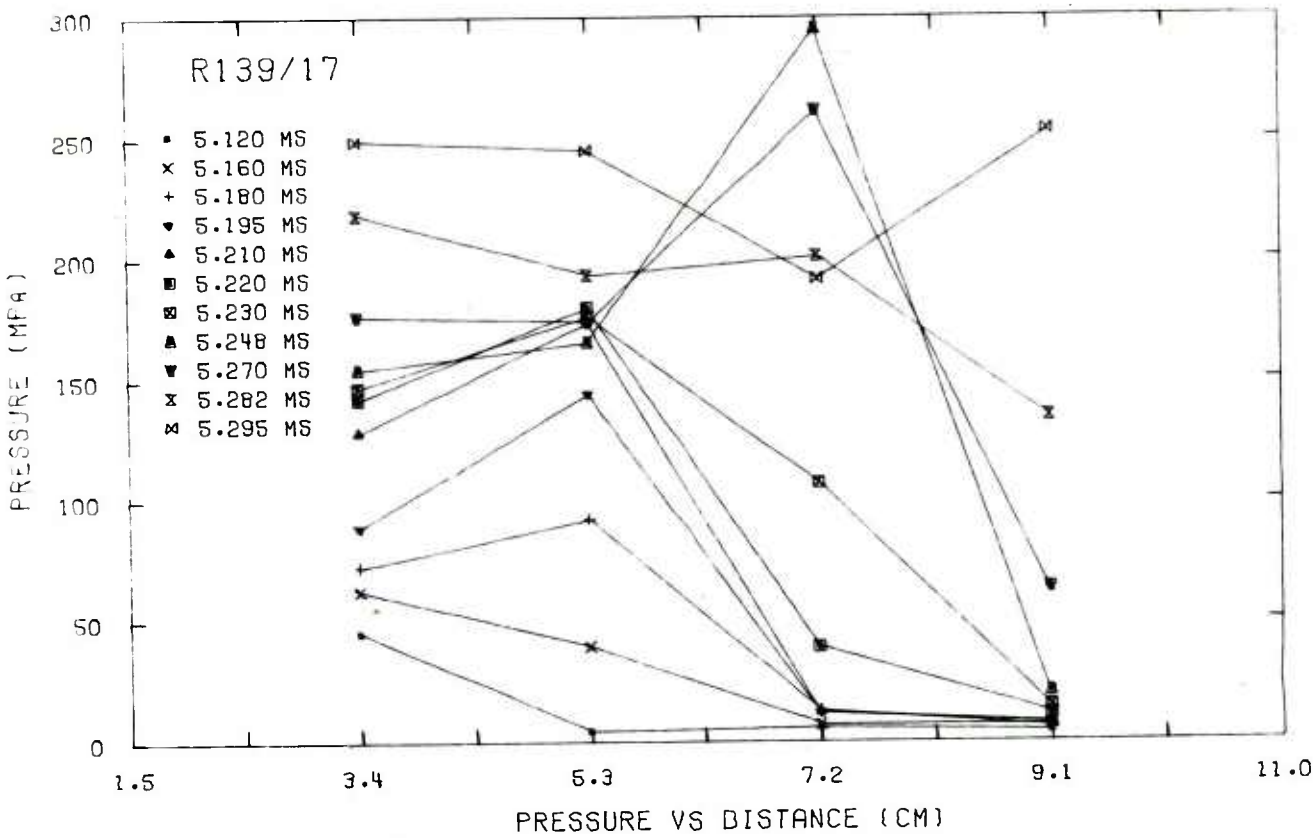
R139/17
5.120 MS
5.160 MS
5.180 MS
5.195 MS
5.210 MS
5.220 MS
5.230 MS
5.248 MS
5.270 MS
5.282 MS
5.295 MS
PRESSURE (MPA)
300
250
200
150
100
50
0
1.5
3.4
5.3
7.2
9.1
11.0
PRESSURE VS DISTANCE (CM)

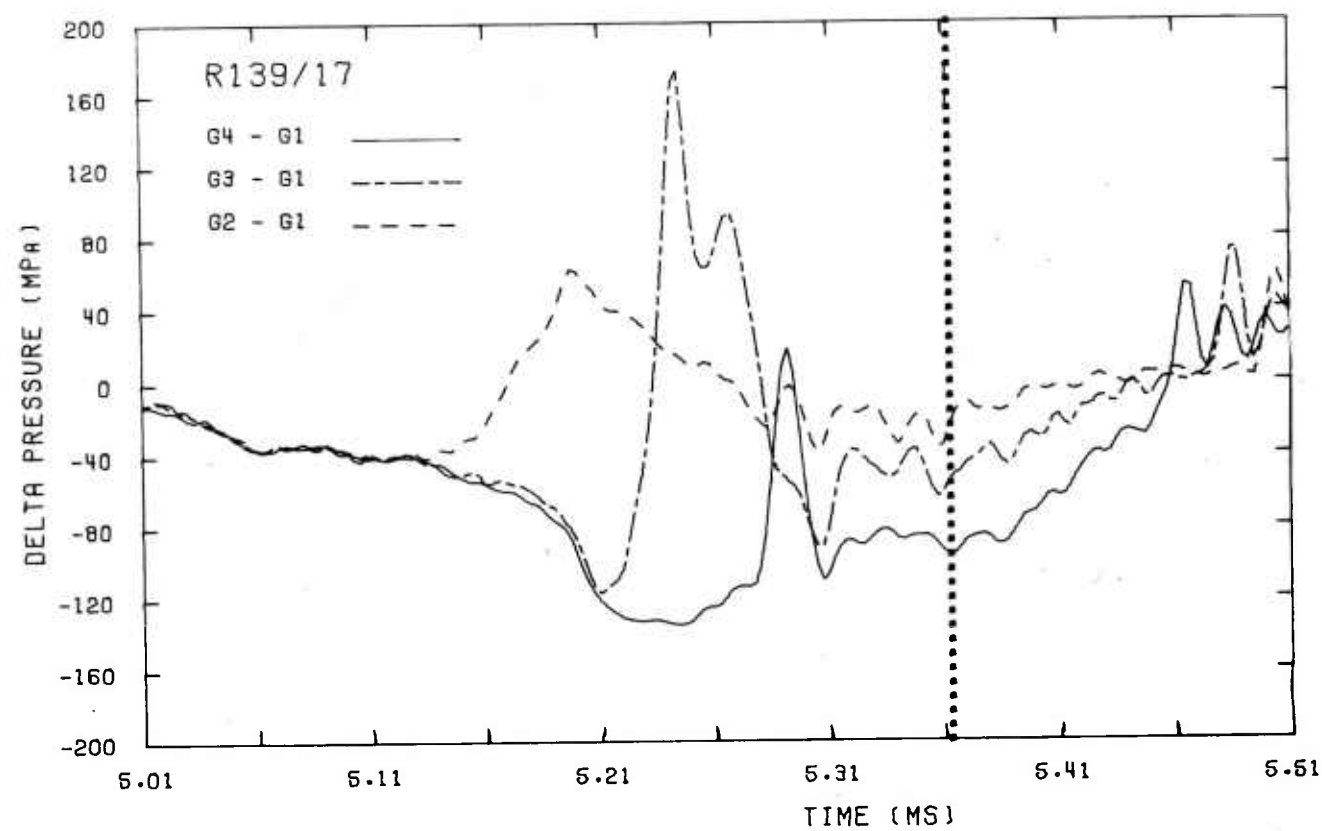
R139/17
G4 - G1
G3 - G1
G2 - G1
DELTA PRESSURE (MPA)
200
160
120
80
40
0
-40
-80
-120
-160
-200
5.01
5.11
5.21
5.31
5.41
5.51
TIME (MS)

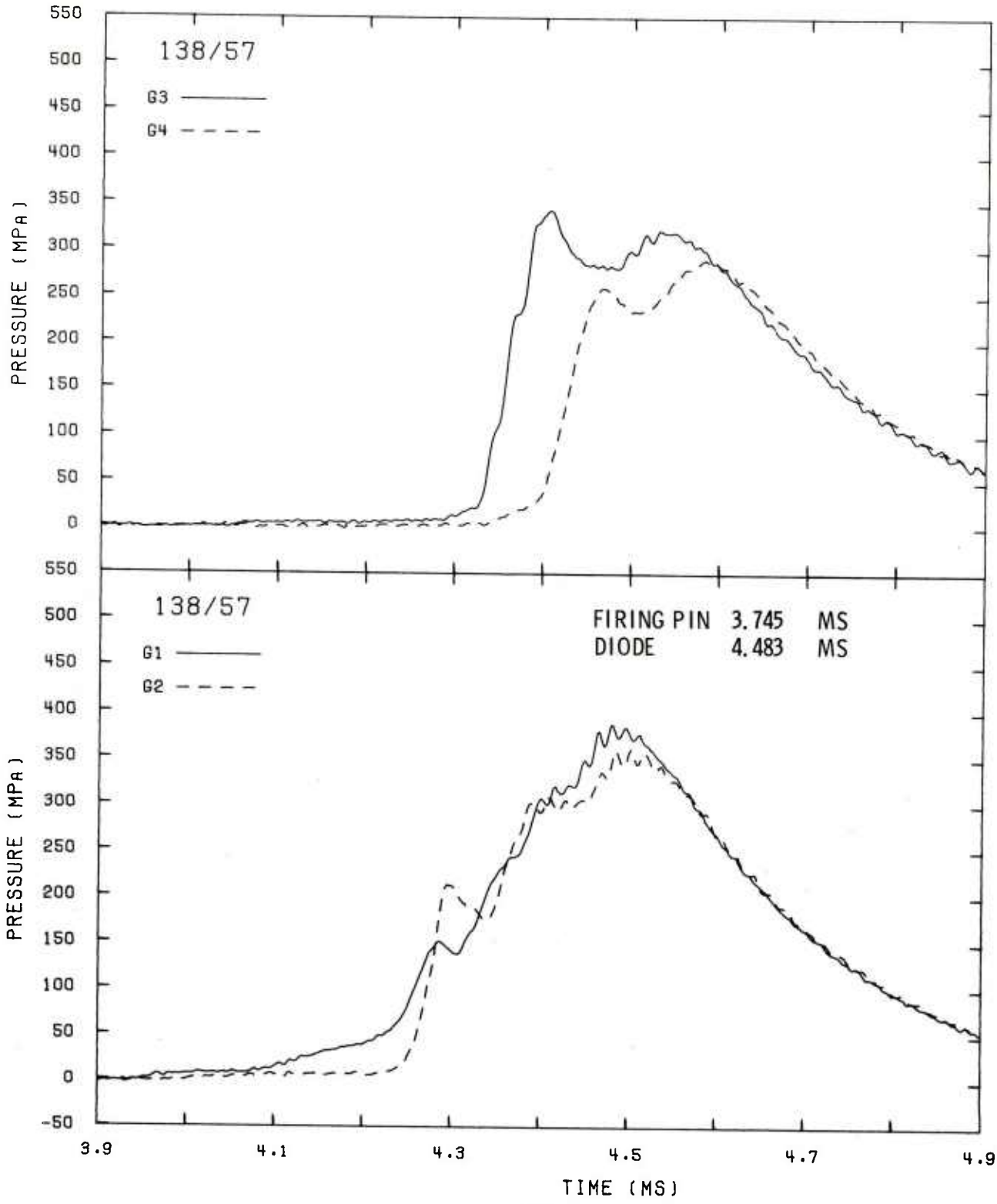
138/57
G3
G4
PRESSURE (MPa)
550
500
450
400
350
300
250
200
150
100
50
0
138/57
G1
G2
FIRING PIN 3.745 MS
DIODE 4.483 MS
PRESSURE (MPa)
550
500
450
400
350
300
250
200
150
100
50
0
-50
3.9
4.1
4.3
4.5
4.7
4.9
TIME (MS)

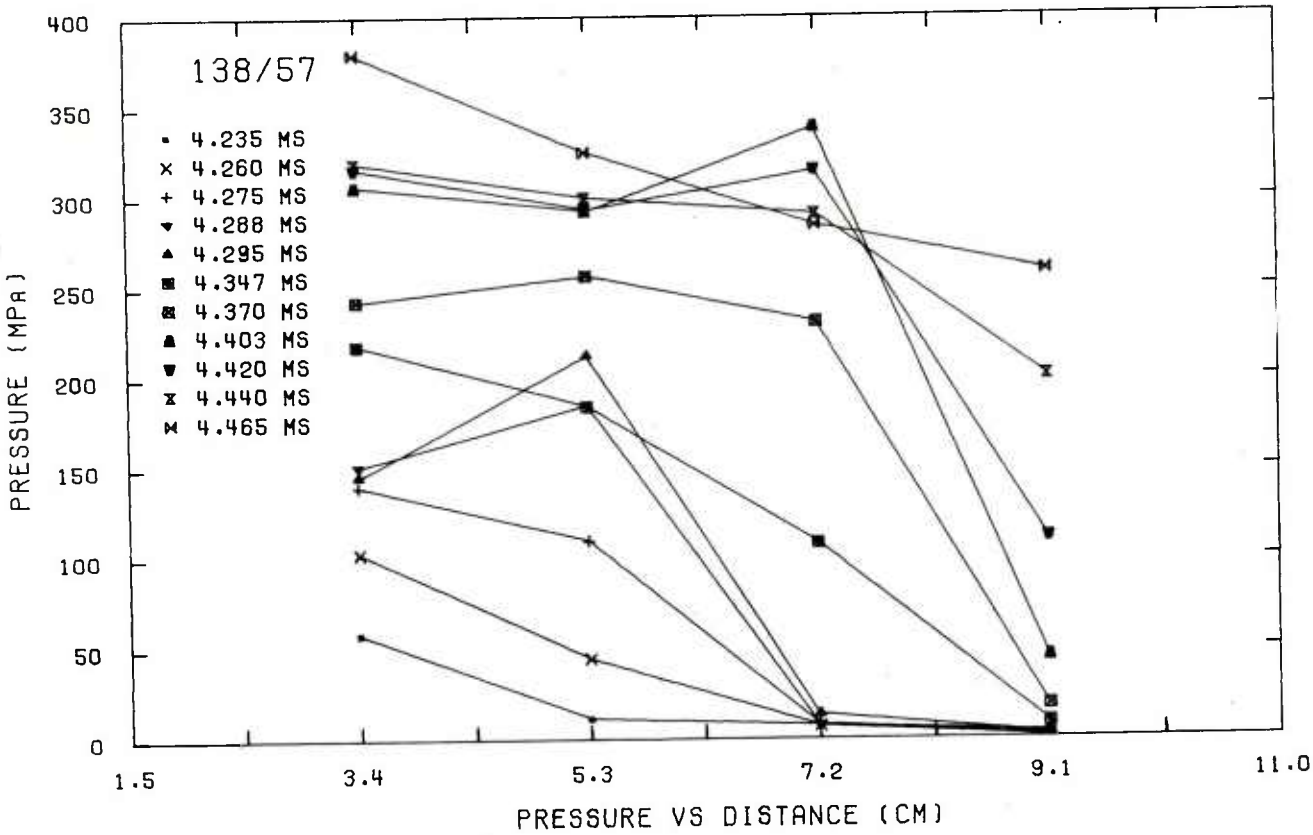
138/57
4.235 MS
4.260 MS
4.275 MS
4.288 MS
4.295 MS
4.347 MS
4.370 MS
4.403 MS
4.420 MS
4.440 MS
4.465 MS
PRESSURE (MPa)
400
350
300
250
200
150
100
50
0
1.5
3.4
5.3
7.2
9.1
11.0
PRESSURE VS DISTANCE (CM)

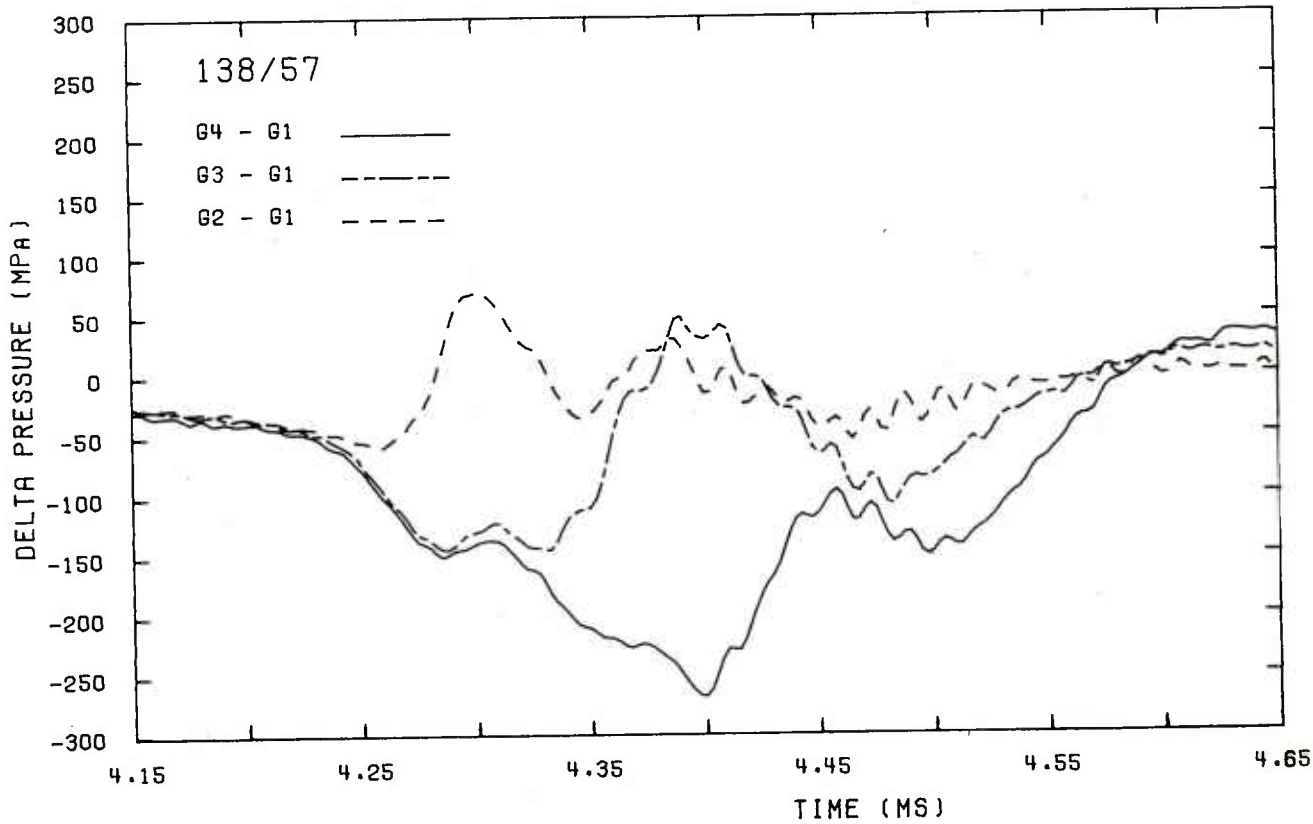
138/57
G4 - G1
G3 - G1
G2 - G1
DELTA PRESSURE (MPa)
300
250
200
150
100
50
0
-50
-100
-150
-200
-250
-300
4.15
4.25
4.35
4.45
4.55
4.65
TIME (MS)

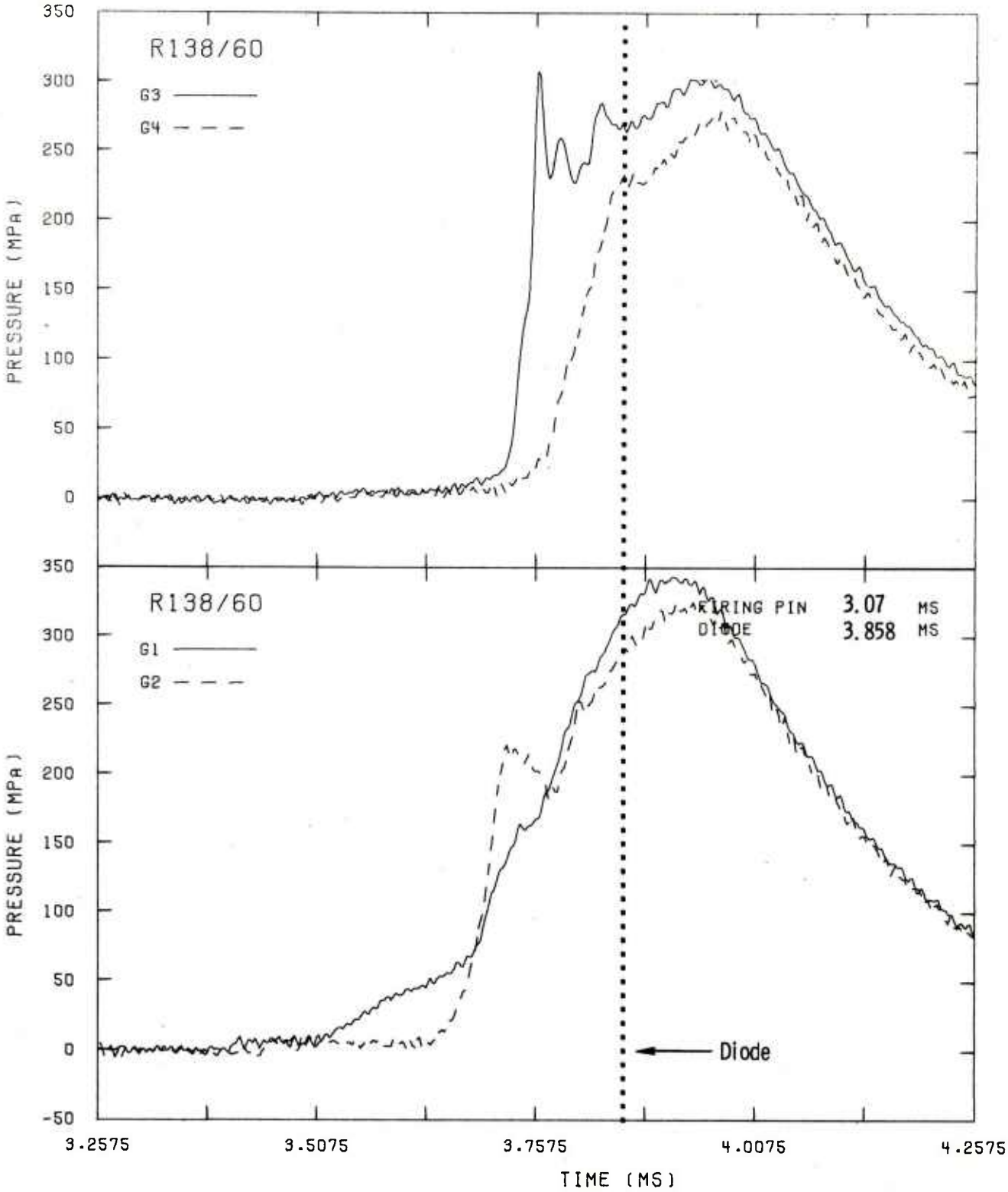
R138/60
G3
G4
PRESSURE (MPa)
350
300
250
200
150
100
50
0
R138/60
G1
G2
FIRING PIN 3.07 MS
DIODE 3.858 MS
Diode
-50
3.2575
3.5075
3.7575
4.0075
4.2575
TIME (MS)

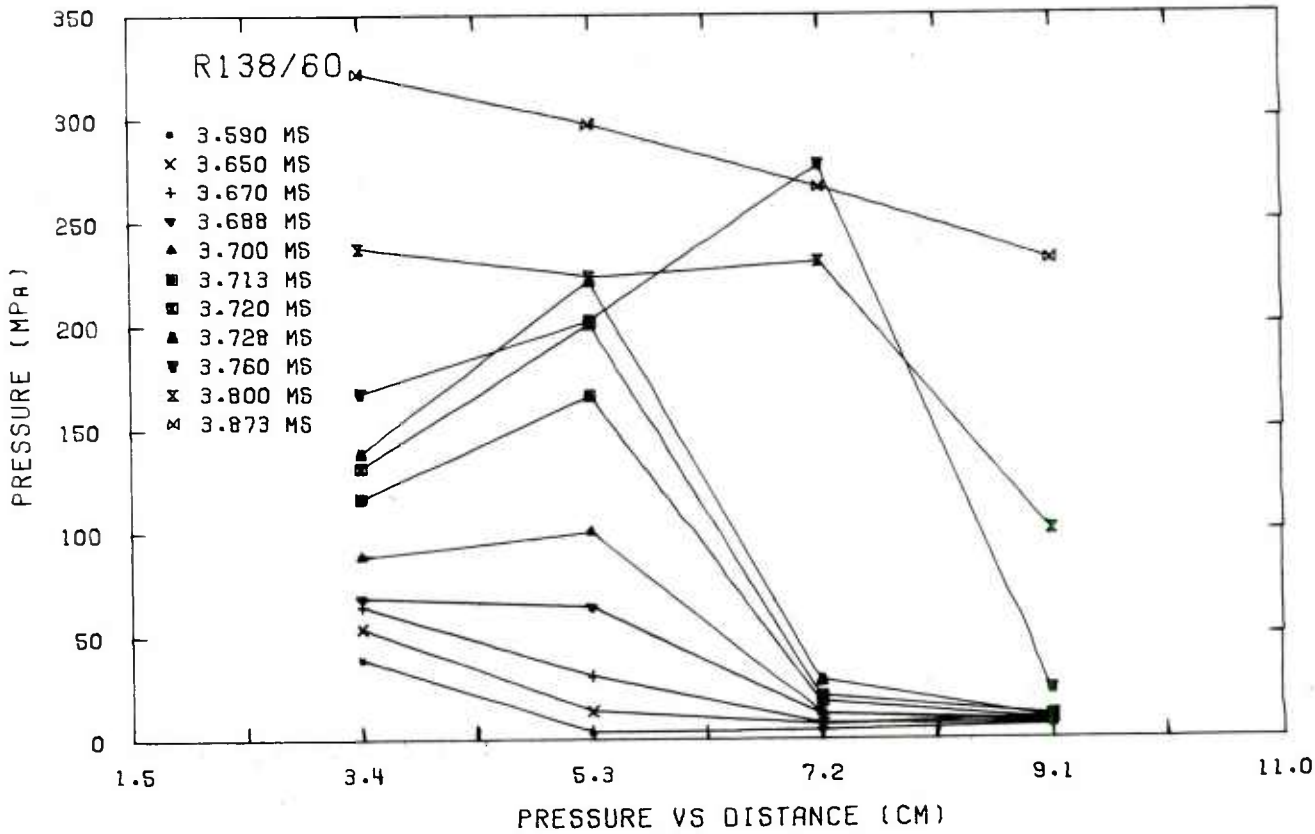
R138/60
3.590 MS
3.650 MS
3.670 MS
3.688 MS
3.700 MS
3.713 MS
3.720 MS
3.728 MS
3.760 MS
3.800 MS
3.873 MS
PRESSURE (MPa)
350
300
250
200
150
100
50
0
1.5
3.4
5.3
7.2
9.1
11.0
PRESSURE VS DISTANCE (CM)

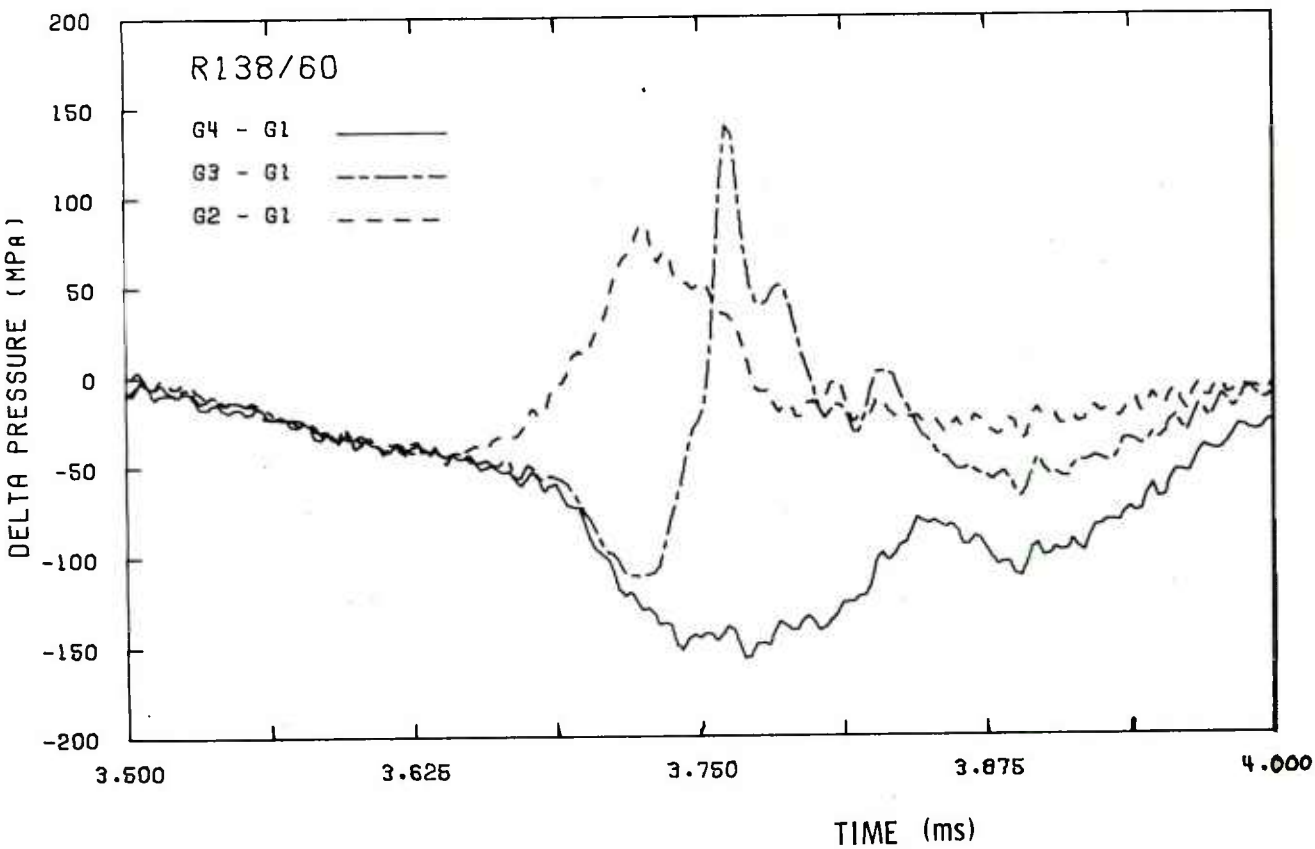
R138/60
G4 - G1
G3 - G1
G2 - G1
DELTA PRESSURE (MPa)
200
150
100
50
0
-50
-100
-150
-200
3.500
3.625
3.750
3.875
4.000
TIME (ms)

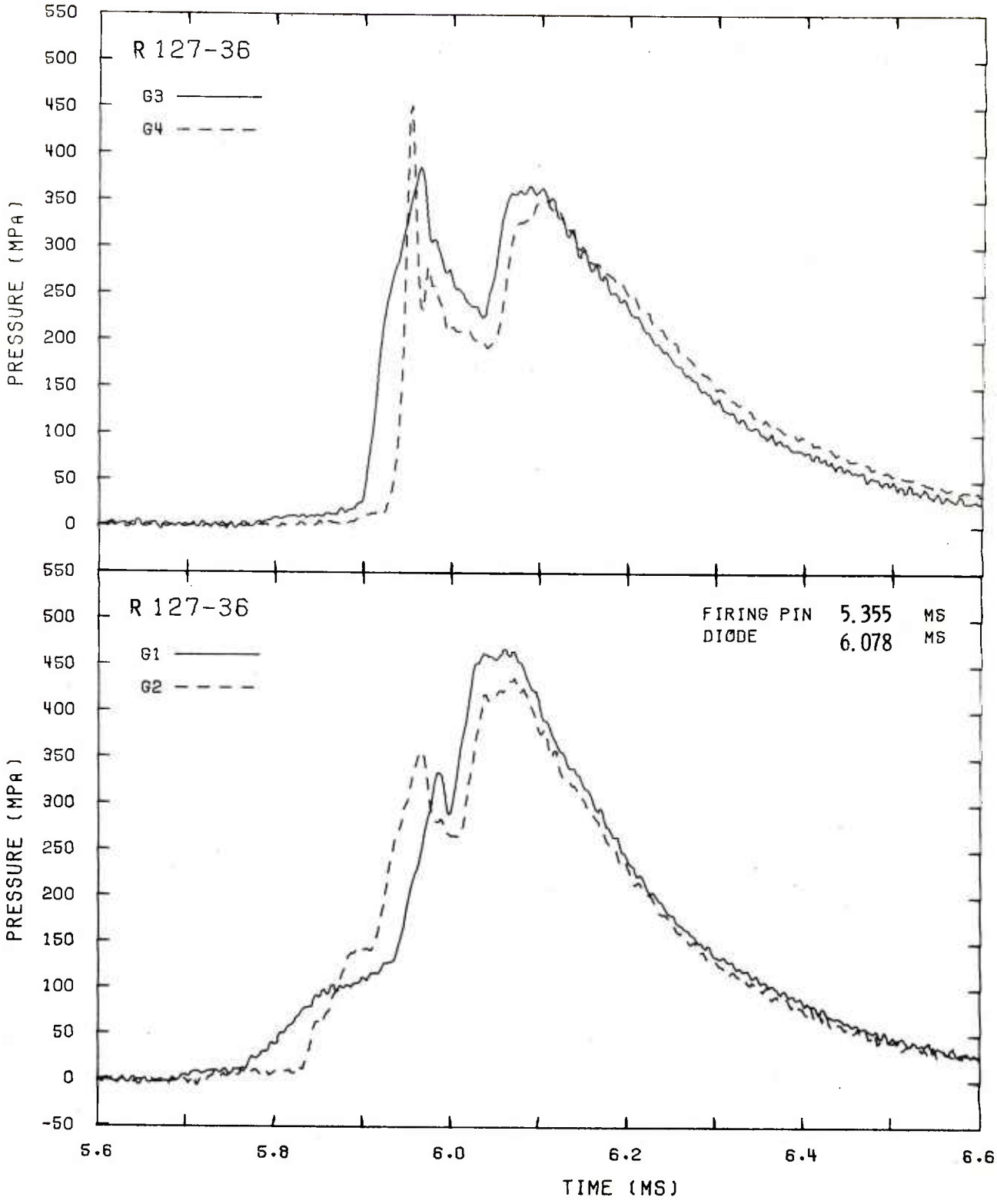
R 127-36
G3
G4
PRESSURE (MPa)
550
500
450
400
350
300
250
200
150
100
50
0
R 127-36
G1
G2
FIRING PIN 5.355 MS
DIODE 6.078 MS
PRESSURE (MPa)
-50
5.6
5.8
6.0
6.2
6.4
6.6
TIME (MS)

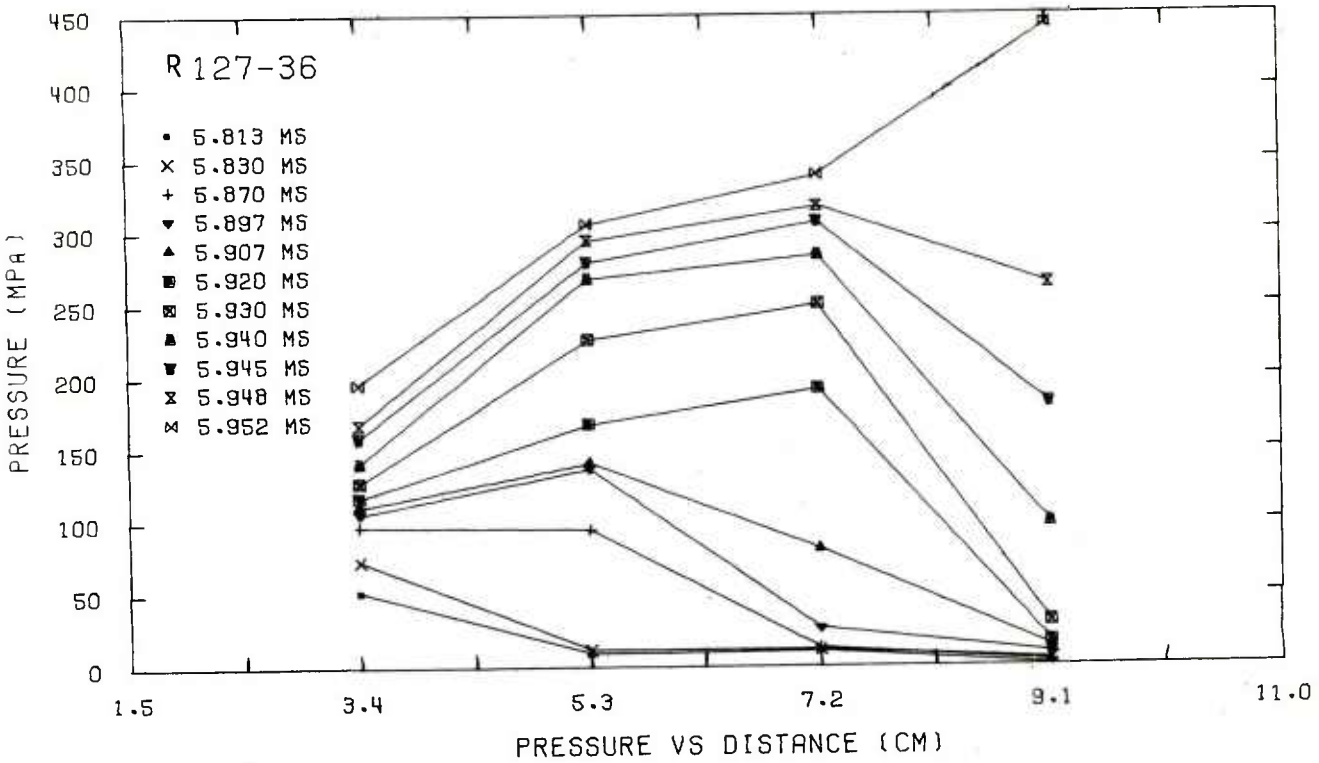
R 127-36
• 5.813 MS
× 5.830 MS
+ 5.870 MS
▼ 5.897 MS
▲ 5.907 MS
■ 5.920 MS
⊠ 5.930 MS
◭ 5.940 MS
▼ 5.945 MS
⧗ 5.948 MS
⋈ 5.952 MS
PRESSURE (MPa)
450
400
350
300
250
200
150
100
50
0
1.5
3.4
5.3
7.2
9.1
11.0
PRESSURE VS DISTANCE (CM)

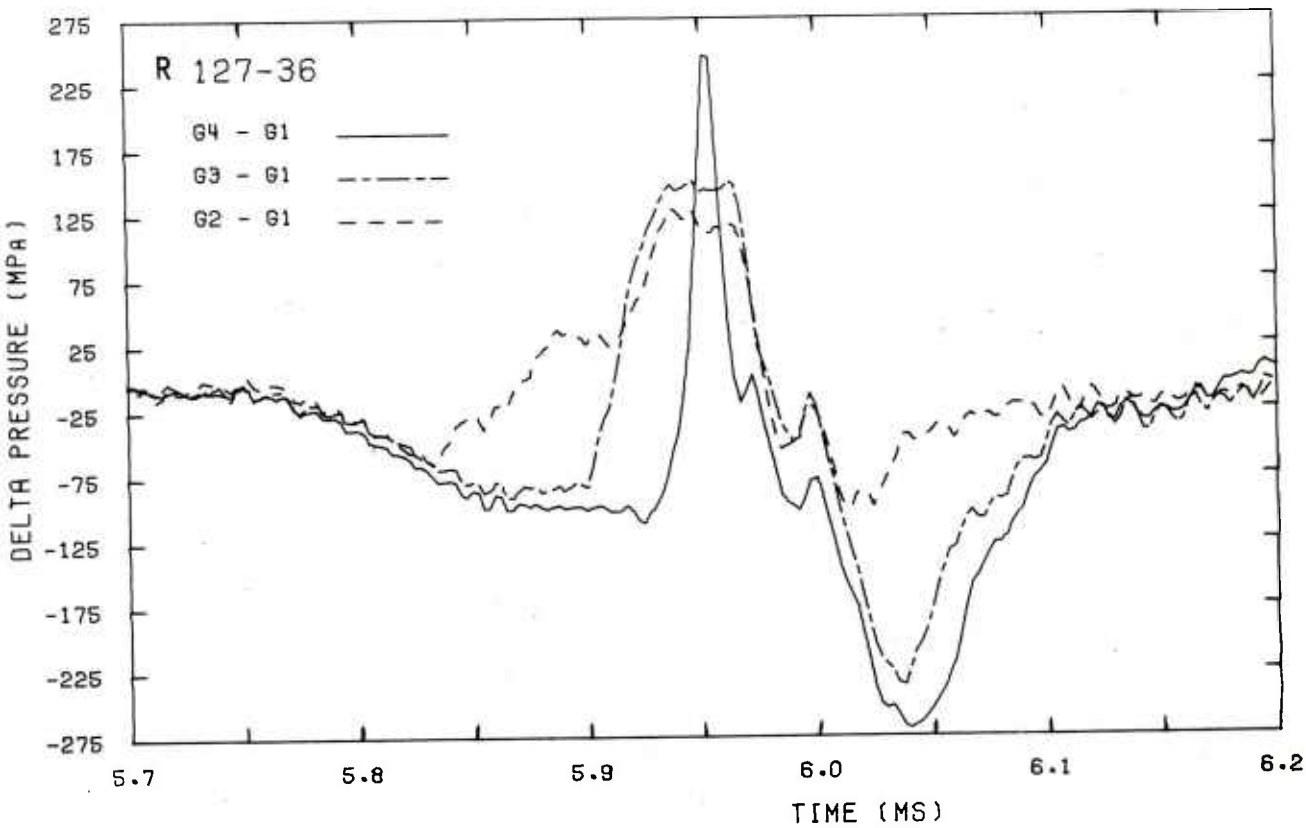
R 127-36
G4 - G1
G3 - G1
G2 - G1
DELTA PRESSURE (MPa)
275
225
175
125
75
25
-25
-75
-125
-175
-225
-275
5.7
5.8
5.9
6.0
6.1
6.2
TIME (MS)

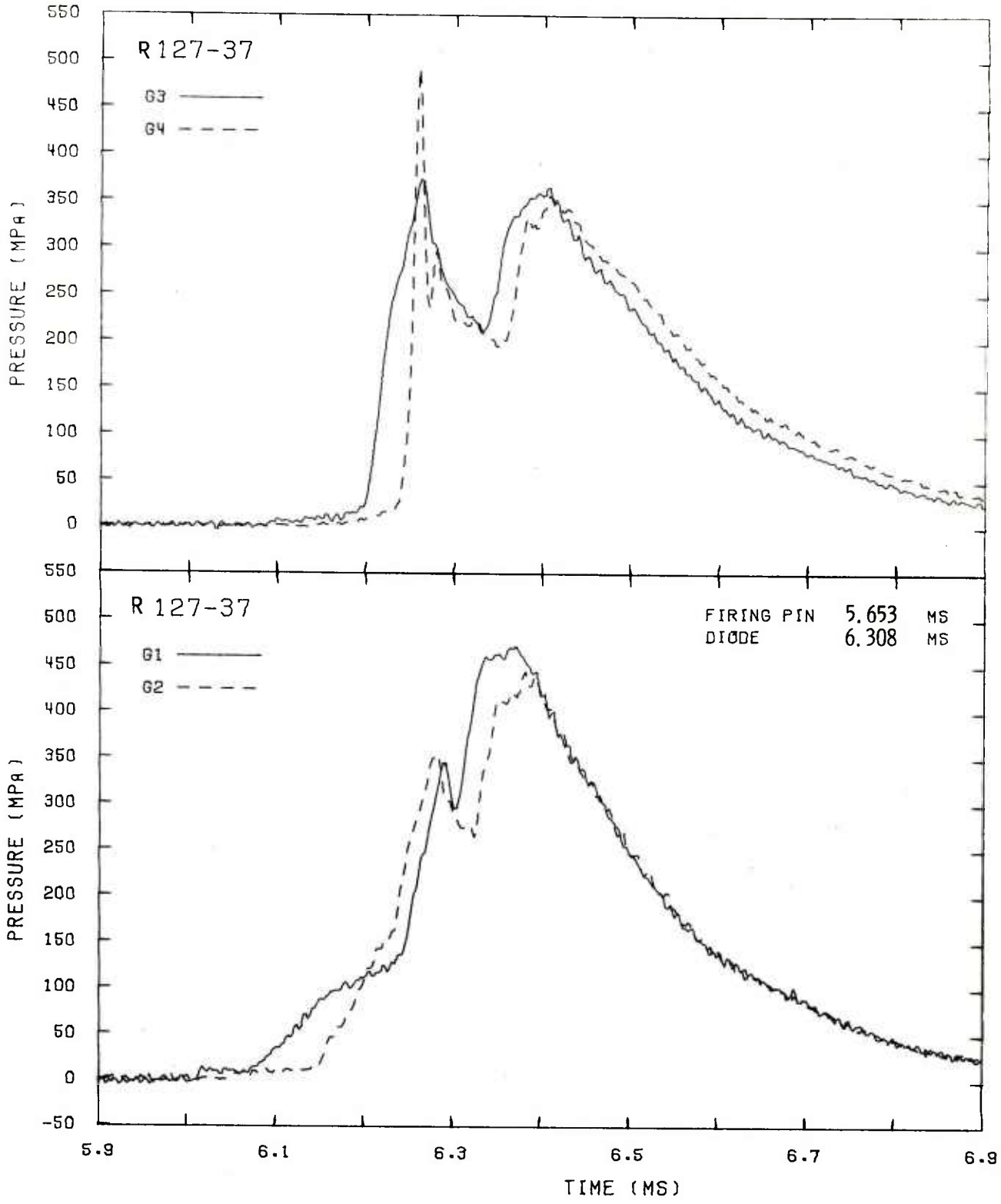
R 127-37
G3
G4
PRESSURE (MPa)
550
500
450
400
350
300
250
200
150
100
50
0
R 127-37
G1
G2
FIRING PIN 5.653 MS
DIODE 6.308 MS
PRESSURE (MPa)
550
500
450
400
350
300
250
200
150
100
50
0
-50
5.9
6.1
6.3
6.5
6.7
6.9
TIME (MS)

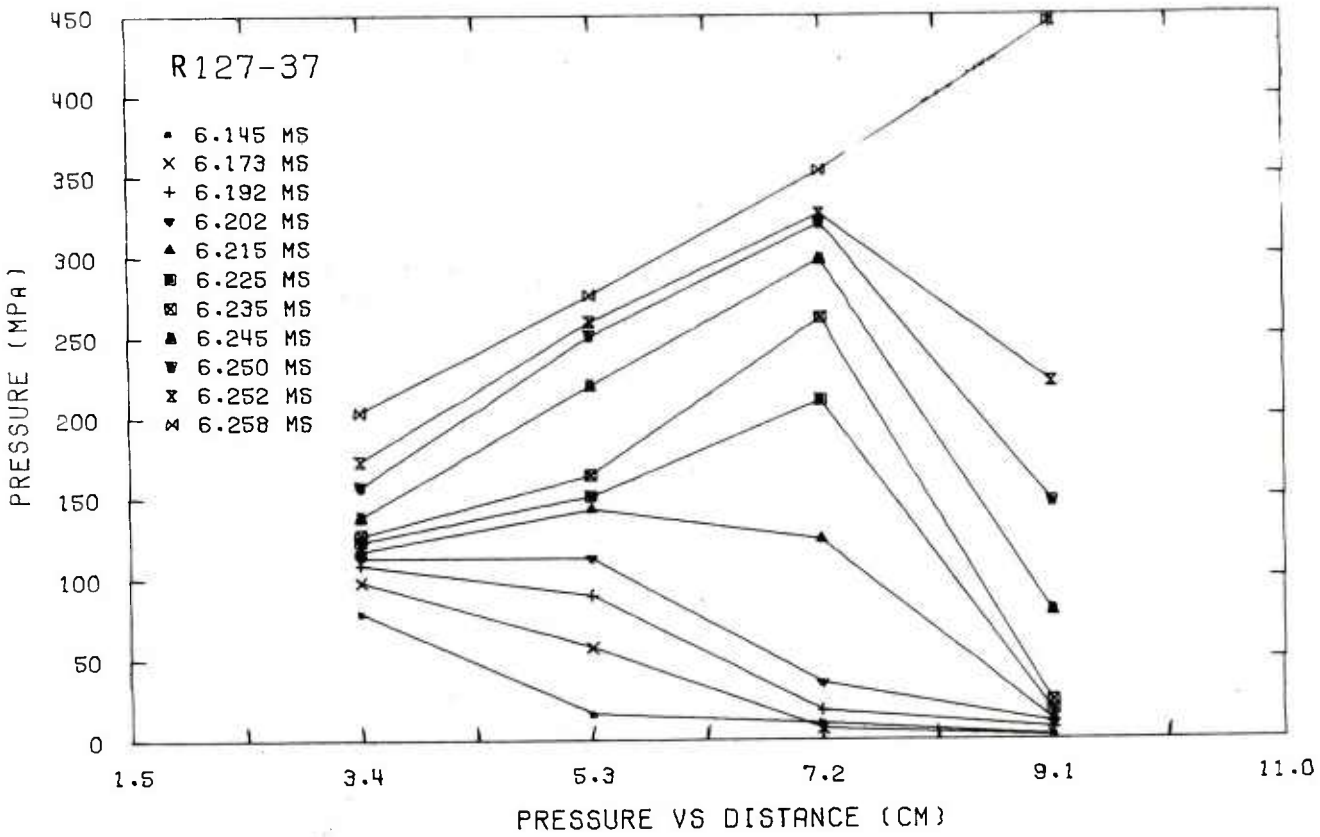
R127-37
6.145 MS
6.173 MS
6.192 MS
6.202 MS
6.215 MS
6.225 MS
6.235 MS
6.245 MS
6.250 MS
6.252 MS
6.258 MS
PRESSURE (MPa)
450
400
350
300
250
200
150
100
50
0
1.5
3.4
5.3
7.2
9.1
11.0
PRESSURE VS DISTANCE (CM)

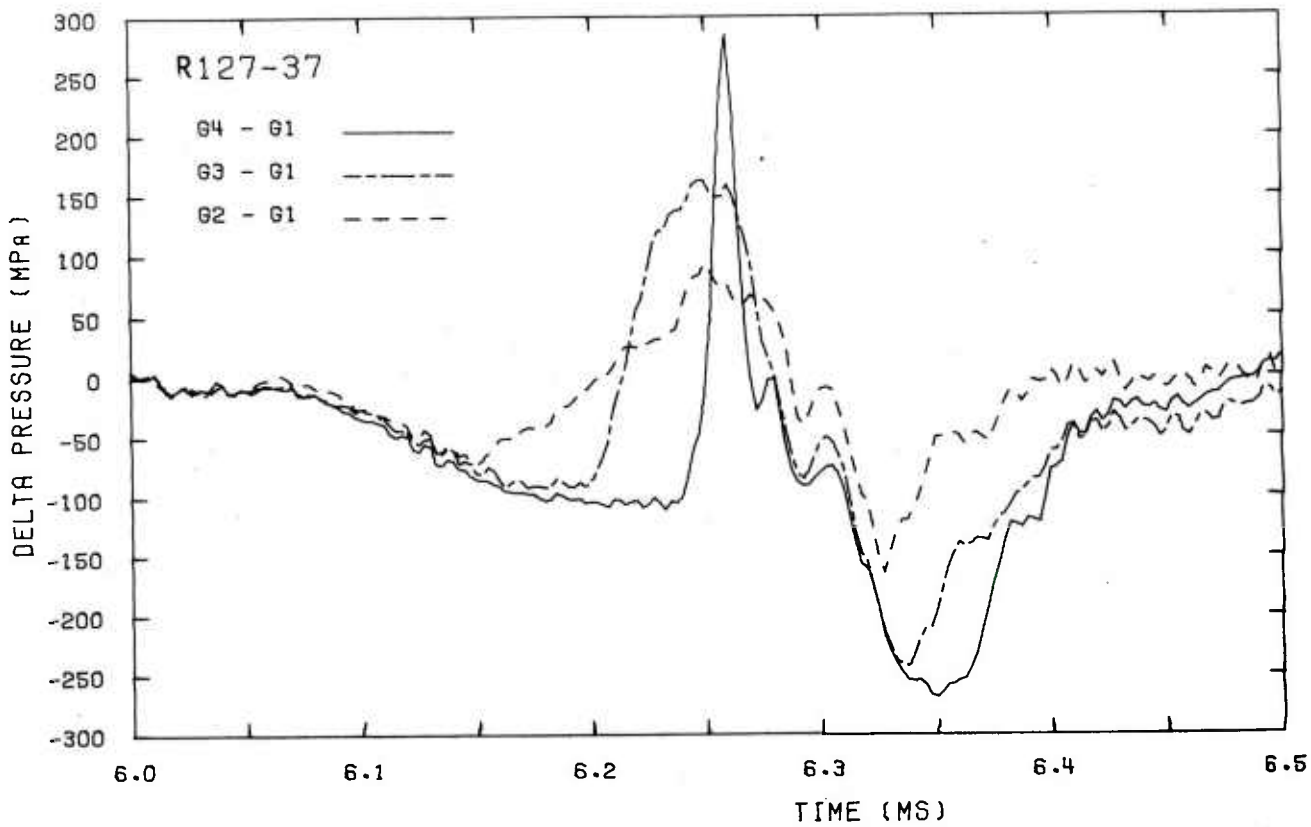
R127-37
G4 - G1
G3 - G1
G2 - G1
DELTA PRESSURE (MPa)
300
250
200
150
100
50
0
-50
-100
-150
-200
-250
-300
6.0
6.1
6.2
6.3
6.4
6.5
TIME (MS)

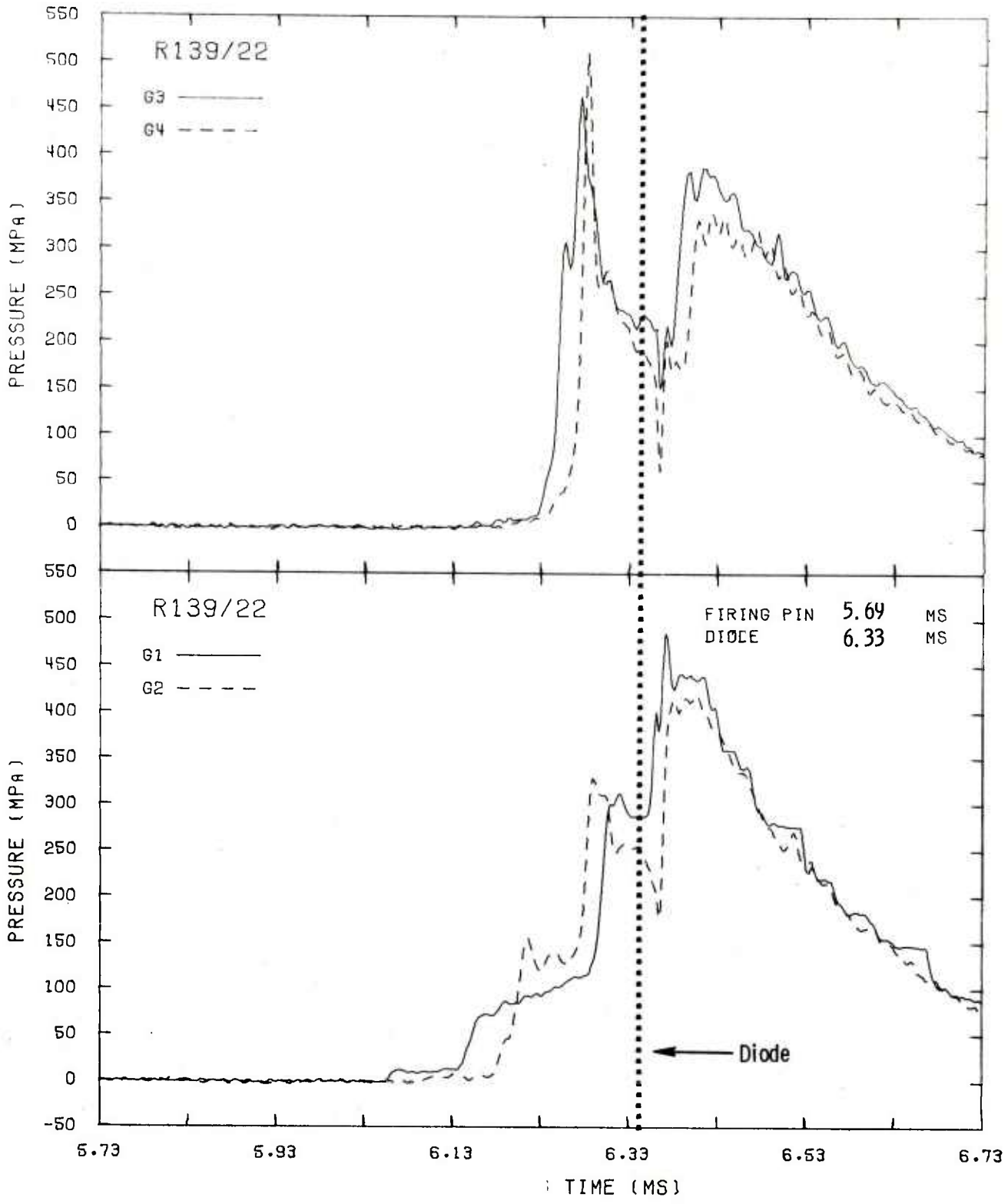
R139/22
G3
G4
PRESSURE (MPa)
550
500
450
400
350
300
250
200
150
100
50
0
R139/22
G1
G2
FIRING PIN 5.69 MS
DIODE 6.33 MS
Diode
-50
5.73
5.93
6.13
6.33
6.53
6.73
TIME (MS)

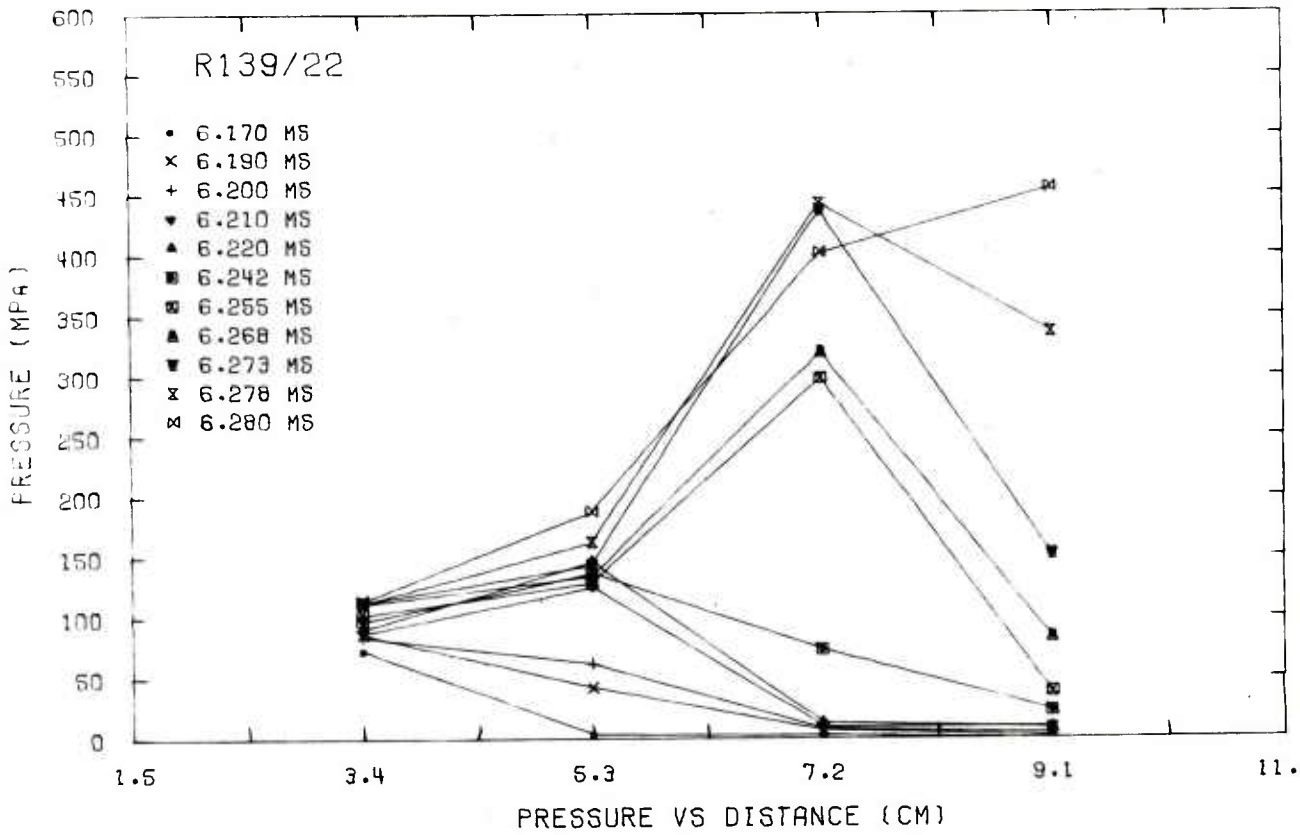
R139/22
6.170 MS
6.190 MS
6.200 MS
6.210 MS
6.220 MS
6.242 MS
6.255 MS
6.268 MS
6.273 MS
6.278 MS
6.280 MS
PRESSURE (MPa)
600
550
500
450
400
350
300
250
200
150
100
50
0
1.5
3.4
5.3
7.2
9.1
11.0
PRESSURE VS DISTANCE (CM)

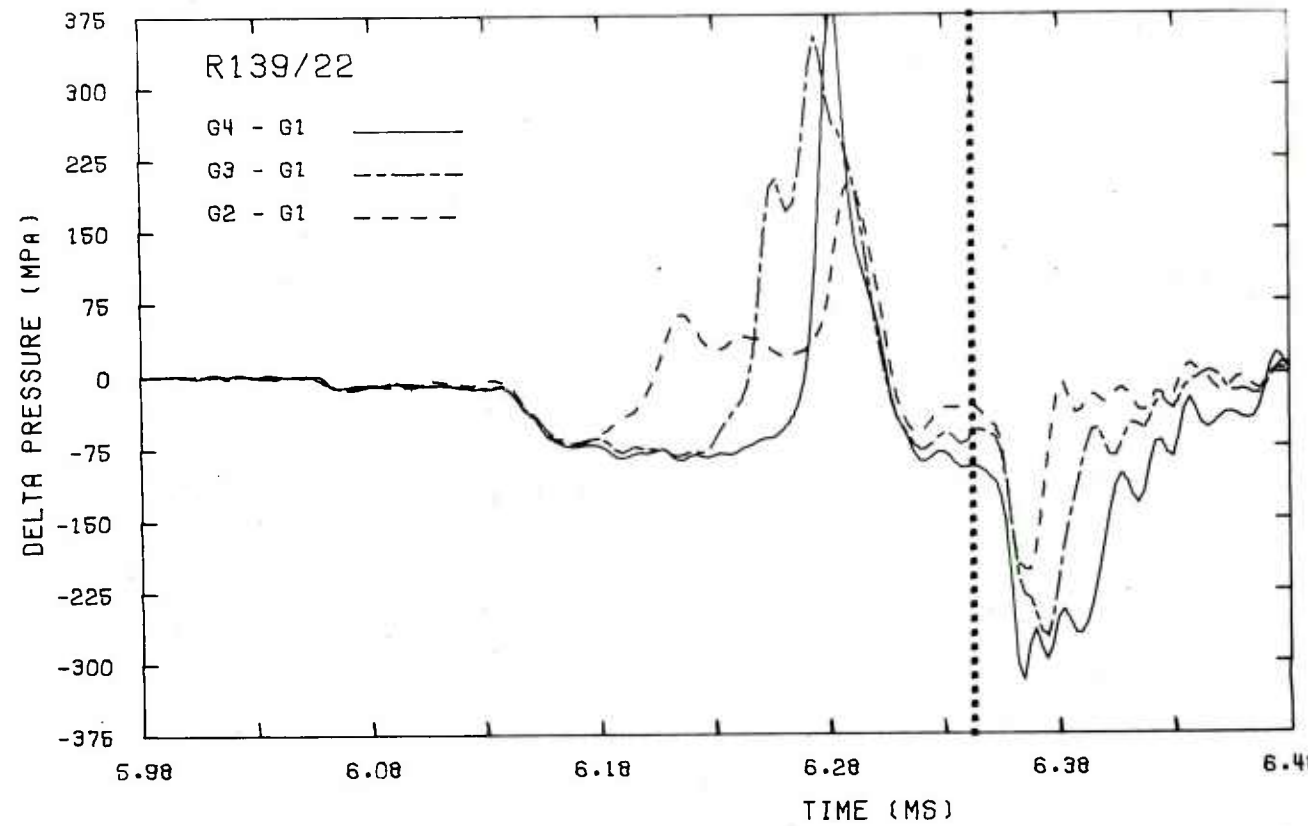
R139/22
G4 - G1
G3 - G1
G2 - G1
DELTA PRESSURE (MPa)
375
300
225
150
75
0
-75
-150
-225
-300
-375
5.98
6.08
6.18
6.28
6.38
6.48
TIME (MS)

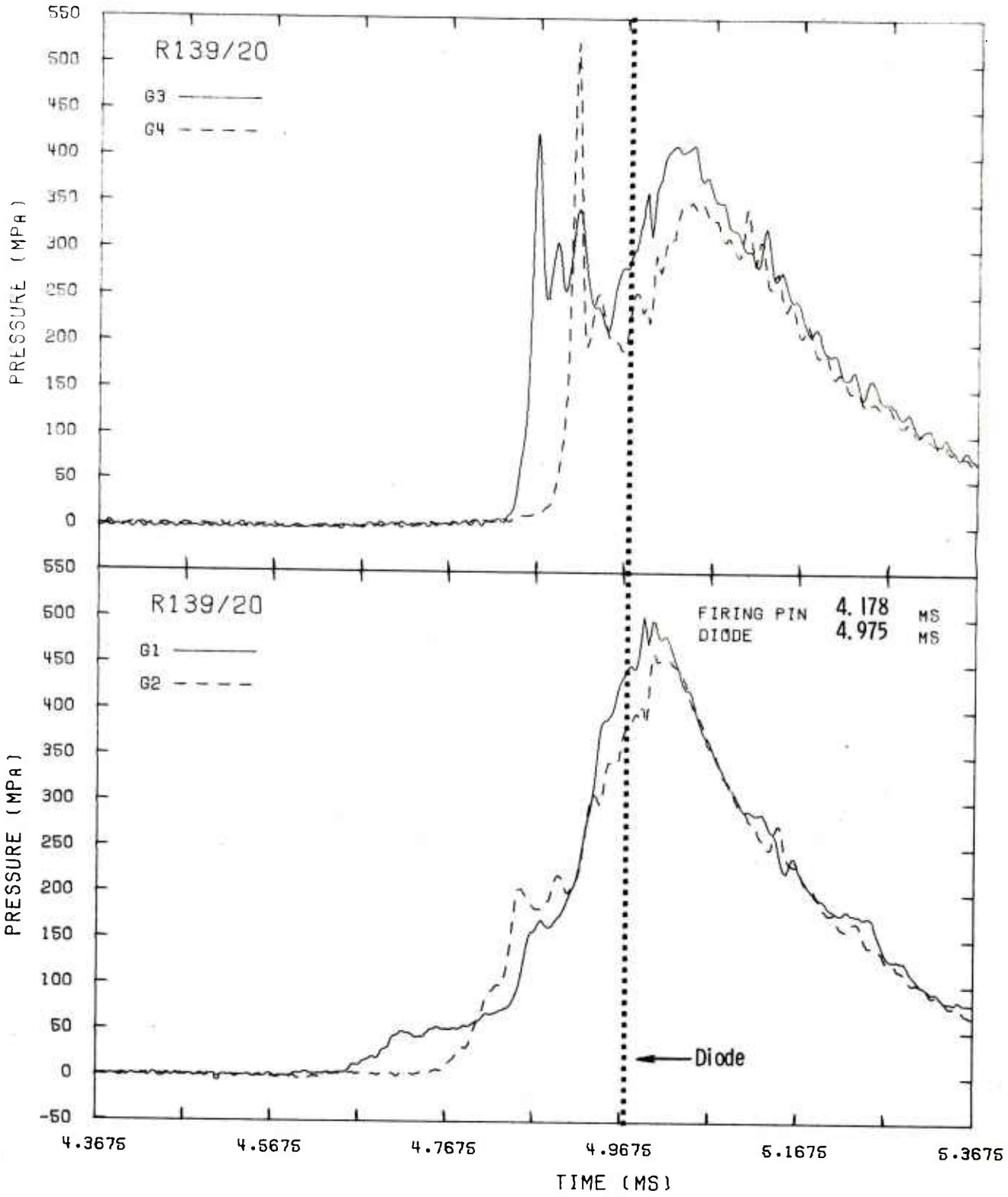
R139/20
G3
G4
PRESSURE (MPA)
550
500
450
400
350
300
250
200
150
100
50
0
R139/20
G1
G2
FIRING PIN 4.178 MS
DIODE 4.975 MS
PRESSURE (MPA)
550
500
450
400
350
300
250
200
150
100
50
0
-50
Diode
4.3675
4.5675
4.7675
4.9675
5.1675
5.3675
TIME (MS)

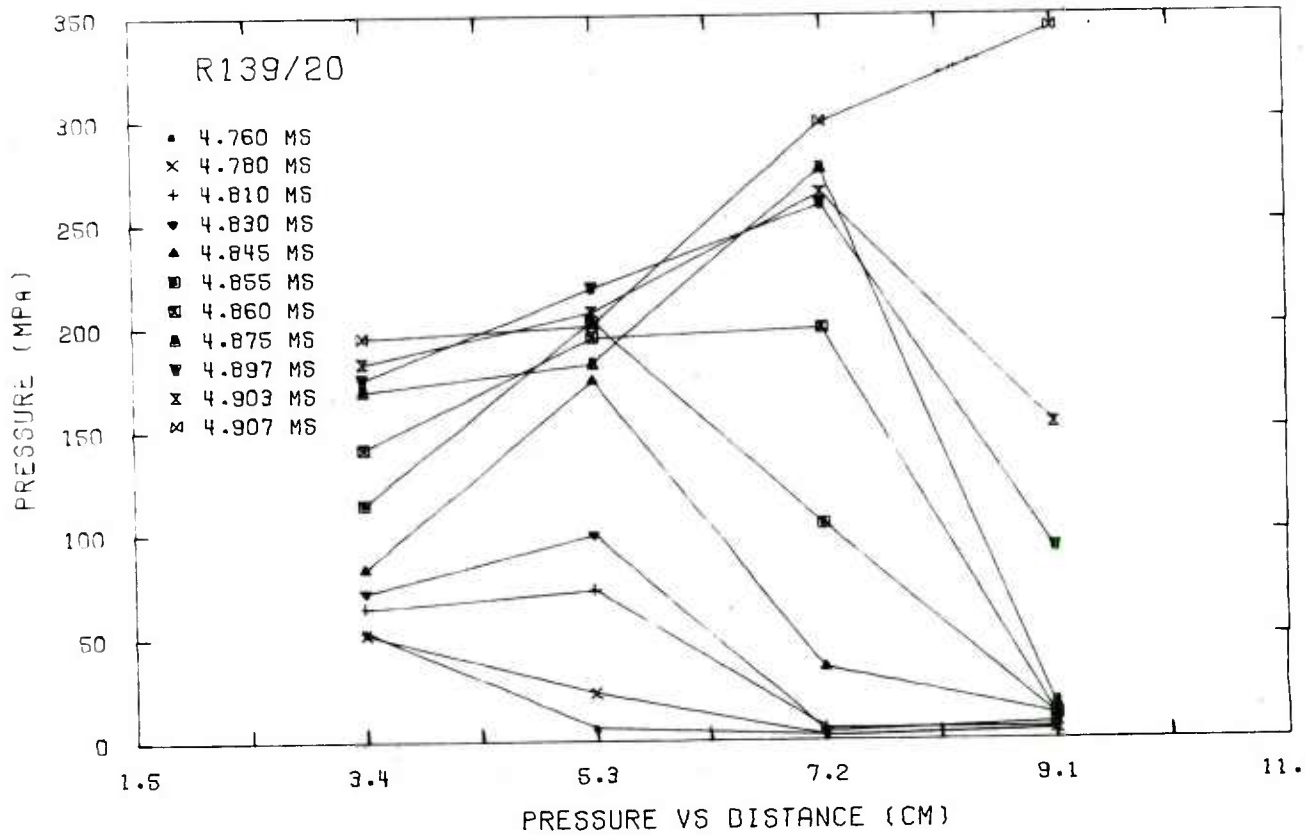
R139/20
4.760 MS
4.780 MS
4.810 MS
4.830 MS
4.845 MS
4.855 MS
4.860 MS
4.875 MS
4.897 MS
4.903 MS
4.907 MS
PRESSURE (MPA)
350
300
250
200
150
100
50
0
1.5
3.4
5.3
7.2
9.1
11.0
PRESSURE VS DISTANCE (CM)

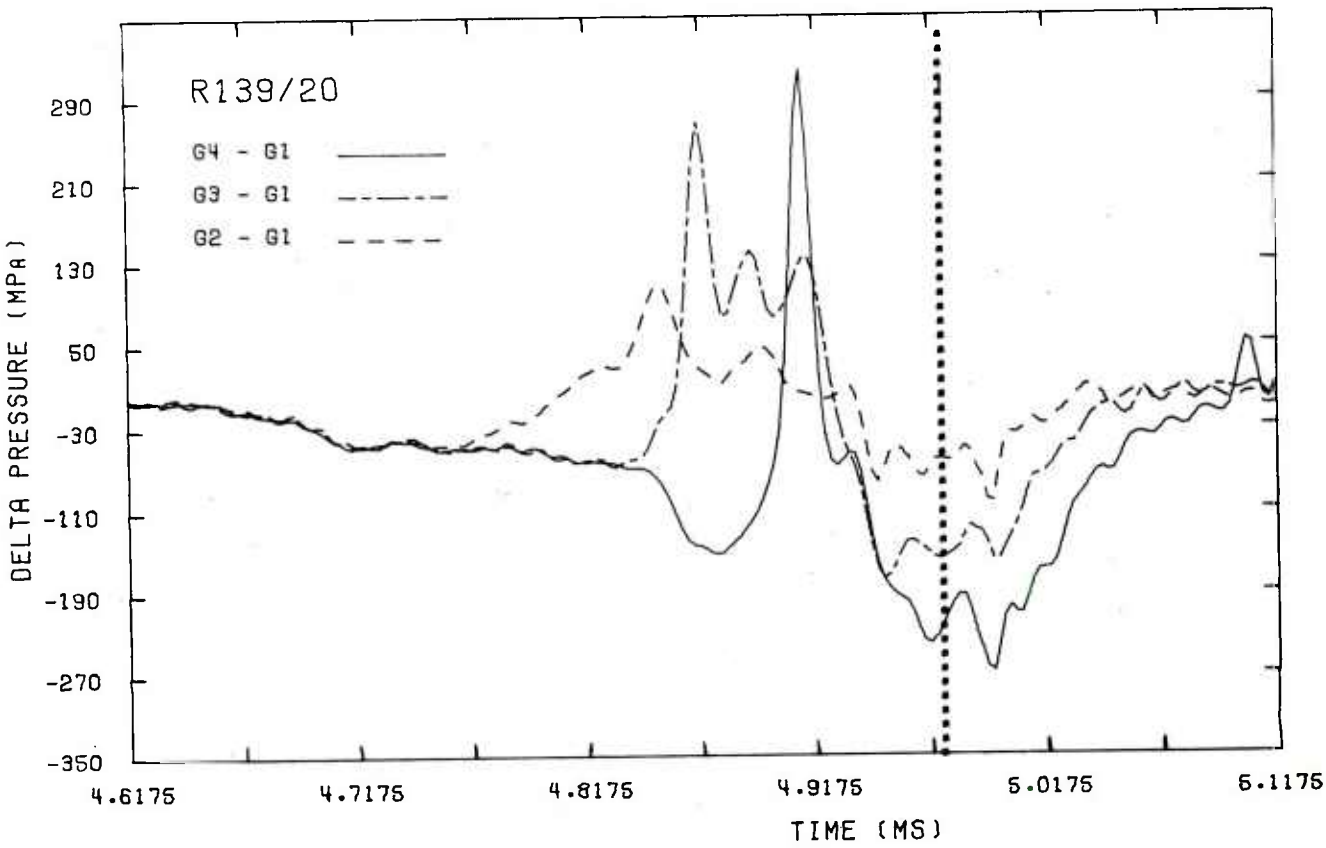
R139/20
G4 - G1
G3 - G1
G2 - G1
DELTA PRESSURE (MPA)
290
210
130
50
-30
-110
-190
-270
-350
4.6175
4.7175
4.8175
4.9175
5.0175
5.1175
TIME (MS)

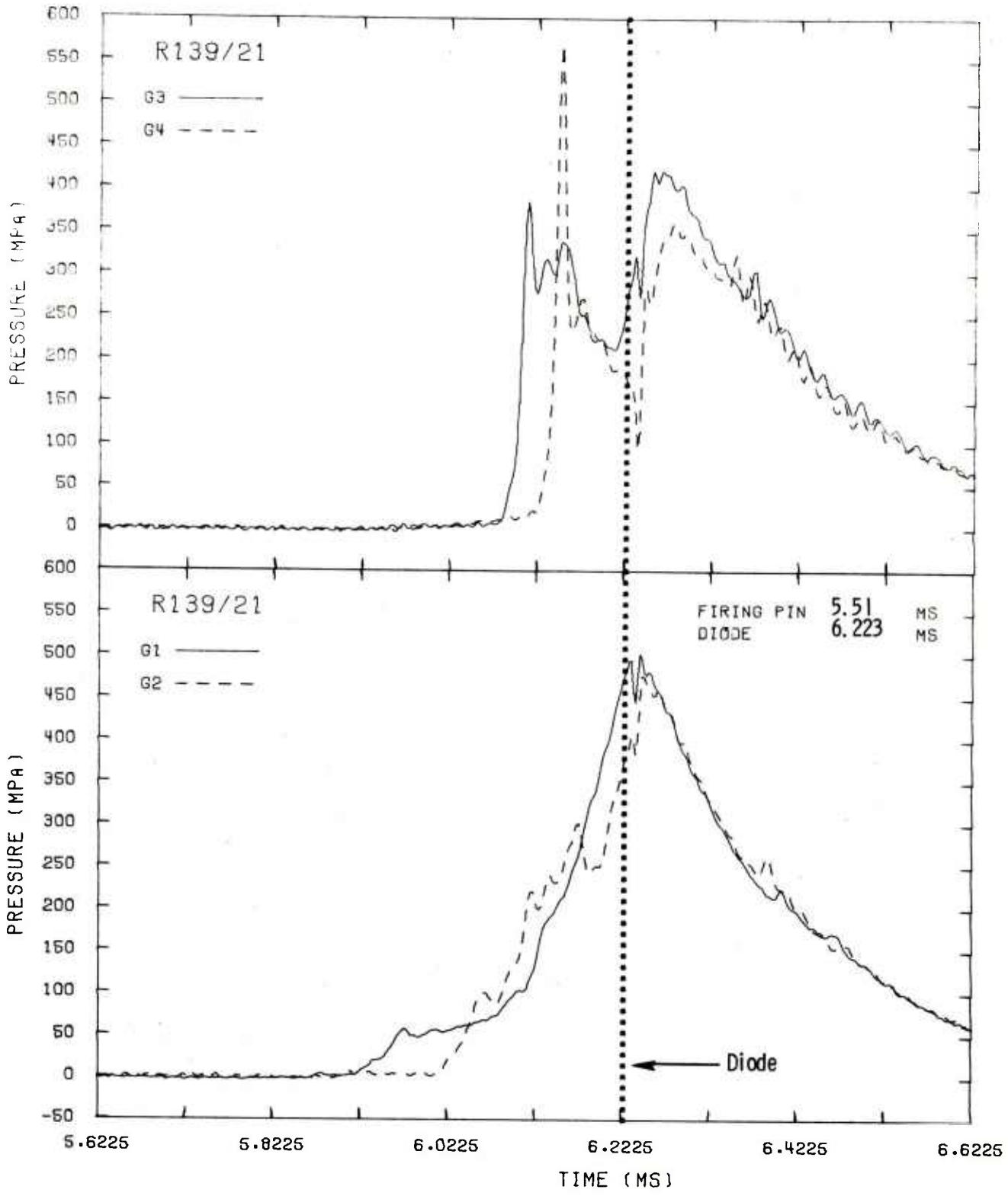
R139/21
G3
G4
R139/21
G1
G2
FIRING PIN 5.51 MS
DIODE 6.223 MS
Diode
PRESSURE (MPa)
PRESSURE (MPa)
TIME (MS)
600
550
500
450
400
350
300
250
200
150
100
50
0
-50
5.6225
5.8225
6.0225
6.2225
6.4225
6.6225

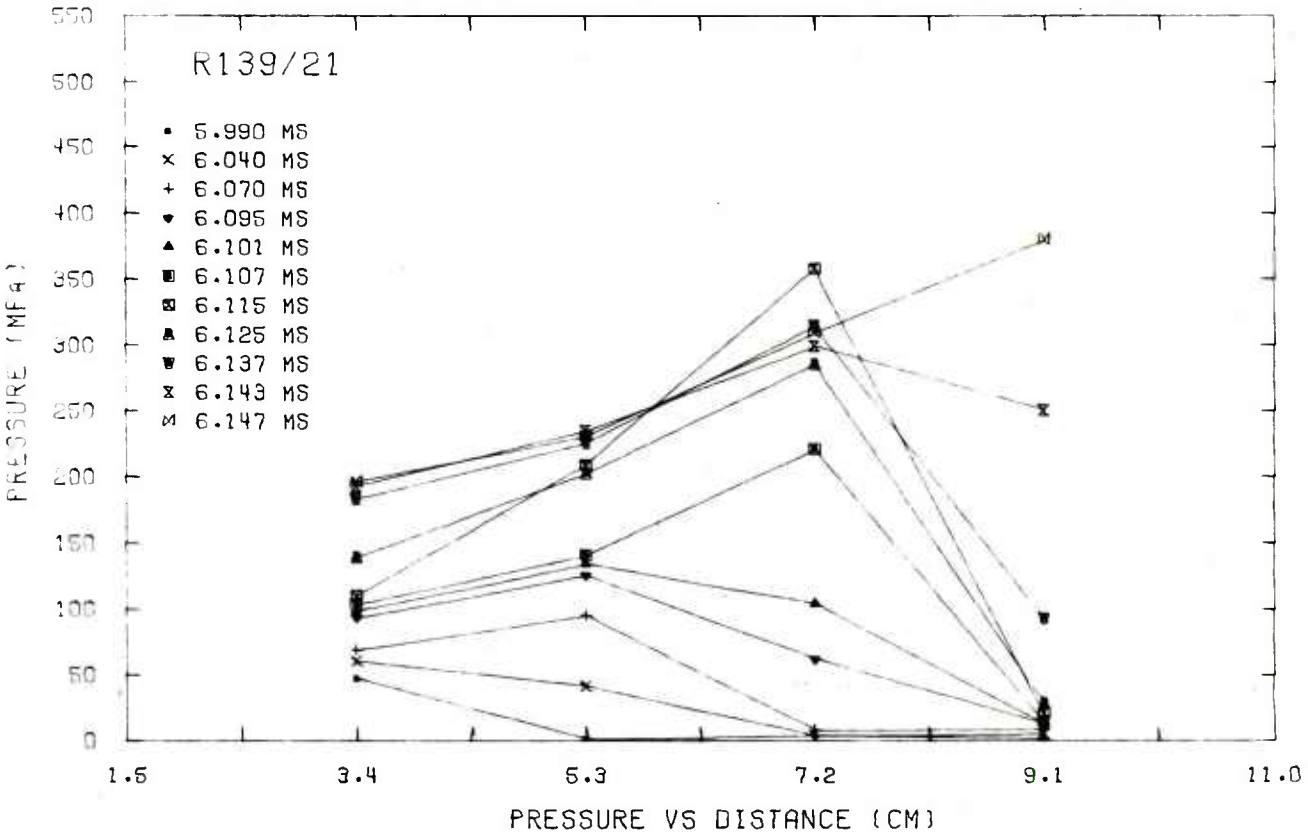
R139/21
5.990 MS
6.040 MS
6.070 MS
6.095 MS
6.101 MS
6.107 MS
6.115 MS
6.125 MS
6.137 MS
6.143 MS
6.147 MS
PRESSURE (MPa)
550
500
450
400
350
300
250
200
150
100
50
0
1.5
3.4
5.3
7.2
9.1
11.0
PRESSURE VS DISTANCE (CM)

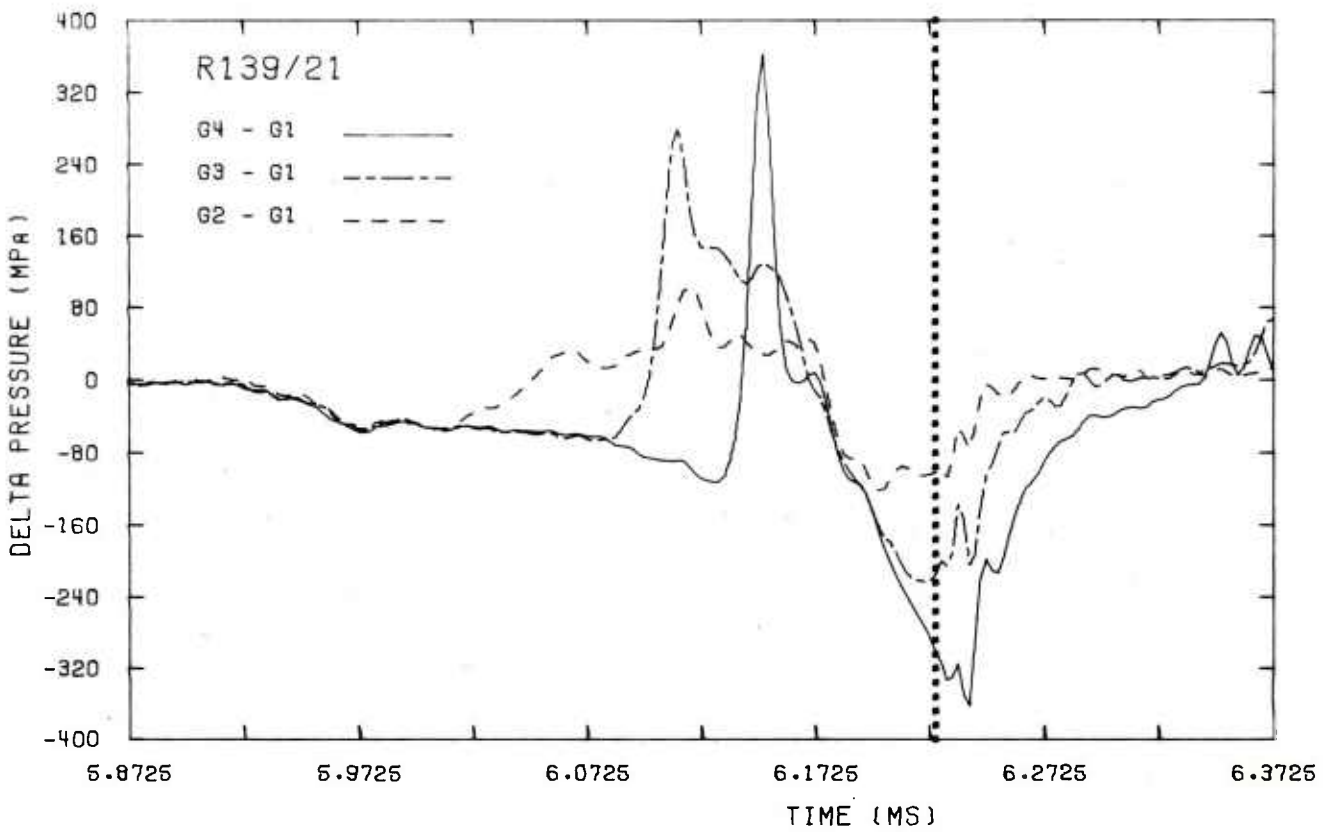
R139/21
G4 - G1
G3 - G1
G2 - G1
DELTA PRESSURE (MPa)
400
320
240
160
80
0
-80
-160
-240
-320
-400
5.8725
5.9725
6.0725
6.1725
6.2725
6.3725
TIME (MS)

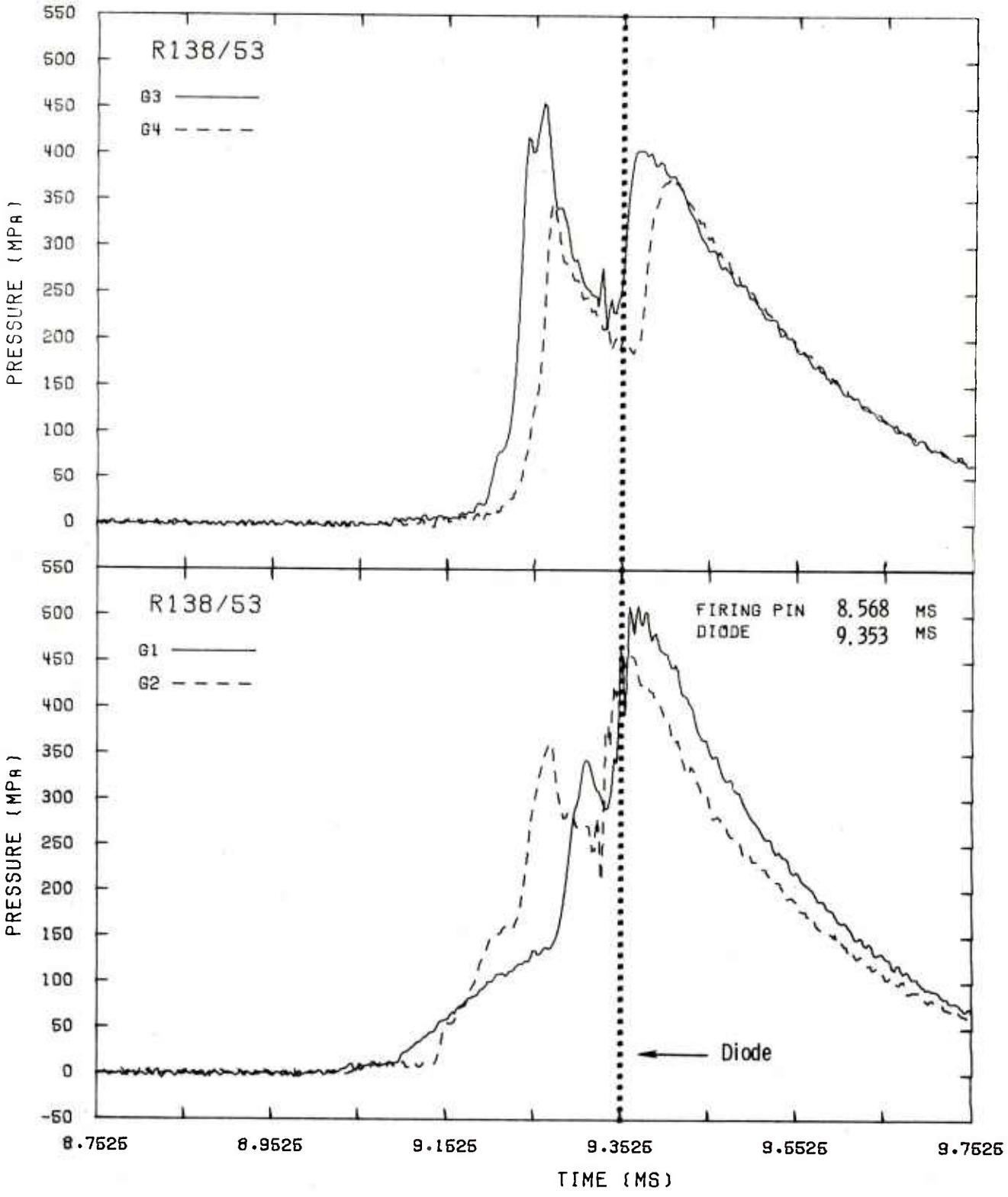
R138/53
G3
G4
PRESSURE (MPa)
R138/53
G1
G2
FIRING PIN 8.568 MS
DIODE 9.353 MS
Diode
PRESSURE (MPa)
TIME (MS)

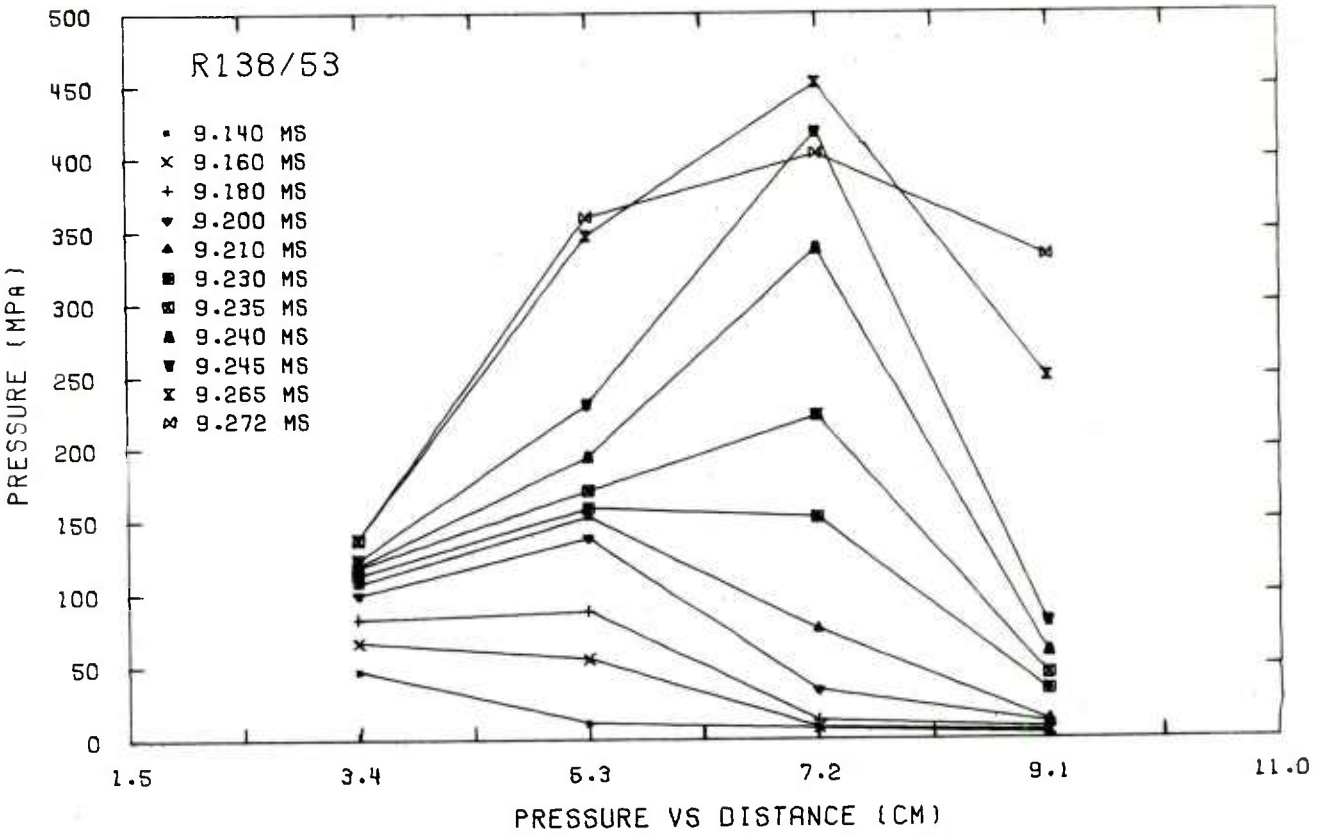
R138/53
9.140 MS
9.160 MS
9.180 MS
9.200 MS
9.210 MS
9.230 MS
9.235 MS
9.240 MS
9.245 MS
9.265 MS
9.272 MS
PRESSURE (MPa)
500
450
400
350
300
250
200
150
100
50
0
1.5
3.4
5.3
7.2
9.1
11.0
PRESSURE VS DISTANCE (CM)

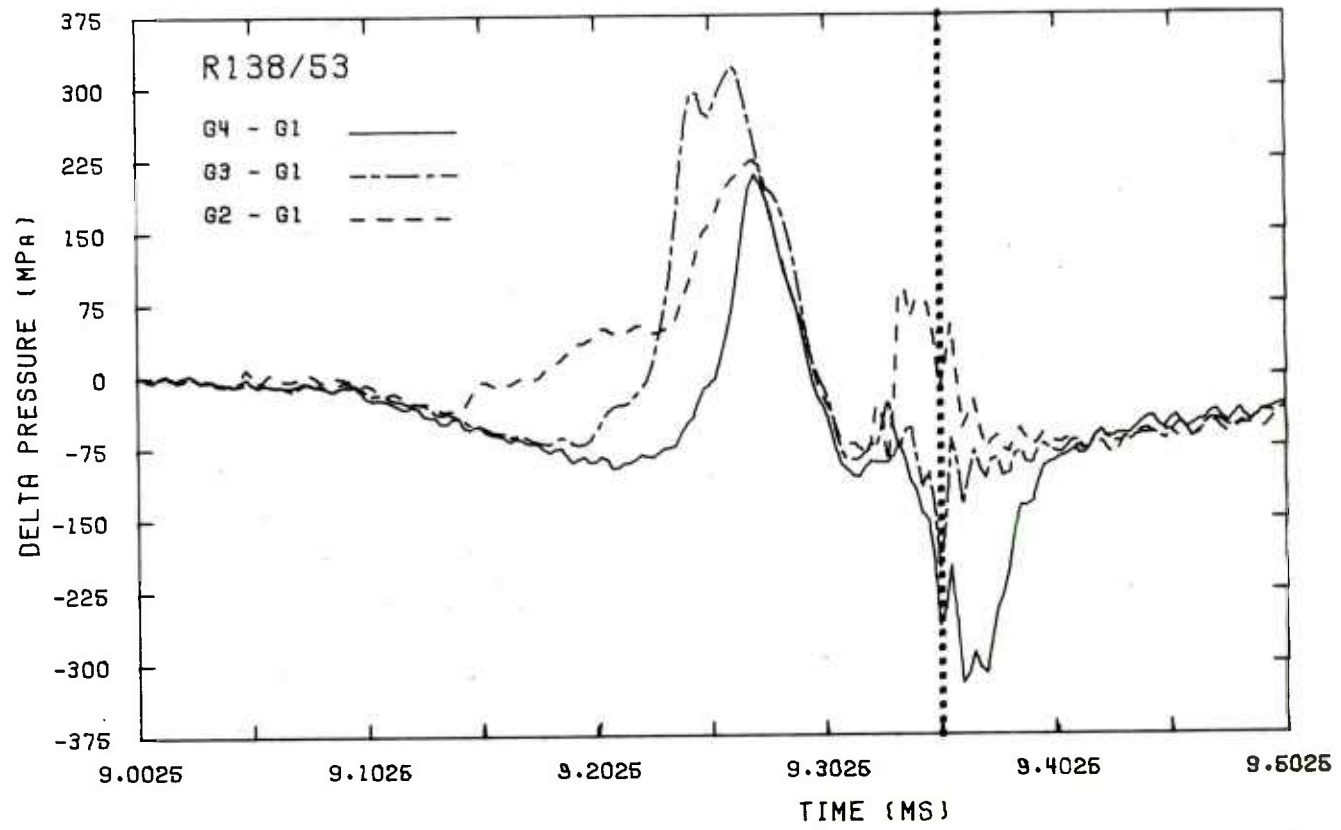
R138/53
G4 - G1
G3 - G1
G2 - G1
DELTA PRESSURE (MPa)
375
300
225
150
75
0
-75
-150
-225
-300
-375
9.0025
9.1025
9.2025
9.3025
9.4025
9.5025
TIME (MS)

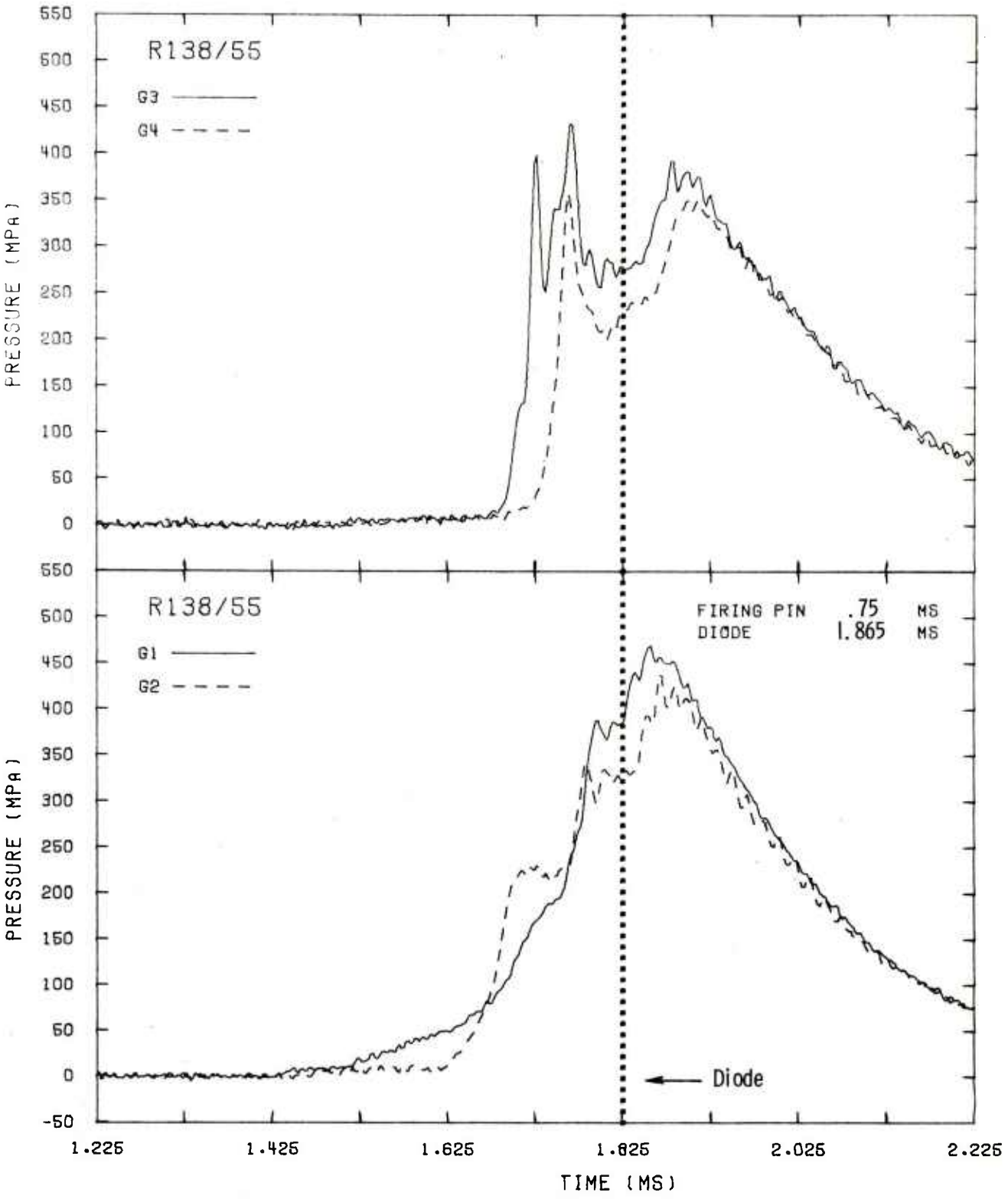
R138/55
G3
G4
PRESSURE (MPa)
550
500
450
400
350
300
250
200
150
100
50
0
R138/55
G1
G2
FIRING PIN .75 MS
DIODE 1.865 MS
Diode
-50
1.225
1.425
1.625
1.825
2.025
2.225
TIME (MS)

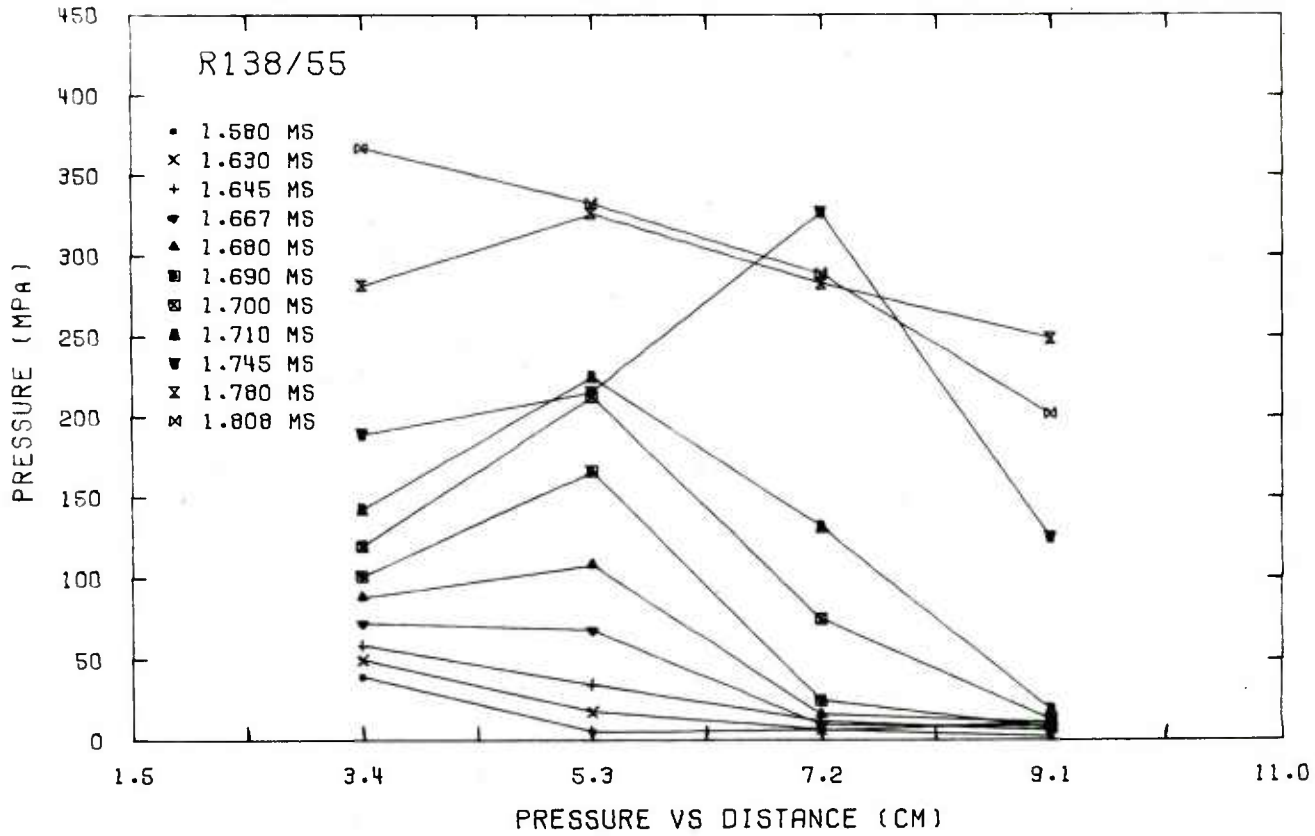
R138/55
1.580 MS
1.630 MS
1.645 MS
1.667 MS
1.680 MS
1.690 MS
1.700 MS
1.710 MS
1.745 MS
1.780 MS
1.808 MS
PRESSURE (MPa)
450
400
350
300
250
200
150
100
50
0
1.5
3.4
5.3
7.2
9.1
11.0
PRESSURE VS DISTANCE (CM)

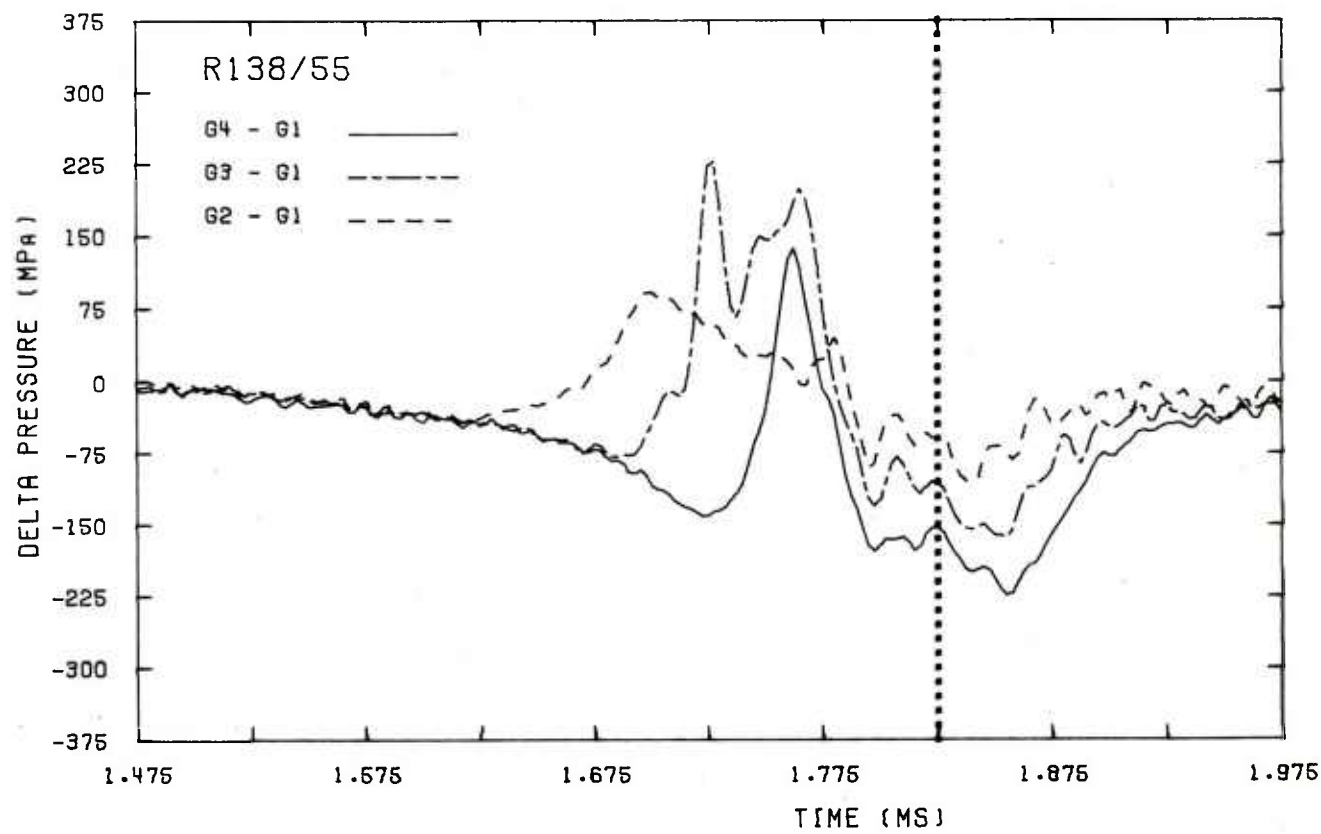
R138/55
G4 - G1
G3 - G1
G2 - G1
DELTA PRESSURE (MPa)
375
300
225
150
75
0
-75
-150
-225
-300
-375
1.475
1.575
1.675
1.775
1.875
1.975
TIME (MS)

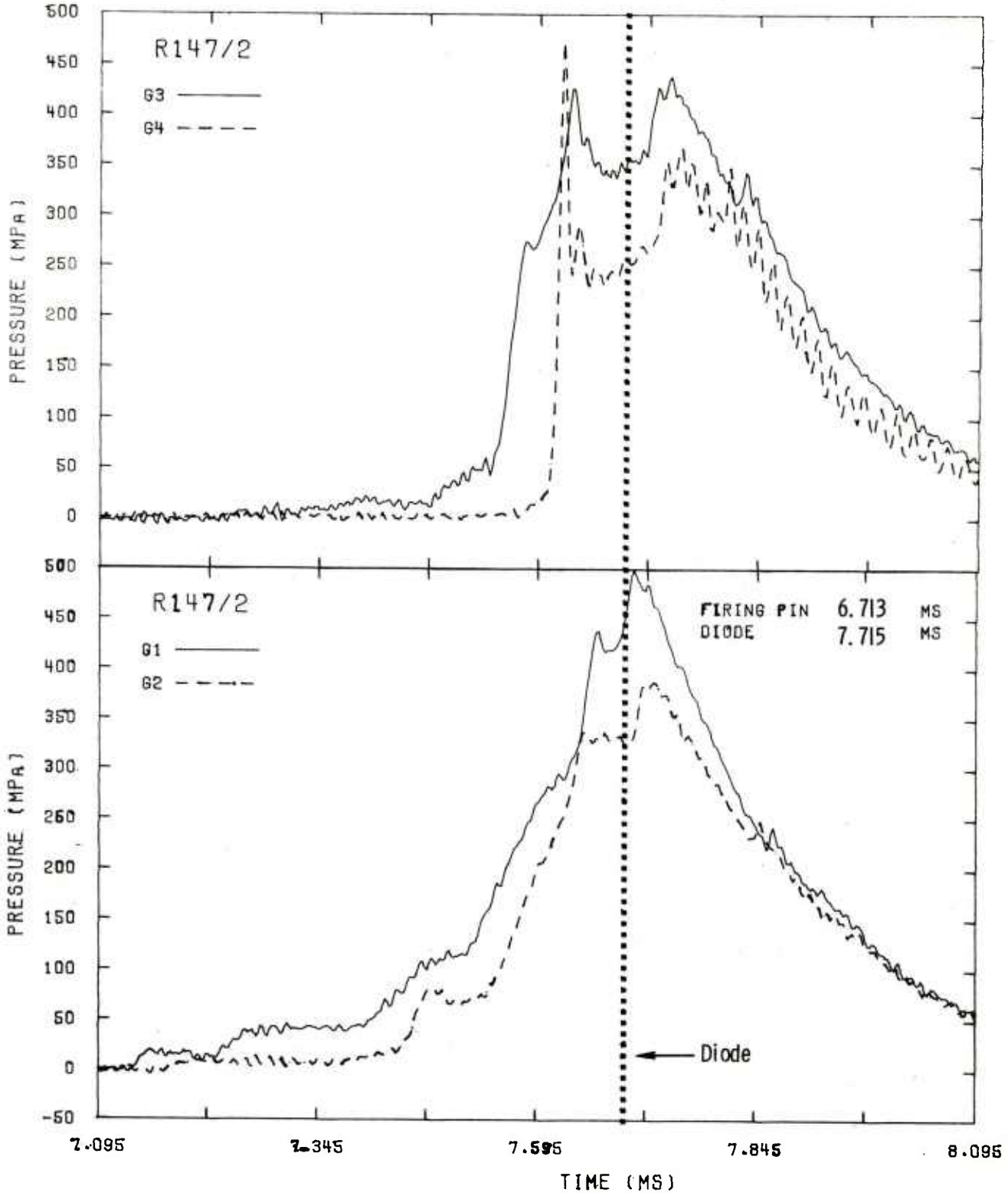
R147/2
G3
G4
PRESSURE (MPA)
R147/2
G1
G2
FIRING PIN 6.713 MS
DIODE 7.715 MS
Diode
PRESSURE (MPA)
TIME (MS)

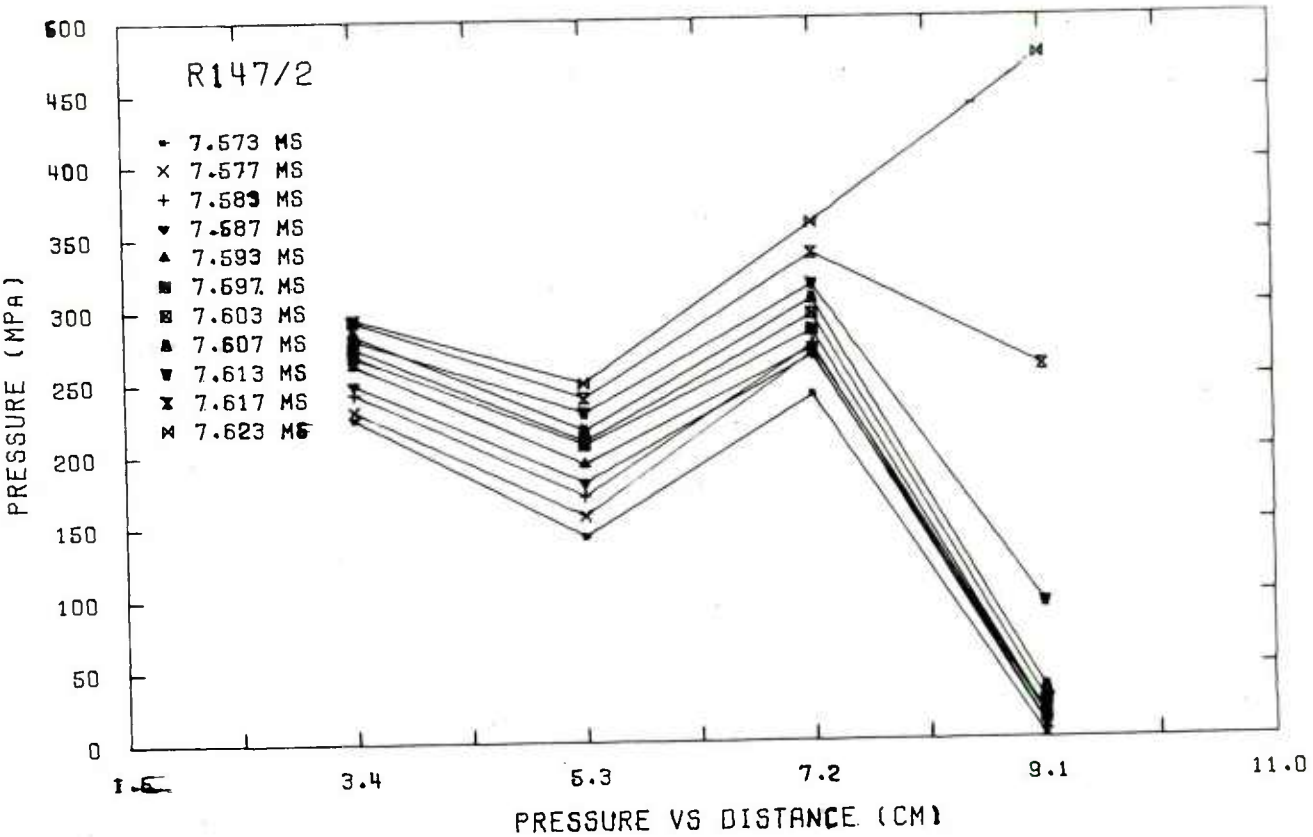
R147/2
7.573 MS
7.577 MS
7.583 MS
7.587 MS
7.593 MS
7.597 MS
7.603 MS
7.607 MS
7.613 MS
7.617 MS
7.623 MS
PRESSURE (MPa)
600
450
400
350
300
250
200
150
100
50
0
1.5
3.4
5.3
7.2
9.1
11.0
PRESSURE VS DISTANCE (CM)

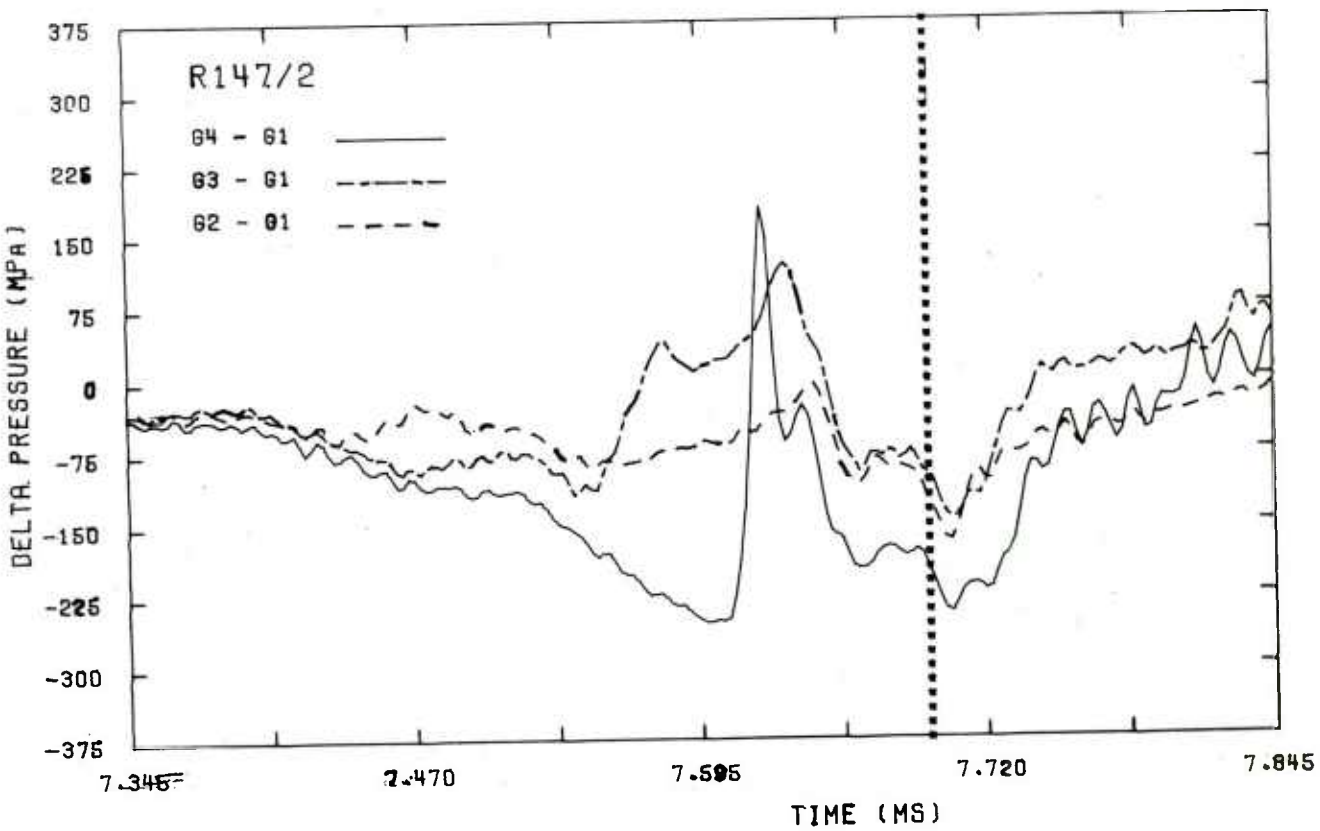
R147/2
G4 - G1
G3 - G1
G2 - G1
DELTA PRESSURE (MPa)
375
300
225
150
75
0
-75
-150
-225
-300
-375
7.345
7.470
7.595
7.720
7.845
TIME (MS)

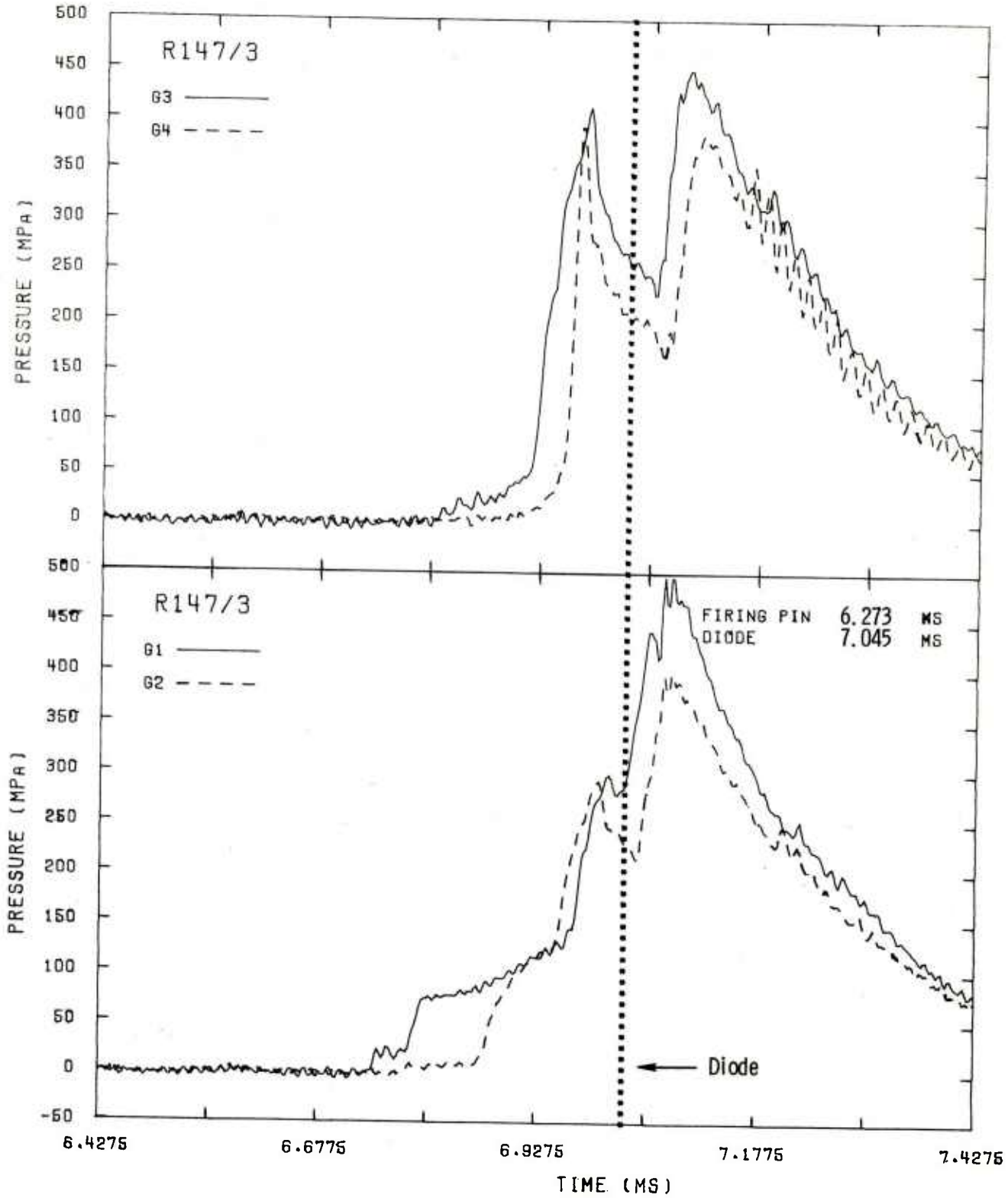
R147/3
G3
G4
PRESSURE (MPA)
500
450
400
350
300
250
200
150
100
50
0
R147/3
G1
G2
FIRING PIN 6.273 MS
DIODE 7.045 MS
Diode
-50
6.4275
6.6775
6.9275
7.1775
7.4275
TIME (MS)

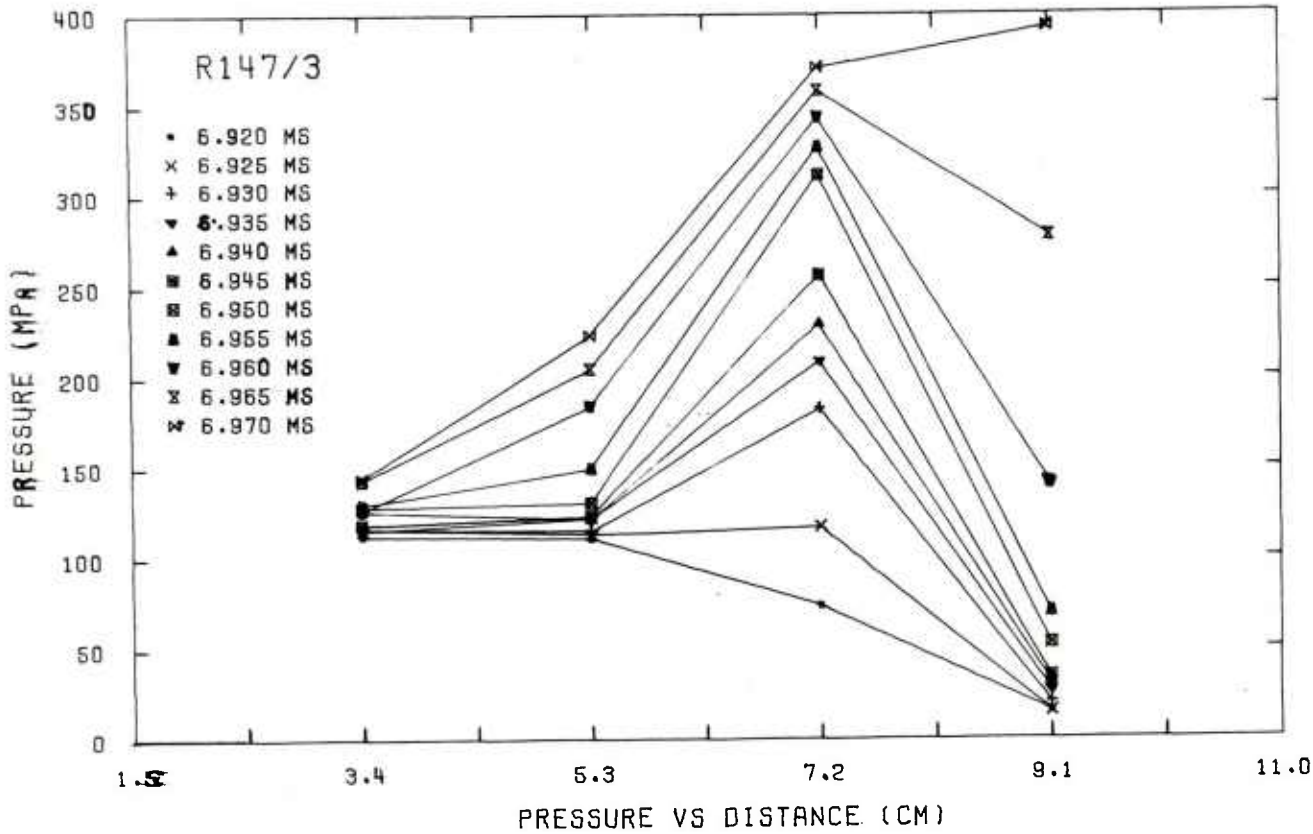
R147/3
6.920 MS
6.925 MS
6.930 MS
6.935 MS
6.940 MS
6.945 MS
6.950 MS
6.955 MS
6.960 MS
6.965 MS
6.970 MS
PRESSURE (MPa)
400
350
300
250
200
150
100
50
0
1.5
3.4
5.3
7.2
9.1
11.0
PRESSURE VS DISTANCE (CM)

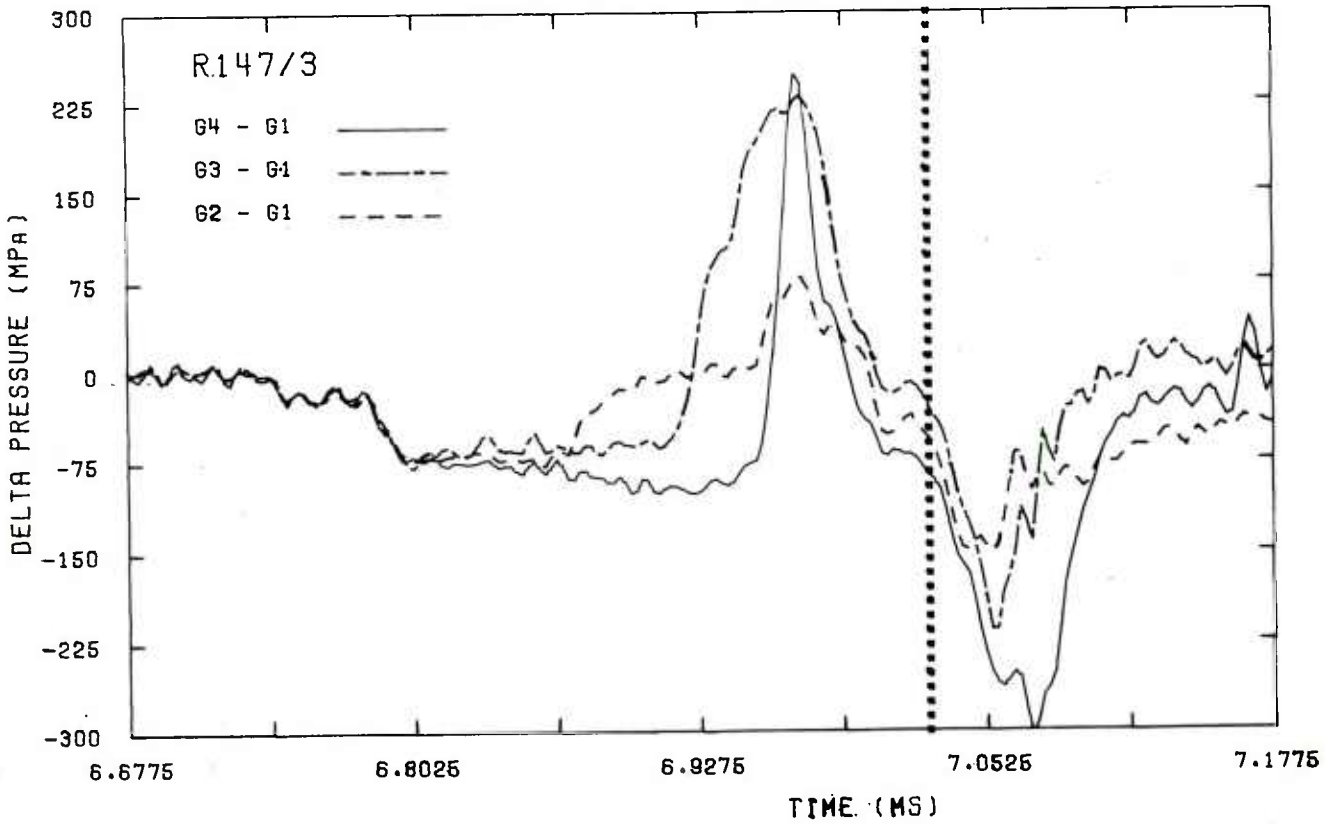
R147/3
G4 - G1
G3 - G1
G2 - G1
DELTA PRESSURE (MPa)
300
225
150
75
0
-75
-150
-225
-300
6.6775
6.8025
6.9275
7.0525
7.1775
TIME (MS)

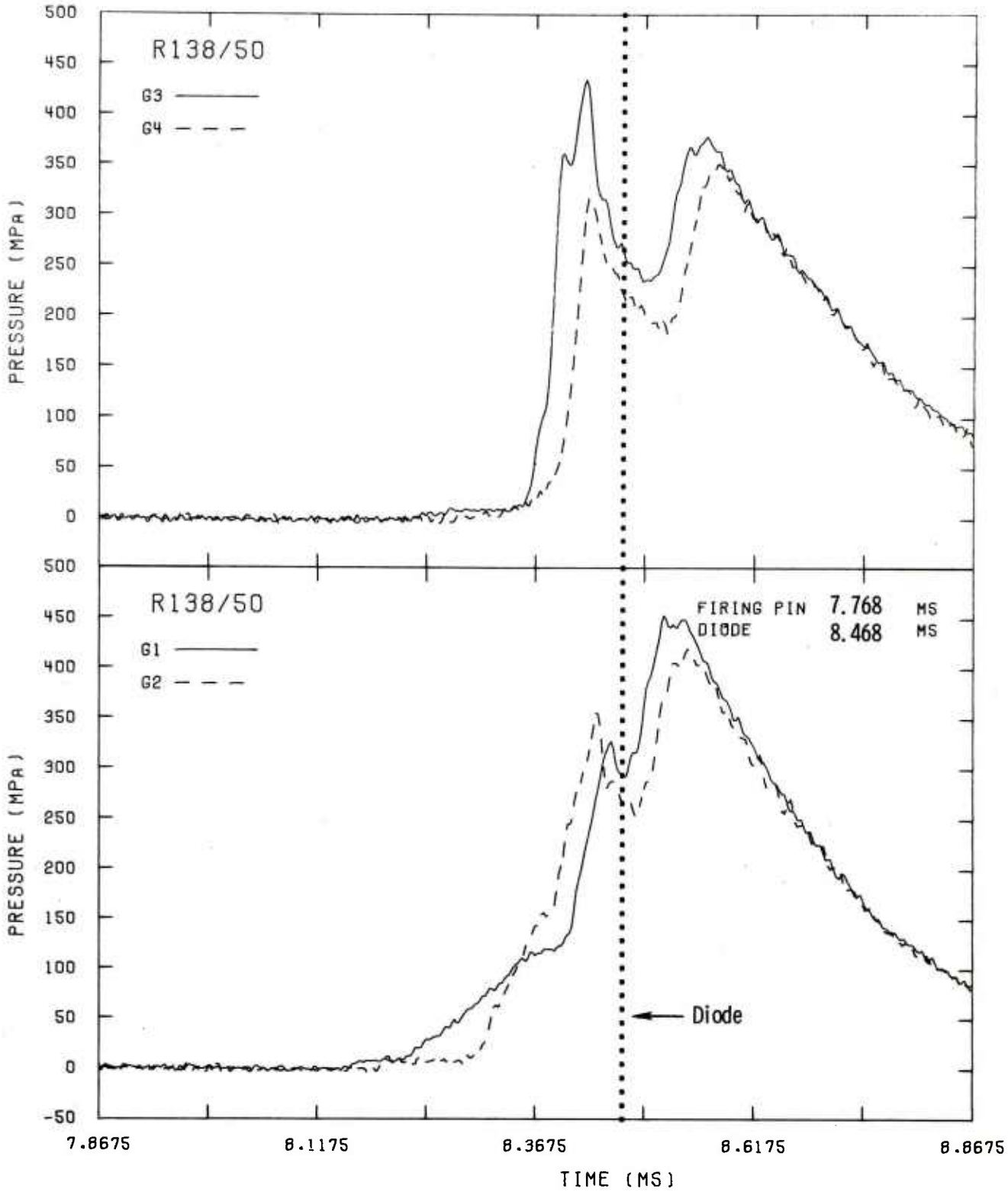
R138/50
G3
G4
PRESSURE (MPa)
500
450
400
350
300
250
200
150
100
50
0
R138/50
G1
G2
FIRING PIN 7.768 MS
DIODE 8.468 MS
Diode
-50
7.8675
8.1175
8.3675
8.6175
8.8675
TIME (MS)

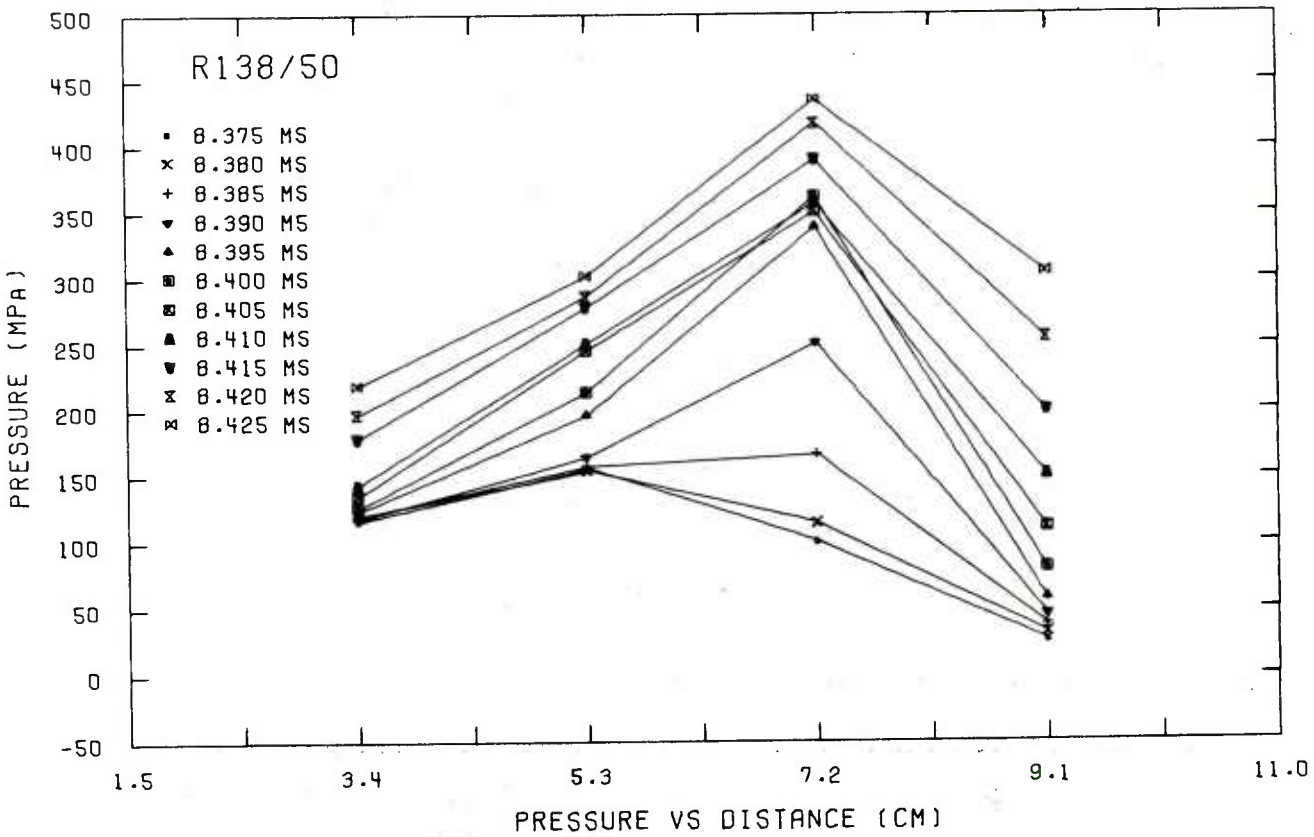
R138/50
8.375 MS
8.380 MS
8.385 MS
8.390 MS
8.395 MS
8.400 MS
8.405 MS
8.410 MS
8.415 MS
8.420 MS
8.425 MS
PRESSURE (MPa)
500
450
400
350
300
250
200
150
100
50
0
-50
1.5
3.4
5.3
7.2
9.1
11.0
PRESSURE VS DISTANCE (CM)

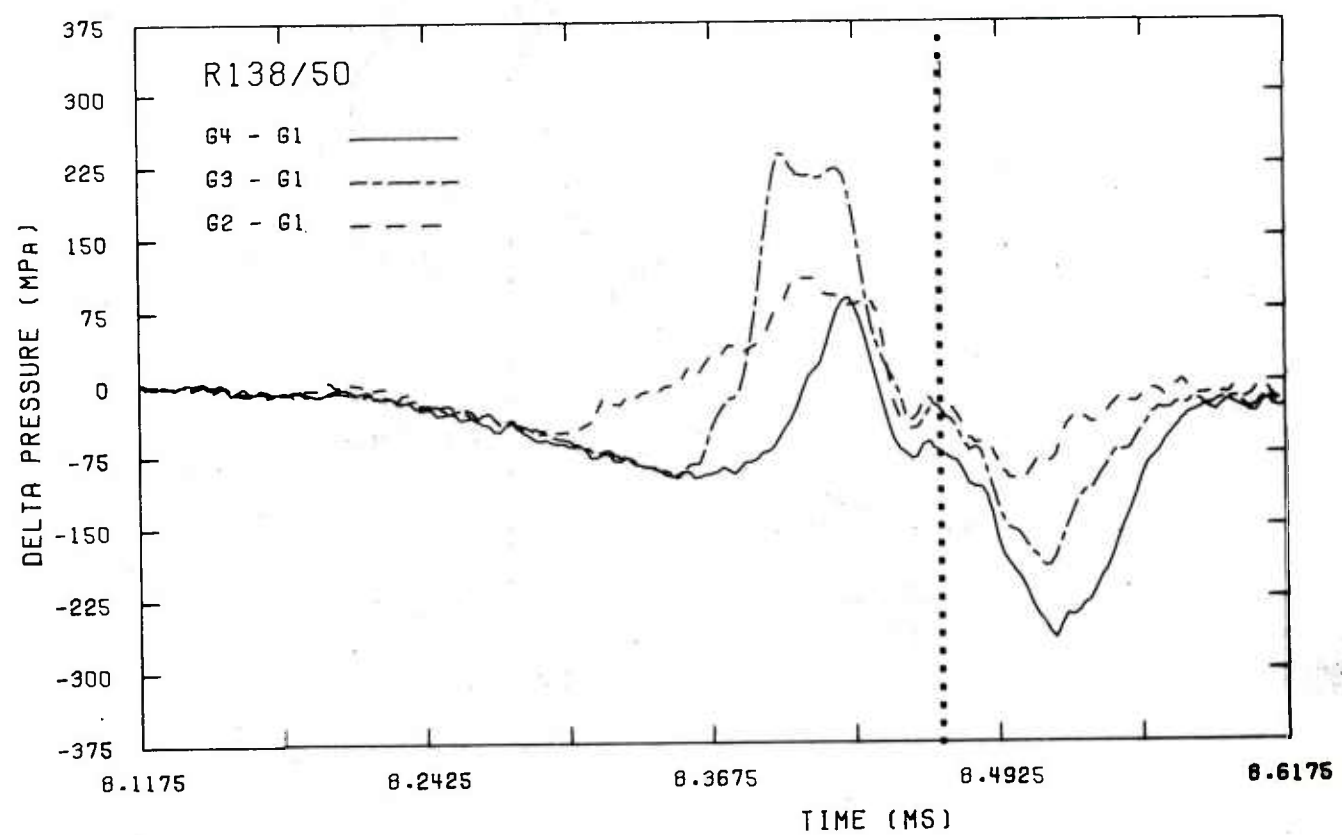
R138/50
G4 - G1
G3 - G1
G2 - G1
DELTA PRESSURE (MPa)
375
300
225
150
75
0
-75
-150
-225
-300
-375
8.1175
8.2425
8.3675
8.4925
8.6175
TIME (MS)

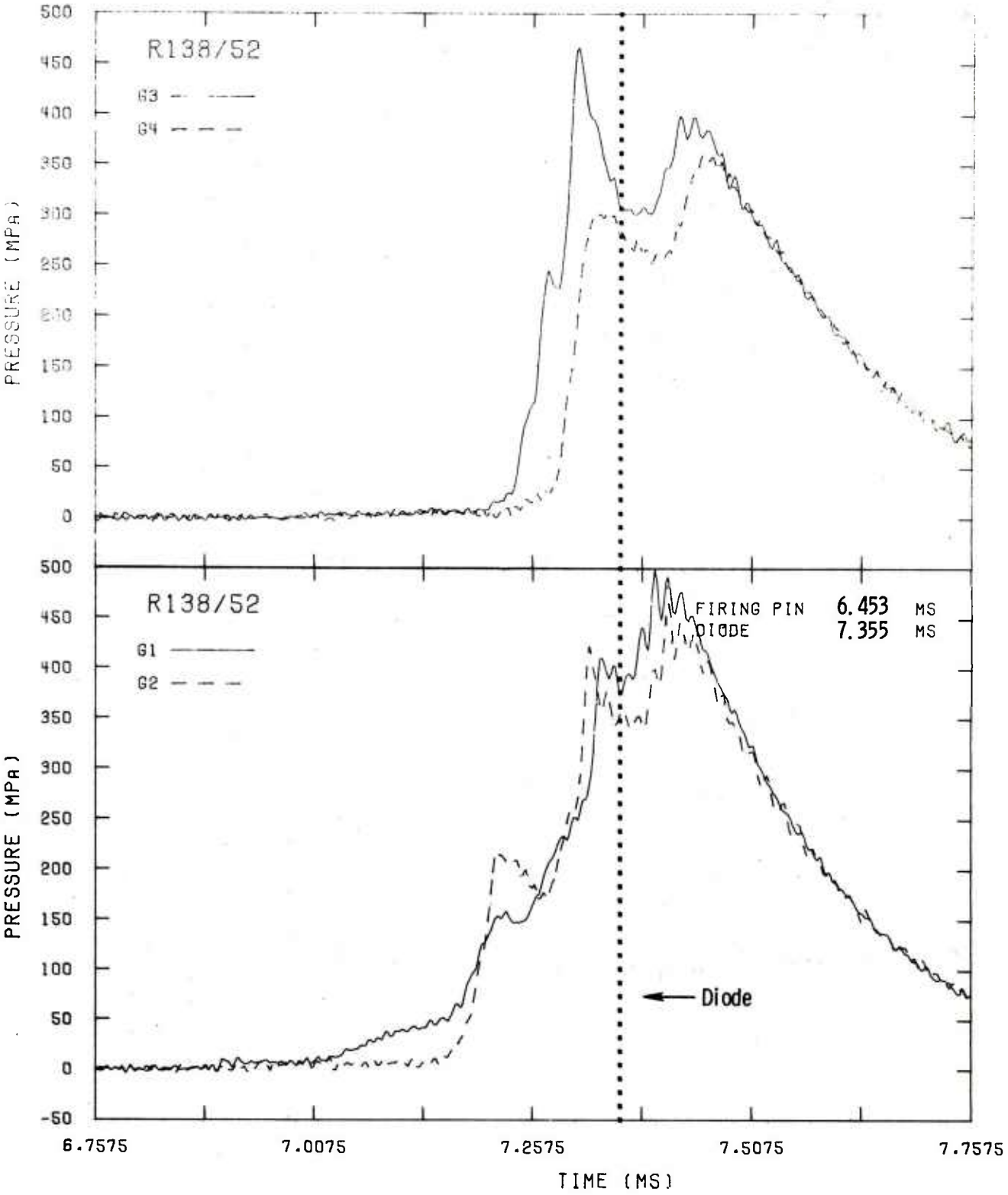
R138/52
G3
G4
PRESSURE (MPa)
R138/52
G1
G2
FIRING PIN 6.453 MS
DIODE 7.355 MS
Diode
PRESSURE (MPa)
TIME (MS)

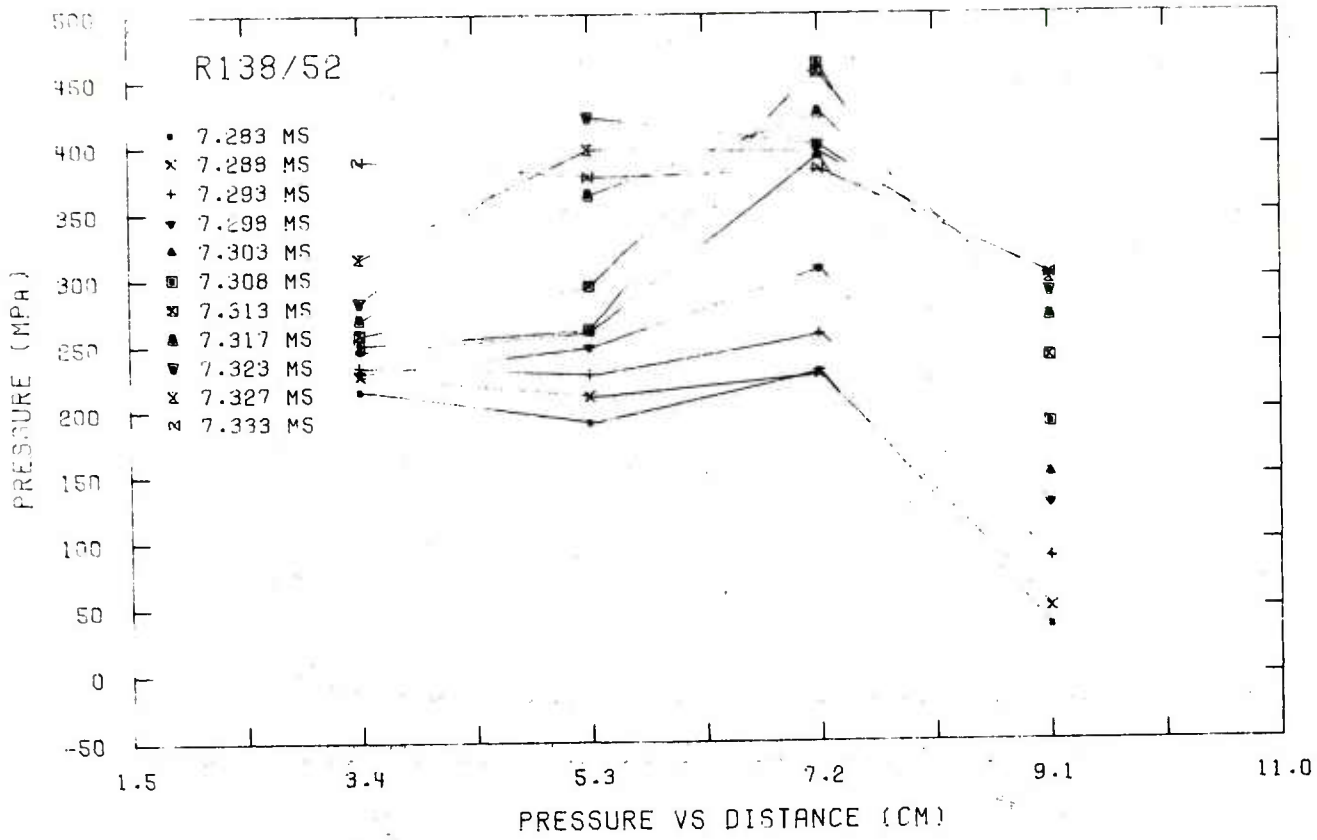
R138/52
7.283 MS
7.288 MS
7.293 MS
7.298 MS
7.303 MS
7.308 MS
7.313 MS
7.317 MS
7.323 MS
7.327 MS
7.333 MS
PRESSURE (MPA)
500
450
400
350
300
250
200
150
100
50
0
-50
1.5
3.4
5.3
7.2
9.1
11.0
PRESSURE VS DISTANCE (CM)

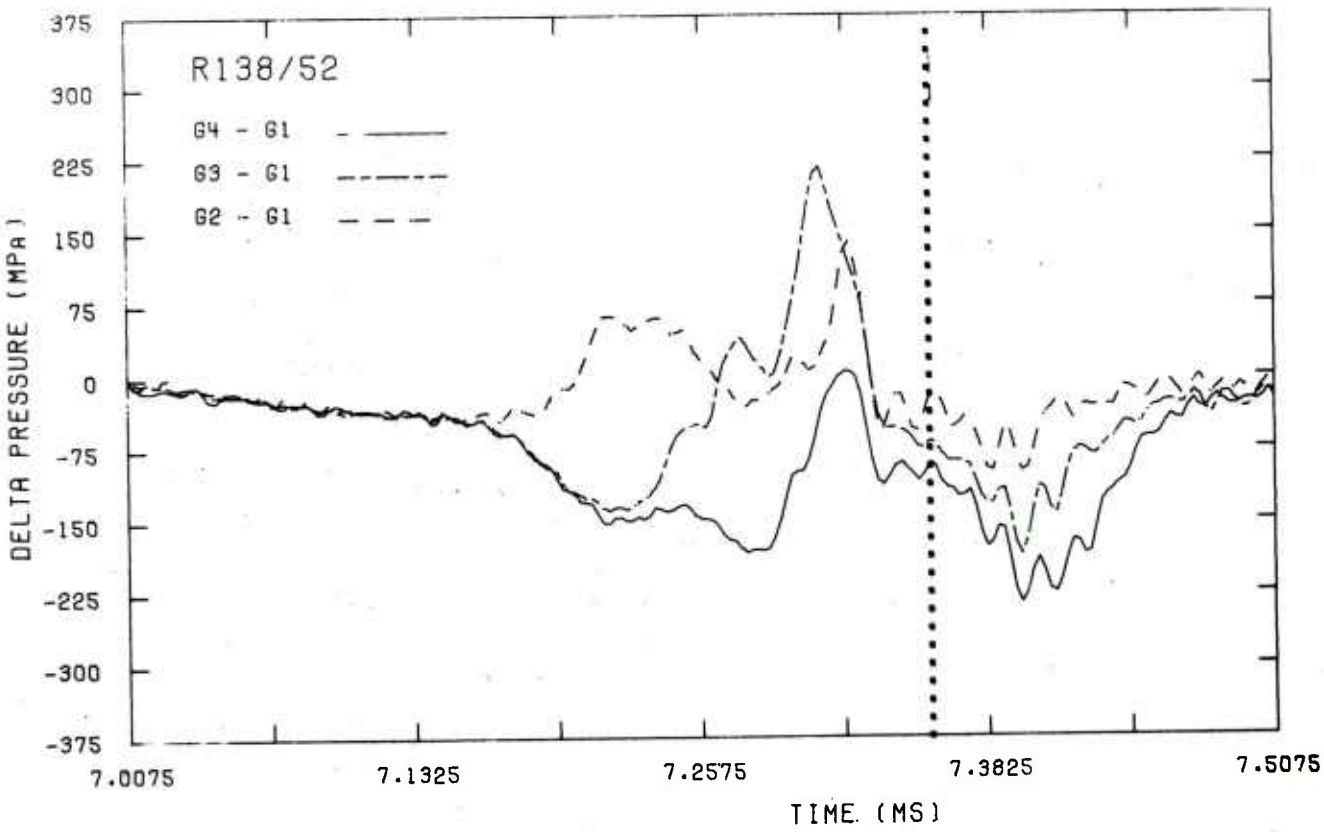
R138/52
G4 - G1
G3 - G1
G2 - G1
DELTA PRESSURE (MPA)
375
300
225
150
75
0
-75
-150
-225
-300
-375
7.0075
7.1325
7.2575
7.3825
7.5075
TIME (MS)

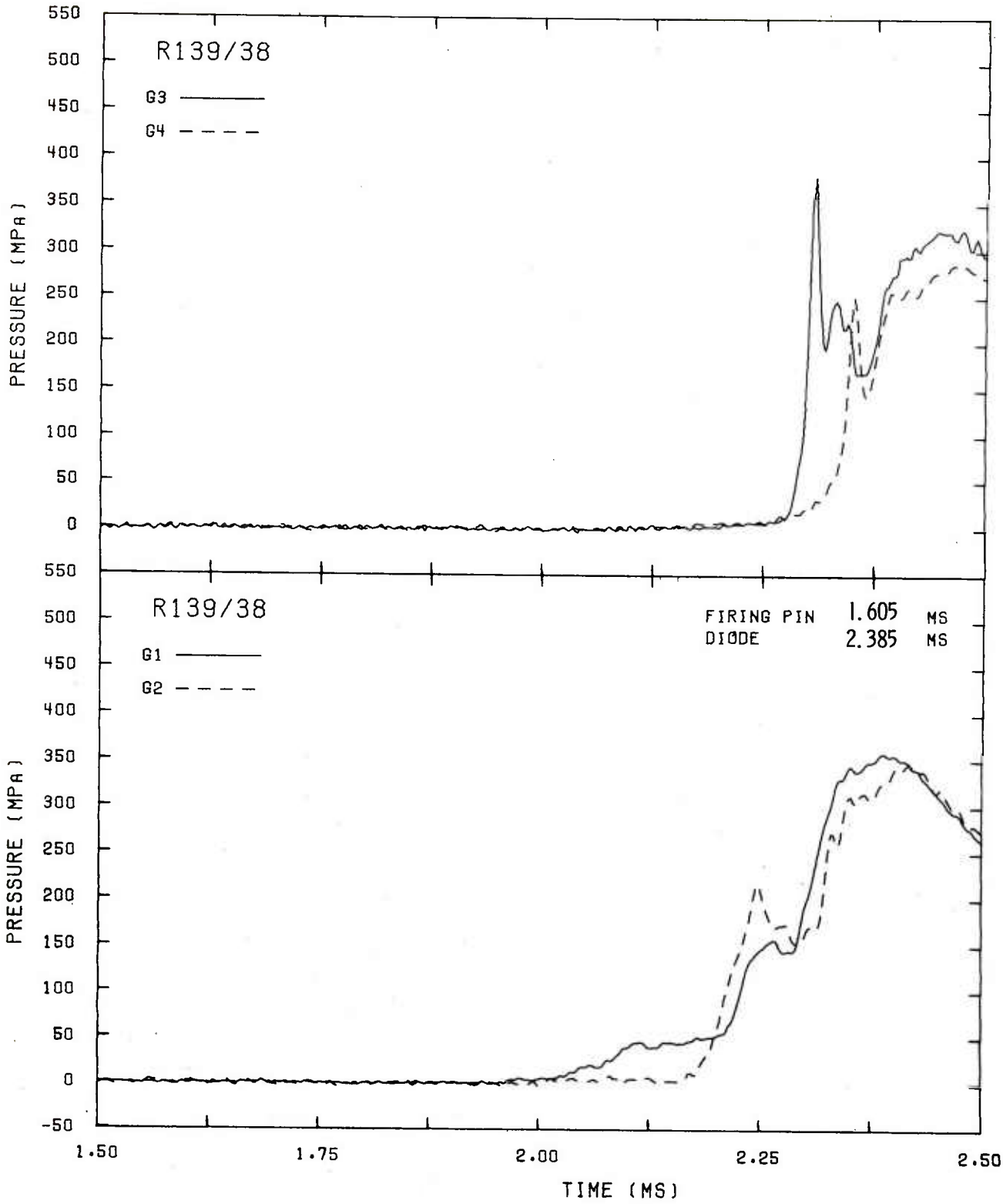
R139/38
G3
G4
PRESSURE (MPa)
550
500
450
400
350
300
250
200
150
100
50
0
R139/38
G1
G2
FIRING PIN 1.605 MS
DIODE 2.385 MS
PRESSURE (MPa)
550
500
450
400
350
300
250
200
150
100
50
0
-50
1.50
1.75
2.00
2.25
2.50
TIME (MS)

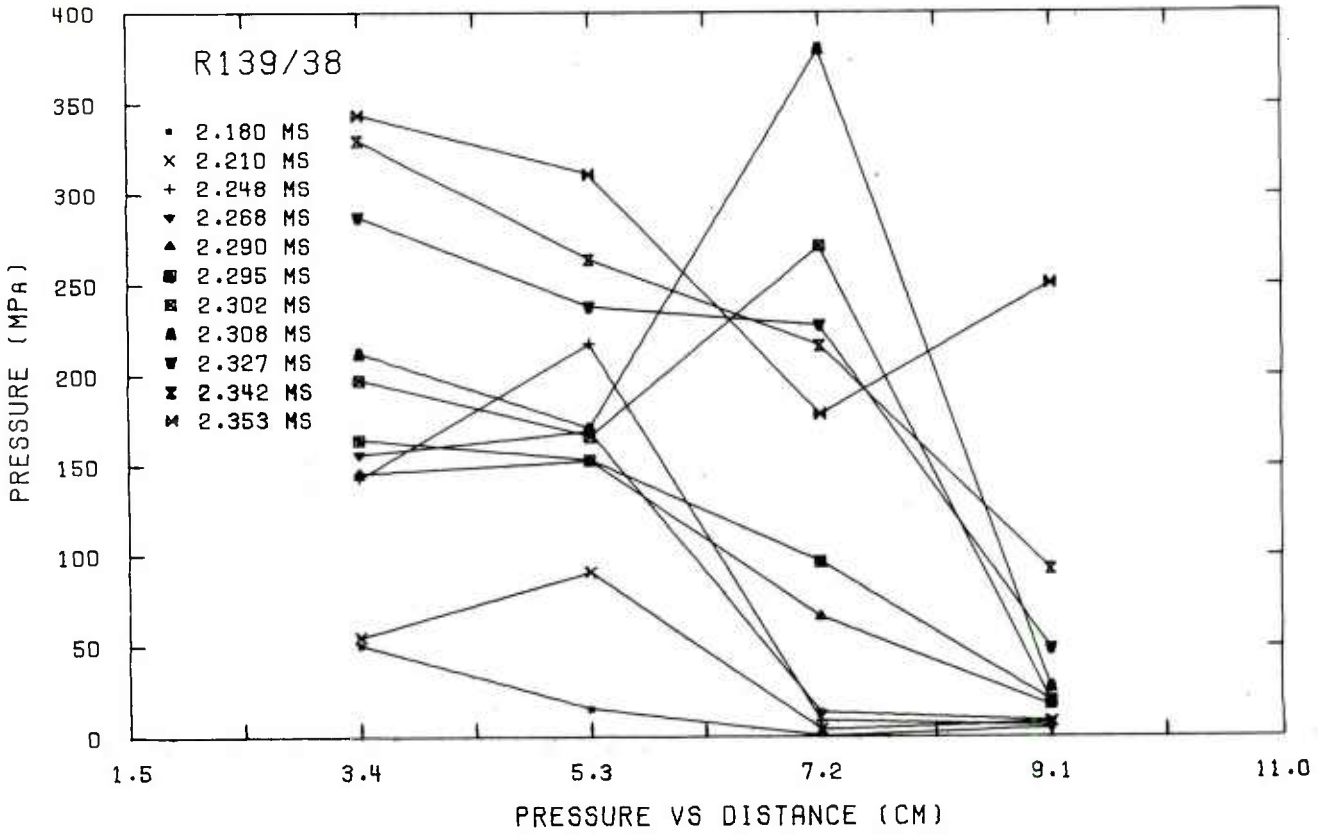
R139/38
2.180 MS
2.210 MS
2.248 MS
2.268 MS
2.290 MS
2.295 MS
2.302 MS
2.308 MS
2.327 MS
2.342 MS
2.353 MS
PRESSURE (MPa)
400
350
300
250
200
150
100
50
0
1.5
3.4
5.3
7.2
9.1
11.0
PRESSURE VS DISTANCE (CM)

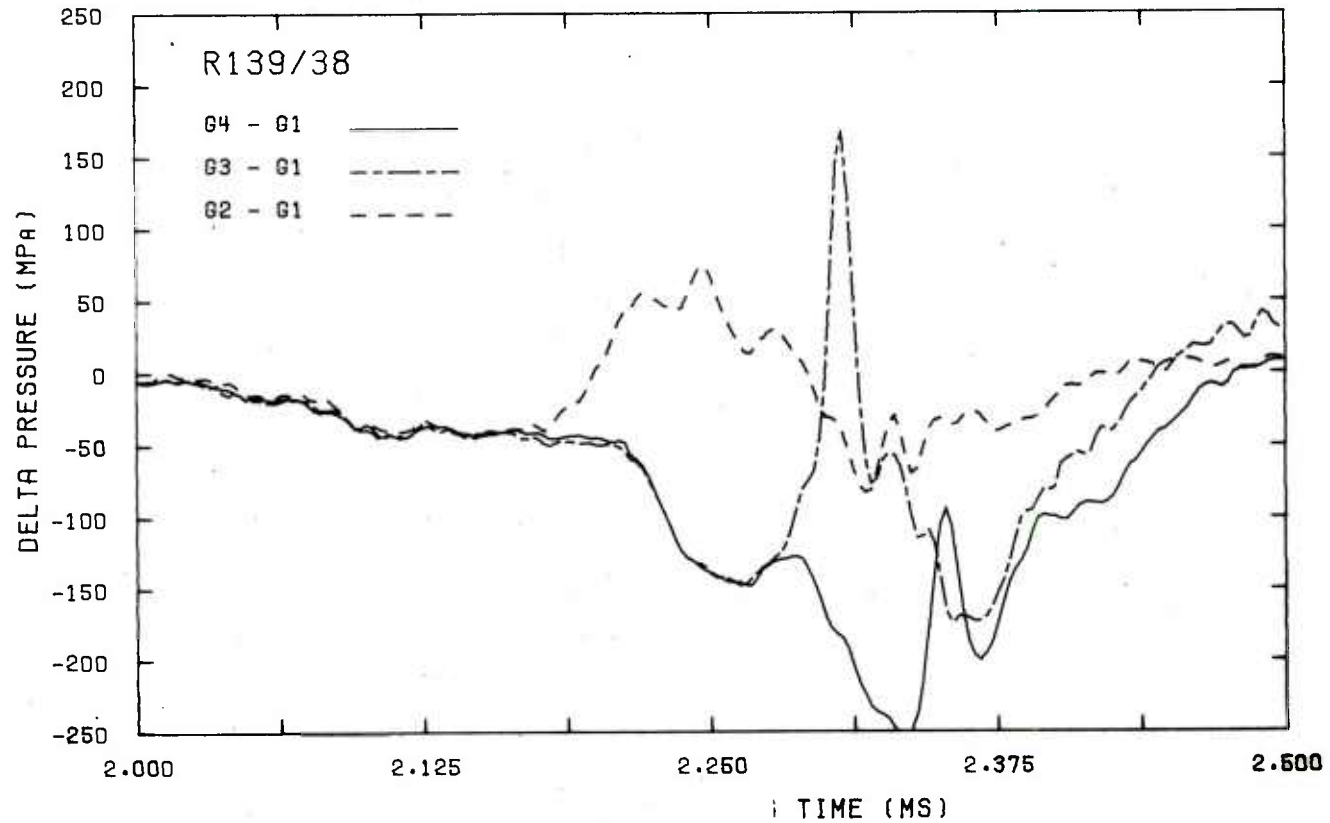
R139/38
G4 - G1
G3 - G1
G2 - G1
DELTA PRESSURE (MPa)
250
200
150
100
50
0
-50
-100
-150
-200
-250
2.000
2.125
2.250
2.375
2.500
TIME (MS)

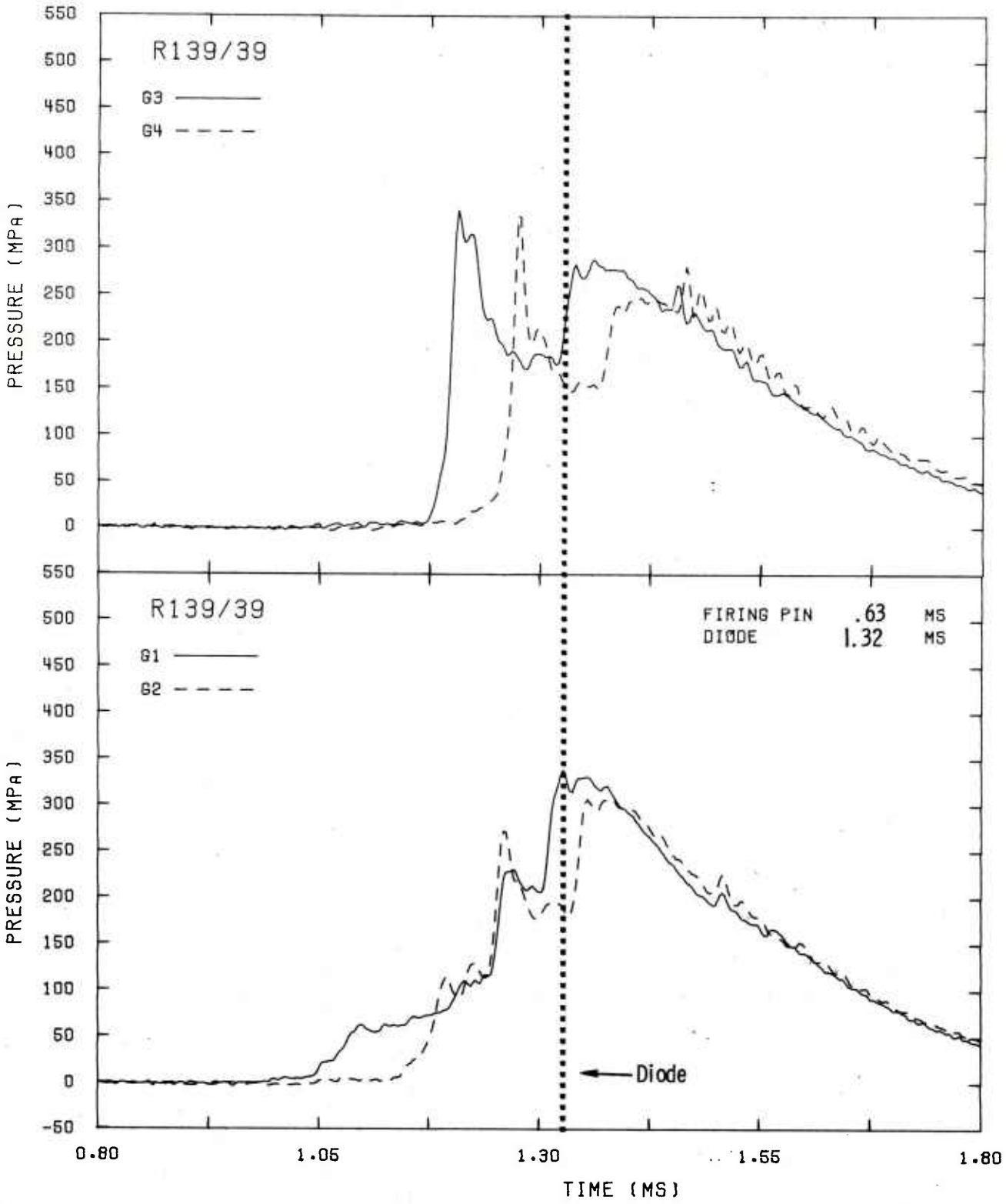
R139/39
G3
G4
R139/39
G1
G2
FIRING PIN .63 MS
DIODE 1.32 MS
Diode
PRESSURE (MPa)
PRESSURE (MPa)
TIME (MS)
550
500
450
400
350
300
250
200
150
100
50
0
-50
0.80
1.05
1.30
1.55
1.80

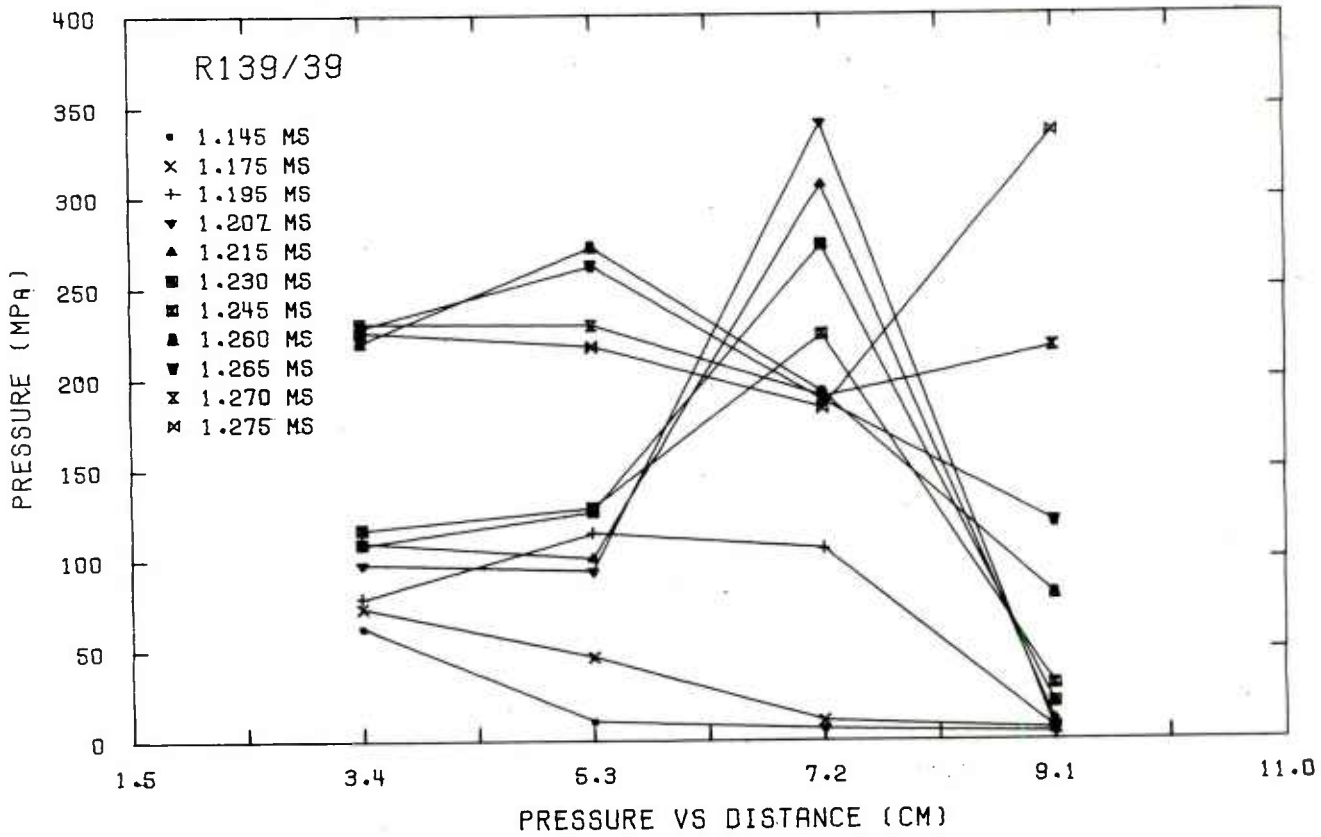
R139/39
1.145 MS
1.175 MS
1.195 MS
1.207 MS
1.215 MS
1.230 MS
1.245 MS
1.260 MS
1.265 MS
1.270 MS
1.275 MS
PRESSURE (MPa)
400
350
300
250
200
150
100
50
0
1.5
3.4
5.3
7.2
9.1
11.0
PRESSURE VS DISTANCE (CM)

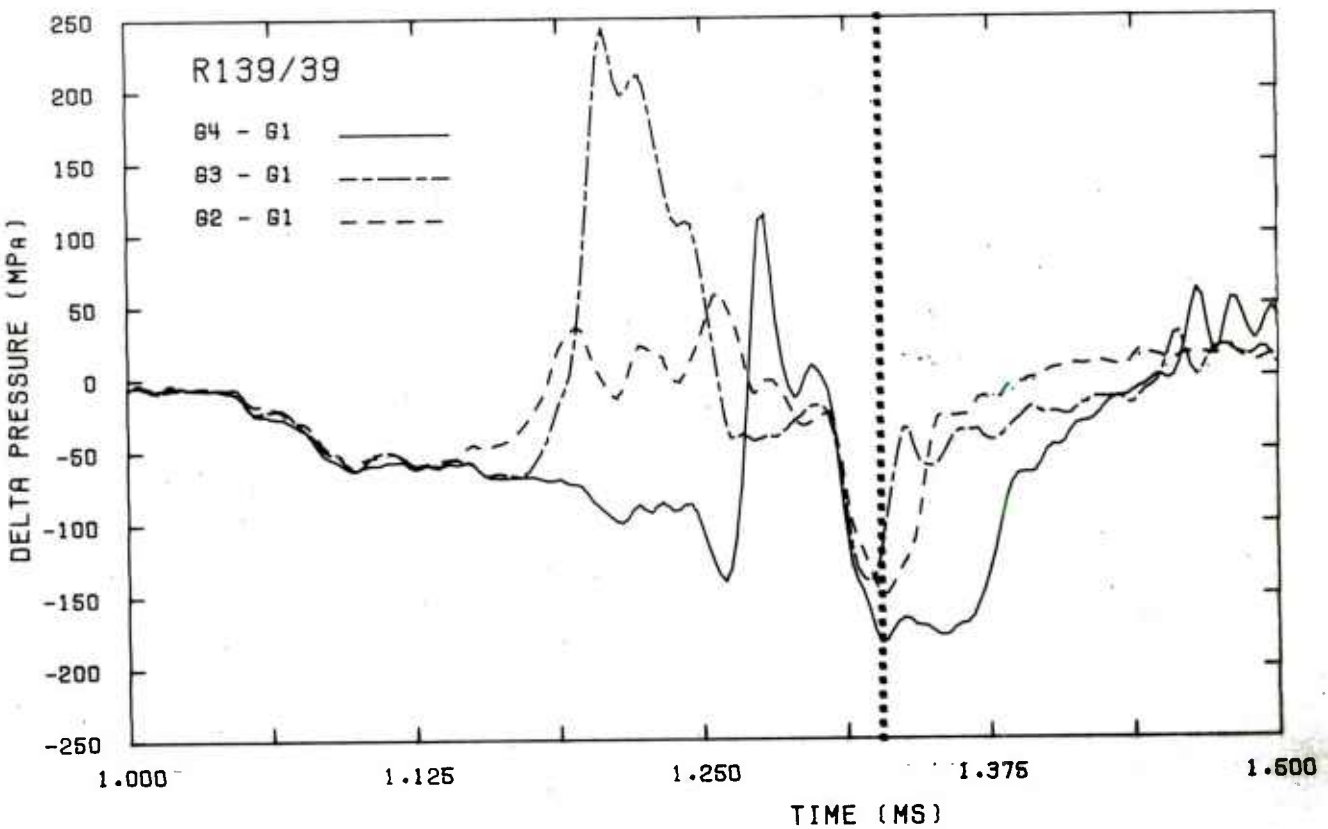
R139/39
G4 - G1
G3 - G1
G2 - G1
DELTA PRESSURE (MPa)
250
200
150
100
50
0
-50
-100
-150
-200
-250
1.000
1.125
1.250
1.375
1.500
TIME (MS)

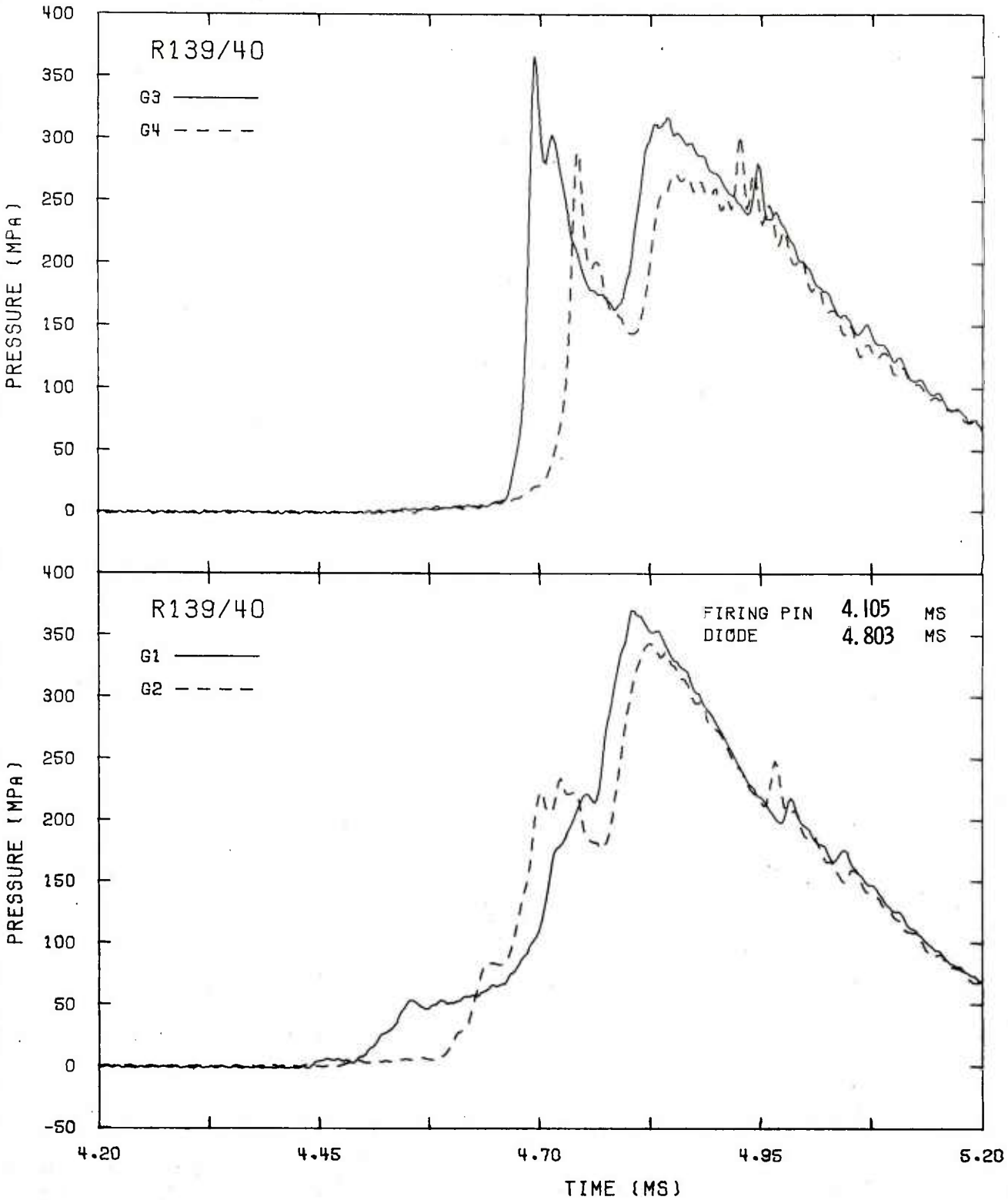
R139/40
G3
G4
R139/40
G1
G2
FIRING PIN 4.105 MS
DIODE 4.803 MS
PRESSURE (MPA)
PRESSURE (MPA)
TIME (MS)
400
350
300
250
200
150
100
50
0
-50
4.20
4.45
4.70
4.95
5.20

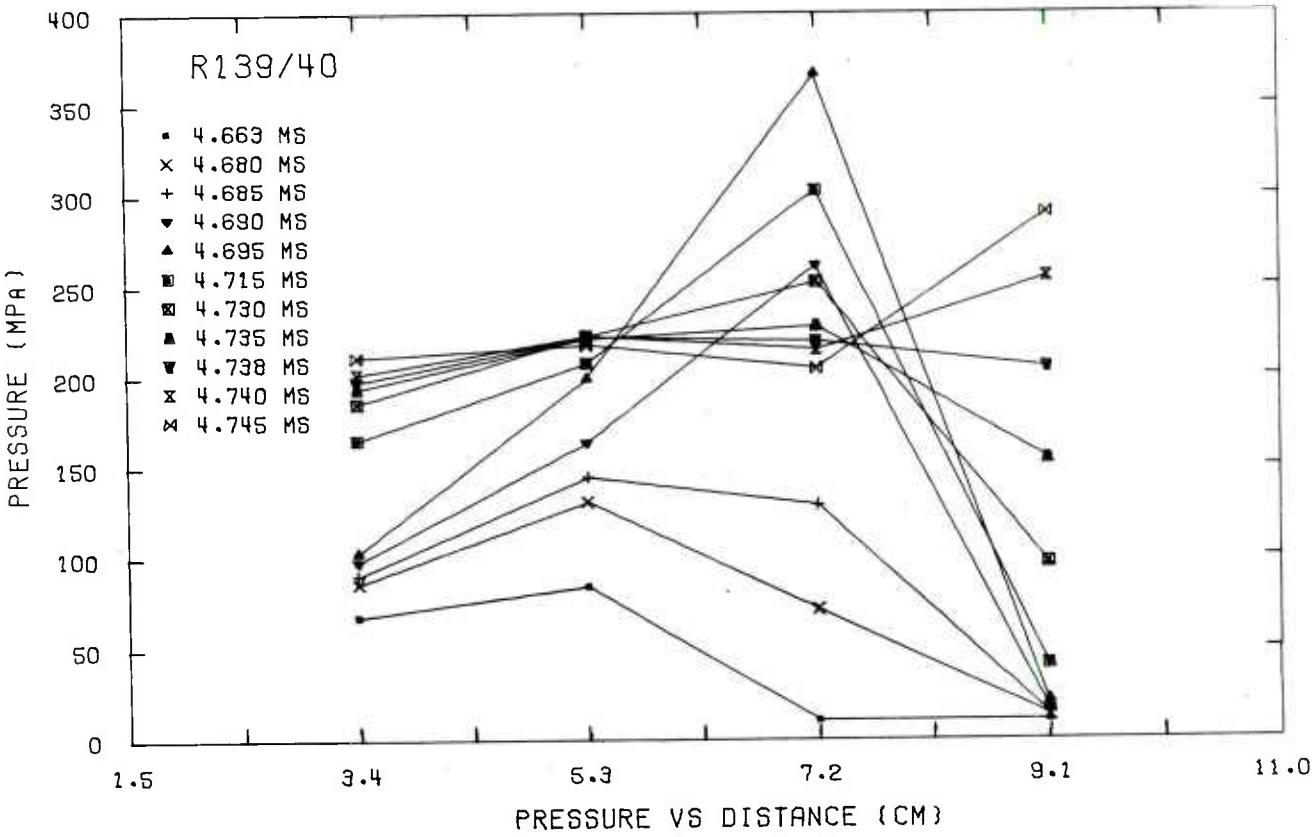
R139/40
4.663 MS
4.680 MS
4.685 MS
4.690 MS
4.695 MS
4.715 MS
4.730 MS
4.735 MS
4.738 MS
4.740 MS
4.745 MS
PRESSURE (MPA)
400
350
300
250
200
150
100
50
0
1.5
3.4
5.3
7.2
9.1
11.0
PRESSURE VS DISTANCE (CM)

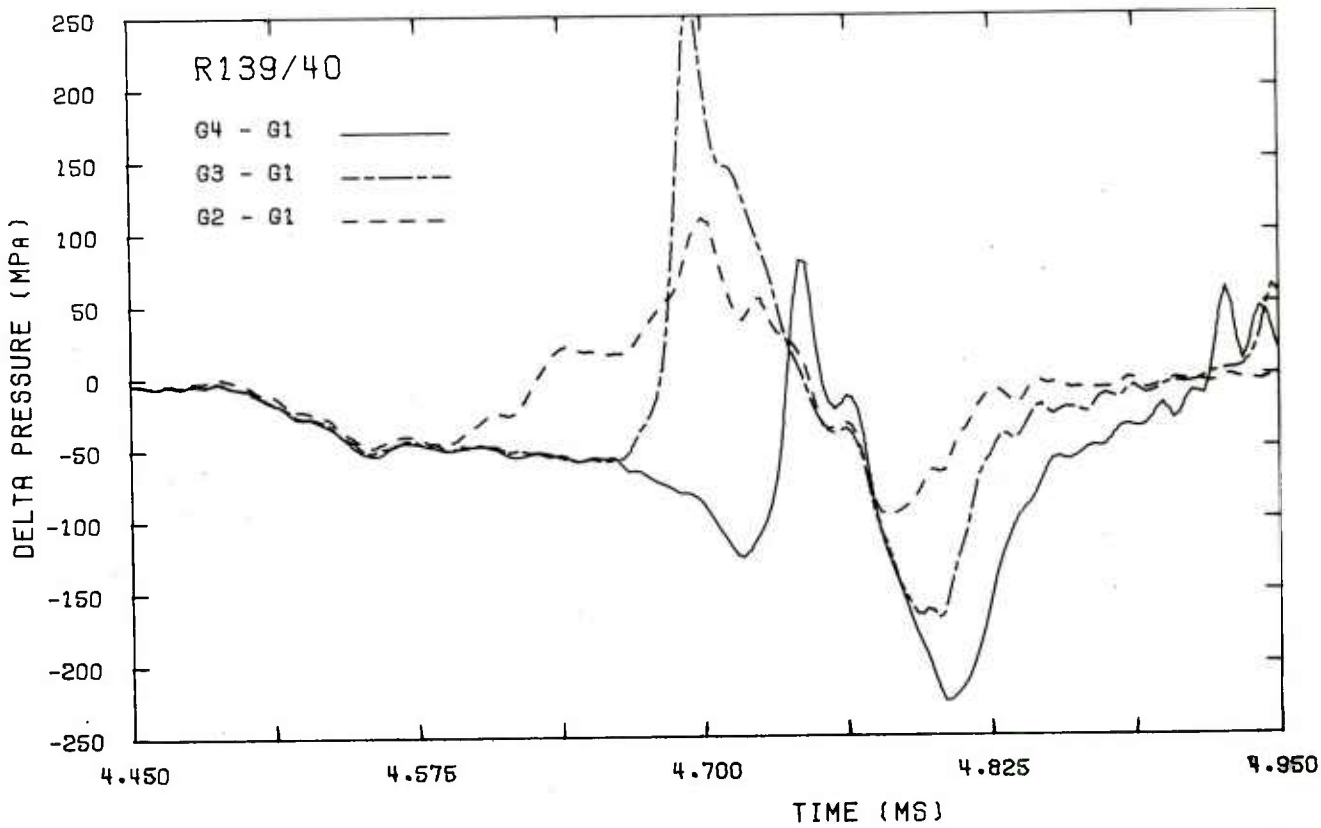
R139/40
G4 - G1
G3 - G1
G2 - G1
DELTA PRESSURE (MPA)
250
200
150
100
50
0
-50
-100
-150
-200
-250
4.450
4.575
4.700
4.825
4.950
TIME (MS)

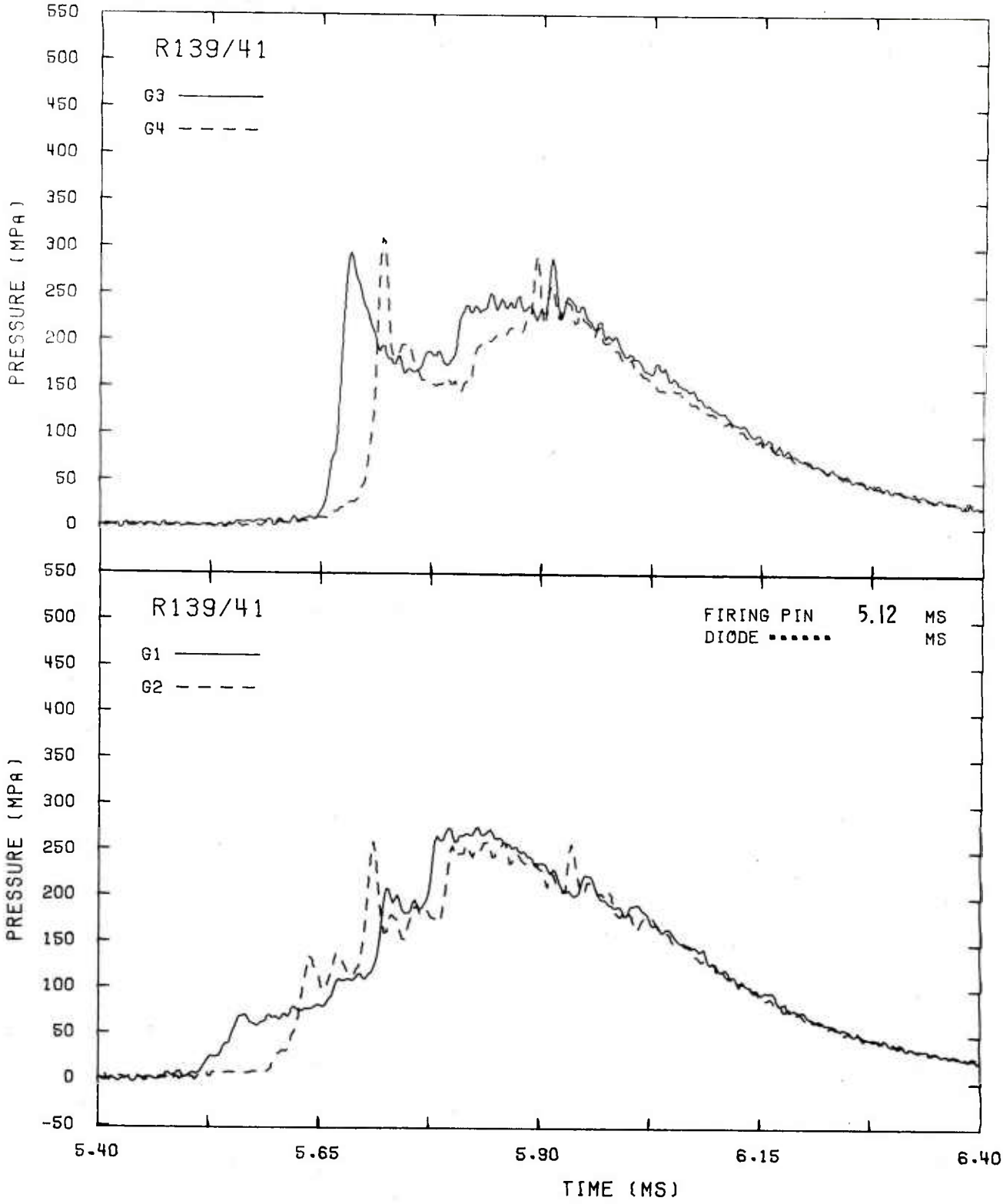
R139/41
G3
G4
PRESSURE (MPA)
550
500
450
400
350
300
250
200
150
100
50
0
R139/41
G1
G2
FIRING PIN 5.12 MS
DIODE ..... MS
PRESSURE (MPA)
550
500
450
400
350
300
250
200
150
100
50
0
-50
5.40
5.65
5.90
6.15
6.40
TIME (MS)

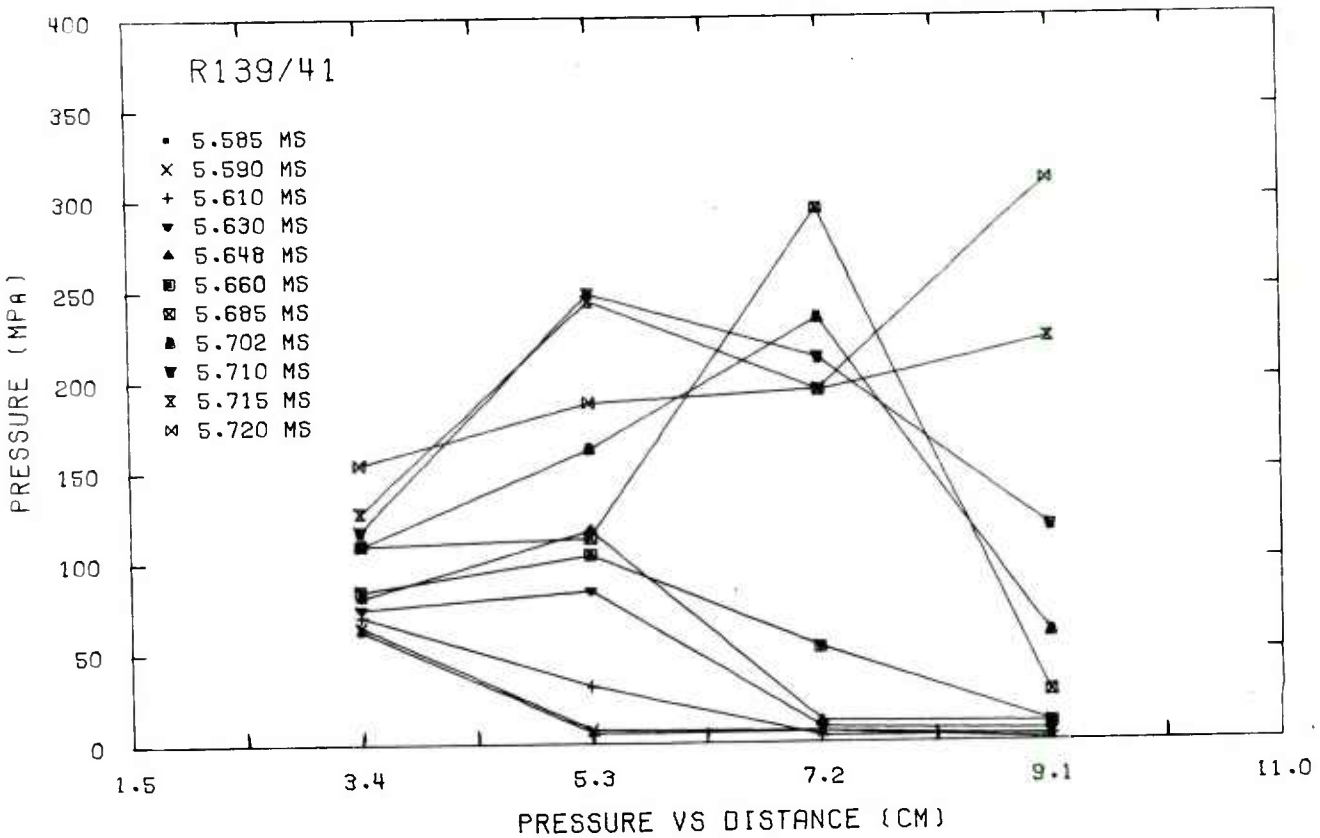
R139/41
5.585 MS
5.590 MS
5.610 MS
5.630 MS
5.648 MS
5.660 MS
5.685 MS
5.702 MS
5.710 MS
5.715 MS
5.720 MS
PRESSURE (MPA)
400
350
300
250
200
150
100
50
0
1.5
3.4
5.3
7.2
9.1
11.0
PRESSURE VS DISTANCE (CM)

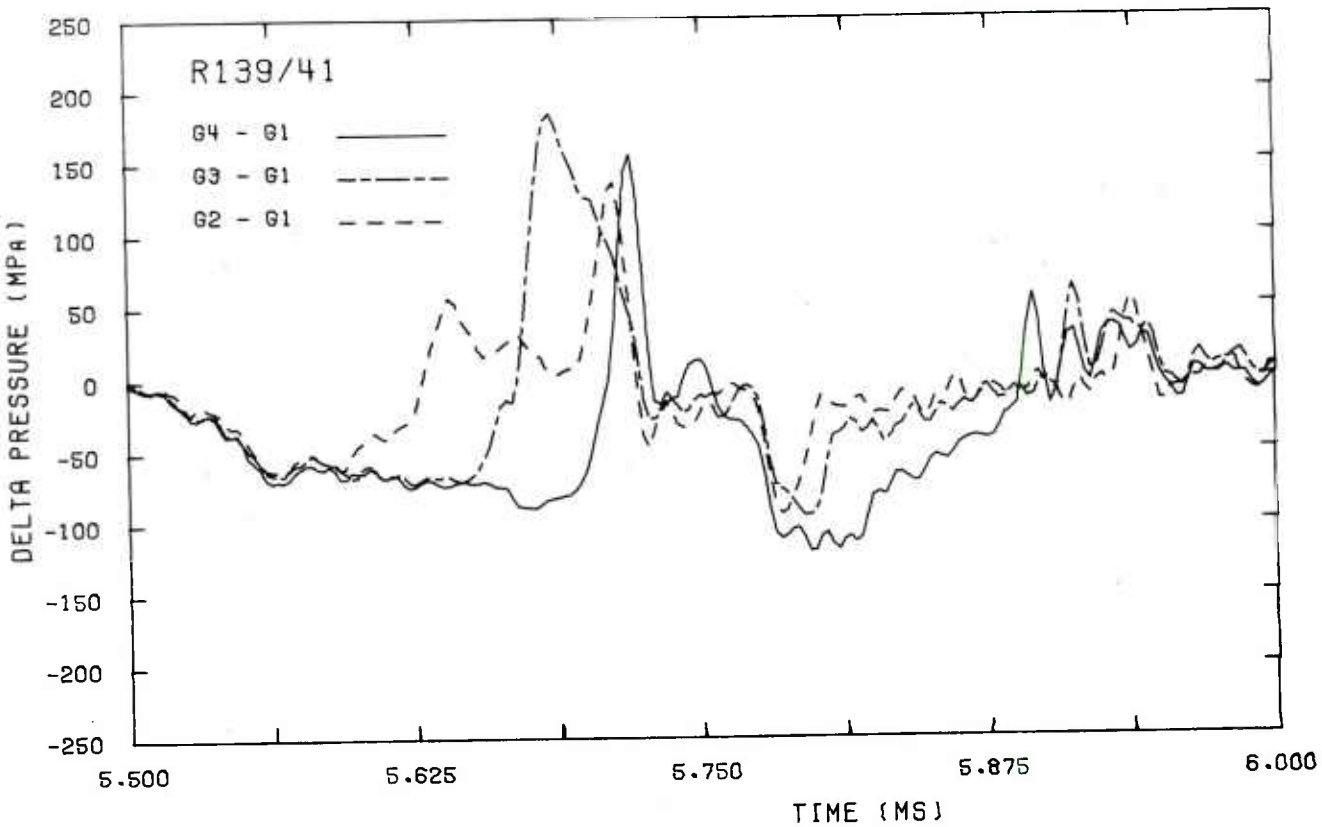
R139/41
G4 - G1
G3 - G1
G2 - G1
DELTA PRESSURE (MPA)
250
200
150
100
50
0
-50
-100
-150
-200
-250
5.500
5.625
5.750
5.875
6.000
TIME (MS)

APPENDIX B. PROPELLANT AND EQUIPMENT SPECIFICATIONS

Propellant Specifications

Designation: Propellant, Ball WC-846, deterred, surface coated

True density (gm/cm^3): 1.60 ± .06

Bulk density (gm/cm^3): 1.01 ± .03

Granulation (mm): .686/.406

Web (mm): .457

Burning rate (m/s): $4.8 \times 10^{-4} P_{(MPa)}$ exp (0.619)

Chemical Composition of Deterred Ball Propellant

Ingredients	PERCENTAGE (%) WC-846	WC-844
Nitroglycerin	9.71	9.71
Dinitrotoluene	0.71	0.71
Diphenylamine	0.90	0.90
Nitrocellulose (13.15% N)	87.01	87.01
Moisture and Volatiles	0.85	0.85
Residual Solvent	0.29	0.29
Calcium Carbonate	0.46	~ 0.05
Sodium Sulfate	0.07	0.07

WC-846 Particle Size Distribution

U.S. Mesh	% Retained	Equivalent Diameter (mm)
20	.89	.84
25	6.92	.71
30	35.18	.59
35	32.89	.50
40	21.97	.42
45	2.15	.35

Chamber Length (mm): 108.4

Chamber Volume (cm^3): 4.91

Nominal Propellant Weight (gm): 4.96
(Standard run, 100% volumetric loading)

Specifications for Primers

Primer	Charge (grams)	Action Time (ms)*
FA-41	0.38 - 0.41	0.23
FA-34	0.48 - 0.60	0.30

* *Time delay from time firing pin strikes the primer to initial primer delivery measured by light sensitive diode.*

Diode Specifications

Diode: Type IN2175-NPN-Diffused Silicon Photo-Duo-Diode

Rise Time: 3 μsec

Sensitivity Range: (.41 - 1.12) microns

Shear Disc Specifications

Diameter (mm)	Static Burst Pressure (MPa)	Thickness (mm)	Material
17	210	0.81	304 SS
17	110	0.38	304 SS

Specifications for Kistler Transducer

Model 607C4

Range: 100,000 psi

Linearity: 1%

Sensitivity: 0.14p Cb/psi

Frequency Response: ±5% - DC to 50,000 Hz

Rise Time: 1.5 μsec

DISTRIBUTION LIST

No. of Copies	Organization
12	Commander Defense Documentation Center ATTN: DCC-TCA Cameron Station Alexandria, VA 22314
1	Director Defense Advanced Research Projects Agency ATTN: C.R. Lehner 1400 Wilson Boulevard Arlington, VA 22209
2	Director Institute for Defense Analyses ATTN: Dr. H. Wolfhard Mr. R.T. Oliver 400 Army-Navy Drive Arlington, VA 22202
1	Commander US Army Materiel Development and Readiness Command ATTN: DRCDMA-ST 5001 Eisenhower Avenue Alexandria, VA 22333
1	Commander US Army Aviation Systems Command ATTN: DRSAV-E 12th and Spruce Streets St. Louis, MO 63166
1	Director US Army Air Mobility Research and Development Laboratory Ames Research Center Moffett Field, CA 94035
1	Commander US Army Electronics Command ATTN: DRSEL-RD Ft. Monmouth, NJ 07703
1	Commander US Army Missile R&D Command ATTN: DRSMI-R Redstone Arsenal, AL 35809
1	Commander US Army Tank Automotive Development Command ATTN: DRDTA-RWL Warren, MI 48090
2	Commander US Army Mobility Equipment Research & Development Command ATTN: Tech Doc Ctr, Bldg. 315 DRSME-RZT Ft. Belvoir, VA 22060
4	Commander US Army Armament Materiel Readiness Command ATTN: DRSAR-RD, Dr. J. Brinkman DRSAR-RDG, Mr. J.G. Blick SARRI-AOF, J. H. Noble Rock Island, IL 61202
3	Commander US Army Frankford Arsenal ATTN: DRDAR-LCE-CI, Dr. J. Lannon SCA-CC, Mr. C. Dickey SCA-PP, Mr. L. Stiefel Philadelphia, PA 19137
8	Commander US Army Armament Research and Development Command ATTN: DRDAR-LC, Mr. R. Corn DRDAR-LCF, Mr. G. Demitrack DRDAR-QAM, Mr. F. Fitzsimmons DRDAR-LCU, Mr. D. Katz DRDAR-TDS, Mr. V. Linder DRDAR-LCE, Mr. C. Lenchitz DRDAR-LC, Dr. J.P. Picard DRDAR-LCE, Dr. R.F. Walker Dover, New Jersey 07801

DISTRIBUTION LIST

No. of Copies	Organization
1	Commander US Army White Sands Missile Range ATTN: STEWS-VT WSMR, NM 88002
1	Commander US Army Watervliet Arsenal ATTN: R. Thierry/Code SWEWV-RD Watervliet, NY 12189
1	Commander US Army Harry Diamond Labs ATTN: DRXDO-TI 2800 Powder Mill Road Adelphi, MD 20783
1	Commander US Army Materials and Mechanics Research Center ATTN: DRXMR-ATL Watertown, MA 02172
1	Commander US Army Natick Research and Development Command ATTN: DRXRE, Dr. D. Sieling Natick, MA 01762
1	Director US Army TRADOC Systems Analysis Activity ATTN: ATAA-SA WSMR, NM 88002
1	Commander US Army Research Office ATTN: Tech Lib P.O. Box 12211 Research Triangle Park, NC 27706
1	Chief of Naval Research ATTN: Code 473 800 N. Quincy Street Arlington, VA 22217
1	Commander US Naval Sea Systems Command ATTN: J.W. Murrin (NAVSEA-0331) National Center, Bldg. 2, Rm 6E08 Washington, DC 20360
2	Commander US Naval Surface Weapons Center ATTN: S.J. Jacobs/Code 240 Code 730 Silver Spring, MD 20910
1	Commander US Naval Surface Weapons Center ATTN: Tech Lib Dahlgren, VA 22338
1	Commander US Naval Underwater Systems Center Energy Conversion Department ATTN: R.S. Lazar/Code 5B331 Newport, RI 02840
2	Commander US Naval Weapons Center ATTN: Dr. R. Derr Mr. C. Thelen China Lake, CA 93555
1	Commander US Naval Research Laboratory ATTN: Code 6180 Washington, DC 20375
3	Superintendent US Naval Postgraduate School ATTN: Tech Lib Dr. David Netzer Dr. Allen Fuhs Monterey, CA 93940
3	Commander US Naval Ordnance Station ATTN: Dr. S. Mitchell Dr. A. Roberts Tech Lib Indian Head, MD 20640

DISTRIBUTION LIST

No. of Copies	Organization
2	AFOSR ATTN: J.R. Masi Dr. B.T. Wolfson Bolling AFB, DC 20332
2	AFRPL (DYSC) ATTN: Dr. D. George Mr. J.N. Levine Edwards AFB, CA 93523
1	Lockheed Palo Alto Rsch Labs ATTN: Tech Info Ctr 3521 Hanover Street Palo Alto, CA 94304
1	Aerojet Solid Propulsion Co. ATTN: Dr. P. Micheli Sacramento, CA 95813
1	ARO Incorporated ATTN: Mr. N. Dougherty Arnold AFS, TN 37389
1	Atlantic Research Corporation ATTN: Dr. M.K. King 5390 Cherokee Avenue Alexandria, VA 22314
1	AVCO Corporation AVCO Everett Research Lab Div ATTN: D. Stickler 2385 Revere Beach Parkway Everett, MA 02149
2	Calspan Corporation ATTN: Dr. E.B. Fisher A.P. Trippe P.O. Box 235 Buffalo, NY 14221
1	ENKI Corporation ATTN: M.I. Madison 9015 Fulbright Avenue Chatsworth, CA 91311
1	Foster Miller Associates, Inc. ATTN: A.J. Erickson 135 Second Avenue Waltham, MA 02154
1	General Electric Company Armament Department ATTN: M.J. Bulman Lakeside Avenue Burlington, VT 05402
1	General Electric Company Flight Propulsion Division ATTN: Tech Lib Cincinnati, OH 45215
2	Hercules Incorporated Alleghany Ballistic Lab ATTN: Dr. R. Miller Tech Lib Cumberland, MD 21501
2	Hercules Incorporated Bacchus Works ATTN: Dr. M. Beckstead Dr. R. Simmons Magna, UT 84044
1	IITRI ATTN: Dr. M.J. Klein 10 West 35th Street Chicago, IL 60615
1	Olin Corporation Badger Army Ammunition Plant ATTN: J. Ramnarace Baraboo, WI 53913
2	Olin Corporation New Haven Plant ATTN: R.L. Cook D.W. Riefler 275 Winchester Avenue New Haven, CT 06504

DISTRIBUTION LIST

No. of Copies	Organization
1	Paul Gough Associates, Inc. ATTN: Dr. P.S. Gough P.O. Box 1614 Portsmouth, NH 03801
1	Physics International Company ATTN: J.D. Watson 2700 Merced Street Leandro, CA 94577
1	Pulsepower Systems, Inc. ATTN: L.C. Elmore 815 American Street San Carlos, CA 94070
1	R&D Associates ATTN: Dr. R.B. Edelman P.O. Box 9695 Marina del Rey, CA 90291
2	Rockwell International Corp. Rocketdyne Division ATTN: Dr. C. Obert Dr. J.E. Flanagan 6633 Canoga Avenue Canoga Park, CA 91304
2	Rockwell International Corp. Rocketdyne Division ATTN: Mr. W. Haymes Tech Lib McGregor, TX 76657
1	Shock Hydrodynamics, Inc. ATTN: Dr. W.H. Anderson 4710-16 Vineland Avenue North Hollywood, CA 91602
1	Thiokol Corporation Elkton Division ATTN: E. Sutton Elkton, MD 21921
3	Thiokol Corporation Huntsville Division ATTN: Dr. D. Flanigan Dr. R. Glick Tech Lib Huntsville, AL 35807
2	Thiokol Corporation Wasatch Division ATTN: Dr. John Peterson Tech Lib P. O. Box 524 Brigham City, UT 84302
1	TRW Systems Group ATTN: Dr. H. Korman One Space Park Redondo Beach, CA 90278
2	United Technology Center ATTN: Dr. R. Brown Tech Lib P. O. Box 358 Sunnyvale, CA 94088
1	Universal Propulsion Co. ATTN: H. J. McSpadden P. O. Box 546 Riverside, CA 92502
1	Battelle Memorial Institute ATTN: Tech Lib 505 King Avenue Columbus, OH 43201
1	Brigham Young University Department of Chemical Engineering ATTN: Prof. R. Coates Provo, UT 84601

DISTRIBUTION LIST

No. of Copies	Organization
1	California Institute of Tech Jet Propulsion Laboratory ATTN: Prof. F.E.C. Culick Pasadena, CA 91103
1	Case Western Reserve Univ. Division of Aerospace Sciences ATTN: Prof. J. Tien Cleveland, OH 44135
3	Georgia Institute of Technology School of Aerospace Engineering ATTN: Prof. B.T. Zinn Prof. E. Price Prof. W.C. Strahle Atlanta, GA 30332
1	Institute of Gas Technology ATTN: Dr. D. Gidaspow 3424 S. State Street Chicago, IL 60616
1	Johns Hopkins University Applied Physics Laboratory Chemical Propulsion Information Agency ATTN: Mr. T. Christian Johns Hopkins Road Laurel, MD 20810
1	Massachusetts Institute of Technology Dept of Mechanical Engineering ATTN: Prof. T. Toong Cambridge, MA 02139
1	Pennsylvania State University Applied Research Lab ATTN: Dr. G.M. Faeth P.O. Box 30 State College, PA 16801
1	Pennsylvania State University Dept of Mechanical Engineering ATTN: Prof. K. Kuo University Park, PA 16801
3	Princeton University Forrestal Campus Library ATTN: Prof. M. Summerfield Dr. L. Caveny Tech Lib P. O. Box 710 Princeton, NJ 08540
2	Purdue University School of Mechanical Engineering ATTN: Prof. J. Osborn Prof. S.N.B. Murthy TSPC Chaffee Hall West Lafayette, IN 47906
1	Rutgers State University Dept of Mechanical and Aerospace Engineering ATTN: Prof. S. Temkin University Heights Campus New Brunswick, NJ 08903
1	Southwest Research Institute Fire Research Section ATTN: W.H. McLain P. O. Drawer 28510 San Antonio, TX 78228
1	Stanford Research Institute Propulsion Sciences Division ATTN: Tech Lib 333 Ravenswood Avenue Menlo Park, CA 94024
1	Stevens Institute of Technology Davidson Laboratory ATTN: Prof. R. McAlevy, III Hoboken, NJ 07030
1	University of California, San Diego AMES Department ATTN: Prof. F. Williams P. O. Box 109 La Jolla, CA 92037

DISTRIBUTION LIST

No. of Copies	Organization
1	University of Illinois Dept of Aeronautical Engineering ATTN: Prof. H. Krier Transportation Bldg, Rm 105 Urbana, IL 61801
1	University of Minnesota Dept of Mechanical Engineering ATTN: Prof. E. Fletcher Minneapolis, MN 55455
2	University of Utah Dept of Chemical Engineering ATTN: Prof. A. Baer Prof. G. Flandro Salt Lake City, UT 84112
	Aberdeen Proving Ground
	Marine Corps Ln Ofc Dir, USAMSAA